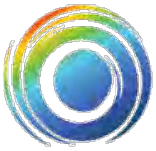

International Ocean Colour Science Meeting 2013

Advancing Global Ocean Colour Observations

SUBMITTED ABSTRACTS

Topical Area

Algorithms and Products

Algorithms and Products

First Name	Name	Institute	Title
Severine	Alvain	LOG - CNRS	**Towards phytoplankton community structure detection thanks to the synergy between theoretical approach and in situ observations.**
Lionel	Arteaga	GEOMAR	**Satellite-derived ocean primary production inferred by an optimality-based phytoplankton model**
Astrid	Bracher	Alfred-Wegener-Institute Helmholtz Centre for Polar and Marine Research	**Ocean colour products from hyper-spectral satellite data of SCIAMACHY using the PhytoDOAS method and the radiative transfer model SCIARAN**
Astrid	Bracher	Alfred-Wegener-Institute Helmholtz Centre for Polar and Marine Research	**Overview on algorithms to derive phytoplankton community structure from satellite ocean colour**
Julien	Brajard	LOCEAN/IPSL/UPMC	**Using the near pixels of ocean colour images to perform the atmospheric correction over turbid waters.**
Nayara	Bucair	Aveiro University	**Diatoms blooms detected by remote sensing**
Ivona	Cetinic	University of Maine	**Multi-sensor, ecosystem-based approaches for estimation of Particulate Organic Carbon**
Sumit	Chakraborty	University of Massachusetts Dartmouth	**Bio-optical properties of the northern Gulf of Mexico: Ship based and satellite observations**
Lesley	Clementson	CSIRO	**A dataset of global in situ observations for the development and comparison of Phytoplankton Functional Type (PFT) algorithms.**
Maycira	Costa	University of Victoria	**MODIS atmospheric correction and chlorophyll products in the Strait of Georgia, British Columbia, Canada.**
Susanne	Craig	Dalhousie University	**Statistical Derivation of Inherent Optical Properties and Chlorophyll a From an Optically Complex Coastal Site**
Miroslaw	Darecki	Institute of Oceanology of the Polish Academy of Science	**A satellite-based operational system for remote sensing of the Baltic ecosystem**
Pierre-Yves	Deschamps	HYGEOS	**Atmospheric scattering and ocean color: errors due to the spherical atmosphere**

First Name	Name	Institute	Title
Roland	Doerffer	Brockmann Consult & HZG	**The Information content of reflectance spectra and the uncertainties of derived IOPs of coastal waters**
Ana	Dogliotti	Instituto de Astronomía y Física del Espacio (IAFE)	**Can a single turbidity algorithm be used in all turbid waters?**
Vincent	Fournier-Sicre	EUMETSAT	**SENTINEL-3 Optical Sensors Products and Algorithms**
Robert	Frouin	Scripps Institution of Oceanography	**Bayesian Methodology for Ocean Color Remote Sensing**
Rodrigo	Garcia	Remote Sensing and Satellite Research Group, Department of Imaging and Applied Physics, Curtin University	**Routine monitoring of bathymetry and habitat maps derived from HICO imagery: Case study of Shark Bay, Western Australia.**
Michelle	Gierach	Jet Propulsion Laboratory	**Biological response to the 1997-98 and 2009-10 El Niño events in the equatorial Pacific Ocean**
Alex	Gilerson	City College of New York	**The retrieval of attenuation and scattering coefficients of marine particles from polarimetric observations**
Jim	Gower	Institute of Ocean Sciences	**An improved FLH product for MERIS and OLCI**
Clémence	Goyens	CNRS, UMR 8187,ULCO, LOG	**A hybrid MUMM NIR-Corrected algorithm for the atmospheric correction of turbid waters**
Taka	Hirata	Hokkaido University	**Satellite Phytoplankton Functional Type Algorithm Intercomparison and validation**
Toru	Hirawake	Hokkaido University	**Retrieval of size fractionated chlorophyll a concentration: an application of particle size distribution**
Chuanmin	Hu	University of South Florida	**Ocean color data product uncertainty, consistency, and continuity: Evaluation with a new algorithm concept**
Ian	Jones	University of Sydney	**Particle Retention in the Moroccan Coastal Ocean**

First Name	Name	Institute	Title
Mati	Kahru	Scripps Institution of Oceanography	**Optimized multi-satellite merger to create time series of inherent optical properties in the California Current**
Tihomir	Kostadinov	University of Richmond	**Carbon-based Phytoplankton Functional Types and Productivity via Remote Retrievals of the Particle Size Distribution**
Susanne	Kratzer	Department of Ecology, Environment and Plant Sciences	**Robust Kd(490) and Secchi depth algorithms for remote sensing of optically complex waters dominated by CDOM**
Zhongping	Lee	University of Massachusetts Boston	**Estimation of spectral attenuation coefficient of downwelling irradiance: from oligotrophic to coastal waters**
Soo Chin	Liew	National University of Singapore	**Deriving suspended sediment and turbidity products from remote sensing reflectance in turbid coastal waters**
Ronghua	Ma	Nanjing Institute of Geography and Limnology, Chinese Academy of Sciences	**Remote sensing of Lake Taihu**
Ronghua	Ma	Nanjing Institute of Geography and Limnology, Chinese Academy of Sciences	**An extension of water color remote sensing: unusual link to particle particulate organic carbon**
Antonio	Mannino	NASA Goddard Space Flight Center	**Development and Analysis of Ocean Color Satellite DOM Products for Studies in Coastal Ocean Dynamics**
Zhihua	Mao	Second Institute of Oceanography,SOA	**A new approach to estimate the aerosol scattering radiance for Case 2 waters**
Salvatore	Marullo	ENEA	**Detecting dominant Phytoplankton Size Classes (micro, nano and pico phytoplankton) from SeaWiFS data in the Mediterranean Sea: spatial and temporal variability**
Mark	Matthews	University of Cape Town	**Distinguishing cyanobacteria from algae in eutrophic near-coastal and inland waters from space: theory and applications**
Frederic	Melin	E.C. Joint Research Centre	**In search of long-term trends in the ocean colour record**
Martin	Montes-Hugo	Université du Québec a Rimouski	**A hybrid halo-optical remote sensing model for characterizing particulates in the Saint Lawrence Estuary**

First Name	Name	Institute	Title
Gerald	Moore	Bio-Optika	**Evolution of the MERIS Bright Pixel Atmospheric Correction: accounting for glint.**
Tim	Moore	University of New Hampshire	**Uncertainty analysis on ocean color products for select semi analytic algorithms**
Wesley	Moses	Naval Research Laboratory	**HICO-Based NIR-red Algorithms for Estimating Chlorophyll-a Concentration in Inland and Coastal Waters – the Taganrog Bay Case Study**
Colleen	Mouw	Michigan Technological University	**Phytoplankton size variability in the global ocean**
Mauricio	Noernberg	Center for Marine Studies - UFPR	**Comparison of atmospheric corrections of HICO images of a subtropical estuarine region in Brazil.**
Emanuele	Organelli	LOV-CNRS/UPMC	**The multivariate Partial Least Squares regression technique for the retrieval of algal size structure from particle and phytoplankton light absorption spectra**
Sherry	Palacios	NASA Ames Research Center	**A novel algal discrimination algorithm based on first principles of aquatic optics and applied to hyperspectral remote sensing imagery of the coastal ocean**
Steef	Peters	Water Insight	**Validation of the WISP algorithm for 9 years of MODIS observations on Dutch monitoring stations**
Andrea	Pisano	CNR-ISAC Rome	**A new oil spill detection methodology for MODIS and MERIS satellite imagery: an application to the Mediterranean Sea**
Cecile	Rousseaux	USRA/GMAO NASA	**Satellite views of global phytoplankton community distributions using an empirical algorithm and a numerical model**
Kevin	Ruddick	RBINS/MUMM	**The saturation reflectance in turbid waters**
Mhd. Suhyb	Salama	ITC faculty, University of Twente	**Calibration and validation of ocean color bio-optical models**
Joseph	Salisbury	University of New Hampshire	**Linking terrestrial fluxes and biogeochemical variability in the coastal ocean: the role of hydrological models and new satellite ocean color and salinity sensors.**

First Name	Name	Institute	Title
Bertrand	Saulquin	ACRI-ST	**Detection of linear trends in multi-sensor time series in presence of auto-correlated noise: application to the chlorophyll-a SeaWiFS and MERIS datasets and extrapolation to the incoming Sentinel 3 - OLCI mission.**
Bertrand	Saulquin	ACRI-ST	**Water typed merge of chl-a algorithms and the daily Atlantic (1km) and global (4km) chlorophyll-a analyses of MyOcean II.**
Mike	Sayers	Michigan Tech Research Institute	**Satellite Derived Primary Productivity Estimates for Lake Michigan**
Thomas	Schroeder	CSIRO	**CDOM a useful surrogate for salinity: Mapping the extent of riverine freshwater discharge into the Great Barrier Reef lagoon from MODIS observations**
Anatoly	Shevyrnogov	Institute of Biophysics SB RAS	**Seasonal dynamics of surface chlorophyll concentration as an indicator of hydrological structure of the ocean (by satellite data)**
Wei	Shi	NOAA/NESDIS/STAR	**Vicarious Calibration Efforts for VIIRS Operational Ocean Color EDR**
Wei	Shi	NOAA/NESDIS/STAR	**Sea ice properties in the Bohai Sea measured by MODIS-Aqua: Satellite Algorithm and Study of Sea Ice Seasonal and Interannual Variability**
David	Siegel	UC Santa Barbara	**A Mechanistic Assessment of Global Ocean Carbon Export From Satellite Observation**
Heidi	Sosik	Woods Hole Oceanographic Institution	**Seasonal to Interannual Variability in Phytoplankton Biomass and Diversity on the New England Shelf: In Situ Time Series to Evaluate Remote Sensing Algorithms**
Knut	Stamnes	Stevens Institute of Technology	**Retrieval of aerosol and marine parameters in coastal environments: The need for improved biooptical models**
François	Steinmetz	HYGEOS	**Polymer: a new approach for atmospheric and glitter correction**
Sindy	Sterckx	VITO	**Validation SIMEC adjacency correction for Coastal and Inland Waters?**
Vyacheslav	Suslin	Marine Hydrophysical Institure of NASU	**Development of the Black Sea bio-optical algorithms: applications and some results based on ocean color scanner data sets**

First Name	Name	Institute	Title
Gavin	Tilstone	Plymouth Marine Laboratory	**Accuracy assessment of satellite Ocean colour products in coastal waters**
Kevin	Turpie	NASA/GSFC	**Coastal and Inland Water Data Product from the Hyperspectral Infrared Imager (HyspIRI)**
Michael	Twardowski	WET Labs, Inc	**Improving remote sensing water quality algorithms**
Maria	Tzortziou	University of Maryland	**Atmospheric trace-gas dynamics and impact on ocean color retrievals in urban estuarine and coastal ecosystems**
Quinten	Vanhellemont	RBINS/MUMM	**A benchmark dataset for the validation of MERIS and MODIS ocean colour turbidity and PAR attenuation algorithms using autonomous buoy data.**
Gianluca	Volpe	Istituto di Scienze dell'Atmosfera e del Clima	**The Mediterranean Ocean Colour Observing System: product validation**
Toby	Westberry	Oregon State University	**The Influence of Raman Scattering on Ocean Color Inversion Models**
Monika	Wozniak	Institute of Oceanography	**Assessment of bio-optical algorithms for satellite radiometers in coastal waters of the Baltic Sea using in situ measurements**
Pengwang	Zhai	SSAI	**Inherent Optical Properties of Coccolithophores: Emiliania Huxleyi**
Yuchao	Zhang	Nanjing Institute of Geography and Limnology, Chinese Academy of Sciences	**Accurate estimation on floating algae area in Lake Taihu, China**
Guangming	Zheng	Scripps Institution of Oceanography	**Evaluation of the Quasi-Analytical Algorithm for estimating the inherent optical properties of seawater from ocean color: Comparison of Arctic and lowerlatitude waters**

Towards phytoplankton community structure detection thanks to the synergy between theoretical approach and in situ observations.

ALVAIN, Severine[1]; Loisel, Hubert[1]; Dessailly, David[1] ; Thyssen Melilotus[3] ;Morin Pascal[2] ;Guiselin Natacha[1] ; Macé Eric[2.]

[1]LOG - CNRS 32 avenue Foch, Wimereux, 62930, France

[2]Station Biologique de Roscoff, CNRS-UPMC, Roscoff France

[3]Mediterranean Institute of Oceanology, 13288 Marseille

Despite observations in good agreement with *in situ* measurements, the underlying theoretical explanation of methods based on radiances anomalies to detect phytoplankton groups (like the PHYSAT one) is missing. This prevents improvements of the methods and limits characterization of uncertainties on the inversed products. In a recent study, radiative transfer simulations have been used in addition to in-situ measurements to understand the organization of the radiances anomalies used in the PHYSAT method. Sensitivity analyses have been performed to assess the impact of the variability of the following three parameters on the reflectance anomalies: specific phytoplankton absorption, colored dissolved organic matter absorption, and particles backscattering. While the later parameter explains the largest part of the anomalies variability, results show that each group is generally associated with a specific bio-optical environment which should be considered in future studies. We will show that the magnitude of the theoretically defined anomalies for the three main PHYSAT groups is in good agreement with specific anomalies empirically highlighted before. Complementary studies, based on large *in situ* database of IOPs measurements, will be necessary in the future to obtain a better agreement between the theoretical and PHYSAT spectral anomalies for the different groups. A project based on automatic in situ measurements approaches on board ferry-box is proposed. We will show also how our recent work opens doors for improving phytoplankton groups' detection when coupled with in situ expertise. For example, the definition of the validity ranges for each group based on their optical properties in order to avoid misclassification. This also opens new potential development by considering phytoplankton groups and composition and their environmental conditions together.

Satellite-derived ocean primary production inferred by an optimality-based phytoplankton model

Lionel Arteaga, Markus Pahlow and Andreas Oschlies

GEOMAR | Helmholtz Centre for Ocean Research Kiel
Email: larteaga@geomar.de

Summary

Optimality-based models of phytoplankton growth offer the potential to help understand the interrelations between phytoplankton stoichiometry and primary production in the ocean. Here we apply an optimality-based model to analyze remote-sensing and in-situ data in order to infer seasonally varying patterns of growth colimitation by light, nitrogen, and phosphorus in the global ocean. Based on these results, we seek to estimate global marine primary production, derived from satellite estimations of nutrient (nitrogen) and light, using a model that accounts for acclimation of the chlorophyll to carbon ratio (Chl:C). One of the aims of this study is to investigate to what extent having a flexible Chl:C ratio alters primary production estimations with respect to more traditional ocean color derived algorithms.

Introduction

Our current understanding of the physical and biogeochemical controls on marine biological production does not allow to accurately describe its future evolution under changing climate and environmental conditions. To better assess how primary production and phytoplankton growth may change in the future, it is essential to know what limits production under present circumstances. While limitation by a single resource is possible, different flavors of colimitation can occur as well [1]. Which combination of factors limits growth may control both magnitude and sign of the response of the ecosystem to CO_2-driven global changes such as warming-induced stratification.

Here we use the optimality-based chain model [3] as a mechanistic foundation for the physiological regulation of nutrient acquisition and light harvesting to diagnose N, P, and light limitation, based on field and satellite data of nutrients, light, and temperature in the surface ocean. Based on these results, we also use the model to estimate global marine primary productivity.

Results and Discussion

Our model-based results indicate nitrogen and light as the main two factors controlling phytoplankton growth in the global ocean. There is essentially no ocean region with dominant phosphorus limitation. While our current version of the model does not include iron, we believe that acounting for this nutrient will accentuate light limitation

in well known iron limited areas such as the Southern Ocean.

As nitrogen is identified as the major limiting nutrient, we use a multiple linear model to estimate nitrate concentrations in the surface ocean, from satellite data of sea surface temperature, mixed layer depth, and chlorophyll. Photosynthetically active radiation is represented by the "Median Mixed Layer Light Level" [I_g, 4]. I_g approximates the average light intensity experienced by phytoplankton in the surface mixed layer.

So far our carbon-based primary production estimates are higher than those obtained by more traditional ocean color models [e.g. 5]. Our next step is to analyze differences in marine productivity resulting from the physiological acclimation of phytoplankton to different seasonal nutrient and light limitation regimes.

This work is a contribution of the Seventh Framework Programme (FP7) - project "Ocean Strategic Services beyond 2015" (www.oss2015.eu).

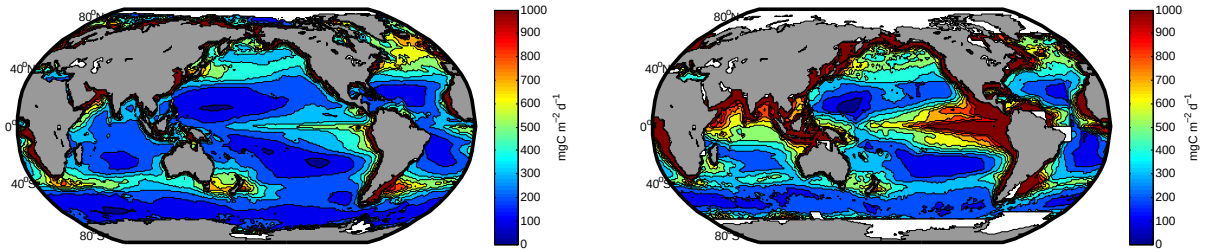

Figure 1: Global marine primary production derived from satellites. Left: Vertical Generalized Production Model (VPGM) [5]. Right: Combined satellite and optimality-based model.

References

[1] Saito, M. A., Goepfert, T. J. & Ritt, J. J. Some thoughts on the concept of colimitation: Three definitions and the importance of bioavailability. *Limnol. Oceanogr.* **53**, 276–290 (2008).

[2] Riebesell, U., Kötzinger, A. & Oschlies, A. Sensitivities of marine carbon fluxes to ocean change. *Proc. Nat. Acad. Sci. USA.* **106**, 20602–20609 (2009).

[3] Pahlow, M. & Oschlies, A. Chain model of phytoplankton P, N and light colimitation. *Mar. Ecol. Prog. Ser.* **376**, 69–83 (2009).

[4] Behrenfeld, M. J., Boss, E., Siegel, D. A. & Shea, D. M. Carbon-based ocean productivity and phytoplankton physiology from space. *Global Biogeochem. Cycles* **19**, GB1006 (2005). Doi:10.1029/2004GB002299.

[5] Behrenfeld, M. J. & Falkowski, P. G. Photosynthetic rates derived from satellite-based chlorophyll concentration. *Limnol. Oceanogr.* **42**, 1–20 (1997).

Overview on algorithms to derive phytoplankton community structure from satellite ocean colour

Astrid Bracher[1], Nick Hardman-Mountford[2]

[1]PHYTOOPTICS Group at the University of Bremen and Alfred Wegener Institute for Polar and Marine Research (AWI), Bussestraße 24, 27570 Bremerhaven, Germany
[2]CSIRO Centre for Environment and Life Sciences, Underwood Avenue, Floreat, Perth, WA 6014, Australia
Email: Astrid.Bracher@awi.de

Summary

Different bio-optical and ecological methods have been established that use ocean color data to identify and differentiate between phytoplankton functional types (PFTs) or phytoplankton size classes (PSCs) in the surface ocean. These can be summarized into four main types: spectral-response methods which are based on differences in the shape of the light reflectance/absorption spectrum for different PFTs/PSCs, methods which use information on the magnitude of chlorophyll biomass or light absorption to distinguish between PFTs or PSCs, methods that retrieve the particle size distribution from satellite-derived backscattering signal and derive PSCs, and ecological-based approaches which use information on environmental factors. Within this presentation we will give an overview over the presently available algorithms. Based on the input we get from the algorithm developers we will try within the short time to present for each product its spatial and temporal coverage, (potential) applications, uncertainties, benefits and short comings.

Ocean colour products from hyper-spectral satellite data of SCIAMACHY using the PhytoDOAS method and the radiative transfer model SCIARAN

Astrid Bracher[1], T. Dinter[1], A. Sadeghi[1], M. Altenburg Soppa[1], B. Taylor[1], J.P. Burrows[2], V. Rozanov[2]
[1]PHYTOOPTICS Group at the Institute of Environmental Physics, University of Bremen and the Alfred Wegener Institute for Polar and Marine Research, Bussestraße 24, 27570 Bremerhaven, Germany
[2]Physics and Chemistry of the Atmosphere, Institute of Environmental Physics, University of Bremen, Otto Hahn Allee 1, 28359 Bremen, Germany
Email: Astrid.Bracher@awi.de

Summary

Quantitative distributions of major functional PFTs of the world ocean improve the understanding of the role of marine phytoplankton in the global marine ecosystem and biogeochemical cycles. Information on the attenuation and light penetration depth tells us the extend of phytoplankton primary production and until which depth satellite obtain information on ocean colour.

In this study, global ocean color satellite products of different dominant phytoplankton functional types' (PFTs') biomass and the vibrational Raman scattering (VRS, i.e. the inelastic light scattering at water molecules, for different wavelength ranges retrieved from hyperspectral satellite data of the satellite sensor SCIAMACHY (SCanning Imaging absorption spectrometer for Atmospheric ChartographY on board ENVISAT, operating 2002-2012) using Differential Optical Absorption Spectroscopy applied to phytoplankton (PhytoDOAS) are presented (see also Vountas et al. 2007, Bracher et al. 2009, Sadeghi et al. 2012a).

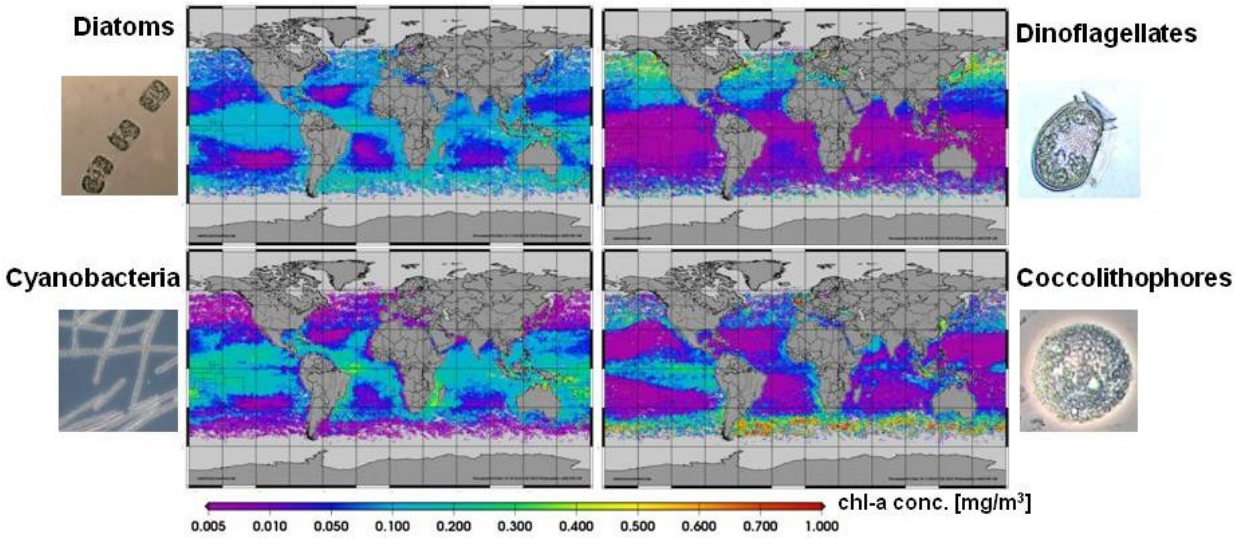

Figure 1 Mean chl-a conc. in March 2007 of different phytoplankton groups derived with PhytoDOAS from SCIAMACHY data. Representative photographs for each group from S. Kranz and S. Wiegmann (AWI).

PhytoDOAS allows the determination of biomass of the four different phytoplankton groups (Sadeghi et al. 2012a, Fig. 1) analytically and independent from a priori information using high spectrally resolved satellite data from SCIAMACHY. The method is an extension of the Differential Optical Absorption Spectroscopy (DOAS by Platt 1974), used for satellite retrievals of trace gas columns (Burrows et al. 1999). In addition to atmospheric compounds, PhytoDOAS also accounts for the differential absorption of water and its constituents.

VRS has been retrieved following the approach of Vountas et al. (2007) but now the radiative transfer model SCIATRAN (Rozanov et al. 2005) now fully coupled for atmospheric and oceanic transfer (Blum et al. 2012) was used to model the pseudo-absorption spectra to be used in PhytoDOAS which account for the differential spectral effect of filling-in of Fraunhofer lines. The radiative transfer calculation were used to calculate inelastic scattering at the whole UV-VIS wavelength range and different wavelength ranges (UV-a, blue) were identified where due to strong differential VRS structures the inelastic scattering effect could be used to retrieve its signature in satellite data. In addition radiative transfer calculations were used to calculate the dependence of VRS at different wavelength ranges to the light penetration depth and attenuation coefficient. By this a UV and blue attenuation coefficient data product is developed with a retrieval which is not influenced by interfering effects of phytoplankton, other particle or CDOM absorption and scattering. As for the PhytoDOAS PFT products, this hyperspectral ocean color products are retrieved analytically, simultaneously with atmospheric components from level-1 (top of atmosphere) SCIAMACHY radiances. The retrieval is less dependent on a-priori assumptions and empirical relationships than multispectral ocean color products. Comparisons of these hyperspectral data to ocean color products from multispectral sensors and application of the hyperspectral data set in studying phytoplankton dynamics are shown (Sadeghi et al. 2012b). Although current hyperspectral sensors have poor spatial resolution (>30 km x 30 km), they are useful for the verification and improvement of the high spatially resolved multi-spectral ocean color products. Future applications of PhytoDOAS retrieval to other hyperspectral sensors and its synergistic use with information gained from multispectral ocean color sensors are proposed.

References

1. Blum M., Rozanov V., Burrows, J. P., Bracher A. (2012) Coupled ocean-atmosphere radiative transfer model in framework of software package SCIATRAN: Selected comparisons to model and satellite data. Advances in Space Research 49(12): 1728-1742

2. Bracher A., Vountas M., Dinter T., Burrows J.P., Röttgers R., Peeken I. (2009) Quantitative observation of cyanobacteria and diatoms from space using PhytoDOAS on SCIAMACHY data. Biogeosciences 6: 751-764

3. Rozanov V.V. Buchwitz M., Eichmann K.-U., de Beek R., Burrows J.P. (2002) SCIATRAN – a new radiative transfer model for geophysical application in the 240-2400 nm region: the pseudo-spherical version. Advances in Space Research 29(12): 1831-1835

4. Sadeghi A., Dinter T., Vountas M., Taylor B., Altenburg Soppa M., Bracher A. (2012) Remote sensing of coccolithophore blooms in selected oceanic regions using the PhytoDOAS method applied to hyper-spectral satellite data. Biogeosciences 9: 2127-2143

5. Sadeghi A., Dinter T., Vountas M., Taylor B., Peeken I., Altenburg Soppa M., Bracher A. (in press) Improvements to the PhytoDOAS method for identification of coccolithophores using hyper-spectral satellite data. Ocean Sciences 8: 1055-1070

6. Vountas M., Dinter T., Bracher A., Burrows J.P., Sierk B. (2007) Spectral Studies of Ocean Water with Space-borne Sensor SCIAMACHY using Differential Optical Absorption Spectroscopy (DOAS). Ocean Science 3: 429-440

Using the near pixels of ocean colour images to perform the atmospheric correction over turbid waters.

J. Brajard[1], C. Jamet[2]
[1]UPMC, LOCEAN/IPSL, Paris, France
[2]ULCO, LOG, Wimereux, France
Email: julien.brajard@locean-ipsl.upmc.fr

Summary

A new approach is proposed to perform atmospheric correction over turbid water. This approach makes no assumption on the water-leaving reflectance spectrum in the near-infrared and uses the spatial context of the pixel. It was applied to MERIS image in the Adriatic Sea.

Introduction

Ocean colour sensors measure the solar flux reflected by the ocean and the atmosphere. In order to estimate the oceanic component, a critical step in the processing of the top-of-atmosphere (TOA) measurements is the so-called atmospheric correction. This involves the removal of the atmospheric signal in order to deduce the contribution of the ocean only.

Following Gordon (1997), we consider (out of the glitter region and neglecting the whitecaps influence):

$$\rho_{toa}(\lambda) = \rho_{path}(\lambda) + t(\lambda)\cdot \rho_w(\lambda) \quad (1)$$

where ρ_{toa} is the total reflectance derived from the satellite measurement ρ_{path} is the atmospheric reflectance (accounting for the scattering and absorption of aerosol and molecules) , t is the diffuse transmittance, ρ_w is the water-leaving reflectance and λ is the wavelength of the measurement.

For most of the non-turbid waters, the atmospheric correction is named "clear water process" hereinafter. We can assume that ρ_w is negligible in the near-infrared part of the signal (λ>700nm). Making this assumption, it is possible to derive the aerosol model from the near-infrared part of the signal. Then the atmospheric contribution ρ_{path} and t can be estimated for the whole spectrum. It is then easy to deduce the water leaving reflectance in visible part of the spectrum applying Eq.1 for which the only unknown term is ρ_w.

Over turbid waters, though, the variability of ocean content (presence of substances other than phytoplankton) induces a signal in the near-infrared part of the signal that can cause errors during the atmospheric correction process. Several solutions were applied to solve this problem (Moore et al. IJRS 1999, Chomko and Gordon AO 2001, Stumpf et al. NASA tech 2003, Stamnes et al. AO 2003, Bailey et al. IJRS 2010, Schroeder et al. IJRS 2007, Brajard et al. RSE 2012). In any case, it is necessary to make a-priori hypothesis on the water-leaving reflectance spectrum in the near-infrared which reduce the generality of the approach. Another family of algorithms proposes to use spatial information of the ocean colour image (Ruddick et al. 2000[1]). The assumption here is that aerosol properties are spatially homogenous on a region of 10km to 100km (Hu et al. 2000[2]). This last approach reduces the number of assumptions to be made on the near-infrared part of the water-leaving reflectance spectrum. The present work addresses this method and proposes to generalize the algorithm making no hypotheses on the turbid water-leaving reflectance spectrum.

Method

The algorithm proposed here can be considered as a generalization of the approach proposed by Hu et al. 2000. In this work, the spatial neighbourhood is used to determine both the aerosol type and optical thickness. An objective spatial interpolation was performed to take into account the spatial correlations. Here are the steps of the algorithm:

1) Classification of the image pixels: turbid or clear water

2) Application of the clear-water process and estimation ,for each clear-water pixel, of the aerosol optical thickness τ and the Angtröm exponent α linked to the aerosol model.
3) For each turbid pixel, τ and α are estimated with the following equation:

$$x_0 = \sum_{i \in V} \lambda_i \cdot x_i \qquad (2)$$

where *x* stands for τ or α, the index 0 designs the turbid pixel, *V* is the ensemble of the 10 clear-water pixels that are the nearest (in the sense of the geographic distance) from the pixel x_0, λ_i are weighted coefficient that decreases with the distance (the furthest a pixel is , the less it is correlated to the turbid pixel).
4) Using τ_0, α_0 determined previously, assuming a Junge size distribution and non-absorbing aerosols, ρ_{path} and *t* are computed at all wavelengths using artificial neural networks (Brajard et al. NN, 2006).
5) The water-leaving reflectance is deduced using Eq. 1.

First result

The algorithm is applied on MERIS image, June 2, 2009 in the north of the Adriatic Sea. The figure 1 presents a comparison between the standard MERIS processing and the modified product using the algorithm described here for the Angström exponent and the water-leaving reflectance at 490nm. The MERIS flags CASE2_S, CASE2_ANOM and CASE2_Y were used to determine turbid waters. For each turbid pixel, the 10 nearest pixels were considered. It can be noticed that the standard Angström exponent is strongly related to the turbidity of the water, which is likely an artefact of the atmospheric correction process. It can be seen, that it is not the case for the new algorithm proposed here (it is particularly visible off the north coast). Even if the new algorithm seems to presents some bias for strong aerosol optical thickness (not shown here), the water-leaving reflectance presents some realistic values and pattern that are to be validated using in-situ data (e.g. Helgoland site P.I. R. Doerffer). It validates the assumption that it is possible to use spatial information to perform atmospheric correction over turbid waters.

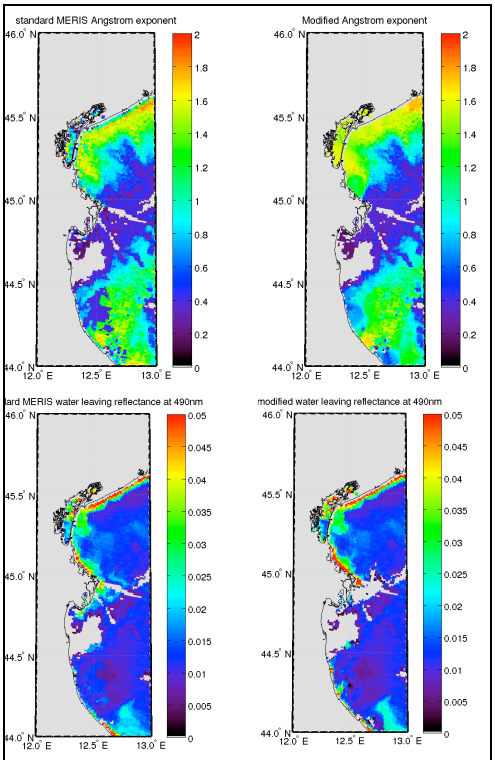

Figure 1. Standard MERIS products (left) compared to the new algorithm products (right) for α (up) and ρ_w(490nm) (bottom).

Conclusion

The method proposes here is a first step to explore the possibilities of using image information to solve inverse problems for ocean colour data. The use of interpolations techniques could give objective criteria to quantify uncertainty of the result. The approach proposed here makes the maximal assumption that the signal over turbid waters cannot be used at all to estimate the aerosol contribution. This simplification was made in order to evaluate the effects of this algorithm only. In the future, it is likely that accurate results can be obtained using a mixed approach using both the neighbouring pixels and the signal over turbid waters.

Principal references

[1] Ruddick, K., Ovidio, F., Rijkeboer, M. (2000). Atmospheric correction of SeaWiFS imagery for trbid coastal and inland waters, App. Opt., 39 (6), 897-912.

[2] Hu C.M., Carder K.L., Muller-Karger F.E. (2000), Atmospheric correction of SeaWiFS imagery over turbid coastal waters: A practical method. Remote Sens. Environ. 74: (2) 195-206.

Diatoms blooms detected by remote sensing

N.M. Bucair[1], P.B. Oliveira[2], J. Dubert[1], A. Silva[2], B. Domingues[2], M.T. Moita[2], R. Nolasco[1]

[1] University of Aveiro, Department of Physics, Aveiro, 3810-193, Portugal
[2] IPMA, Av. Brasilia, Lisboa, 1449-006, Portugal
Email: nayarabucair@ua.pt

Summary

Diatom blooms are recurrent along the Portuguese coast during summer in response to the prevailing upwelling conditions. Preexistent algorithms to differentiate this group from other phytoplankton communities were used and adapted for the study area. Normalized water-leaving radiance (nLw) was analyzed to distinguish the specific diatoms group for the particular conditions of the region. The satellite data were compared with in situ data, obtained from an oceanographic cruise carried out in summer 2011. An empiric approach demonstrates that diatoms correspond to high reflectance on the wavelength of 412nm.

Introduction

Early satellite ocean color missions were designed to provide synoptic chlorophyll a (Chl.a) concentration fields. Currently, the foremost application is to monitor the response of the marine ecosystem to climate change. This has been mainly accomplished by the ability to trace changes in the spatial and temporal distribution of the phytoplankton concentration. In addition to its contribution to the ocean's primary production, marine phytoplankton takes part of important biogeochemical cycles. Some species incorporate nitrogen as feedstock, as the cyanobacteria's group, while others as coccolithophores are responsible to capture calcium carbonate from the system to build their calcite plates. Another representative group are the diatoms, that contribute to about 40% of the total marine primary production. This group is usually found in nutrient-rich waters, dominating the phytoplankton assemblages during the spring blooms in temperate and Polar regions [1]. Both diatoms and coccolithophores have high sinking rates contributing to the carbon export into the deep ocean [2].

Previous studies show that summer oceanographic conditions along the west Portuguese coast are influenced by coastal upwelling driven by persistent equatorward winds [3], providing the necessary conditions for phytoplankton growth [4]. Studies on coastal upwelling ecosystems revealed that diatoms are also the dominating group during the intensification phase of upwelling events [5].

Aiming to detect the occurrence of diatom blooms in the central Portuguese coast, the concept of Plankton Functional Type (PFT) has been adopted. The specific absorption coefficients of phytoplankton cells can vary because of differences in the pigment composition and size structure of phytoplankton populations [6]. As chl.a are present in almost all marine phytoplankton, the discrimination of PFT must be performed analyzing accessories pigments (biomarkers)[7].

Discussion

Diatom populations are known to be related to high chl.a concentration [7]. Their signature is readily observed on the images obtained during the 2011 summer cruise off the NW Portuguese coast, using a

range of Chl.a between 0.04 and 3.0 mg m^{-3}. The use of this range allows to focus the analysis on areas out of both the influence of oceanic oligotrophic and continental sediment dominated waters (figure 1).

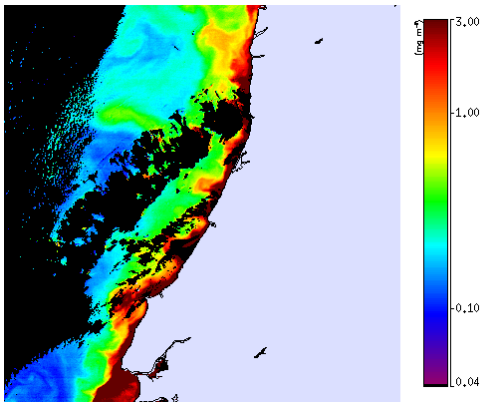

Figure 1: Chlorophyll a concentration

The higher Chl.a concentrations detected on the satellite data are comparable with in situ diatom distribution.

Water dominated by diatoms is associated with the highest backscattering, and exhibit much lower absorption coefficient than other phytoplankton populations [6]. Being in some cases, detectable at short wavelength (412 and 443 nm) however, the absorption by the yellow substance is a potential error source because it may influence nLw values on this spectral range.

Conclusions

Using adequate algorithms, it is possible to associate same parameters to distinguish diatoms from the other marine phytoplankton groups, mainly due to the high nLw at short wavelengths, such as Rrs 412. The results suggest that an empirical approach may be used to discriminate diatoms blooms using remote sensing off the Portuguese coast.

References

[1] Sarthou, G., Timmermans, K.R., Blain, S., Tréguer, P. (2005). Growth physiology and fate of diatoms in the ocean: a review. J Sea Res, 53: 25–42.

[2] Nair, A., Sathyendranath, S., Platt, T., Morales, J., Stuart, V., Forget, M-H., Devred, E., Bouman, H.(2009). Remote sensing of phytoplankton functional types. Remote Sens Environ, 112: 3366–75.

[3] Oliveira, P.B., Nolasco, R., Dubert, J., Moita, T., Peliz, Á. (2009). Surface temperature, chlorophyll and advection patterns during a summer upwelling event off central Portugal. Cont Shelf Res, 29: 759–74.

[4] Largier, J.L., Lawrence, C.A., Roughan, M., Kaplan, D.M., Dever, E.P., Dorman, C.E., et al. (2006). WEST: A northern California study of the role of wind-driven transport in the productivity of coastal plankton communities. Deep-Sea Res II, 53: 2833–49.

[5] Oliveira, P.B., Moita, T., Silva, A., Monteiro, I.T., Sofia, P. A. (2009). Summer diatom and dinoflagellate blooms in Lisbon Bay from 2002 to 2005: Pre-conditions inferred from wind and satellite data. Prog Oceanogr, 83: 270–7.

[6] Sathyendranath, S., Watts, L., Devred, E., Platt, T., Caverhill, C., Maass, H. (2004). Discrimination of diatoms from other phytoplankton using ocean-colour data. Mar Eco Prog Ser, 272: 59–68.

[7] Alvain, S., Moulin, C., Dandonneau, Y., Bréon, F.M. (2004). Remote sensing of phytoplankton groups in case 1 waters from global SeaWiFS imagery. Deep-Sea Res I, 52: 1989–2004.

Multi-sensor, ecosystem-based approaches for estimation of Particulate Organic Carbon

I. Cetinić[1], M.J. Perry[1], N. Poulton[2], W.H. Slade[3]

[1]University of Maine, School of Marine Sciences and
Ira C. Darling Marine Center, Walpole ME 04573-3307, USA
[2]Bigelow Laboratory for Ocean Sciences, East Boothbay, ME 04544, USA
[3]Sequoia Scientific, Inc., Bellevue, WA 98005, USA
Email: icetinic@gmail.com

Summary

Uncertainties in remote-sensing retrieval of the particulate organic carbon concentration in the ocean can be attributed in part to differences in methodology among researchers and in part to inherent variability in the nature of oceanic particles themselves and the relationships between these particles and their optical properties. Here we present a novel approach that could lead to a better understanding of the underlying mechanisms that govern the variability of particulate organic carbon optical relationships. By using new and improved *in-situ* optical methodologies, we aim to develop a new multi-sensor, ecosystem-based remote sensing algorithm for assessing particulate organic carbon.

Introduction

Particulate organic carbon (POC) in the surface ocean is a major, dynamic carbon reservoir, and through the biological pump, provides a means for the transfer and potential storage of atmospheric CO_2 into the deep ocean. Total POC, as well as the phytoplankton fraction, is of great interest in biogeochemical studies, in part because of the potential changes in the biological pump due to climatic impacts. However, the variability of POC both regionally and globally is poorly understood due to a lack of direct measurements at sufficient spatial and temporal scales. The availability of high-resolution optical measurements from ocean color remote sensing and *in-situ* optical instrumentation has stimulated interest in the development of optical POC proxies that allow quantification of POC on temporal and spatial scales that surpass traditional, discrete water sampling methods. Current POC algorithms are based on both particulate beam attenuation and particulate backscattering coefficients (e.g., Fig. 1), but both display great variability as a function of geographical regime and/or investigator, leading us to ask the following questions:

1. What are the mechanisms responsible for the observed variability in optical proxy algorithms? Is the variability natural (inherent to the specific ecosystem or regime) or due to methodology (both chemically-measured and optical proxy POC)?

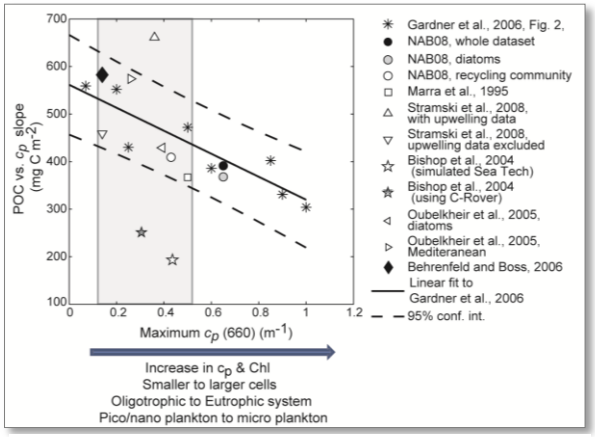

Figure 1. *POC vs. c_p slope as a function of maximum c_p observed for each data set from [1]. The regression includes eight data sets summarized by [2] (r^2=0.82). Most of the literature values fall within the 95% confidence interval (dashed line). Gray shaded area depicts the oceanic c_p threshold range (from the ACE/PACE white paper appendix).*

2. If the variability is natural, what are the drivers of the observed variability? We hypothesize that part of the variability in the optical proxy algorithms is related to differences in phytoplankton taxa and community composition, composition of non-phytoplankton particles, and ecosystem function (i.e., recycling community or not).
3. Can we build better proxies by taking these differences, as well as other environmental parameters that can be remotely sensed, into consideration?

Discussion

We are entering an era (*or we are already there?*) when most estimates of POC are derived using optical proxies (both *in-situ* and remotely sensed). These estimates of POC have been - and will continue to be used - to derive carbon budgets and ecosystem predictions, with potential impacts on environmental public policy and decision-making. Hence, it is an imperative to improve the understanding of POC optical proxy algorithms by evaluating all aspects of variability for POC and optical measurements, and by assessing uncertainties in the proxy-derived POC concentrations.

In order to address these issues, the "Multi-sensor, ecosystem-based approaches for estimation of particulate organic carbon" project goals are to:

- Conduct an intensive field program (taking advantage of ship time and space provided by collaborators) that will allow us to collect data on hydrography, inherent optical properties (including polarized angular scattering), POC, suspended particulate matter (SPM), particle size distribution (PSD), HPLC pigments, and plankton size and carbon biomass from a dynamic range of ecosystem types.
- Use best-practice POC and other biogeochemical parameter sampling and analysis protocols and use carefully calibrated (and inter-calibrated) optical instruments to constrain methodological sources of variability in both optical and POC measurements.
- Use this extensive dataset to develop a multi-sensor, ecosystem-based remote sensing algorithm that will improve estimation of the oceanic POC pool, thereby allowing new insights into the dynamics of POC, as well as SPM and phytoplankton carbon biomass, in the surface ocean.
- Evaluate the applicability of newly available remote sensing products such as Sea Surface Salinity (Aquarius/NASA) and polarized scattering measurements (PARASOL/CNES, future PACE and ACE/NASA) to improve retrieval of POC, and reduce uncertainty in its estimation.

References

[1] I. Cetinić, M. J. Perry, N. T. Briggs, E. Kallin, E. A. D'Asaro, and Lee, C. M. (2012). Particulate organic carbon and inherent optical properties during 2008 North Atlantic Bloom Experiment. J. Geophys. Res. 117, C06028.
[2] W. D. Gardner, A. Mishonov, and Richardson, M. J. (2006). Global POC concentrations from in-situ and satellite data**.** Deep-Sea Res. (Part II: Top. Stud. Oceanogr.) 53, 718-740.

Bio-optical properties of the northern Gulf of Mexico: Ship based and satellite observations

Sumit Chakraborty [1] and Steven. E. Lohrenz[1]

University of Massachusetts Dartmouth
School of Marine Science and Technology
New Bedford-02744, Massachusetts, U.S.A
Email: schakrabortyl@umassd.edu

Summary

This study examines the seasonal and regional variability in the spectral absorption coefficients of phytoplankton (a_ϕ), non-algal particles (aNAP) and colored dissolved organic matters (aCDOM) in the northern Gulf of Mexico (NGOM) using data collected during eight research cruises from 2008 to 2010 and quasi analytical algorithm (QAA) derived MODIS (Moderate resolution Imaging Spectroradiometer) data. Significant differences in bio-optical properties were observed. Seasonal fluctuations in river discharge, wind fields, wind driven transport and mixing processes explained majority of the observed variability. Comparisons between log- transformed in-situ a_{dg} (λ) (aNAP+ aCDOM) data and log-transformed QAA derived a_{dg} (λ) showed reasonable agreement with r^2 values between 0.82-0.99 while QAA retrievals for a_ϕ (λ) were characterized by slightly lower r^2 values of 0.6-0.7

Introduction

Application of remote sensing algorithms in coastal waters are particularly challenging because of their optically complexity. The NGOM influenced by Mississippi (MS) and Atchafalaya (ATF) rivers provide a clear example of a system largely dominated by Case 2 waters [1]. The main goal of this study was to be describe the variability of the bio-optical properties in the region using both in-situ and satellite derived data and to test the potential of the Quasi Analytical Algorithm [2] for the retrieval of absorption by phytoplankton, non-algal particles and colored dissolved matter.

Results and Discusssion

In general QAA was able to capture the spatio-temporal gradients but over-estimated at the inner-shelf regions and underestimated at the estuarine and offshore waters (Fig. 1). The results obtained for QAA_a_{dg} (low bias: ranged ± 0.04 -0.08) were better than QAA_a_ϕ. Uncertainty estimates for QAA_a_{dg} was better at all wavelength. (Table not shown). QAA_ a_ϕ retrievals were particularly poor at shorter wavelengths.

Factors that affected the a_ϕ (λ) estimates include variations related to phytoplankton pigmentation and package effects [3]. Large variability in pigment composition in the region might account for some of the variability in the relationship between satellite-derived and in situ observations. Retrieval of R_{rs} at short wavelengths is particularly challenging in coastal waters given the high light attenuation and uncertainties in atmospheric corrections particularly at shorter wavelengths [4] Cloud cover and solar glint are additional factors that affects the accuracy of the satellite-derived R_{rs} estimates and associated QAA retrievals. Finally, small scale spatial heterogeneity in distributions as well as rapidly

changing conditions over the time window for matchups (± 24hrs) may have contributed to observed differences between the QAA-derived products and in-situ observations.

Besides choice of spectral slope value of a_{dg} can influence the performance of the QAA. Spectral slopes of CDOM (S_{CDOM}) and NAP (S_{NAP})are known to vary widely in continental margins [5]. The S_{CDOM} values determined during this study ranged from 0.01-0.022 nm^{-1}, while S_{NAP} ranged from 0.005 -0.02 nm^{-1}. The QAA uses a standard spectral slope of 0.015 nm^{-1} for S_{dg}. Ideally in-situ S_{dg} values should be used as it is difficult to accurately determine just from R_{rs} values [4]. Since $a_{\phi}(\lambda)$ is calculated by subtraction of $a_{dg}(\lambda)$ from a(λ), uncertainty in the spectral slope used in the QAA can be an additional source of error in $a_{\phi}(\lambda)$

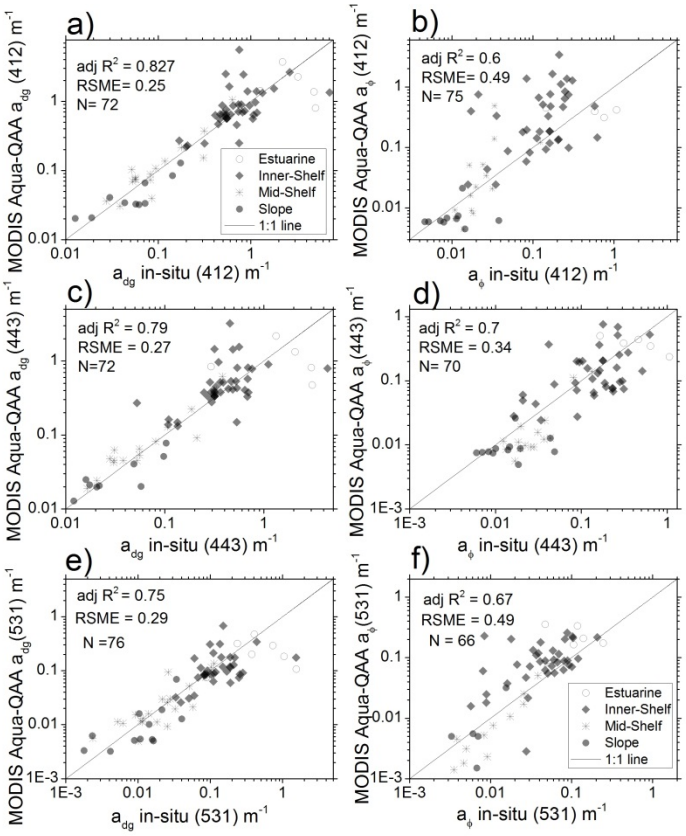

Figure 1.Scatter plot showing the comparison between log-transformed in-situ adg and QAA retrieved adg (MODIS Aqua) at 412 (a), 443 (c), 531 (e) and similarly b,d and f shows the relationship between log-transformed QAA derived aϕ versus in-situ aϕ at 412 (b), 443(d) and 531(f).

Conclusion

The low uncertainty associated with the QAA_a_{dg} values are particularly promising and provides confidence to the quantitative use of satellite derived QAA_a_{dg} maps in NGOM. Repeated validation of QAA with in-situ data and R_{rs} data from multi-platform should be undertaken in future. The use of in-situ R_{rs} to derive QAA products would provide much needed information to further investigate the uncertainty budget in the region and is thus recommended for future assessment of remote sensing algorithms and derived products in NGOM.

R**eferences**

[1] Sathyendranath, S., Remote Sensing of ocean color in coastal and other optically-complex waters in International Ocean-Color Coordination Group (IOCCG) Report 3 (2000), S. Sathyendranath, Editor 2000: Dartmouth, Nova Scotia, Canada. p. 140.

[2.] Lee, Z., K.L. Carder, and R.A. Arnone, Deriving inherent optical properties from water color: A multiband quasi-analytical algorithm for optically deep waters. Applied Optics, 2002. **41**(27): p. 5755-5772.

[3] Bricaud, A, et.al. Natural variability of phytoplanktonic absorption in oceanic waters: Influence of the size structure of algal populations. J. Geophys. Res., 2004. **109**(C11): p. C11010.

[4] Lee, Z. and K.L. Carder, Absorption spectrum of phytoplankton pigments derived from hyperspectral remote-sensing reflectance. Remote Sensing of Environment, 2004. **89**(3): p. 361-368.

[5] Kirk, J.T.O., Light and photosynthesis in Aquatic Ecosystems. (1994). Cambridge, UK: Cambridge University Press.

A dataset of global in situ observations for the development and comparison of Phytoplankton Functional Type (PFT) algorithms.

Clementson, L.A.[1], Hardman-Mountford, N.[2], Hirata, T.[3], Barlow, R.[4], Hirawake, T.[3], Brewin, R.[5], Bracher, A.[6]

[1] CSIRO Marine and Atmospheric Research, Hobart, Tasmania, Australia

[2] CSIRO Marine and Atmospheric Research, Floreat, WA, Australia

[3] Hokkaido University, Sapporo, Japan

[4] Bayworld Centre Research and Education, Cape Town, South Africa

[5] Plymouth Marine Laboratory, Plymouth, UK

[6] PHYTOOPTICS Group, Alfred-Wegener Institute Helmholtz Center for Polar and Marine Research and Institute of Environmental Physics at University of Bremen, Germany

Email: lesley.clementson@csiro.au

Summary

The International Working Group for PFT Algorithm Development aims to establish an in situ dataset specifically for the calibration and validation of PFT algorithms. The dataset will include multiple coincident parameters such as HPLC pigments (including size fractionated pigments where available), flow cytometry, microscopic cell counts, particle size and in-water optical measurements from both the northern and southern hemispheres. It is envisaged that the first version of this dataset will be publically available in 2014.

Introduction

Since the launch of SeaWiFS, in 1997, satellite-retrieved estimates of chlorophyll-a (chl-a) have been used as a proxy for phytoplankton biomass. The unprecedented spatial and temporal coverage of satellite-generated products, such as chl-a, has enhanced our knowledge of trends in productivity and extended our understanding of biogeochemical processes, on both regional and global scales. However in recent years researchers have required greater detail about the phytoplankton community composition responsible for the productivity and whether the phytoplankton community consisted of taxonomic groups with specific functions, such as silicification, calcification and nitrogen fixation. Phytoplankton with these functions have been termed Phytoplankton Functional Types (PFTs) and in response to the requirement for greater detail about the phytoplankton community composition, PFT algorithms have been developed. Some of the algorithms generate estimates of phytoplankton composition by determining size structure while others estimate taxonomic groupings. At present it is difficult to compare the outputs of PFT algorithms as each algorithm has used an individual input dataset.

It is the intention of the International Working Group for PFT Algorithm Development to establish an in situ dataset specifically for the calibration and validation of PFT algorithms. The dataset will include

multiple coincident parameters such as HPLC pigments (including size fractionated pigments where available), flow cytometry, microscopic cell counts, particle size and in-water optical measurements from both the northern and southern hemispheres. The availability of the dataset will allow better comparison of the outputs from different PFT algorithms and also allow validation of the algorithms over different regions. The Working Group acknowledge that databases and datasets such as SeaBASS and NOMAD (NASA) already exist, but believe that the PFT dataset with the added phytoplankton-specific parameters will only enhance the information available to researchers.

Discussion

Collection of in situ data from various investigators is underway, building on existing datasets (e.g. Hirata et al. 2011) and it is envisaged that by May 2013 the PFT dataset will contain substantial data from the southern hemisphere. This data will come from the Australian, South African, New Zealand and Southern Ocean regions. By mid-year, data from the northern hemisphere will be added to the dataset.

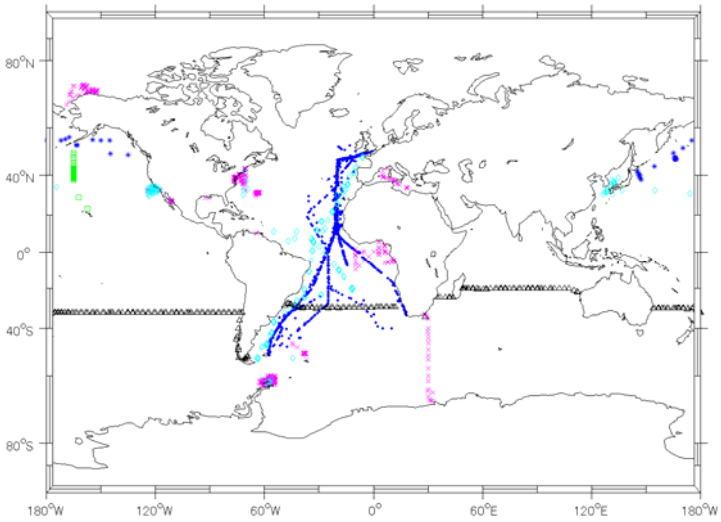

Fig. 1. In situ data used for the development of a global PFT algorithm by Hirata et al. (2011).

Acknowledgements

The authors Clementson and Hardman-Mountford acknowledge funding to assist this work from the EOI-TCP for the AEsOP project.

References

Hirata, T., Hardman-Mountford, N.J., Brewin, R.J.W., Aiken, J., Barlow, R. (2011). Synoptic relationships quantified between surface Chlorophyll-a and diagnostic pigments specific to phytoplankton functional types. *Biogeosciences* **8**: 311-327

MODIS atmospheric correction and chlorophyll products in the Strait of Georgia, British Columbia, Canada.

M. Costa[1], T. Carswell[1], E. Young[1], N. Komick[2], L. Zhai[3]
[1]University of Victoria, Department of Geography, Victoria, BC, Canada
[2]Department of Fisheries and Ocean, Pacific Biologic Station, Nanaimo, BC, Canada
[3]Bedford Institute of Oceanography, Halifax, NS, Canada
Email:maycira@uvic.ca

Summary

MODIS derived aerosol optical depth (AOD) and chlorophyll (Chl) and were compared with in situ AERONET and extracted chlorophyll, respectively, and weekly binned for deriding bloom metrics for the Strait of Georgia (SOG), an optically complex estuarine environment on the West Coast of Canada. A total of 101 images were considered in the evaluation of the atmospheric strategies: (1) the management unit of the North Sea mathematical models (MUMM) with SWIR band, (2) the fixed Angstrom coefficient derived from AERONET, and (3) the standard NIR approach. In the next step, the sensor derived chlorophyll estimates were determined using the OC3M model and compared with extracted chlorophyll acquired within 24 hrs, 6hrs, and 2 hrs on imagery acquisition. The results showed indicated that the MUMM+SWIR (r^2= 0.6-0.7; average slope ~1.1; $RMSE_{443nm}$= 0.7% and $RMSE_{869nm}$= 0.9% compared with in situ AERONET AOD) and the MUMM+SWIR and OC3M chlorophyll (24hrs: n=42, r^2=0.4, and slope=0.6; 6hrs: n=21, r^2=0.6, and slope=0.9; and 2hrs: n=11, r^2=0.7, and slope=1.1 compared with in situ chlorophyll) resulted in the best estimates of chlorophyll. These products were further weekly binned and bloom metrics derived.

Introduction

Fraser River salmon, specifically sockeye, are one of the most important fisheries for the British Columbia commercial and recreational fishing sectors. However, the stocks have experienced variations of return rates in the past 50 years, and a general decline in the past decade, thus adding several uncertainties in the management of this valuable resource [1]. Return rate variability of Fraser sockeye have been attributed to several factors, including oceanographic variability in the Strait of Georgia (SoG) [2] such as zooplankton availability, which is to a certain extent groups related to the phytoplankton bloom conditions in the SoG [3]. As such, the important role of the spring bloom on the survival of juvenile salmon has been hypothesized [1]. The objective of this work is to define the appropriate method to determine phytoplankton bloom metrics (initiation, amplitude, and duration) in the SoG based on MODIS imagery. The first step is the validation of the atmospheric correction strategy; second step the validation of the estimated chlorophyll model; and third, the binning of imagery and generation of temporal bloom metrics.

Results and Discussion

Image data (level 1a) were accessed from NASA's OceanColor web portal, and processed in SeaDAS (Seawifs Data Analysis System) environment. All available MODIS-Aqua images (n=465, 2007, 2008, and 2012) were processed. In the first step, a total of 101 images were considered in the evaluation of three different atmospheric strategies: (1) the management unit of the North Sea mathematical models (MUMM) with SWIR band, (2) the fixed Angstrom coefficient derived from AERONET, and (3) the standard NIR approach. The results showed significant agreement between in situ AERONET AOD at visible and near-infra red wavelengths and MODIS derived AOD for the different atmospheric

approaches: MUMM+SWIR (r^2= 0.6-0.7; average slope ~1.1; $RMSE_{443nm}$= 0.7% and $RMSE_{869nm}$= 0.9%); fixed Angstrom (r^2= 0.7-0.8; average slope ~1.3; $RMSE_{443nm}$= 1.3% and $RMSE_{869nm}$= 0.8%); and standard NIR (r^2= 0.7-0.8; average slope ~1.1; $RMSE_{443nm}$= 1.2% and $RMSE_{869nm}$= 0.6%).

In the second step, the sensor derived Chl estimates were determined using the OC3M model [4] and compared with extracted chlorophyll acquired within 24 hrs, 6hrs, and 2 hrs on imagery acquisition. The results indicated that the MUMM+SWIR and OC3M Chl resulted in the best estimates when compared with in situ data acquired within 2 hrs of imagery acquisition (24hrs: n=42, r^2=0.4, and slope=0.6; 6hrs: n=21, r^2=0.6, and slope=0.9; and 2hrs: n=11, r^2=0.7, and slope=1.1) compared with the NIR and OC3M approach (24hrs: n=48, r^2=0.12, slope=0.8; 6hrs: n=23; r^2=0.4, and slope=0.9; 2hrs: n=12, r^2=0.6, slope=0.6). There were no images corrected with the fixed Angstrom coefficient coincident with in situ data acquisition, thus highlighting the issue of needing AERONET data to guide the atmospheric correction step.

After the previous evaluation, the MUMN+SWIR and OC3M Chl derived images were spatially binned and finally temporally binned to derive mean 'weekly' Chl concentrations. Mean weekly Chl values were collected for a central region the south SoG. The number of available binned (weekly) images were 20 (2007); 19 (2008); 21 (2012). In order to derive bloom dynamics that help describe underlying physical and biological forcing, a set of objective metrics were derived based on a shifted Gaussian function of time fitted to the time-series of binned weekly imagery mean *chl* concentrations [5]. The earliest timing of initiation (week 6.6 – mid February) was defined in 2008. This is much earlier than 2007 and 2012 years, 12.0 (~end March) and 12.9 (~beginning of April) week, respectively. Further, 2007 and 2012 are also similar in regard to week of maxima observed Chl (~week 15) and maximum observed concentrations (~16.0 mg m^-3). Much lower maximum Chl were determined in 2008 (3.4 mg m^{-3}) but for a long duration (~ 10 weeks). The determined week of initiation of bloom conditions in 2012 was beginning of April. Our methods further defined that the 2012 maximum Chl was approximately 16.0 mg m^{-3} and the bloom last for about 4 weeks. Determining inter-annual relationships between the timing/magnitude/duration of the spring bloom and the residence/condition of juvenile salmon entering from lotic systems may be paramount for ecological based fisheries management. Our approach applied to a 10 years time series of data will help to understand these relationships.

References

[1]Marmorek, D., D. Pickard, A. Hall, K. Bryan, L. Martell, C. Alexander, K. Wieckowski, L. Greig and C. Schwarz. 2011. Fraser River sockeye salmon: data synthesis and cumulative impacts. ESSA Technologies Ltd. Cohen CommissionTech. Rep. 6. 273p. Vancouver, B.C. www.cohencommission.ca.
[2]Thomson, R.E.; Beamish R. R.; Beacham, T.D.; Trudel, M.; Whitfield, P.H.; Hourston, R.A.S. (2012). Anomalous ocean conditions may explain the recent extreme variability in Fraser River sockeye salmon production. *Marine and costal Fisheries: Dynamics, Management, and Ecosystem Sciences*, 4:415-437.
[3]Kleppel,G. (1993). On the diets of calanoid copepods. *Marine Ecology Progress Series*, 99, 183-195.
[4]Komick, N., Costa, M., Gower, J. (2009). Bio-optical algorithm evaluation for MODIS for western Canada coastal waters: an exploratory approach using *in-situ* reflectance. *Remote Sensing of Environment,* 113(4), 794-804.
[5]Zhai, L., Platt, T., Tang, C., Sathyendranath, S., Hernandez Walls, R. (2011). Phytoplankton phenology on the Scotian Shelf. *ICES Journal of Marine Science*, 68(4),781-791.

Statistical Derivation of Inherent Optical Properties and Chlorophyll *a* From an Optically Complex Coastal Site

Susanne E. Craig[1], Jennifer Cannizzaro[2], Chuanmin Hu[2], Chris T. Jones[1], Paul Carlson[3]
[1]Dalhousie University, Dept. of Oceanography, B3H 4R2, Canada; [2]University of South Florida, College of Marine Sciences, FL 33701, USA; [3]Florida Fish & Wildlife Research Institute, FL 33701, USA
Email: susanne.craig@dal.ca

Summary

A statistically based model, trained using regional data, accurately derives chlorophyll *a* concentration and various inherent optical properties (IOPs) from *in situ* measurements of remote sensing reflectance in the waters of Big Bend, FL, USA – an area where conventional approaches often yield poor results due to optical complexity (high CDOM absorption, bottom reflectance) and challenges in achieving atmospheric correction. The approach is also successfully applied to MODIS data, and, despite imperfect atmospheric correction, successfully derives accurate estimates of chlorophyll *a* and IOPs. Results indicate the potential of the approach to derive important biogeochemical parameters from ocean colour under very challenging conditions in this ecologically and commercially important coastal region.

Introduction

Big Bend, Florida, USA is an area of both commercial and ecological importance and is home to several large fisheries, seagrass habitat and popular tourist destinations. Measurement of ocean colour offers a powerful means to achieve such monitoring and can capture synoptic patterns in biological and physical processes at various temporal and spatial scales. However, accurate retrieval of proxies for these processes (e.g. chlorophyll a concentration or backscattering coefficient) from ocean colour is often challenging in this region due to the non co-varying nature of the optically active water constituents and to the difficulty in achieving accurate atmospheric correction. Here we present a region specific, statistical approach[1] for deriving inherent optical properties (IOPs) and chlorophyll *a* concentration from measurements of ocean colour around the Big Bend region of FL, USA. We first show results for an extensive *in situ* dataset, then use the same approach for MODIS measurements of the study area.

The algorithm of Craig *et al.*[1] was used to derive chlorophyll *a* concentration (*Chl a*; mg m^{-3}) and IOPs from *in situ* measurements of remote sensing reflectance ($R_{rs}(\lambda)$; sr^{-1}). This is a statistical approach that uses empirical orthogonal function (EOF) analysis to identify the dominant modes of variance in the shape of $R_{rs}(\lambda)$ spectra and then builds a model based on the relationship of the EOF modes with either *Chl a* or IOPs. The model was trained using a subset (70%) of an extensive *in situ* radiometric and water sample dataset that covered various water types including those dominated by coloured dissolved organic material (CDOM) absorption and those influenced by bottom reflection. The model was then tested on the remaining 30% of the dataset. Following

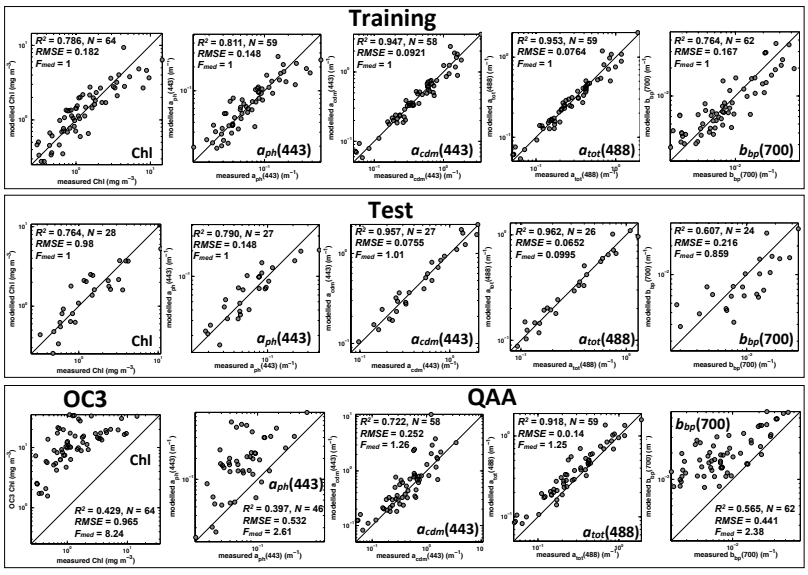

Fig. 1. Training, test and comparison of EOF models. F_{med} is a metric of bias: 1 = no bias, 2 = model overestimates x2, 0.5 = model underestimates x2

implementation of the model on the *in situ* data, the approach was also tested on MODIS imagery of the same region.

Discussion

Training and test results for the model for *Chl a*, phytoplankton absorption at 443 nm ($a_{ph}(443)$; m^{-1}), detrital and CDOM absorption at 443 nm ($a_{cdm}(443)$; m^{-1}), total absorption at 488 nm ($a_{tot}(488)$; m^{-1}) and particulate backscattering at 700 nm ($b_{bp}(700)$; m^{-1}) are shown in Fig. 1, rows 1-2. The models performed very well, especially in deriving absorption coefficients. Many of the spectra were obtained from sites where CDOM absorption comprised up to 80% of total absorption or where $R_{rs}(\lambda)$ spectral shape was significantly modified by bottom reflectance, showing the ability of the EOF approach to accurately detect very small variations in spectral shape that may otherwise be 'swamped' by more dominant signals. Test results showed only a modest decrease in modest skill, suggesting that the model had been adequately trained. For comparison, *Chl a* derived using the OC3 algorithm[2] and IOPs using the quasi-analytical algorithm (QAA)[3] are shown in Fig. 1, row 3. It should be pointed out that the EOF algorithm is trained using regional data, whereas both the OC3 and QAA algorithms are global models. It is not unexpected, therefore, that our model performed better. However, what we present here is the application of a *generic approach* that is computationally inexpensive, straightforward to apply and that can be applied in any instance in which a modestly sized[1] radiometric and corresponding validation dataset is available.

The models derived from the *in situ* data were then applied to MODIS $R_{rs}(\lambda)$ from the same region, but *Chl a* and IOP estimates were poor. Upon comparison of MODIS $R_{rs}(\lambda)$ with match up *in situ* $R_{rs}(\lambda)$, it was evident that inadequate atmospheric correction was likely deforming the spectral shape, meaning that the model coefficients derived from the *in situ* data were not appropriate. It was decided, therefore, to train a new set of models using only MODIS $R_{rs}(\lambda)$ in order to account for the deformation of the spectral shape, especially in the blue. The MODIS dataset was split into 60:40 training:test subsets and the results are shown in Fig. 2. $a_{tot}(488)$ and $a_{cdm}(443)$ are estimated most accurately, and in general, model skill is comparable to the *in situ* models (Fig. 1). Only 33 data points were available for the training and testing procedures, but these initial results are very encouraging and suggest that accurate estimates of biogeochemical parameters in this optically complex site can be derived even under conditions of imperfect atmospheric correction. This is a significant finding, indeed, and underscores the ability of the EOF approach to 'tease out' spectral signatures of optically active water constituents from imperfectly atmospherically corrected satellite data.

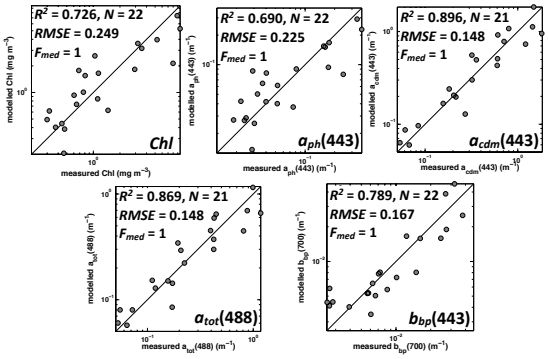

Fig. 2. EOF model results for MODIS data

Conclusions

A statistically based, computationally inexpensive, regional model accurately estimates *Chl a* and various IOPs from both *in situ* and satellite measurements of $R_{rs}(\lambda)$ from very optically complex waters. The model performs very well despite modification of $R_{rs}(\lambda)$ spectral shapes from high CDOM concentration, bottom reflectance and imperfect atmospheric correction, pointing strongly to its potential as a valuable tool in coastal ocean colour applications.

References

1 Craig, S. E. *et al.* Deriving optical metrics of coastal phytoplankton biomass from ocean colour. *Remote Sensing of Environment* **119**, 72-83, doi:10.1016/j.rse.2011.12.007 (2012).

2 O'Reilly, J. E. *et al.* SeaWiFS postlaunch calibration and validation anlayses, part 3. 58 (NASA, Greenbelt, Maryland, 2000).

3 Lee, Z. P., Carder, K. L. & Arnone, R. A. Deriving inherent optical properties from water colour: a multiband quasi-analytical algorithm for optically deep waters. *Applied Optics* **41**, 5755-5772 (2002).

A satellite-based operational system for remote sensing of the Baltic ecosystem

M. Darecki[1], B. Woźniak[1], M. Ostrowska[1], A. Krężel[2], D. Ficek[3], K. Furmańczyk[4]

[1] Institute of Oceanology of the Polish Academy of Science, Sopot, Poland
[2] Institute of Oceanography, University of Gdańsk, Gdańsk, Poland
[3] Institute of Physics, Pomeranian University, Słupsk, Poland
[4] Institute of Marine and Coastal Sciences, University of Szczecin, Szczecin,Poland
Email: darecki@iopan.gda.pl

Introduction

The Baltic Sea is of great importance to the countries surrounding it and its ecosystem is evolving as a result of human activities. This requires a regular monitoring of environmental processes in the Baltic Sea which, together with in situ analysis at selected sites and times, can only be effective with the implementation of remote sensing technology.
To meet these needs, a consortium of four Polish research institutions execute in years 2010 - 2014 the SatBałtyk project [1]. The project is aiming to prepare a technical infrastructure and set in motion operational procedures for the satellite monitoring of the Baltic ecosystem. The system will deliver on a routine basis the variety of structural and functional properties of this sea, based on data provided by relevant satellites and supported by hydro-biological models. Among them: the solar radiation influx to the sea's waters in various spectral intervals, energy balances of the short- and long-wave radiation at the Baltic Sea surface and in the upper layers of the atmosphere over the Baltic, sea surface temperature distribution, dynamic states of the water surface, concentrations of chlorophyll a and other phytoplankton pigments in the Baltic water, distributions of algal blooms, the occurrence of upwelling events, and the characteristics of primary organic matter production and photosynthetically released oxygen in the water and many others. It is also intended to develop and, where feasible, to implement satellite techniques for detecting slicks of petroleum derivatives and other compounds, evaluating the state of the sea's ice cover, and forecasting the hazards from current and future storms and providing evidence of their effects in the Baltic coastal zone.

Discussion

The satellite component of the SatBaltic operational system is based on the most efficient of the available modern algorithms applicable to the Baltic Sea, most of them developed within DESAMBEM project carried out in Poland in years 2001- 2005 [2,3]. Due to high cloudiness typical over the Baltic, which partially or wholly precludes the use of satellite sensors for remote sensing of the water properties based on DESAMBEM algorithms, the system has to be supplemented by the component, which provides reliable data in these situations. The most rational means of providing such a data is to use data generated by prognostic ecohydrodynamic models. The development and implementation of a packet of prognostic models together with procedures for assimilating satellite data are the second component of the system (see Figure).
To secure the highest quality of data delivered by SatBaltic system, also the development and implementation of methods for the continuous calibration of the system (systematic measurements from research vessels, platforms and sea buoys) is also carried out within the Project.
Only when all above described system components are developed and synchronized, the SatBaltic operational system will be launched. The system, designed and equipped with appropriate procedures for the continuous spatial and temporal monitoring of the main structural and functional characteristics

of the entire Baltic Sea, and not just of instantaneous and local situations from the very restricted study areas accessible from ships and buoys or from often limited by clouds the satellite data.

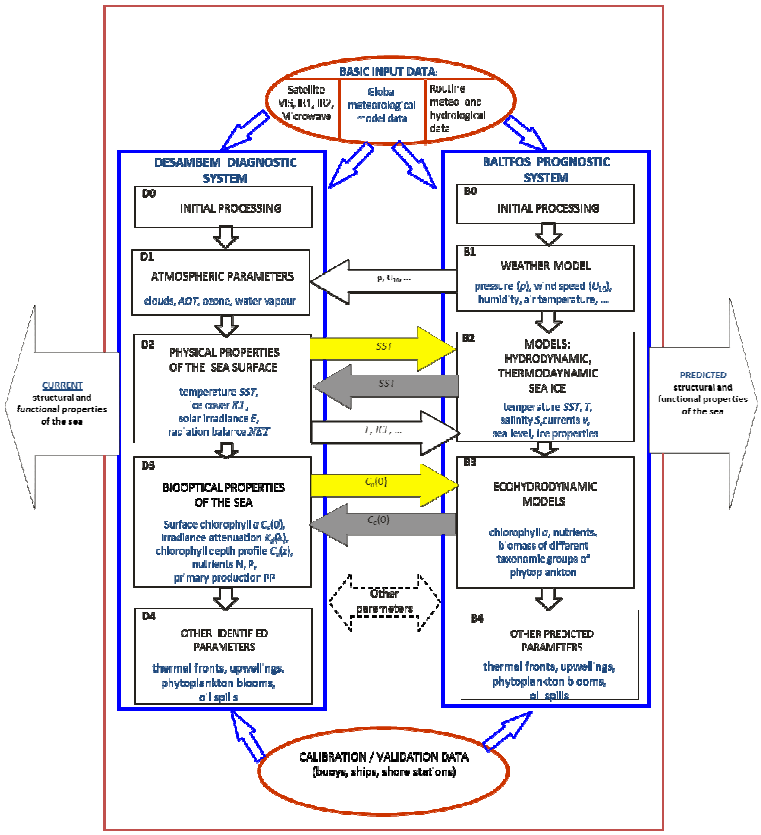

Figure illustrates the main components of the SatBaltic operational system. The system consists of two independent but coordinating subsystems: the DESAMBEM Diagnostic System and the Baltic Forecasting System (BALTFOS).

References

[1] Woźniak B., Bradtke K., Darecki M., Dera J., Dudzińska-Nowak J., Dzierzbicka-Głowacka L., Ficek D., Furmańczyk K., Kowalewski M., Krężel A., Majchrowski R., Ostrowska M., Paszkuta M., Stoń-Egiert J., Stramska M., Zapadka T., 2011a, SatBaltic – a Baltic environmental satellite remote sensing system-an ongoing project in Poland. Part 1: Assumptions, scope and operating range, Oceanologia 53(4) 897-924.

[2] Woźniak B., Krężel A., Darecki M., Woźniak S.B., Majchrowski R., Ostrowska M., Kozłowski Ł., Ficek D., Olszewski J., Dera J., 2008, Algorithm for the remote sensing of the Baltic ecosystem (DESAMBEM). Part 1: Mathematical apparatus, Oceanologia, 50 (4), 451–508.

[3] Darecki M., Ficek D., Krężel A., Ostrowska M., Majchrowski R., Woźniak S.B., Bradtke K., Dera J., Woźniak B., 2008, Algorithms for the remote sensing of the Baltic ecosystem (DESAMBEM). *Part 2:* Empirical validation, Oceanologia, 50(4), 509-538.

Atmospheric scattering and ocean color: errors due to the spherical atmosphere

D. Jolivet, D. Ramon, P. Y. Deschamps
HYGEOS, Lille, 59000, France
Email: pyd@hotmail.com

Summary

The atmospheric correction for ocean color requires very accurate computations of the scattering by aerosols and molecules. This is usually done assuming an infinite plane parallel atmosphere. In order to evaluate the errors due to this approximation, we have developed a radiative transfer code for a spherical atmosphere. The results of the computations by the two codes, plane parallel and spherical, both of them using a Monte Carlo method, have been compared. The relative error between the two computations remains below 1 % up to an incidence angle of about xxx° above which it is necessary to use the spherical atmosphere for atmospheric correction. Nevertheless, even at nadir, the error is significant enough to suggest to systematically computing the atmospheric scattering of a spherical atmosphere for atmospheric correction of ocean color.

Atmospheric scattering for a spherical atmosphere – Monte Carlo Code

Calculations are performed with a Monte Carlo radiative transfer code used in backward mode. It includes polarization, a rough sea surface, Rayleigh scattering, aerosols and gaseous absorption. The atmosphere is vertically extended up to 100 km altitude to take into account high-level molecules.

Comparison of the spherical and plane parallel results

Figure 1 shows a comparison between results for plane parallel and spherical atmosphere. It is actually the ration of the two computations so that a one value means no error. The relative error increases with the wavelength, but remains critical at the shorter wavelengths where the molecular scattering is important. Most of the effect comes from the scatterers at the highest altitude Adding aerosol with a lower altitude profile does not change much these results. The errors increases rapidly at viewing and solar zenith angles above 60 °, so that spherical calculations are strictly necessary for ocean color observations at high latitudes or with a large swath. For nadir observations, the error may still be within 1 % and using the computations for a spherical atmosphere is recommended.

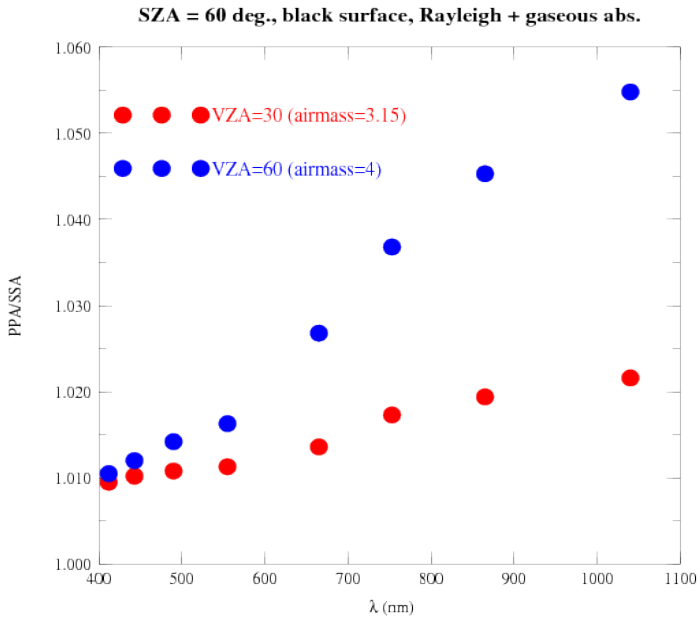

Figure 1: Wavelength dependence of the ration of plane parallel (PPA) to spherical (SSA) atmospheric scatterings.

Discussion

Our results show a larger effect of the sphericity of the atmosphere, contrary to a previous study [1] that misses part of the effect by using a molecular layer limited to a 8 km altitude. We recommend that advanced atmospheric corrections make a systematic use of computations of atmospheric scattering with a realistic spherical atmosphere, in particular when having a wide swath and large incidence angles (VIIRS, geostationary)

References

[1] Ding, K. and Gordon, H. R. (1994). Atmospheric correction of ocean color sensors: effects of the Earth's curvature. Appl. Opt., 33, 30, 7096-7106

The Information content of reflectance spectra and the uncertainties of derived IOPs of coastal waters

Roland Doerffer[1,2], Carsten Brockmann[1], Rüdiger Röttgers[2], Marc Bouvet[3]

[1] Brockmann Consult Geesthacht, Geesthacht, 21502, Germany,
[2] Helmholtz Zentrum Geesthacht, Geesthacht, 21502, Germany,
[3] ESA-ESTEC, Nordwijk, Netherlands
Email: roland.doerffer@hzg.de

Summary

Optical properties of coastal waters are characterized in many cases by a large number of different water constituents, including different phytoplankton species, mineralic and organic particles and dissolved matter such as humic substances. This large variety together with the impact of the atmosphere makes it difficult to determine inherent optical properties (IOPs) and the concentration of water constituents from reflectance spectra with an uniform quality. Sensitivity analysis of different constellations of water constituents, demonstrate that the uncertainties can be so large that the data become useless. To take these problems into account, we have developed a system of algorithms, which allows us to estimate the uncertainty and also to identify reflectance spectra, which are out of scope of the retrieval algorithm.

Introduction

Top of atmosphere radiance or reflectance spectra of coastal waters are determined by a large number of factors. Even in case 1 water, which is defined as water, the optical properties of which can be described by only one component, i.e. phytoplankton, uncertainties occur already due to the variability of the optical properties of phytoplankton [1, 2]. On the other hand, the information content of spectra in most cases is limited to a few (2-3) components, which can be derived with sufficient accuracy. The nature of these components may vary with the optical water type and depends on the dominating water constituents, aerosols, thin clouds etc., s. figure 1. Furthermore, the importance of spectral bands changes with optical water types. Different algorithms or systems of algorithms exist, to decompose reflectance spectra [3, 4], which partly include also the determination of uncertainties [5].

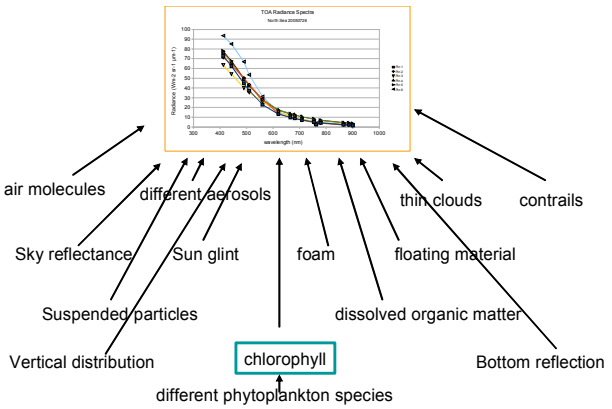

A large number of factors determine TOA radiance spectra, here of the North Sea. On the other side, these spectra are rather similar and the information content is much smaller, than the number of factors, which determine the spectra.

Discussion

The large number of factors, which determine top of atmosphere (TOA) and water reflectances of some

types of coastal waters imply issues and uncertainties when we derive water reflectances from TOA reflectances and, in turn, IOPs from water reflectances. Uncertainties can be large for components, which are sub-dominant and thus above the acceptance level. In particular high concentrations of suspended matter may totally mask the effect of other substances on reflectance spectra, such as phytoplankton. In these cases the uncertainty can easily surmount a factor of 2 or even 10. User of such data without any warning can easily be misleaded. In extreme cases also the atmospheric correction may lead to large uncertainties in water reflectances or may even fail. Sensitivity studies within the ESA Water Radiance project have demonstrated that the determination of the uncertainty range is crucial for the use of remote sensing data of coastal waters. Thus, it is necessary to determine these uncertainties on a pixel by pixel bases. For this purpose a system of algorithms has been developed (1) to check if a reflectance spectrum is within the scope of the algorithm, and (2) to determine the uncertainty range. This system is based on neural networks [6], which have been trained using a case 2 water bio-optical model and radiative transfer simulations [7] for water and atmosphere.

Conclusions

Uncertainties of IOPs and concentrations of coastal water constituents, when derived from reflectance spectra, can be variable and large so that products such as concentration maps of coastal waters provided from data of earth observing satellites, should be complemented by co-registered maps of uncertainties and flags, which indicates out of scope conditions.

References

[1] Bricaud, A., M. Babin, A. Morel and H. Claustre. 1995. Variability in the chlorophyll-specific absorption coefficients of natural phytoplankton: analysis and parameterization, J. Geophys. Res., 100, 13321–13332.

[2] Röttgers, R., C. Häse, and R. Doerffer. 2007. Determination of the particulate absorption of microalgae using a point-source integrating-cavity absorption meter: verification with a photometric technique, improvements for pigment bleaching, and correction for chlorophyll fluorescence. Limnol. Oceanogr. Methods 5: 1-12.

[3] IOCCG. 2006. IOCCG Report 5: Remote Sensing of Inherent Optical Properties: Fundamentals, Tests of Algorithms, and Applications. Edited by ZhongPing Lee, pp. 126.

[4] Franz, B.A. and P.J. Werdell. 2010. A Generalized Framework for Modeling of Inherent Optical Properties in Remote Sensing Applications. White Paper, Proc. Ocean Optics 2010, Anchorage, Alaska, USA.

[5] Maritorena S., D.A. Siegel and A. Peterson. 2002. Optimization of a Semi-Analytical Ocean Color Model for Global Scale Applications. Applied Optics, 41(15), 2705-2714.

[6] Doerffer R. and H. Schiller (2007). The MERIS Case 2 water algorithm, , International Journal of Remote Sensing, 28, (3-4): 517-535.

[7] Mobley, C. D. 1994. Light and water. Radiative transfer in natural waters. San Diego. Academic Press.

Can a single turbidity algorithm be used in all turbid waters?

A.I. Dogliotti[3], K.G. Ruddick[2], B. Nechad[2], D. Doxaran[1], E., E. Knaeps[4]

[1] Instituto de Astronomía y Física del Espacio (IAFE), CONICET/UBA. Buenos Aires, Argentina
[2] Royal Belgian Institute for Natural Sciences (RBINS), 100 Gulledelle, 1200 Brussels, Belgium
[3] Laboratoire d'Océanographie de Villefranche (LOV), CNRS/UPMC, B.P. 8, Villefranche-sur-Mer, 06230, France
[4] Flemish Institute for Technological Research (VITO), Boeretang 200, B-2400 Mol, Belgium
Email: adogliotti@iafe.uba.ar

Summary

Ocean color remote sensing has shown to be a useful tool to map turbidity (T) and total suspended sediment (TSM) concentration in turbid coastal waters. Different algorithms to retrieve T and TSM from water reflectance already exist. However there are important questions as to whether these algorithms need to be calibrated specifically for different regions. In the present work we use a set of 180 simultaneous measurements of water reflectance and turbidity in five different highly turbid regions to validate a single band algorithm using the near infrared (NIR) band at 859 nm. The good performance of the algorithm for all these regions, despite different sediment characteristics, suggests the global applicability of the algorithm to map turbidity within a certain range.

Introduction

Suspended particles modify the transmission of light under water affecting the biological productivity and underwater visibility as well as pollutant and nutrient transport. Turbidity (T), defined from the measurement of 90° scattered light at 860nm, is a relevant optical parameter for certain water quality applications, like water transparency. It is relatively cheap and easy to measure, and is highly correlated to the total suspended sediment (TSM) concentration (which is more expensive and time consuming to measure), making it an interesting parameter to retrieve from optical remote sensing. Even though many regional algorithms to estimate T and TSM have been already developed [e.g. 1, 2], the generality of these algorithms for remotely estimating sediment concentrations and/or turbidity is currently not established because of possible regional variation of specific optical properties.

In a previous work, a single band turbidity algorithm [1] using reflectance at 859 nm was re-calibrated using *in situ* T and reflectance measurements performed in the Southern North Sea (SNS) and the Scheldt River (SR) with T values higher than 10 FNU [3]. The algorithm was applied to MODIS satellite-retrieved Rayleigh-corrected reflectance data in the Samborombón Bay region (located to the south of Río de la Plata River, Argentina) and validated with in situ T measurements. A good agreement between modelled and *in situ* measurements was found, but no *in situ* water reflectance measurements were available to directly validate the algorithm. The objective of the present study is to validate the single band algorithm and test its generality using water reflectance and turbidity measurements performed in five different turbid regions of the world: the Southern North Sea (SNS), French Guyana (FG), and the Scheldt (SC, in Belgium), Gironde (GIR, in France), Río de la Plata (RP in Argentina) rivers; these regions have quite different sediment composition (refractive index, density) and range of concentrations.

Discussion

Turbidity measured in the five regions covered a wide range of values, from 10 to 900 FNU (Formazin Nephelometric Units). Good performance of the algorithm was found with correlations > 0.75 for each site and a higher correlation ($r=0.96$, $p<0.00001$) for all sites together (Figure 1).

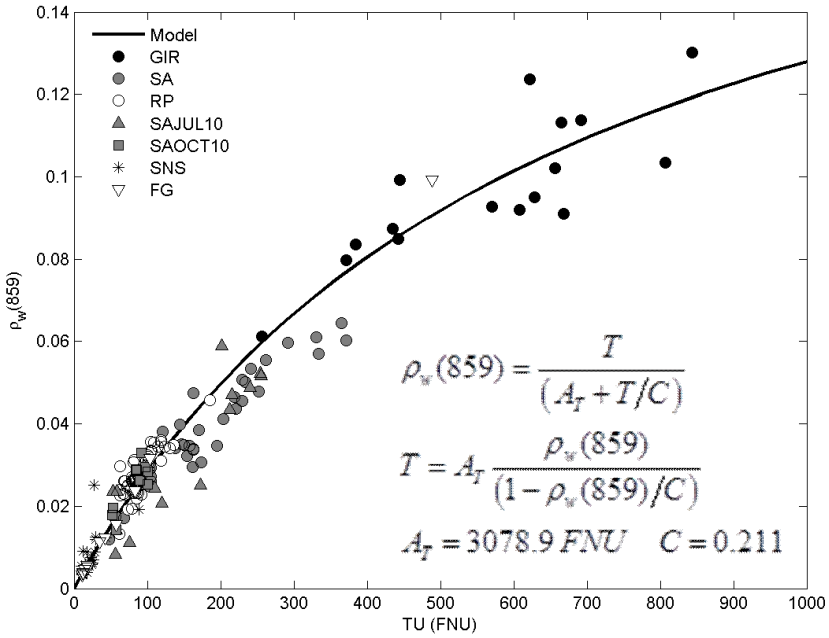

Fig. 1: In situ water reflectance and T values measured for various regions (see text for abbreviations) and the single band model validated in the present study (solid line)

Even though the algorithm was calibrated with a dataset from two specific regions (SNS and SC), it showed good performance in all five regions analyzed here, suggesting the general applicability of the algorithm for coastal/estuarine waters with this turbidity range.

Conclusions

A single band algorithm [1, 2] using 859nm was validated using *in situ* turbidity and reflectance measurements from five different turbid water regions. A good agreement between modelled and *in situ* measurements was found. These results suggest that a general algorithm can be used for mapping turbidity using NIR bands present in different ocean colour satellites such as MODIS, MERIS, SeaWIFS, GOCI, OLCI, HIOC, etc provided atmospheric correction is possible. The impact of the regional variability of the relationship between T and ρ_w859 is expected to be low because: a) unlike TSM, T is an optical property closely related to the side/backscattering processes affecting ρ_w859, b) ρ_w859 is hardly affected by particulate absorption which may vary significantly between regions. The main limitation of this algorithm will be related to the range of T rather than geographic region or particle type. TSM concentration, the parameter of main interest in sediment transport studies, could subsequently be retrieved by ocean colour remote sensing if a region-specific relation between T and TSM is known.

References

[1] Nechad B., K. G. Ruddick & Neukermans, G. (2009). Calibration and validation of a generic multisensor algorithm for mapping of turbidity in coastal waters. In: SPIE, Rem Sens of the Ocean, Sea Ice, and Large Water Regions. Vol. 7473, 74730H.

[2] Doxaran, D., J.M. Froidefond, S. Lavender and Castaing, P. (2002) Spectral signature of highly turbid waters Application with SPOT data to quantify suspended particulate matter concentrations. *Rem Sens Env 81 (2002);* pp. 149-161.

[3] Dogliotti A. I., K. G. Ruddick, B. Nechad, C. Lasta, A. Mercado, C. Hozbor, R. Guerrero, G. Riviello López, and Abelando, M. (2011). Calibration and validation of an algorithm for remote sensing of turbidity over La Plata River estuary, Argentina. *EARSeL eProceedings*, 10(2): 119-130.

SENTINEL-3 Optical Sensors Products and Algorithms

Carla Santella [(1)], Roberto Sciarra[(1)], Philippe Goryl[(2)], Alessandra Buongiorno[(2)], Vincent Fournier-Sicre [(3)], Vincenzo Santacesaria[(3),] Hilary Wilson[(3)]

(1) SERCO SpA (c/o ESA-ESRIN), Italy (2) ESA-ESRIN, Italy (3) EUMETSAT, Germany

The Sentinel-3 mission objectives encompass the commitment to consistent, long-term collection and operational provision of remotely sensed marine and land data, to measure sea surface topography, sea/land surface temperature and ocean/land surface colour in support of ocean forecasting systems and for environmental and climate monitoring.

The objective of this poster is to introduce the Sentinel-3 Level 2 geophysical products generated from data acquired by the OLCI and SLSTR optical sensors, with a special focus on ocean color products and the algorithms used for products retrieval.

An overview of the complete set of Sentinel-3 optical sensors products and their characteristics will be also provided to offer a complete view of the “Sentinel-3 Optical Products” that will be generated within the Sentinel-3 Payload Data Ground Segment by the Sentinel-3 Instrument Processing Facilities (IPFs) and disseminated to the users.

Bayesian Methodology for Ocean Color Remote Sensing

Robert Frouin, Scripps Institution of Oceanography, La Jolla, USA
Bruno Pelletier, University of Rennes 2, Rennes, France

The inverse ocean color problem, i.e., the retrieval of marine reflectance from top-of-atmosphere (TOA) reflectance, is examined in a Bayesian context. The solution is expressed as a probability distribution that measures the likelihood of encountering specific values of the marine reflectance given the observed TOA reflectance. This conditional distribution, the posterior distribution, allows the construction of reliable multi-dimensional confidence domains of the retrieved marine reflectance. The expectation and covariance of the posterior distribution are computed, which gives for each pixel an estimate of the marine reflectance and a measure of its uncertainty. The p-value is also computed to identify situations for which forward model and observation are incompatible. Prior distributions of the forward model parameters that are suitable for use at the global scale, as well as a noise model, are determined. Numerical approximations of the expectation and covariance are defined and implemented. Performance is evaluated on simulated data, and the ill posed nature of the inverse problem is illustrated and discussed. The theoretical concepts and inverse models are applied to SeaWiFS imagery, and comparisons are made with estimates from the standard atmospheric correction algorithm and in situ measurements. Conclusions are given in terms of performance, robustness, and generalization. Regionalization of the inverse models is a natural development to improve retrieval accuracy, for example by including explicit knowledge of the space and time variability of atmospheric variables.

Routine monitoring of bathymetry and habitat maps derived from HICO imagery: Case study of Shark Bay, Western Australia.

R.A. Garcia [1], P.R.C.S. Fearns [1], L.I.W. McKinna [1]
[1] Curtin University, Department of Imaging and Applied Physics, Bentley, WA 6102, Australia
Email: Rodrigo.Garcia@postgrad.curtin.edu.au

Summary
The purpose of this study was to investigate and develop approaches to atmospheric correction, level-2 (L2) processing, and geo-location of HICO imagery for routine monitoring of shallow coastal water ecosystems. A total of nine HICO images, spanning November 2011 - August 2012, over the Shark Bay World Heritage Area, Western Australia, were examined. We have implemented a semi-analytical shallow water inversion model to retrieve bathymetry and a two class benthic habitat map. Within this research, challenges regarding atmospheric correction of HICO imagery, tide correction of bathymetry products, and geo-location accuracy are discussed.

Introduction
The Hyperspectral Imager for the Coastal Ocean (HICO) is a prototype sensor, onboard the International Space Station, designed with the necessary specifications for the remote sensing of coastal marine environments [1]. HICO has a spatial resolution of 100 × 100 m with 87 contiguous spectral bands between 400-900 nm, which has the potential for the generation of improved shallow water remote sensing products such as bathymetry and benthic habitat maps.

Bathymetry and benthic habitat maps are important not only for coastal resource managers, but also for research utilizing hydrodynamic models in which depth and benthic habitat type influence tide, currents, wave energy and consequently sediment/nutrient transportation mechanisms [2]. Furthermore, coastal resource managers and researchers often require 'environmental baselines' to assess the natural/seasonal variability in benthic habitat type(s) and bathymetry prior to industrial/commercial development or anthropogenic disturbances. This, however, requires routine monitoring of such products within coastal regions of interest. To date, there has been limited work reported on the routine monitoring of bathymetry and benthic habitats using standardized processing of satellite hyperspectral imagery.

A case study showing the routine monitoring of HICO-derived bathymetry and benthic habitat maps is presented for the World Heritage Area of Shark Bay, Western Australia. In this study, the semi-analytical shallow water inversion algorithm, BRUCE [3], was implemented to retrieve imagery of water column depth (bathymetry), inherent optical properties (IOPs) of the water column and the benthic albedos of sand and seagrass.

Discussion and conclusion
Several processing steps have been implemented that convert HICO L1B, calibrated radiances, to the desired bathymetry and benthic habitat map L2 products. Briefly, these steps include: (1) Tafkaa 6S [4] atmospheric correction to generate the above water remote sensing reflectances; (2) a per-pixel quality control that masks land, cloud and pixels that were over-corrected in step 1; (3) sunglint removal; (4) derivation of L2 products using the BRUCE model (Figure 1); (5) uncertainty propagation through the inversion model using the method proposed by Hedley et al. [5]; (6) Image smoothing and tide correction of the bathymetry product and; (7) Geo-referencing and manual geo-rectification using ground control points.

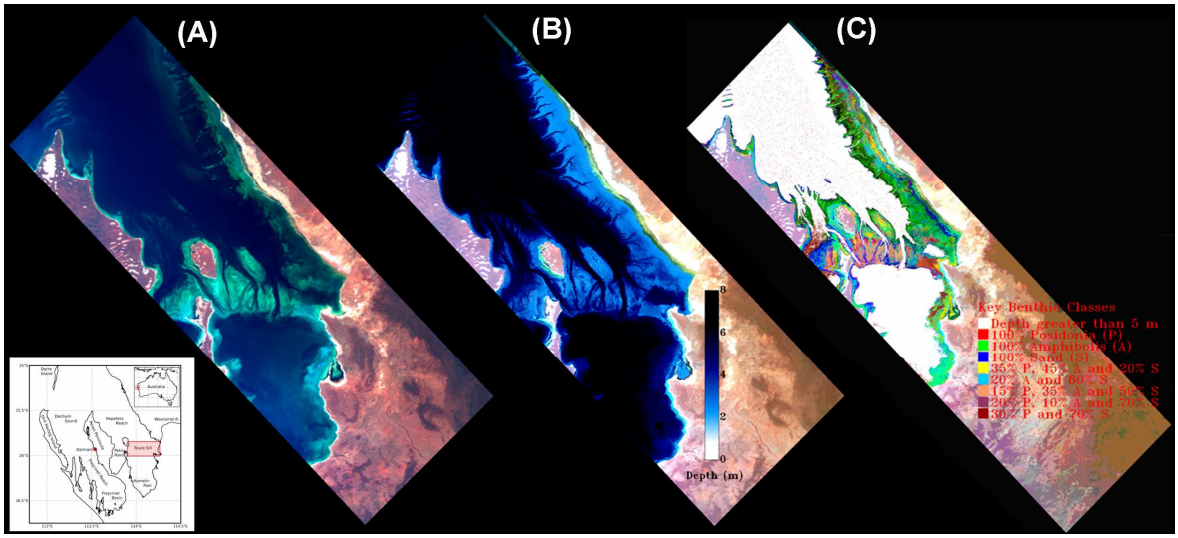

Figure 1: HICO imagery of Shark Bay, Western Australia (central latitude/longitude 25.62°S/ 113.89 °E) on 01 June 2012; (a) quasi-true color image; (b) derived bathymetry, and; (c) derived substrate classification of sand and seagrass and various proportions of these two classes.

Preliminary results show relative changes through time between the two substrate classes (sand and seagrass). This may be attributed to seasonal variability in the proportion of seagrass present. However, further work is needed to assess if this variation is statistically significant above the uncertainty propagated through the BRUCE model.

The routine monitoring of bathymetry of Shark Bay has also raised the following key issues: (1) Tafkaa 6S often overcorrects the atmospheric radiance signal, resulting in non-physical reflectance signatures in the blue and red portions of the spectrum. This overcorrection is particularly evident in HICO swaths captured during high solar zenith angles. Further work is needed to improve atmospheric correction; (2) Geo-referencing using the distributed geographic lookup tables does not generate the desired geospatial consistency through time. Analysis showed that clearly identifiable land features varied by approximately 1° in latitude and longitude across the HICO images. Additional geo-registration using distinct land features as ground control points improved the geo-location. Based on analysis of image features, we estimate the geo-location accuracy has improved to within 100-300 m, and; (3) Tide correction proved challenging over shallow regions of Shark Bay where shallow water tidal harmonics are prevalent. The lack of water level height data prevented direct correction of these tidal influences, and thus an empirical image based tide correction technique was employed to correct all bathymetry images to a relative datum.

References

[1] Lucke, R.L., Corson, M., McGlotlin, et al. (2011), Hyperspectral imager for the coastal ocean: instrument description and first images, *Appl Optics*, 50: 1501-1516.

[2] Burling, M.C., Pattiaratchi, C. B., Ivey, G.N. (2003), The tidal regime of Shark Bay, Western Australia, Estuar Coast Shelf Sci. 57: 725-735

[3] Klonowski, W.M., Fearns, P.R.C.S., Lynch, M.J. (2007), Retrieving key benthic cover types and bathymetry from hyperspectral imagery, J Appl Rem Sens, 1: 011505

[4] Gao, B-C., Montes, M.J., Ahmad, Z., Davis, C.O. (2000), Atmospheric correction algorithm for hyperspectral remote sensing of ocean color from space. Appl Optics, 39: 887-896.

[5] Hedley, J., Roelfsema, C., Phinn, S.R. (2010), Propagating uncertainty through shallow water mapping algorithm based on radiative transfer model inversion, In: *Proceedings of Ocean Optics XX*, Anchorage Alaska.

Biological response to the 1997-98 and 2009-10 El Niño events in the equatorial Pacific Ocean

Michelle M. Gierach[1], Tong Lee[1], Daniela Turk[2,3], and Michael McPhaden[4]
[1]Jet Propulsion Laboratory / California Institute of Technology
[2]Dalhousie University
[3]Lamont-Doherty Earth Observatory, Earth Institute at Columbia University
[4]NOAA Pacific Marine Environmental Laboratory

Gierach, M.M., T. Lee, D. Turk, and M.J. McPhaden (2012), Biological response to the 1997-98 and 2009-10 El Niño events in the equatorial Pacific Ocean, *Geophys. Res. Lett.*, 39, L10602, doi:10.1029/2012GL051103.

El Niño-Southern Oscillation (ENSO) significantly influences atmospheric and ocean circulations in the Pacific Ocean, which in turn affect biological production and ecosystem characteristics. Much of our existing knowledge about the relationship between ENSO and biology is with respect to the classic El Niño (i.e., EP-El Niño), which has maximum warming in the eastern equatorial Pacific (EEP) (Fig. 1e). However, since the 1990s, there have been frequent occurrences of a new flavor of El Niño (i.e., CP-El Niño) that has maximum warming in the central equatorial Pacific (CEP) (Fig. 1f). The impact of the latter on biology is not well understood. Biophysical responses in the equatorial Pacific Ocean to the 1997-98 and 2009-10 El Niño (i.e., the strongest EP- and CP-El Niño event in the last three decades) are analyzed using satellite observations and reanalysis products. Significant differences in chlorophyll-a (chl-a) are found between the two events associated with different patterns of anomalies for the physical variables (Fig. 1). An adjoint tracer analysis is used to examine the difference in the origin and pathway of water masses in the upper equatorial Pacific Ocean that control the difference in nutrient supply and thus chl-a.

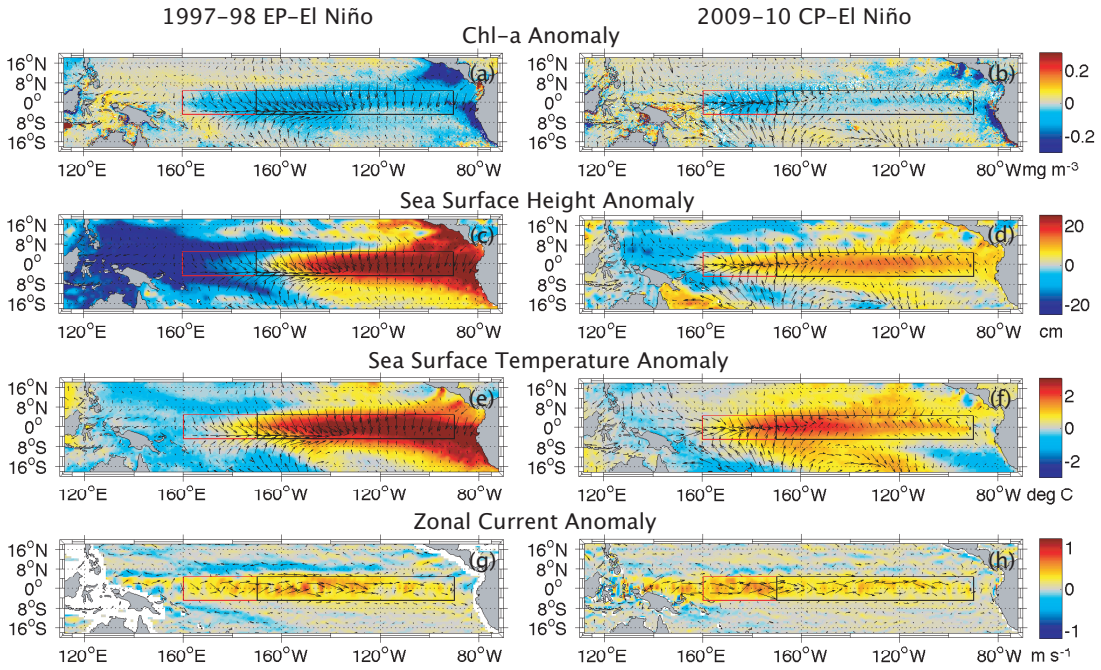

Fig. 1. November-December-January averaged anomalies of (a-b) chl-a, (c-d) sea surface height, (e-f) sea surface temperature, and (g-h) zonal ocean surface currents for the 1997-98 EP-El Niño and 2009-10 CP-El Niño. Wind vector anomalies are overlaid on (a-f) and ocean surface current vector anomalies on (g-h). The black and red boxes denote the EEP (5°S-5°N, 170°W-90°W) and CEP (5°S-5°N, 160°E-170°W) regions.

The retrieval of attenuation and scattering coefficients of marine particles from polarimetric observations

A. Gilerson, A. Ibrahim, J. Stepinski, A. El-Habashi, S. Ahmed

Optical Remote Sensing Laboratory, the City College of the City University of NY,
New York, NY, 10031, United States
Email: gilerson@ccny.cuny.edu

Summary

Polarized light in the oceans carries intrinsic information that can be utilized to estimate the optical and microphysical properties of the oceanic hydrosols. It is especially sensitive to the scattering coefficient, which cannot be retrieved from the unpolarized light used in current ocean color remote sensing algorithms. Based on extensive simulations using the vector radiative transfer program RayXP, the attenuation-to-absorption ratio (c/a), from which b is readily computed, is shown to be closely related to the DoLP. The relationship is investigated for the upwelling polarized light for several wavelengths in the visible part of the spectrum, for a complete set of viewing geometries, and for varying water compositions including open ocean and coastal waters. A large dataset of Stokes components is collected for various water compositions, measured in the field with a hyper-spectral and multi-angular polarimeter for validation purposes.

Introduction

Light-scattering properties of particles in the ocean and atmosphere have been extensively studied [1]. Taking note that solar radiation is initially completely unpolarized, once it reaches the Earth's atmosphere, scattering events, such as Rayleigh (molecular) and particulate scattering, cause it to become partially polarized. Light exhibits, as a result of scattering, some degree of polarization (DoP) in different directions and this polarization is directly related to the source of the radiation and to the properties of the scatterers. Thus, the polarization state of light carries information about the atmosphere-ocean system (AOS) that can be utilized for remote sensing of microphysical and optical properties of particulates including the oceanic hydrosols and it is sensitive to the scattering coefficient. Through the unpolarized remote sensing reflectance (R_{rs}), the classical algorithms can only estimate *back*scattering coefficients b_b, but the *total* scattering coefficient b could be retrieved based on the characteristics of polarized light.

Discussion

Based on extensive simulations using the vector radiative transfer program RayXP, the attenuation-to-absorption ratio (c/a), from which b is readily computed, is shown to be closely related to the degree of linear polarization (DoLP). The relationship is investigated for the upwelling polarized light for several wavelengths in the visible part of the spectrum, for a complete set of viewing geometries, and for varying concentrations of phytoplankton, non-algal particles, and color dissolved organic matter (CDOM) in the aquatic environment that resembles coastal waters (Case II waters) [2]. Another dataset of bio-optical properties for open ocean (Case I waters) that includes only phytoplankton particles and its bi-products has been ingested into the RayXP program to simulate the polarized radiance. It is shown, for Case I and Case II waters, that there is an excellent correlation between the DoLP and c/a for a wide range of viewing geometries. That correlation is investigated theoretically using fitting techniques, which show that it depends not only on the general composition of water but also on the particle size

distribution (PSD) of the (mainly non-algal) particles for Case II waters according to the power law in Equation (1).

$$\left\{\left(\frac{c}{a}\right)_{\text{fit}}\right\}_{\xi_{\text{nap}}=3.5,4.0,4.5} = \left\{\chi(DoLP)^{\gamma}\right\}_{\xi_{\text{nap}}=3.5,4.0,4.5}, \quad (1)$$

where a and c are the absorption and attenuation coefficients, respectively; χ and γ are the fitting coefficients and ξ_{NAP} is a PSD slope. The relationship between the IOPs (c/a ratio) and the DoLP is parameterized as a power law as in Equation (1) with a good coefficient of determination R^2 opening the possibility for an accurate retrieval technique of the c/a ratio and further attenuation and scattering coefficients.

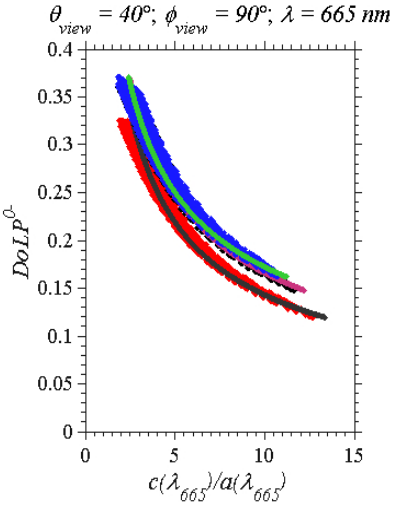

Fitted relationship between DoLP and c/a at 665 nm

An interesting result is that the fits for both ξ_{nap} of 4.0 and 4.5 are similar for the all three wavelengths 440, 550 and 665nm (only results for 665nm are shown in the figure). In coastal waters, the slope ξ_{nap} of PSD of NAP largely falls in the range of 4.0-4.5, where these particles are small in size. Since the relationship weakly depends on the PSD of chlorophyllic particles, a rough estimate of ξ_{nap} to be in its typical range may not induce large errors in, for example, retrieval analysis. On the other hand, the relationship between the DoLP and c/a for Case I waters is more linear especially at the 550 nm where maximum dependency in relationship falls onto the optical properties of the phytoplankton particles. At the blue and red wavelengths, the relationship becomes more dependent on the optical properties of the water molecules (Rayleigh scattering at the blue and high water absorption at the red spectral region).

Conclusions

While attenuation and scattering coefficients are not retrievable from the scalar reflectance measurements, a relationship between the degree of linear polarization (DoLP) and the attenuation to absorption coefficients ratio (c/a) has been investigated using vector radiative transfer simulations for open ocean and coastal waters for conditions just below and above the air-water interface. The parameterized relationship allows the direct retrieval of the scattering coefficient b of the hydrosols using polarimetric observations of the ocean. A large dataset of Stokes components for various water compositions, measured in the field with a hyper-spectral and multi-angular polarimeter, then provides the opportunity to validate the parameterized relationship between DOLP and c/a. This study opens the possibility for the retrieval of additional inherent optical properties (IOPs) from air- or space-borne DoLP measurements of the ocean.

References

[1] Timofeyeva, V. A. (1970) “Degree of polarization of light in turbid media,” Izvestiya Akademii Nauk SSSR Fizika Atmosfery. I. Okeana. **6**, 513.

[2] Ibrahim, A., Gilerson, A., Harmel, T., Tonizzo, A., Chowdhary, J., and Ahmed, S. (2012) "The relationship between upwelling underwater polarization and attenuation/absorption ratio," Opt. Express **20**, 25662-25680.

An improved FLH product for MERIS and OLCI

J.F.R. Gower[1], S.A. King[2], E. Young[3]

[1]Institute of Ocean Sciences, Fisheries and Oceans Canada, Sidney, BC, Canada
[2]Sea This Consulting, Nanaimo, BC, Canada
[3]University of Victoria, Geography Department, Victoria, BC, Canada
Email: jim.gower@dfo-mpo.gc.ca

Summary

ESA should make available a level 3 global MERIS FLH product, to provide new insight into productivity and blooms in coastal areas. MODIS ocean colour data, including fluorescence, are made widely available through the NASA Oceancolor and Giovanni web systems, but fluorescence does not appear to be widely used. We show problems with the Giovanni fluorescence data that may partly explain this. For fluorescence imaging, MERIS has the technical advantage over MODIS of better band placing (including the additional 709 nm band) and of higher spatial resolution (300m compared to 1000m). MERIS ocean colour data, including fluorescence, need to be made more easily available to encourage the work that needs to be done on FLH in preparation for OLCI.

Introduction

Both MERIS and MODIS were designed to map chlorophyll using FLH (Fluorescence Line Height) at wavelengths near 680 nm, as well as using the more standard green-to-blue ratio estimates based on measurements in the range 440 to 560 nm. The standard green-to-blue product has proven inadequate in many coastal areas, and we believe FLH to be a viable alternative. We have applied FLH in the coastal waters of Western Canada [1,2] and documented cases where FLH provides a superior result [3].

Discussion

We show here an example of the way fluorescence is made available by the Giovanni system developed and maintained by the NASA GES DISC, but note problems which probably contribute to its relative lack of use. We conclude that MERIS data should be made available using tools of this type. This applies to both fluorescence and the more conventional chlorophyll products. It will greatly improve global acceptance of OLCI data if such a system were tested and in place before launch of Sentinel 3

At present we notice two problems with Giovanni's fluorescence data. The first is the description of NFLH (Normalized Fluorescence Line Height) data as dimensionless. The normalization applied here is to scale the signal up to the radiance that would be observed under zenith sun, on the assumption that fluorescence increases proportional to incident solar irradiance. This will still have units of radiance. The second problem is the fact that the fluorescence data should not be normalized. The fluorescence data show that this is inappropriate (see Figure), and studies of the fluorescence mechanism [eg 4] confirm this. It has long been known that the fluorescence signal tends to saturate under high insolation. Data summarized in [4] support the conclusion that for all sun elevations over about 20 degrees, that is, when insolation is sufficient for ocean colour satellites to produce reliable results, fluorescence is fully stimulated, and the fluorescence signal is independent of the value of solar irradiance.

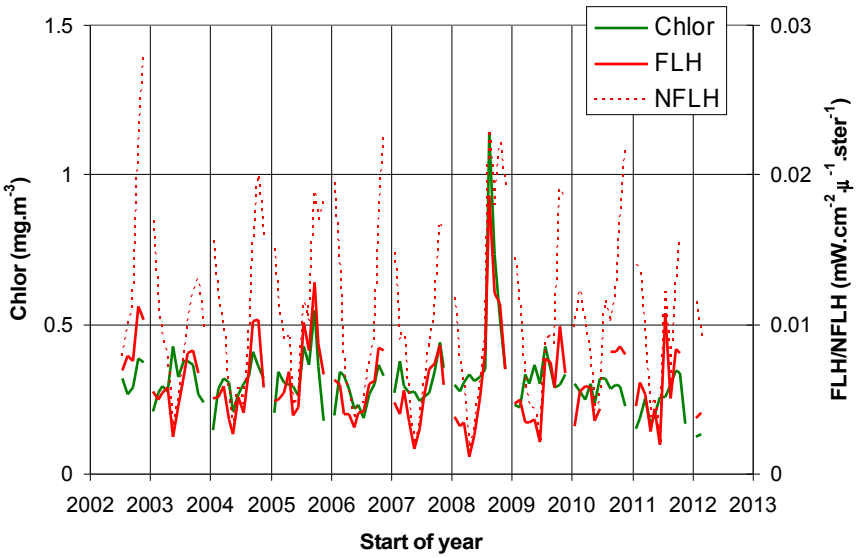

MODIS Aqua monthly average chlorophyll (green) and fluorescence (FLH, red), plotted as normalized fluorescence (NFLH, dotted red) and as FLH (solid red) for a 2-degree square centred on Ocean Station Papa in the NE Pacific. FLH values agree well with chlorophyll. NFLH data show a spurious annual cycle

Conclusions

We are finding successful applications of FLH data and believe that with more users, more successes would appear. We have found problems with the way fluorescence data are handled and believe that these are limiting their use. We note that MERIS data are not distributed using a simple, widely accessible web tool similar to NASA Giovanni. MERIS fluorescence data need to be made more widely available in this way. It would greatly improve international acceptance of OLCI data if such a system were tested with MERIS fluorescence and other data, and in place before launch of Sentinel 3.

Acknowledgements

This work has been supported by Fisheries and Oceans Canada and the Canadian Space Agency. The author thanks colleagues at IOS and the Universities of British Columbia and Victoria for useful discussions.

8. REFERENCES

1. Gower, J.F.R., Brown, L and Borstad, G.A., 2004. Observation of chlorophyll fluorescence in west coast waters of Canada using the MODIS satellite sensor. Can. J. Remote Sens. 30(1), 17-25.
2. Gower, J.F.R. and King, S.A., 2007. Validation of chlorophyll fluorescence derived from MERIS on the west coast of Canada. Int. J. Remote Sens. 28(3-4), 625-635.
3. Gower, J. and King, S., 2012. Use of satellite images of chlorophyll fluorescence to monitor the spring bloom in coastal waters. Int. J. Remote Sens. 33(23), 7469-7481. http://dx.doi.org/10.1080/01431161.2012.685979.
4. Behrenfeld, M.J., Westberry, T.K., Boss, E.S., O'Malley, R.T., Siegel, D.A., Wiggert, J.D., Franz, B.A., Mcclain, C.R., Feldman, G.C., Doney, S.C., Moore, J.K., Dall'Oolmo, G., Milligan, A.J., Lima, I., and Mahowald, N., 2009, Satellite-detected fluorescence reveals global physiology of ocean phytoplankton, *Biogeosciences*, **6**, pp. 779-794.

A hybrid MUMM NIR-Corrected algorithm for the atmospheric correction of turbid waters

C. Goyens[1], C. Jamet[1] and K. Ruddick[2]
[1]CNRS, UMR 8187, Univ Lille Nord de France, ULCO, LOG, F-62930 Wimereux, France
[2]MUMM | BMM | UGMM, B-1200 Brussels, Belgium
Email: clemence.goyens@univ-littoral.fr

Summary
In extremely turbid waters, the relation between water leaving reflectance ($\rho_w(\lambda)$) at two bands in the near infra-red (NIR) was shown to be well approximated by the polynomial function suggested by Wang et al. [1] for the atmospheric correction (AC) algorithm of GOCI. Accordingly, a new hybrid MUMM NIR-corrected AC algorithm is developed consisting to replace the constant NIR reflectance ratio in the MUMM AC algorithm [2,3] by the polynomial function of Wang et al. [1]. Based on a sensitivity study we conclude that the hybrid MUMM NIR-corrected AC algorithm results in improved $\rho_w(\lambda)$ retrievals in turbid waters.

Introduction
The use of satellites to retrieve $\rho_w(\lambda)$ requires effective removal of the atmospheric signal. This can be performed by extrapolating the aerosol optical properties to the visible from the NIR spectral region assuming that seawater is totally absorbent in this latter part of the spectrum, the so-called black pixel assumption. However, in turbid waters the scattering and absorption of coloured dissolved organic matter and non-algal particles result in non-zero $\rho_w(NIR)$. To extent the black pixel assumption AC algorithm, Ruddick et al. [2, 3] assumed a constant reflectance ratio, $\alpha(\lambda_{NIR1},\lambda_{NIR2})$, and spatial homogeneity in aerosol reflectance. Recently, Wang et al. [1] suggested a NIR-corrected AC algorithm for GOCI retrieving $\rho_w(\lambda)$ at two wavelengths in the NIR and including a polynomial function relating $\rho_w(\lambda_{NIR1})$ to $\rho_w(\lambda_{NIR2})$.

The polynomial function and the constant $\alpha(\lambda_{NIR1},\lambda_{NIR2})$, suggested by Wang et al. [1] and Ruddick et al. [3], respectively, are validated with 131 highly accurate *in situ* $\rho_w(\lambda)$ data. Next, a study is conducted to evaluate the sensitivity of the AC algorithm to the NIR marine reflectance model. *In situ* $\rho_w(\lambda)$ are therefore combined with a simplified power law model for aerosol reflectance. With the assumption that only single scattering occurs and that the diffuse atmospheric transmittance is equal to 1, we compute the Rayleigh corrected reflectance. The latter is than inverted using the AC algorithms to give the retrieved $\rho_w(\lambda)$, which for a perfect model should be equal to the *in situ* $\rho_w(\lambda)$. According to the results of the sensitivity test, a new AC algorithm is suggested to provide satisfactory $\rho_w(\lambda)$ retrievals over moderately, very and extremely turbid waters.

Discussion
The validation exercise shows that the polynomial function relating $\rho_w(748)$ to $\rho_w(869)$ [1] has a larger validity range compared to the constant reflectance ratio $\alpha(748,869)$ [3]. However, when evaluating the sensitivity of the AC algorithms to the NIR marine reflectance models, we observe that the NIR-corrected AC algorithm largely overestimate $\rho_w(\lambda)$ at all wavelengths and for all water types (median difference between *in situ* and retrieved $\rho_w(\lambda)$ ranging between 0.001 and 0.01, Fig.

1 (a-c)). With the MUMM AC algorithm and provided that the aerosol model is correctly retrieved, for moderate to very turbid waters the difference between observed and retrieved $\rho_w(\lambda)$ remains very small (median difference < -0.0001, Fig. 1 (a,b)). In contrast, for extremely turbid waters, $\rho_w(\lambda)$ are underestimated with a median difference between *in situ* and retrieved $\rho_w(\lambda)$ of about -0.003 (Fig. 1 (c)). Including an error of 40% on the angstrom coefficient for the selection of the aerosol model results in larger errors on the $\rho_w(\lambda)$ retrievals (not shown here). However, these $\rho_w(\lambda)$ retrievals are still closer to ground truth compared to the NIR corrected AC retrieved $\rho_w(\lambda)$ values.

To improve $\rho_w(\lambda)$ retrievals in extremely turbid waters, a hybrid MUMM NIR-corrected AC algorithm is suggested consisting to replace the constant NIR reflectance ratio in the MUMM AC algorithm [2,3] by the polynomial function of Wang et al. [1]. Indeed, this AC algorithm yields in median differences between retrieved and *in situ* $\rho_w(\lambda)$ below 0.001 in extremely turbid waters (Fig. 1 (c)). Nonetheless, for ρ_w(NIR) above 0.05, the hybrid MUMM NIR corrected AC algorithm still retrieves negative $\rho_w(\lambda)$ values in the blue suggesting a refinement of the polynomial function.

Conclusion

To improve $\rho_w(\lambda)$ retrievals in extremely turbid waters the constant NIR reflectance ratio suggested by Ruddick et al. [2,3] for the MUMM AC algorithm is replaced by the polynomial function used within the NIR-corrected AC algorithm of GOCI [1]. Future work will include a refinement of the polynomial function to account for the most turbid water masses and a validation of MODIS Aqua ocean color images processed with the new hybrid MUMM NIR-corrected AC algorithm.

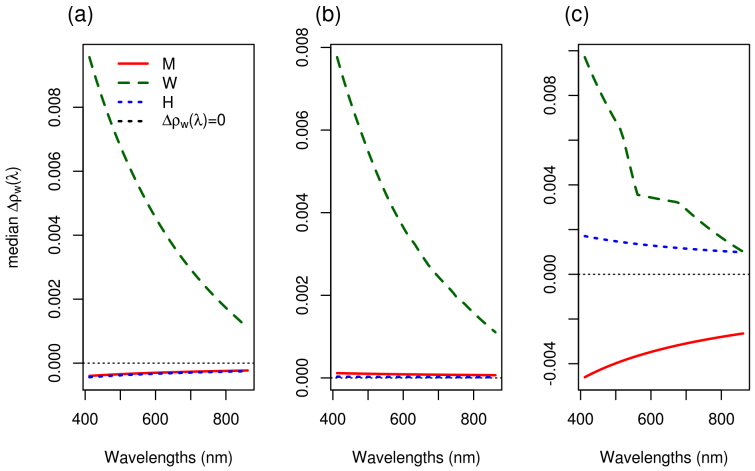

Fig.1: Median difference between in situ and retrieved $\rho_w(\lambda)$ for (a) moderately, (b) very and (c) extremely turbid water. M: MUMM AC algorithm assuming the correct aerosol model, W: NIR-corrected algorithm and H: Hybrid MUMM NIR-corrected AC algorithm assuming the correct aerosol model.

References

1. M. Wang, W. Shi and L. Jiang (2012). ''Atmospheric correction using near-infrared bands for satellite ocean color data processing in the turbid western pacific region,'' Opt. Express, 20, 741-753.
2. K. G. Ruddick, F. Ovidio, and M. Rijkeboer (2000). ''Atmospheric correction of SeaWiFS imagery for turbid coastal and inland waters, '' Appl. Opt., 39, 897-912.
3. K. G. Ruddick, V. De Cauwer, Y. Park and G. Moore (2006). ''Seaborne measurements of near infrared water-leaving reflectance: The similarity spectrum for turbid waters,'' Limnol. Oceanogr. 51, 1167-1179.

Satellite Phytoplankton Functional Type Algorithm Intercomparison and Validation

T. Hirata[1], R. J.W. Brewin[2], N. Hardman-Mountford[3], L. Crementson[4], R. Barlow[5], T. Kostadinov[6], T. Hirawake[7], C. Mouw[8]

[1] Hokkaido University, Sapporo, 060-0810, Japan

[2] Plymouth Marine Laboratory, Plymouth, PL1-3DH, UK

[3] CSIRO, Floreat, 6010, Australia

[4] CSIRO, Hobart, 3195, Australia

[5] Bayworld Centre for Science and Education, CapeTown,7806, South Africa

[6] University of Richmond,Richmond, 23173, USA

[7] Hokkaido University, Hakodate, 041-8611, Japan

[8] Michigan Technological University, 49931, USA

Email: tahi@ees.hokudai.ac.jp

Summary

A satellite phytoplankton functional type algorithm intercomparison project was launched in 2011. The project was tasked to: (i) produce a PFT algorithm user-guide; (ii) collect in situ data for use in algorithm testing; (iii) conduct an algorithm intercomparison; and (iv) conduct an algorithm validation. In this presentation, preliminary results of the intercomparison are presented. The algorithm comparison exercise showed that global micro- and picoplankton distributions did not diverge among algorithms, although some differences were found, notably between algorithms using input data obtained from different satellite sensors.

Introduction

A number of new ocean colour algorithms have been developed to derive global phytoplankton community structure for better understandings of biogeochemical cycles as well as food web structure and trophic energy efficiency of marine ecosystems. Improving the algorithms and obtaining a community consensus as to how phytoplankton community is composed and maintained in our planet, are necessary steps. Therefore, a satellite phytoplankton functional type algorithm intercomparison project was organized in 2011. The project is composed of 4 working groups (WGs): (1) User guide WG,

(2) In situ data compilation WG, (3) Intercomparison WG, (4) Validation WG. In this presentation, we show initial results of from the intercomparison and validation WGs.

Algorithm Comparison

Algorithms used in the current comparisons include: Alvain et al., 2012; Brewin et al., 2010; Bricaud et al., 2012; Bracher et al, 2009; Fujiwara et al., 2011; Hirata et al., 2011; Kostadinov et al., 2010; Roy et al., 2012; and Uitz et al., 2006. While Bracher et al. (2009) model is applicable only to the SCHYMACHY instrument, all other algorithms used SeaWiFS L3 9km data as inputs. The comparison was made for the 2003-2007 period. Monthly climatologies and average fields over the period were generated for comparison of global distributions of micro- and picoplankton as well as their seasonality.

Most algorithms showed a consistent distribution of microplankton (Fig.1). The largest differences were observed between the SCHYMACHY-based algorithm and SeaWiFS-based algorithms, partly because the SCHYMACHY-based algorithm estimates diatoms, not exactly same as "microplankton" defined in the other algorithms, and partly because input satellite data are different. In spite of providing a different output ("frequency of dominance" in Alvain et al., 2008, "% Chla" in others), the Alvain et al (2008) approach showed a distribution of relative abundance of pico-sized phytoplankton similar to these derived from other SeaWiFS-based algorithms However, in both microplankton and picoplankton distributions, the similarity among algorithms do not guarantee results are accurate, and a validation using in situ data is required to give a better understanding as to the accuracy of our current estimation of PFT distributions.

Ongoing validation efforts

In situ datasets (collected within the in situ data compilation WG) are to be matched in space and time with satellite observations. The satellite observations will be used by algorithm developers to process and estimate PFTs, meanwhile, in situ data will be also processed to estimate PFTs based on a method agreed by the community. An objective methodology to test the performance of the satellite algorithm is currently being developed. This includes simple statistical tests such as Type II regression, RMSE and bias, with reference to a similar methodology used in the ESA OC-CCI project.

Retrieval of size fractionated chlorophyll *a* concentration: an application of particle size distribution

Y. Arakawa[1], T. Hirawake[2]* and A. Fujiwara[3]

[1] Hokkaido University, Graduate School of Fisheries Sciences, Hakodate, Hokkaido 041-8611, Japan

[2] Hokkaido University, Faculty of Fisheries Sciences, Hakodate, Hokkaido 041-8611, Japan

[3] National Institute of Polar Research, Tachikawa, Tokyo 190-8518, Japan

***Email**: hirawake@salmon.fish.hokudai.ac.jp

Summary

We have developed an algorithm to estimate size fractionated chlorophyll *a* (chl *a*) concentration using inherent optical properties (IOPs). A function of particle size distribution based on the Junge distribution was applied to express the size fractionated chl *a* and a slope of power function was determined for each sample. This method can estimate three phytoplankton size classes (micro, nano and picoplankton) with root mean square errors less than 36 % when the IOPs were calculated from remote sensing reflectance. Advantage of applying the particle size distribution is possibility to represent other size factions. Algorithm developed in this study succeeded to derive a fraction of ultraplankton (< 5 μm) from *in situ* IOPs.

Introduction

Size of phytoplankton cells are strongly related to limitation factors of photosynthesis such as light and nutrients [1]. Meanwhile sinking speed of the cells and number of trophic levels in marine food web are strongly influenced by the size [2, 3]. Therefore, large spatio-temporal scale observation of the phytoplankton size distribution is important to understand the global carbon cycle and marine ecosystems. While the phytoplankton size distribution has been determined frequently by measuring size fractionated chlorophyll *a* (chl *a*) concentration using several kinds of filters with different pore or mesh size, pigments composition measured with the high performance liquid chromatography (HPLC) is utilized to estimate phytoplankton size class, particularly for development of ocean color algorithms recently [e.g. 4]. However, gaps between the two methods are expected and algorithm to derive phytoplankton size from the former method has not been developed. In this study, we provide a new way to estimate size fractionated chl *a* concentration using light absorption coefficient of phytoplankton and spectral slope of backscattering coefficient and evaluate the performance of algorithm.

Discussion

A function of particle size distribution based on the Junge distribution [5] was applied to express the size fractionated chl *a* concentraions of three size classes (pico, nano and microphtyoplankton defined as fraction of <2, 2-10, >10µm, respectively). For each sample, a slope of power function (η) was determined assuming the minimum and maximum size is 0.7 and 200 µm, respectively. The slope η was derived from spectral slope of backscattering coefficient (γ) and a ratio of absorption coefficients of phytoplankton (a_{ph}) at two wavelengths using a multiple linear regression (Fig. 1).

This method can estimate fraction of three phytoplankton size classes with root mean square errors (RMSE) less than 36 % when the IOPs were calculated from remote sensing reflectance. If η is possible to derive without error, RMSE in estimation of the fractions reduces to <10.5%. Although further improvements in derivation of η from IOPs, a fraction of ultraplankton (< 5 µm) was able to be estimated from *in situ* IOPs (RMSE = 18%). This algorithm is appropriate to compare with typically measured size fractionated chl *a in situ* for oceanographic and marine ecological studies.

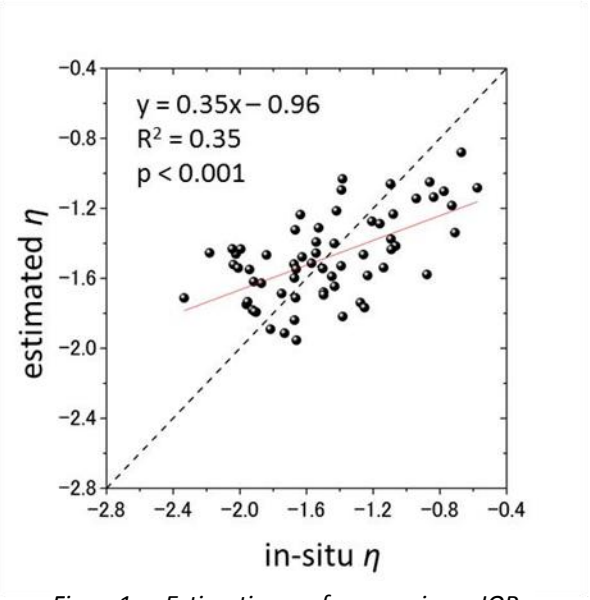

Fig. 1. Estimation of η using IOPs. Comparison between in situ and modeled values.

References

[1] Aiken, J., Pradhan, Y., Barlow, R., Lavender, S., Poulton, A., Holligan, P., and Hardman-Mountford, N. (2009). Phytoplankton pigments and functional types in the Atlantic Ocean: A decadal assessment, 1995-2005. Deep-Sea Res. II, 56: 899-917.

[2] Buesseler, K. O., et al. (2007). Revisiting carbon flux through the ocean's twilight zone. Science, 316: 567– 570.

[3] Lalli, C. M., Parsons, T. R. (1997). Biological Oceanography: An Introduction, Pergamon Press, Oxford.

[4] Hirata, T., Hardman-Mountford, N. J., Brewin, R. J. W., Aiken, J., Barlow, R., Suzuki, K., Isada, T., et al. (2011). Synoptic relationships between surface Chlorophyll-a and diagnostic pigments specific to phytoplankton functional types. Biogeosci., 8: 311-327.

Acknowledgement

This work was supported by JAXA GCOM-C program.

Ocean color data product uncertainty, consistency, and continuity: Evaluation with a new algorithm concept

Hu, Chuanmin[1]; Lee, Zhongping[2]; Franz, Bryan[3], Feng, Lian[4,1];
[1]University of South Florida 140 Seventh Avenue, S., St. Petersburg, FL, 33701, United States, huc@usf.edu;
[2]University of Massachusetts at Boston, Boston, Massachusetts, 02125, United States;
[3]NASA/GSFC, Greenbelt, MD, 20771, United States;
[4]State Key Laboratory of Information Engineering in Surveying, Mapping and Remote Sensing, Wuhan University, Wuhan 430079, China.

ABSTRACT

Studies of long-term ocean changes in response to climate variability call for the most accurate and consistent data products across multiple ocean color missions, and a thorough understanding of the uncertainties is the first step towards a seamless, multi-sensor data record. For a well-calibrated sensor, data product uncertainties result primarily from two sources: the sensor's signal-to-noise ratio (SNR) and the algorithms to derive the products. Using statistics and a recently developed chlorophyll-a (Chl) algorithm (the ocean color index (OCI) algorithm) to determine the highest-quality data, we quantified SNRs, uncertainties in the remote sensing reflectance (R_{rs}) products, noises in the band-ratio OCx Chl products and OCI Chl products from several ocean color instruments including SeaWiFS, MODIS/Aqua, MERIS, and VIIRS. MODISA ocean bands show 2-4 times higher SNRs than SeaWiFS and comparable SNRs to MERIS-RR (reduced resolution, 1.2-km) data. Correspondingly, MODISA Chl products show the least uncertainties when evaluated using a spatial homogeneity test. While MERIS and VIIRS data are still being analyzed, both SeaWiFS and MODISA showed R_{rs} uncertainties within mission specifications, with higher uncertainties in SeaWiFS R_{rs} data possibly due to its lower SNRs. When comparing the global and regionally monthly means for deep oceans, the sensors often showed significant differences (> 5-10%) in the OCx Chl products. These differences may overwhelm real ocean changes and may also bring questions to the fidelity of the global data when only one sensor is operational in orbit. The cross-sensor differences in the product uncertainties are believed to result primarily from different SNRs and imperfect atmospheric corrections. In contrast, the OCI Chl algorithm was designed to be much more tolerant to noises and atmospheric correction errors for clear waters (Chl ≤ 0.25 mg m^{-3}), which indeed led to a much more consistent multi-sensor Chl data record from all sensors evaluated (SeaWiFS, MODISA, MODIST, MERIS, VIIRS) for the deep ocean, with most of the cross-sensor differences reduced by more than half. While some of these uncertainties may be removed using empirical approaches (Fig. 1), the new OCI algorithm provides a solution to bring all sensors together to form a multi-sensor Chl data record (Fig. 2). As we are now entering a transition period to use VIIRS and to design several ocean color continuity missions, it may be time to change the 40-year band-ratio paradigm to a band-subtraction concept or other mechanistic algorithms in order to establish more consistent multi-sensor ocean color data records.

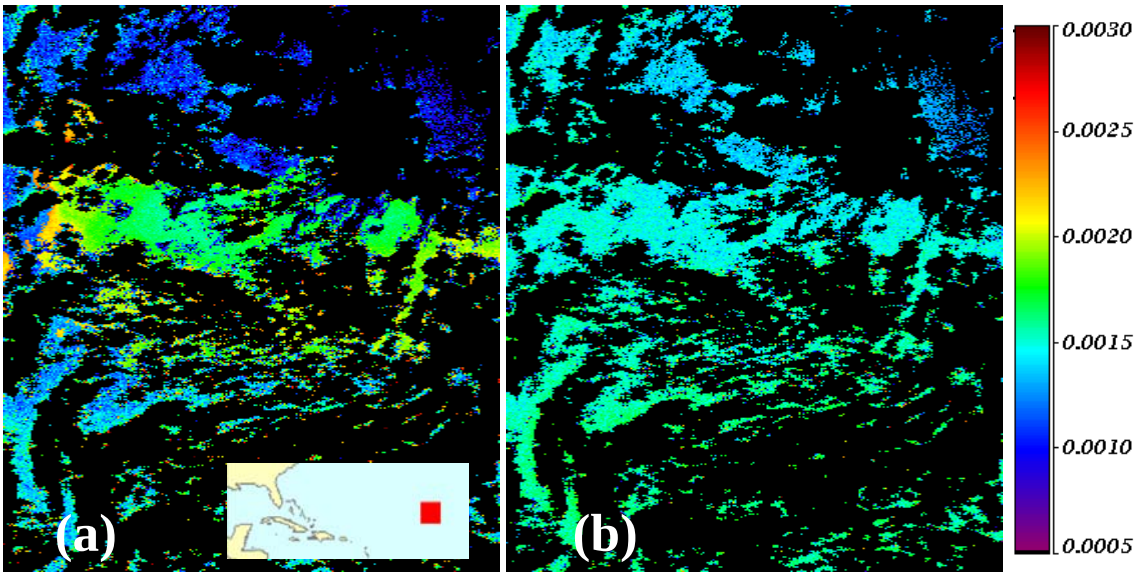

Fig. 1. SeaWiFS $R_{rs}(555)$ (sr^{-1}) in the North Atlantic Gyre (~1500 km x 1500 km centered at 23°N 47°W) on 27 December 2006 from the default SeaDAS processing (a) and after an empirical correction (b). In this oligotrophic gyre $R_{rs}(555)$ is expected to be homogeneous.

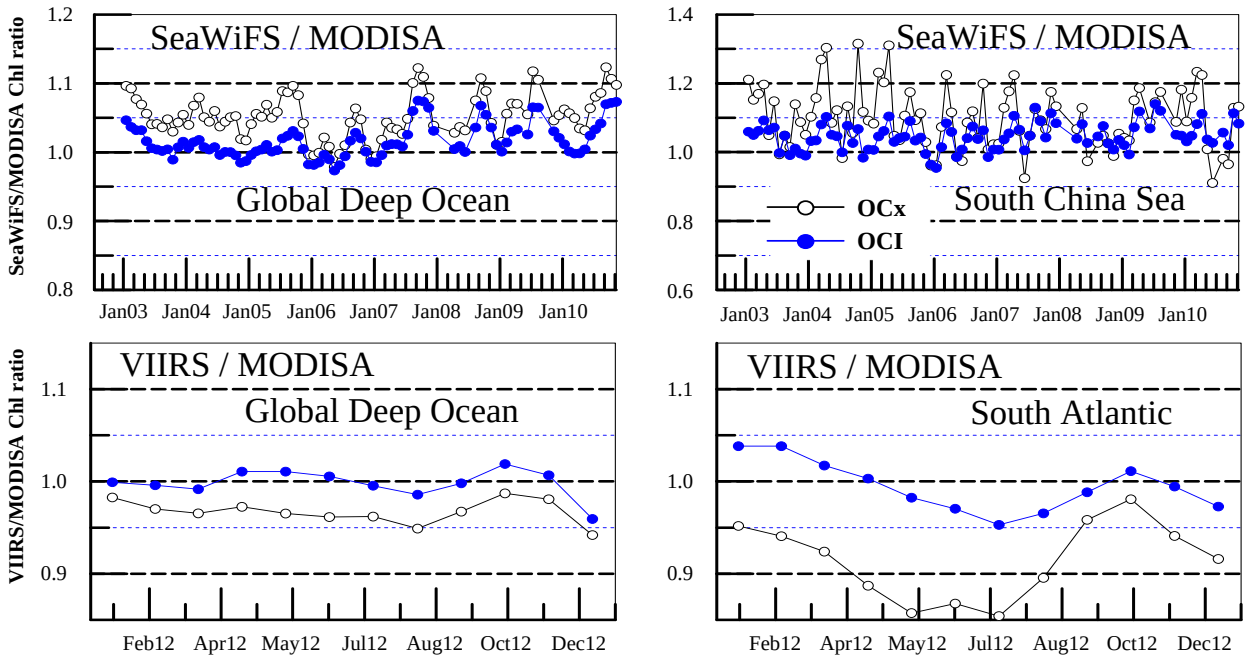

Fig. 2. Chl ratios between different satellite sensors using two algorithms: the default OCx band-ratio algorithm and the new OCI algorithm. The latter is shown to improve cross-sensor consistency significantly.

Particle Retention in the Moroccan Coastal Ocean

Dale A Kiefer[1] and Ian S F Jones[2]

[1] University of Southern California
[2] University of Sydney
Email: ian.s.f.jones@hotmail.com

Summary

Superpositioning of surface current vectors produced by a numerical model and the monthly chlorophyll concentration in the Atlantic ocean near Morocco have revealed a surface eddy trapped by the Canary Islands adjacent to the coast. Near the eddy chlorophyll concentrations are higher 100 km off shore that at more distant locations. There are implications for larvae retention of the northern sardine stocks.

Text

Pelagic fisheries are an important element in the Moroccan economy and the fluctuations in the magnitude and location of the stocks present difficulties for the management of the resource. Schooling small pelagic fish in an upwelling region such as the Moroccan coastal region are able to spawn in the Canary current and have the juveniles develop to adults in the same geographic region. The eggs provided by small pelagic fish float passively in the water column and take order 30 days to develop swimming skills able to counter in the prevailing current.

We used satellite ocean colour data [1] and 0.1 degree resolution hydrodynamic ocean model outputs fused by EASy [2] software to examine the Moroccan coastal ocean from the Gibraltar Straits to the Canary Islands. Monthly averages of the surface current from the hydrodynamic model ECCO2 was used. During the period 1997 to2007 a topographically trapped counter clockwise eddy north of the Canary Islands persistently provided recirculation of chlorophyll rich water. The time for a passive scalar to make one circuit of the eddy is order 40 days.

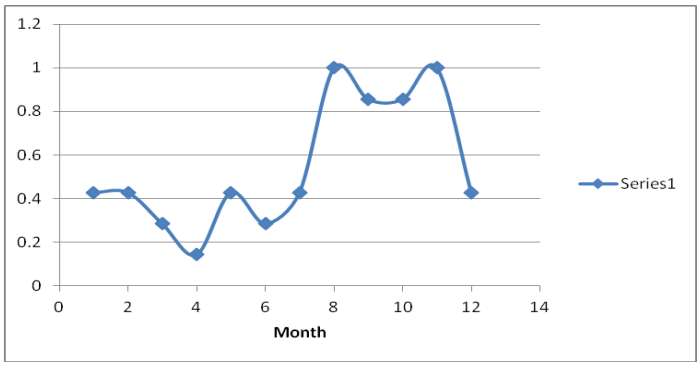

The probability of finding an eddy at 30 degrees N for the period 1997 to 2007.

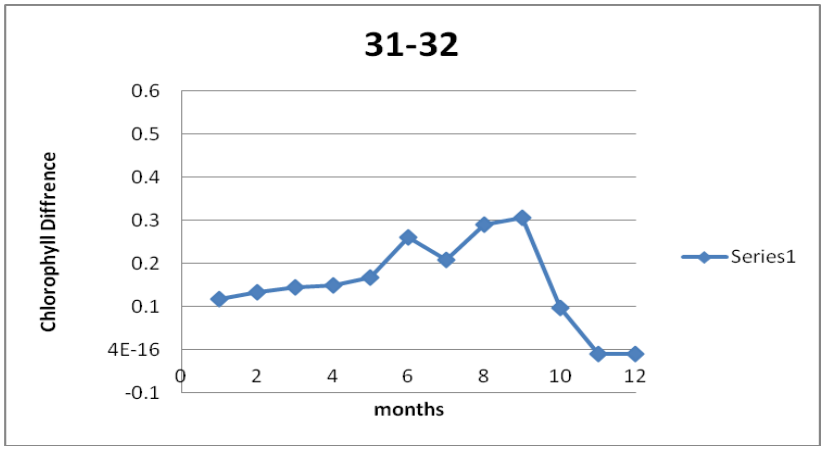

The difference in chlorophyll concentration mg/m^3 100 km from the coast at latitude 31 degrees N and 32 degrees N during the period 1997 to 2007.

Kifani [3] identified two reproduction areas on this portion of the Moroccan Coast and one is near latitude 32 degrees N where in autumn there is a very high probability of finding the counter clockwise rotating eddy. Chlorophyll levels at 100 km from the coast are higher near the eddy than further to the north providing potential food for larvae that remain within this eddy. The eddy probability of occurrence and the larger chlorophyll concentration is shown as a function of the month of observation.

Key words:

Fisheries, Morocco, recruitment, small pelagic

References

[1] Jones, I S F, Y. Sugimori & R. W. Stewart (1993) *Satellite remote sensing of the oceanic environment*. Seibutsu Kenkyusha, Tokyo, pp 528, 1993.

[2] Tsontos, V.M.; Kiefer, D.A. (2000). Development of a dynamic biogeographic information system for the Gulf of Maine *Oceanography 13(3)*: 25-30.

[3] Kifani, S (1998) Climate Dependent Fluctuations of the Moroccan Sardine and their Impact on Fisheries.

Optimized multi-satellite merger to create time series of inherent optical properties in the California Current

M. Kahru[1], Z. Lee[2], R.M. Kudela[3], M. Manzano-Sarabia[4]
B.G. Mitchell[1]

[1]University of California San Diego, Scripps Institution of Oceanography, La Jolla, CA 92093, USA
[2]University of Massachusetts, Dept. of Environmental, Earth and Ocean Sciences, Boston, USA
[3]University of California Santa Cruz, Ocean Sciences Department, Santa Cruz, CA 95064, USA
[4]Universidad Autónoma de Sinaloa, Mazatlán, Sinaloa, México

Summary

We have developed empirically optimized versions of the QAA semianalytic algorithm for 4 ocean color sensors (OCTS, SeaWiFS, MODIS-Aqua and MERIS) by applying a complex optimization process that minimizes the differences in estimated inherent optical properties (IOPs) between match-ups of *in situ* and satellite data and also between the estimated IOPs of the overlapping satellite sensors (SeaWiFS, MODIS-Aqua, MERIS). We then apply the algorithms to standard satellite remote sensing reflectance (*Rrs*) estimates and create merged multi-sensor time series of the near-surface optical characteristics in the California Current region for a time period of over 16 years (November-1996 to December-2012).

Introduction and Results

Satellite observations of ocean color have become the most important method of monitoring global distributions of phytoplankton and ocean productivity, and validating various models. However, the primary output product, the concentration of chlorophyll-a (*Chla*), when estimated with the standard band ratio algorithms primarily represents a change in the total absorption coefficient at the blue wavelength (~440 nm) and is often biased compared to *in situ Chla*. Here we estimate the following set of IOPs using a tuned version of the QAA semianalytic algorithm [1]: the total absorption coefficient at 490 nm (*a490*), phytoplankton absorption coefficient at 440 nm (*aph440*), absorption by dissolved and detrital organic matter at 440 nm (*adg440*) and particle backscattering coefficient at 490 nm (*bbp490*). By tuning the coefficients of the QAA models we were able to remove most of the bias when compared to the *in situ* measurements and between individual sensors (Fig. 1). However, due to the limited number of *in situ* match-ups and their uneven distribution as well as the large errors in the satellite-derived *Rrs*, the uncertainty in the retrieved IOPs is still significant and the differences between the IOPs derived from different sensors cannot be completely eliminated. The merged time series show the dominant annual cycle (Fig. 2) but also significant variability at interannual time scales. The ratio of *adg440* to *aph440* is around 1 in the transition zone of the California Current (100-300 km from coast), is >1 in the coastal zone (0-100 km from coast) and generally <1 offshore (>300

km from coast). *adg440* decreases towards south and towards offshore.

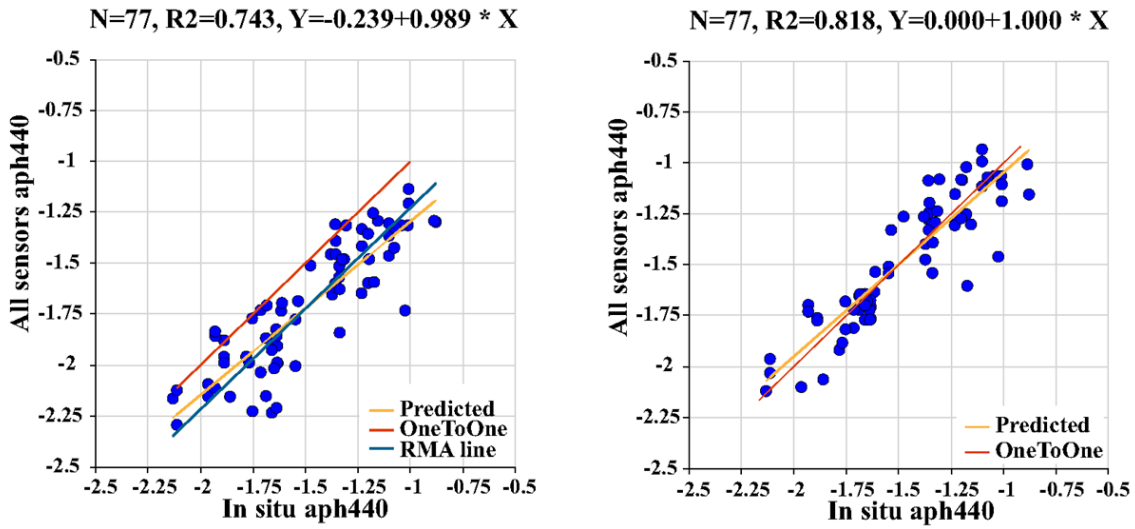

Fig. 1. Combined (OCTS, SeaWiFS, MODISA, MERIS) match-ups (blue dots) of *aph440* between satellite estimates and *in situ* using the standard QAA model (left) and the tuned QAA (right).

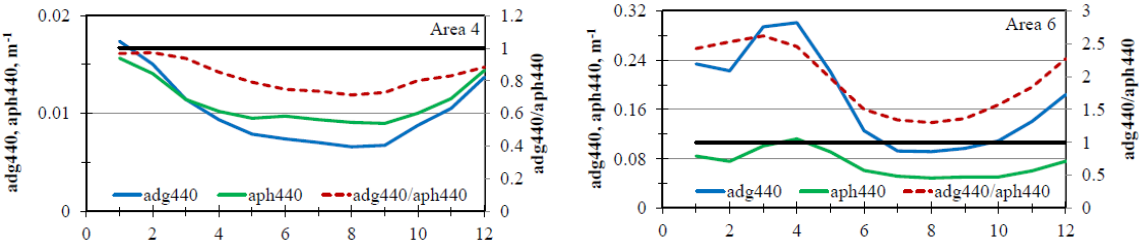

Fig. 2. Mean annual cycle of the merged multi-sensor *adg440*, *aph440* (left axis) and the ratio of *adg440* to *aph440* (right axis) for offshore (left panel, 300-1000 km from coast) and coastal (right panel, 0-100 km from coast) of Southern California. The horizontal black line shows where *adg440*/ *aph440* = 1.

Conclusions

We created a consistent multi-sensor time series of the surface IOPs in California Current region. The merged 16-year time series (1996-2012) show an increasing trend until 2012 in the proxies of phytoplankton biomass in the California Current which is consistent with some observations [2] and model predictions of either increased upwelling or increased nutrient content in the upwelled waters. Also, a trend of decreasing phytoplankton biomass in the oligotrophic subtropical Pacific was shown. However, uncertainties in our estimates of IOPs are still large and require further work.

References

[1] Lee, Z. P., et al. (2002). Deriving inherent optical properties from water color: A multi-band quasi-analytical algorithm for optically deep waters. Applied Optics, 41, 5755-5772.

[2] Kahru, M., Kudela, R., Manzano-Sarabia, M., Mitchell, B.G. (2009). Trends in primary production in the California Current detected with satellite data. J. Geophys. Res., 114, C02004.

Carbon-based Phytoplankton Functional Types and Productivity via Remote Retrievals of the Particle Size Distribution

Tihomir S. Kostadinov[1], Svetlana Milutinović[2], Irina Marinov[2]

1. Department of Geography and the Environment, Univ. of Richmond, Richmond, VA, USA
2. Department of Earth and Environmental Science, Univ. of Pennsylvania, Philadelphia, PA, USA

E-mail: tkostadi@richmond.edu

Assessment of the ocean's role in biogeochemical cycling and climate formation requires characterization of oceanic ecosystems' structure and function. This can be accomplished by understanding the spatio-temporal variability of phytoplankton functional types (PFTs) and its physical drivers. Satellite remote sensing of ocean color is the best available tool for sustained continuous oceanic ecosystem observation. Various algorithms for the retrievals of PFTs have been developed in recent years, using different theoretical bases and PFT definitions [1]. The algorithm of Kostadinov et al. [2,3] defines the PFTs in terms of percent contribution to biovolume of three size-based PFT groups: picophytoplankton (here, cell diameter between 0.2 and 2 μm), nanophytoplankton (2–20 μm) and microphytoplankton (20–50 μm). This method is based upon retrievals of the parameters of an assumed power-law particle size distribution (PSD), using existing spectral backscattering retrievals [4] and a theoretically derived look-up table.

Phytoplankton carbon biomass (rather than biovolume) is more closely related to biogeochemical cycling and climate and it is needed for deriving carbon-based phytoplankton productivity from ocean color [5]. Here, we develop a procedure to recast the PFTs in terms of relative contribution to carbon biomass, rather than volume. We start with the same PSD retrievals as the volume-based approach (here, derived from monthly SeaWiFS r2010.0 imagery), but convert cell volumes in each size class to carbon biomass before PFT calculation. We use the allometric relationships of Menden-Deuer and Lessard [6], as in the initial effort by [7]. Fig. 1 illustrates the SeaWiFS mission climatology for picoplankton (A) and microplankton (B). As expected, picoplankton dominate oligotrophic areas and microplankton are abundant only in eutrophic areas.

Partitioned carbon biomass estimates were also uses as input to the vertically-integrated version of the carbon-based productivity algorithm (CbPM) [5] in order to estimate PFT-specific NPP. PFT-specific maximum growth rates were based on [8], and PFT-specific chlorophyll concentrations were based on SeaWiFS chlorophyll (r2010.0) and the size fractions of Uitz et al. [9]. Results for the August 2007 image are presented in Fig. 1C for picoplankton and Fig. 1D for microplankton.

At this stage the presented products are preliminary and retrieved variables may not be necessarily geophysically accurate. While this especially applies to the absolute values of carbon biomass and productivity, carbon-based PFTs (Fig. 1A-B) are defined by ratios of biomass. Our goal is to assess the feasibility of using ocean color-based retrievals of the particle size distribution parameters to estimate size-partitioned carbon-based biomass and productivity. Next steps will focus on further methodology

improvements, comparison to existing algorithms [1, 10, see also 7], and validation of these novel satellite ocean color products.

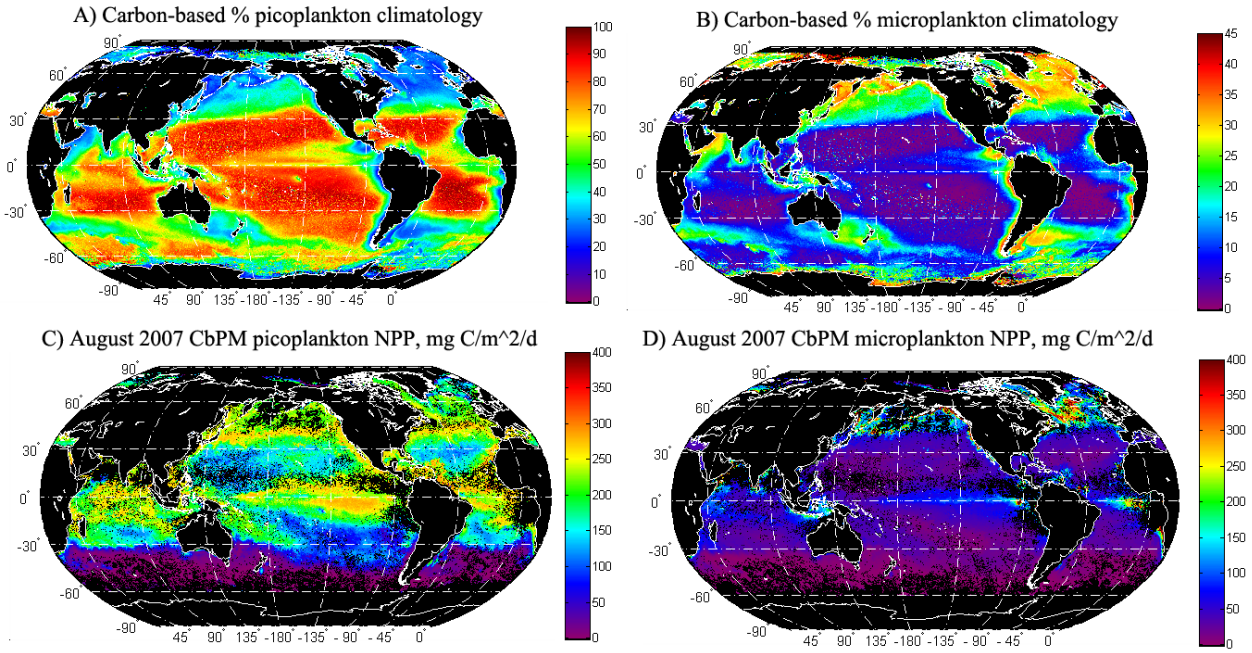

Figure 1. *SeaWiFS mission climatology (1997-2010) of percent allometric carbon biomass due to (A) picoplankton (0.2 -2 μm) and (B) microplankton (20-50 μm). Note the different colorbar scales. August 2007 CbPM net primary productivity due to (A) picoplankton (0.2-2 μm), and (B) microplankton (20-50 μm), using allometric PSD-based carbon estimates.*

References

[1] Hirata, T., et al. (2012), Comparing satellite-based phytoplankton classification methods, Eos Trans. AGU, 93(6).

[2] Kostadinov, T. S., D. A. Siegel, and S. Maritorena (2009), Retrieval of the particle size distribution from satellite ocean color observations, *Journal of Geophysical Research-Oceans*, *114*, 22.

[3] Kostadinov, T. S., D. A. Siegel, and S. Maritorena (2010), Global variability of phytoplankton functional types from space: assessment via the particle size distribution, *Biogeosciences*, *7*(10), 3239-3257.

[4] Loisel, H., Nicolas, J.-M., Sciandra, A., Stramski, D., and Poteau, A. (2006), Spectral dependency of optical backscattering by marine particles from satellite remote sensing of the global ocean, J. Geophys. Res., 111, C09024, doi:10.1029/2005JC003367.

[5] Behrenfeld, M., E. Boss, D. Siegel, and D. Shea (2005), Carbon-based ocean productivity and phytoplankton physiology from space, *Global Biogeochemical Cycles*, *19*(1), GB1006.

[6] Menden-Deuer, S., and E. Lessard (2000), Carbon to volume relationships for dinoflagellates, diatoms, and other protist plankton, *Limnology and Oceanography*, *45*, 569–579.

[7] Kostadinov, T. S. (2009), Satellite Retrieval of Phytoplankton Functional Types and Carbon via the Particle Size Distribution, Ph.D. thesis, 217 pp, University of California, Santa Barbara, CA, USA.

[8] Ward, B. A., S. Dutkiewicz, O. Jahn, and M. J. Follows (2012), A size-structured food-web model for the global ocean, Limnology and Oceanography, 57(6), 1877-1891.

[9] Uitz, J., H. Claustre, A. Morel, and S. B. Hooker (2006), Vertical distribution of phytoplankton communities in open ocean: An assessment based on surface chlorophyll, Journal of Geophysical Research-Oceans, 111(C8).

[10] Uitz, J., H. Claustre, B. Gentili, and D. Stramski (2010), Phytoplankton class-specific primary production in the world's oceans: Seasonal and interannual variability from satellite observations, Global Biogeochem. Cycles, 24, GB3016, doi:10.1029/2009GB003680.

ROBUST $K_d(490)$ AND SECCHI DEPTH ALGORITHMS FOR REMOTE SENSING OF OPTICALLY COMPLEX WATERS DOMINATED BY CDOM

Alikas, Krista[1]; Kratzer, Susanne[2,3]; Reinart, Anu[1]
[1]Tartu Observatory, Tartumaa, Toravere, 61602, Estonia; e-mail: alikas@ut.ee
[2]Stockholm University, Stockholm, Stockholm, SE-106 91, Sweden
[3]Brockmann Consult GmbH, Max-Planck-Str. 2, 21502 Geesthacht, Germany

ABSTRACT

We developed and compared different empirical and semi-analytical algorithms for optically complex waters to retrieve the diffuse attenuation coefficient of downwelling irradiance, $K_d(490)$, and tested them against an independent data set, in order to ultimately suggest a robust algorithm that is valid for optically complex water bodies with high concentrations of CDOM.

In the first approach, developed by Austin and Petzold (1981), revisited by Mueller (2000), $K_d(490)$ was estimated from the empirical relation between $K_d(490)$ and the ratio of remote-sensing reflectance at two wavelengths within the visible spectrum. Due to MERIS characteristics, several bands in the longer wavelengths (560, 620, 660, 710 nm) were available to retrieve better reference conditions over CDOM dominated coastal waters. Various sets of band ratios were tested to achieve the best estimate for *Kd*(490) where reflectance data was retrieved either using MERIS standard algorithms (ODESA) or an alternative processor for atmospheric correction and water quality parameters (FUB WeW). In the second approach, $K_d(490)$ was expressed as a function of inherent optical properties (IOP) after the algorithms by Lee et al. (2005b) and Kirk (1994). The IOPs needed as an input for these algorithms were retrieved from MERIS level 2 products (algal_2, total_susp and yellow_subs) or taken from the literature.

We compared the MERIS derived $K_d(490)$ values by various algorithms with values measured in optically complex coastal waters in the Baltic Sea which showed very good estimates for both methods. The results indicate that for empirical algorithm, the RMSE (%) decrease and the coefficients of determination (R2) increase when using the longer wavelengths in the visible spectrum as reference band. The best estimates were retrieved by using the reflectance ratio of MERIS bands *Rrs*(490)/*Rrs*(710), which provides a promising approach (RMSE 14%, R2=0.98, N=14) for estimating $K_d(490)$over a wide range of values (0.2 - 2.5m^{-1}). Figure 1 shows $K_d(490)$ for the Baltic Sea on 22 May 2002 using the best algorithm.

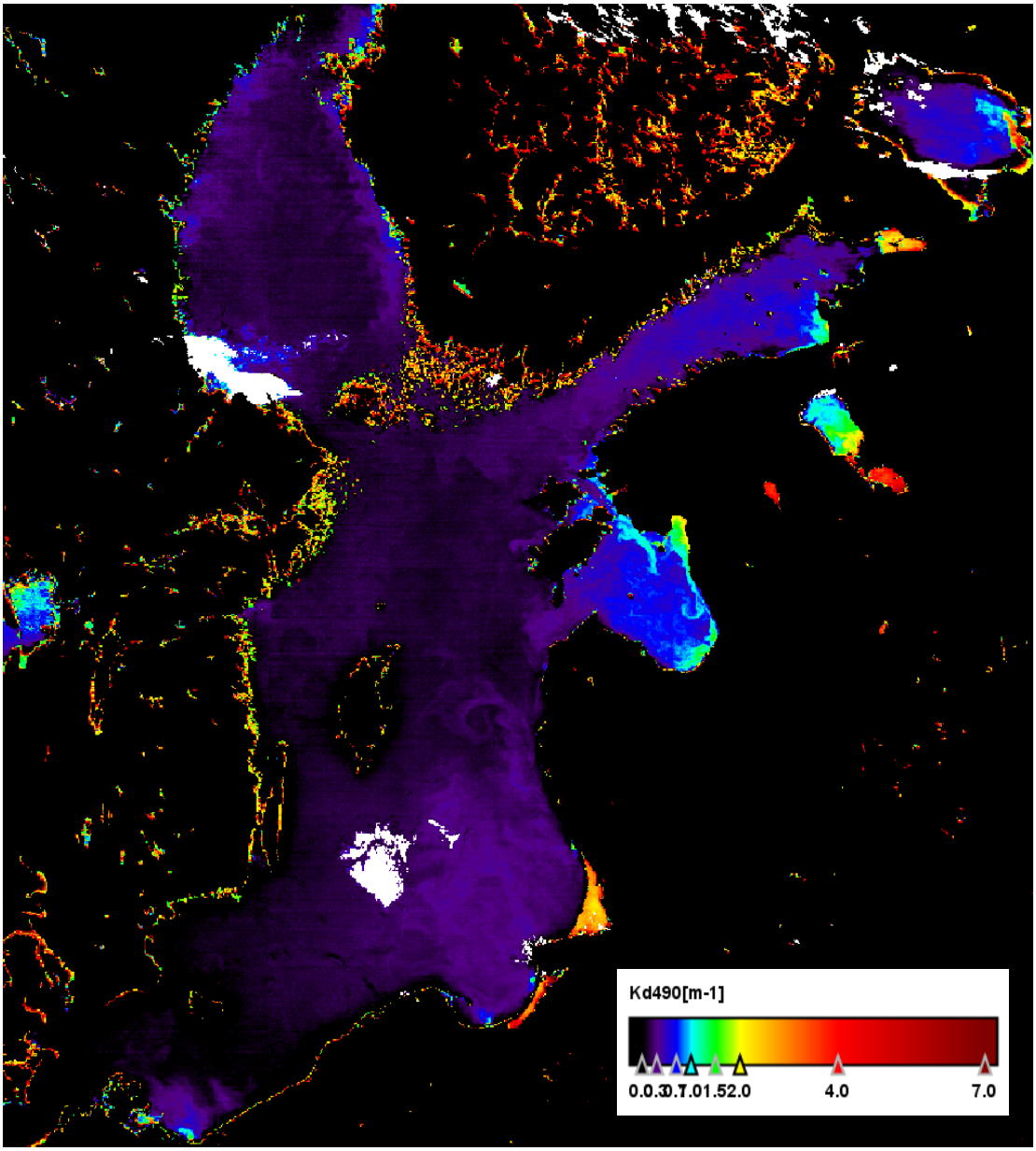

Figure 1 $K_d(490)$ image of the Baltic Sea on 22 May 2002 using MERIS bands *Rrs*(490)/*Rrs*(710).

Estimation of spectral attenuation coefficient of downwelling irradiance: from oligotrophic to coastal waters

Zhongping Lee[1], Chuanmin Hu[2], Shaoling Shang[3], Keping Du[4], Marlon Lewis[5], Robert Arnone[6]

[1] University of Massachusetts Boston

[2] University of South Florida

[3] Xiamen University

[4] Beijing Normal University

[5] Dalhousie University

[6] University of Southern Mississippi

The attenuation coefficient of downwelling irradiance at 490 nm (Kd490) is a standard product for satellite ocean color missions. Presently Kd490 is derived from the ratio of remote sensing reflectance (Rrs) at ~490 nm and ~555 nm, and it is limited to this single spectral band. Studies from photosynthesis to heat transfer, however, require spectral Kd, where empirical band ratios could be cumbersome for its generation. In principle, Kd is a function of sun angle and water's inherent optical properties (IOPs) including absorption and backscattering coefficients. Because these IOPs products are also generated routinely from satellite measurements, it is logical to evolve the empirical Kd product to semi-analytical Kd product that is not limited to one wavelength but flexible for hyperspectral data. The semi-analytical Kd product also explicitly accounts for the impact of sun angle and the contribution of backscattering coefficient. Furthermore, the analytical nature makes it straightforward to quantify the product uncertainty pixel-by-pixel. Here, using field data collected from oligotrophic ocean to coastal waters covering >99% of the range of global oceans, we evaluate the semi-analytical Kd product and demonstrate the applicability of the algorithm as well as the quality of the product. Data products generated from ocean-color sensors are also presented to provide a global perspective.

Deriving suspended sediment and turbidity products from remote sensing reflectance in turbid coastal waters

Soo Chin Liew, Chew Wai Chang and Boredin Saengtuksin

National University of Singapore, Centre for Remote Imaging, Sensing and Processing,
Singapore 119260, Singapore
Email: scliew@nus.edu.sg

Summary

Remote sensing reflectance measured by high resolution satellite sensors is used to map water turbidity and total suspended sediment concentration (TSS) in turbid coastal waters. Empirical relations between water turbidity, backscattering coefficient and TSS were derived using in-situ measurement data. These relations were applied to satellite derived backscattering coefficient to produce maps of turbidity and TSS.

Introduction

Water reflectance depends on the intrinsic optical properties, primarily the absorption and scattering coefficients. Hence, it is possible to derive the water turbidity and TSS, both related to scattering by suspended particles, from remote sensing reflectance measured by satellite sensors. In this paper, we describe our experience in providing a user service for mapping water turbidity and TSS in turbid coastal waters using high resolution SPOT-5 satellite. The service was provided in conjunction with the environmental impact assessment of a bridge construction project. The visible bands have considerable penetrating power through water. Hence, the signals from these bands are likely to be influenced by water depth. We used the NIR band to derive water turbidity and TSS to minimize this problem.

Method

The SPOT satellite data were converted to the top-of-atmosphere reflectance, and corrected for Rayleigh scattering and molecular absorption using routines in the 6S package [1] with considerations of the sensor spectral response. The SWIR band is used to correct for surface glints. The water reflectance is converted to sub-surface remote sensing reflectance and the backscattering coefficient was computed using an algorithm based on the Quasi-Analytical Algorithm (QAA) [2] [3]. In-situ measurements of water reflectance, suspended sediment concentration and water turbidity were performed to establish the relations between water backscattering coefficient, turbidity and TSS. The relations were applied to convert the satellite measured water backscattering coefficient to water turbidity (in nephelometric turbidity unit, NTU) and TSS.

Results and discussion

Results of in-situ measurements conducted during seven field trips indicate that the backscattering coefficient has a linear relation with water turbidity (R^2 = 0.93). The backscattering coefficient values were derived from above-water reflectance spectra measurement by a hand-held spectroradiometer using a spectral matching method [4]. TSS (in mg/l, measured by the filtration method) was found to

have a power-law relation with turbidity (R^2 = 0.84) (see Fig. 1). The field trips were conducted over a period of 3 years from Sep 2009 to Sep 2012 at twenty sampling locations. The turbidity values ranged from about 1.5 NTU to over 100 NTU. Only samples with turbidity below 70 NTU (136 out of 140 samples) were used in establishing the regression relations. These relations were applied to the backscattering coefficient derived from satellite data to produce maps of water turbidity and TSS at about half yearly interval.

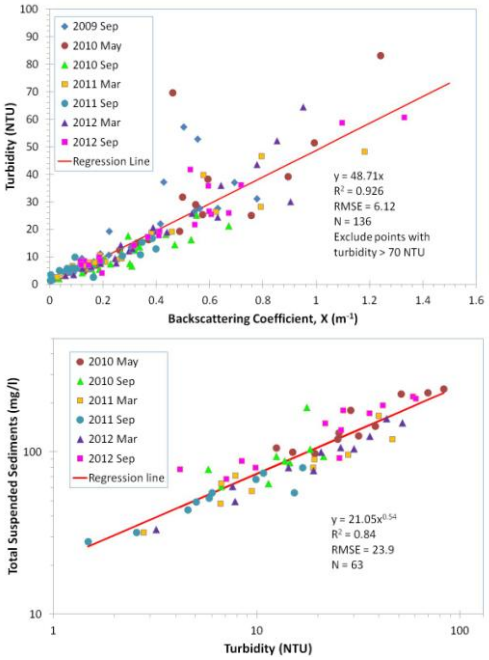

Fig. 1: Relations between backscattering coefficient and turbidity (top), turbidity and TSS (bottom).

Due to prevalence of cloud covers in the region, most of the field trips did not coincide with satellite data acquisition dates. In one occasion (13 March 2012), the satellite derived values of backscattering coefficient were found to agree quite well with those derived from in-situ spectral reflectance measurements collected within an hour of the satellite pass (bias = 0.07 m^{-1}, R^2 = 0.50)

Conclusion

We demonstrated that water turbidity and TSS maps can be derived from high resolution satellite data such as those acquired by the SPOT and Landsat satellites. Our experience with measurements across different water types seem to indicate that the relation between turbidity and backscattering coefficient is quite robust. This is probably due to the fact that turbidity and backscattering coefficient are both determined by the scattering properties of suspended particles. Our method of deriving backscattering coefficient does not require the availability of external data and hence can be used for routine operational applications in monitoring water turbidity for different water types. On the other hand, The relation of TSS with turbidity is expected to depend on the bulk density, refractive index and size distribution of the suspended particles. This relation needs to be established before TSS can be derived from remote sensing measurements.

References

[1] Vermote, E., Tanre, D., Deuze, J. L., Herman, M., Morcette, J. J. (1997). Second simulation of the satellite signal in the solar spectrum: An overview. IEEE Transactions on Geoscience and Remote Sensing, 35: 675-686.

[2] Lee, Z. P., Carder, K.L., Arnone, R. (2002). Deriving inherent optical properties from water color: A multiband quasi-analytical algorithm for optically deep waters. Applied Optics, 41: 5755-5772.

[3] Liew, S. C., He, J. (2008). Uplift of a coral island in the Andaman Sea due to the 2004 Sumatra earthquake measured using remote sensing reflectance of water. IEEE Geoscience and Remote Sensing Letters, 5: 701-704.

[4] Lee, Z. P. et. al. (1999). Hyperspectral remote sensing for shallow waters. 2. Deriving bottom depths and water properties by optimization. Appl. Opt. 38: 3831–3843.

An extension of water color remote sensing: unusual link to particle particulate organic carbon

Ronghua Ma Guangjia Jiang

(Nanjing Institute of Geography and Limnology, Chinese Academy of Sciences, Nanjing 210008, China; rhma@niglas.ac.cn; +86-25-86882168)

The retrieval of only three parameters by water color remote sensing seems to lead to a narrow road, which may inversely limit the development of water color remote sensing. This manuscript aims to discover an unusual link between phytoplankton pigments with particulate organic carbon (POC), which extends the retrieval water parameters by remote sensing.

Study Area

Taihu Lake, a typical eutrophic lake with a water surface area of 2338 km^2, is located in the middle and lower reaches of Yangtze River, Easten China (Fig.1). Cyanobaceria blooming always happen especially in summer in the last 20 years (Duan et al., 2009; Ma et al., 2009).

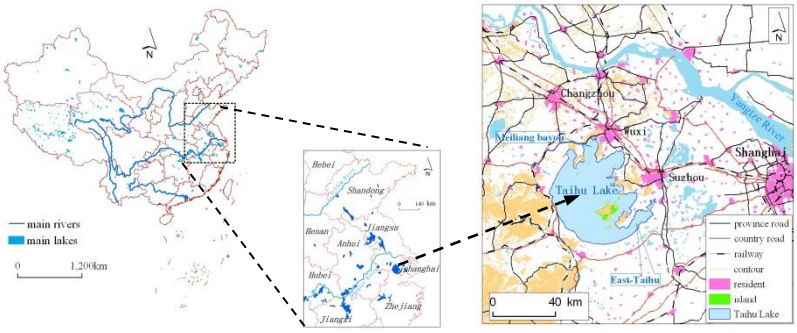

Fig.1 Location of Taihu Lake

Data

Five campaigns with 137 surface water samples were made during January, March, May, August and November 2011. The measured parameters included remote sensing reflectance, backscattering, absorption (due to phytoplankton pigment, non-algal particulate matter and CDOM), Chla, POC, SPM, SPIM (suspended particulate inorganic matter) and SPOM (suspended particulate organic matter). MERIS images were used.

Results

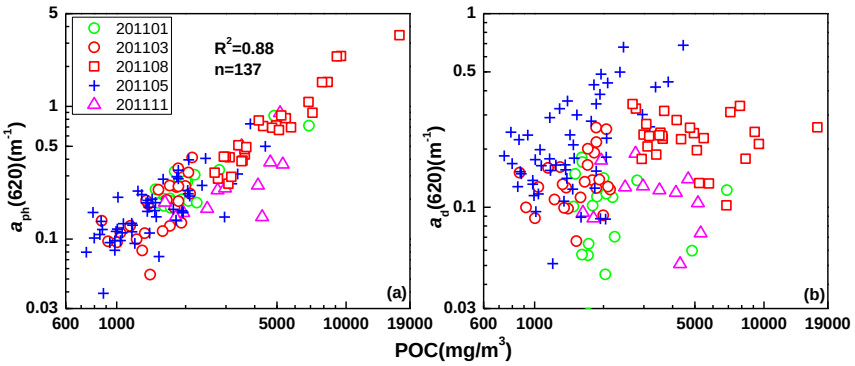

Fig.2 Relationships between POC and (a) phytoplankton pigment absorption at 620 nm ($a_{ph}(620)$ and (b)

detritus absorption at 620 nm ($a_d(620)$).

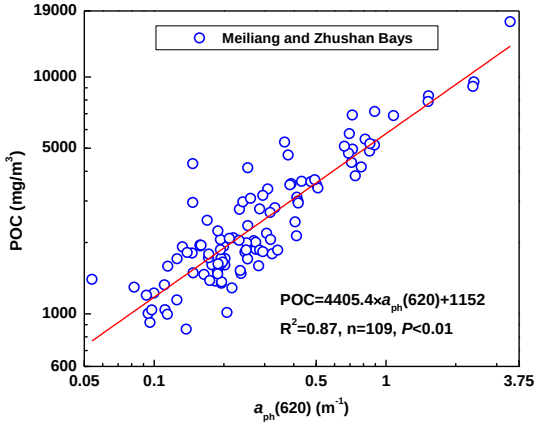

Fig.3 Estimation of POC concentration from $a_{ph}(620)$) using data sampled from Meiliang and Zhushan Bays in the 5 cruises in Taihu Lake.

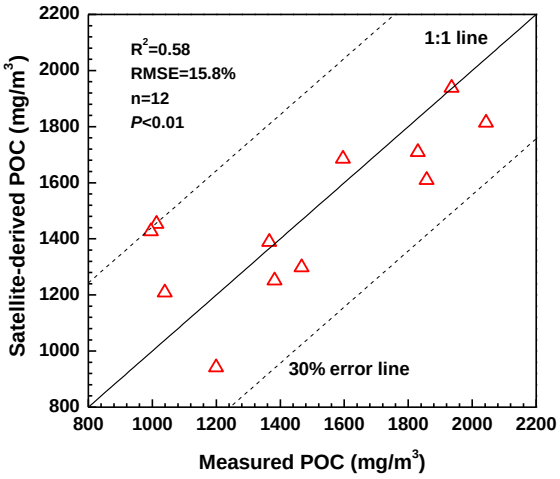

Fig. 4 Comparison of measured POC and MERIS-derived POC using data from the measurement campaign in May 2011.

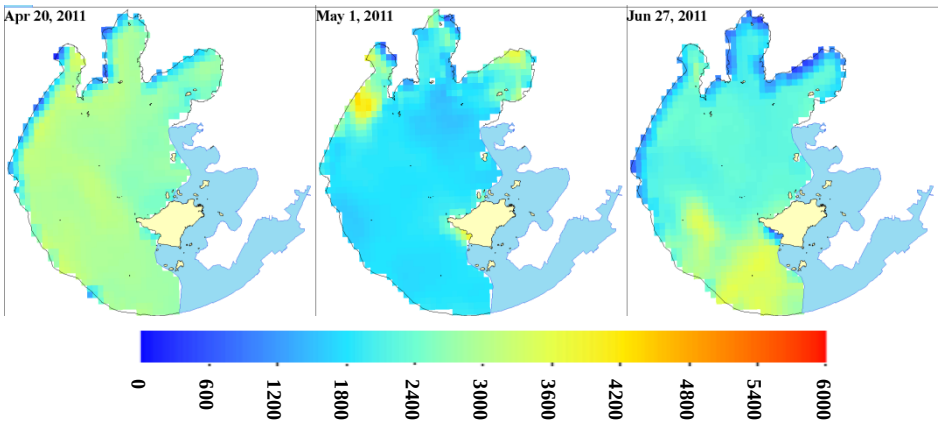

Fig.5 MERIS-derived POC in Taihu Lake surface waters using the link relationship

Conclusions

By linking POC to $a_{ph}(620)$ and then to remote sensing reflectance, it was possible to develop a new algorithm to examine the spatio-temporal dynamics of surface POC in Taihu Lake. It provides a needed new tool to explore carbon cycling in inland waters.

Remote sensing of Lake Taihu

Ronghua Ma

State Key Laboratory of Lake Science and Environment, Nanjing Institute of Geography and Limnology, Chinese Academy of Sciences, Nanjing 210008, China

Email: rhma@niglas.ac.cn

Summary

Lake Taihu, the third largest freshwater lake in China, is one of the main drinking water sources for 40 million people in the Jiangsu and Zhejiang provinces, and Shanghai municipality. In recent years, it has experienced significant pollution due to rapid economic growth in the surrounding region. Increasing eutrophication and reoccurring algal blooms pose a significant threat to the millions of people who rely on the lakes for drinking water supply. Around Lake Taihu, we did a series of water colour research including IOPs, AOPs, phytoplankton pigments and algal blooms. We also try to develop new algorithm to estimate DOC and POC. Here I'm going to introduce all of these.

Introduction

According to ecological theory and *in situ* observations in Lake Taihu, a four-phase development hypothesis has been proposed for the process of the cyanobacterial bloom forming: dormancy in winter, recruitment in spring, growth and float to the water surface in summer, and sink to the sediment in autumn [1]. During the early bloom stage, it is crucial to detect and quantify cyanobacterial blooms [2]. Early detection allows local authorities to make appropriate changes in water supply and catchment management. In summer and autumn, it's important to monitor the blooms and focus on the complex integration of many environmental factors on algal blooms.

To better explore carbon cycling in the aquatic ecosystems, it is necessary to understand the concentrations and fate of the main organic components. The role of particulate organic carbon (POC) and dissolved organic carbon (DOC) is particularly important and plays a fundamental role in the attenuation of solar radiation.

Discussion

The phytoplankton species variations from early recruitment to bloom formation pose

significant challenges in remote sensing algorithm development, as most algorithms depend on the mass-specific phytoplankton pigment absorption coefficient either explicitly (such as the Gons and Simis algorithms) or implicitly (such as the band-ratio algorithms). This effect was clearly shown in the algorithm performance after local parameterizations. One potential explanation of the high mass-specific absorption coefficient in the local data that the pigment concentrations may have been underestimated due to inefficient pigment extraction. However, we have no evidence to support this speculation, but rather believe that the high mass-specific absorption is more likely caused by the changing pigment composition (Chla in all phytoplankton, Chlb in green algae, and Chlc in diatoms) in different species, which makes universal parameterizations difficult.

Conclusions

From a practical point of view, all algorithms need to be applied to satellite imagery to test their performance, validity, and applicable range. Unfortunately, such tests for the cited algorithms have rarely been available due to a variety of reasons. For our case study here, direct validation using MERIS satellite data suffered from lack of high-quality (cloud-free, glint-free, relatively low aerosols) data. Among all polar-orbiting satellite sensors, MERIS is perhaps the most applicable sensor for its 620-nm and 709-nm bands, 300-m spatial resolution, 2-3 day revisit time, and high signal-to-noise ratio. Unfortunately, of all MERIS data collected during the cruise survey period (23 April to 3 May 2010) or adjacent days, no image was sun glint free with minimal cloud cover. Although data from the Moderate Resolution Imaging Spectroradiometers (MODIS) are available for their much wider swath width than MERIS, the sensors are not equipped with the required spectral bands (620 and 709-nm). Likewise, the Geostationary Ocean Color Imager (GOCI) launched in 2010 measures the study region 8 times a day at 500-m spatial resolution, the lack of spectral bands makes it difficult for using these algorithms. In the future, MERIS-like sensors on geostationary platforms may provide the ultimate solution on routine monitoring and quantitative assessment of cyanobacterial blooms in these inland water bodies.

References

[1] F. X. Kong, and G. Gao, “Hypothesis on cyanobacteria bloom-forming mechanism in large shallow eutrophic lake,” Acta Ecologica Sinica, vol. 25, no. 3, pp. 589-595, 2005.

[2] H. Duan, R. Ma, and C. Hu, “Evaluation of remote sensing algorithms for cyanobacterial pigment retrievals during spring bloom formation in several lakes of East China,” Remote Sensing of Environment, vol. 126, no. 0, pp. 126-135, 2012.

Development and Analysis of Ocean Color Satellite DOM Products for Studies in Coastal Ocean Dynamics

Antonio Mannino[1], Rachael Dyda[2], Peter Hernes[2], Michael Novak[1], Stan Hooker[1], Kim Hyde[3]
[1]NASA Goddard Space Flight Center, [2]UC-Davis, [3]NOAA NEFSC

In the coastal ocean, multiple source inputs and removal processes yield variable distributions of colored dissolved organic matter (CDOM), dissolved organic carbon (DOC) and particles on a seasonal to inter-annual basis. Our objectives entail development and validation of regional ocean color satellite algorithms for the CDOM absorption coefficient (a_{CDOM}), DOC and lignin phenols (as proxies for terrigenous DOM), and application of these algorithms to quantify seasonal to interannual distributions, inventories, cross-shelf fluxes and study the processes that contribute and remove organic matter from coastal zone. Field measurements of remote sensing reflectance (Rrs) and a_{CDOM} are used to develop regional satellite algorithms to retrieve a_{CDOM} and CDOM spectral slope (S). Empirical relationships of a_{CDOM} and S with DOC and lignin phenols from field observations will be applied to retrieve DOC and lignin phenols from ocean color satellite data. We have demonstrated strong linear relationships between a_{CDOM} and discrete measurements of DOC throughout the northeastern U.S. continental margin and between lignin phenols and a_{CDOM} or S within the southern Middle Atlantic Bight and Chesapeake Bay. The correlations between DOC and CDOM vary seasonally and between regions requiring variable coefficients for each region (southern Middle Atlantic Bight, Hudson estuarine plume and western Gulf of Maine). Nevertheless, the regional and seasonal a_{CDOM} to DOC correlations enable satellite retrieval of DOC through the a_{CDOM} algorithm.

A new approach to estimate the aerosol scattering radiance for Case 2 waters

Zhihua Mao, Delu Pan, Difeng Wang , Fang Gong

State Key Laboratory of Satellite Ocean Environment Dynamics,

Second Institute of Oceanography, State Oceanic Administration

36 Bochubeilu, Hangzhou, 310012, China

ABSTRACT

The atmospheric correction of satellite remote sensing data for turbid waters meets some problems in which the aerosol scattering reflectance is the most uncertain term to be determined. The standard method of the atmospheric correction is based on the dark pixel assumption of the water-leaving reflectance in the two NIR bands and this assumption usually becomes invalid for turbid coastal waters. A new approach was developed to accurately estimate the aerosol scattering reflectance for the turbid coastal waters. This approach is based on the idea that the aerosol scattering reflectance can be obtained from the known water-leaving reflectance of the satellite measured reflectance at the top of the atmosphere. The water-leaving reflectance is determined from the choice of a look-up table of in situ measurements based on the Angstrom law of the candidate aerosol scattering reflectance using the best non-linear least squares fit function. The performance of the approach was evaluated using the simulated reflectance at the top of the atmosphere, the Sea-viewing Wide Field-of-view Sensor (SeaWiFS) imagery, and in situ measured aerosol optical thickness. This approach is based on the assumption of the aerosol scattering reflectance following the Angstrom law instead of the standard dark pixel assumption, providing a new approach of the atmospheric correction of satellite remote sensing data.

Keywords: Atmospheric correction; Aerosol scattering reflectance; Satellite remote sensing; Coastal waters

Detecting dominant Phytoplankton Size Classes (micro-, nano- and pico-phytoplankton) from SeaWiFS data in the Mediterranean Sea: spatial and temporal variability

A. Di Cicco[1,2], M. Sammartino[3,4], S. Marullo[1], R. Santoleri[4] , [1]F. Artuso

[1]ENEA - Technical Unit Development of Applications of Radiations - Diagnostic and Metrology Laboratory – Frascati (Italia)
[2]Università degli Studi della Tuscia - DEB - Laboratorio di Oceanologia Sperimentale ed Ecologia Marina, Civitavecchia (Italia)
[3]Università di Pisa, facoltà di scienze Ambientali, Dipartimento di Scienze della Terra, Pisa (Italia)
[4]Istituto di Scienze dell'Atmosfera e del Clima – CNR – Gruppo Oceanografia da Satellite – Roma (Italia)
Email: salvatore.marullo@enea.it

Summary

In this paper we present the analysis of the spatial and temporal distribution of the Phytoplankton Size Classes in the Mediterranean Sea derived from a SeaWiFS satellite dataset produced using a Mediterranean regional algorithms for case 1, case 2 and transition waters. The results show the open Mediterranean water are mainly dominated by picoplankton all around the year with a maximun during summer and minima in autumn and winter in open sea regions not affected by intense spring blooms. Coastal and intense bloom regions, instead, show the dominance of nano and micro plankton.

Introduction

In recent years several models have been proposed to identify the contribute of different Phytoplankton Size Classes (PSCs) and Phytoplankton Functional Types (PFTs) to the total phytoplankton chlorophyll-*a* biomass or to estimate Particle Size Distribution from remote sensing Ocean Color data. These bio-optical algorithms can provide an important instrument for a synoptic studies of the Phytoplankton community structure and its spatial and temporal variability and then improve our knowledge about the ecological and biogeochemical dynamics connected with it. Validation exercises performed at global scale using data representative of a variety possible situations have shown that the models are able to capture the general trend of the size-specific chlorophyll-a concentration [1], [2], [3]. Of course, at regional scale deviation from this trends agreement can be observed.

Discussion

In this work we concentrated our investigation over the Mediterranean an Black Seas region applying two models, based on biological and ecological approaches , proposed by Brewin and co-authors [2] and by Hirata and co-authors [3] to the SeaWiFS mission data from 1998 to 2010. The regional

Mediterranean case 1 and case2 merged product were provided by MyOcean Ocean Colour Thematic Assembling Centre.

The two models were tested using a Mediterranean subset of the NOMAD SeaBASS *in-situ* dataset [4],[5],[6] and HPLC data collected by the authors group in several cruises in the West Mediterranean Sea. The matchup analysis indicates that the first model [2] tends to slightly to underestimate the concentration of nanoplakton chlorophyll and overestimate the concentration of picoplankton chlorophyll. In the second model [3] the nanoplankton underestimation is less evident as well as the picoplakton overestimation.

The analysis of the spatial and temporal distribution of the three PSC components, derived from satellite data, indicates that Picoplankton dominates all around the year with a maximum during summer and minima in autumn and winter in open sea regions not affected by intense spring blooms. Coastal and intense bloom regions, instead, in general show the dominance of nano and micro plankton.

Figure 1 shows an example of the yearly cycle for Pico, Nano Micro-planktonin the Ligurian Sea. The yearly cycle of the three components is well marked by a minimum of picoplankton concentration in spring (March - April) and maximum in summer. Microplankton dominated from March to April. In the Ionian Sea, where the spring bloom is less intense, the picoplankton maximum occurs from December to February.

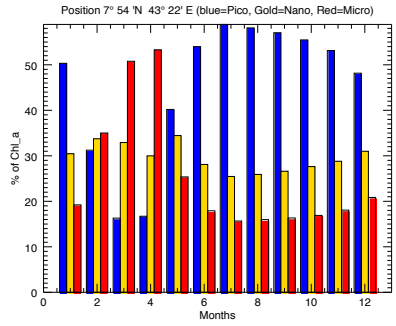

Figure 1. Mean monthly PSC distribution in the Ligurian Sea (NW Mediterranean). Picoplakton percent (blue), Nanoplankton percent(yellow), microplankton percent (red)

References

[1] Brewin R. J. W.. An intercomparison of bio-optical techniques for detecting dominant phytoplankton size class from satellite remote sensing (2011). Remote Sensing of Environment 115 (2011) 325–339

[2] Brewin R. J.W., E. Devred E, S. Sathyendranath, S. J. Lavender, and N. J. Hardman-Mountford. Model of phytoplankton absorption based on three size classes (2011), App. optics ,Vol. 50, No. 22.

[3] Hirata, T., Hardman-Mountford, N. J., Brewin, R. J. W., Aiken, J., Barlow, R., Suzuki, K., Isada, T., Howell, E., Hashioka, T., Noguchi-Aita, M., and Yamanaka, Y.: Synoptic relationships between surface Chlorophyll-*a* and diagnostic pigments specific to phytoplankton functional types (2011), Biogeosciences, 8, 311-327

Distinguishing cyanobacteria from algae in eutrophic near-coastal and inland waters from space: theory and applications

M.W. Matthews[1], S. Bernard[12]

[1]Marine Remote Sensing Unit, Department of Oceanography, University of Cape Town, Cape Town, South Africa

[2] Earth Systems Earth Observation, Council for Scientific and Industrial Research, 15 Lower Hope Street, Rosebank, 7700, Cape Town, South Africa

Email: MTTMAR017@myuct.ac.za

Summary

Cynobacteria may be distinguished from eukaryotic algae on the basis of the magnitude of the peak near 709 nm from top of atmosphere MERIS FR data. A new approach called the maximum peak height (MPH) algorithm is presented for estimating trophic status (chlorophyll a), surface scums and floating vegetation in inland and near coastal waters. Evidence is presented from a two-layered sphere model for enhanced backscattering from cyanobacteria due to intracellular gas vacuoles. Cyanobacteria dominant waters may be distinguished from those dominated by eukaryotes using a flagging procedure based on the unique pigmentation and fluorescence features of cyanobacteria.

Introduction

Cyanobacterial blooms in marine and fresh waters represent an increasing and substantial global health threat. A new approach is presented which enables cyanobacteria-dominant waters to be distinguished from those dominated by eukaryotic algae from space [1]. A dataset consisting of 74 coincident top-of-atmosphere reflectance spectra from the Medium Resolution Imaging Spectrometer (MERIS) and *in situ* chlorophyll-a (chl-a) observations is used to derive an algorithm for estimating phytoplankton biomass (chl-a) over a wide trophic range (0.5 mg/m^3<chl-a<362 mg/m^3). The algorithm makes use of the chl-a fluorescence and backscatter/absorption features in the red/NIR MERIS wavebands to calculate the maximum-peak height. By plotting the MPH variable in chl-a space, waters dominated by *Microcystis* cyanobacteria may be distinguished from those dominated by diatom/dinoflagellate eukaryotes on the basis of the magnitude of the MPH variable. This, we hypothesize, is due to an enlarged chl-a specific backscatter in the red/NIR associated with vacuolate cyanobacteria.

Results: Distinction of cyanobacteria and eukaryotic phytoplankton

Using a two-layered sphere model to simulate the optical properties of algae and cyanobacteria, evidence is presented for enhanced backscatter resulting from internal vacuoles in prokaryote species as opposed to eukaryotes and non-vacuolate prokaryotes. Two layered sphere population model results and radiometry are used to provide some evidence for the increased magnitude of the 709 nm reflectance observed in *Microcystis* dominant waters. Furthermore, a new flagging procedure based on cyanobacteria-specific spectral pigmentation and fluorescence features between 620 and 681 nm enables cyanobacteria-dominant waters to be further distinguished.

Applications: Time series analysis

Time-series applications of the MPH algorithm and the cyanobacteria-flag to South African and global study areas demonstrate how these techniques might be applied for effective monitoring and frequency analysis of high-biomass cyanobacterial blooms. The MPH algorithm also provides a suitable alternative when targeting high-biomass (chlorophyll-a > 20 mg/m^3), turbid and spatially constrained waters since conventional ocean colour algorithms are generally poorly parameterised for use in these environments.

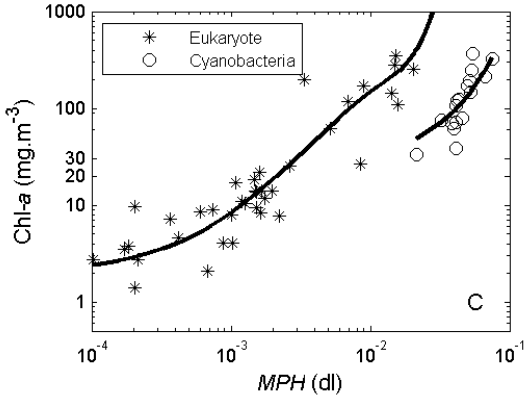

Figure 1 Chl-a versus MPH variable showing separation of cyanobacteria and eukaryotic algae

References

[1] Matthews, M. W., Bernard, S., & Robertson, L. (2012). An algorithm for detecting trophic status (chlorophyll-a), cyanobacterial-dominance, surface scums and floating vegetation in inland and coastal waters. Remote Sensing of Environment, 124, 637–652. doi:10.1016/j.rse.2012.05.032b

In search of long-term trends in the ocean colour record

F. Mélin[1]

[1] E.C. Joint Research Centre, Institute for Environment and Sustainability, Italy
Email: frederic.melin@jrc.ec.europa.eu

Summary

The use of ocean colour data records for trend detection and climate research is presented, particularly in terms of requisites and challenges. A major concern is the existence of significant differences between mission-specific data sets that need to be properly accounted for before these data sets can be combined for time series analyses. The cases of the remote sensing reflectance and the chlorophyll-a concentration are illustrated and their quality as consistent multi-mission data records is discussed.

Introduction

Constructing a long-term record of ocean colour data suitable for monitoring activities or climate research necessitates a suite of successive satellite missions, considering that missions may have a typical life time of 5-10 years. But flying a continuous suite of missions is obviously not sufficient to allow quantitative temporal analyses such as trend detection. First, each mission-specific series needs to possess certain characteristics minimizing the possibility that variations in the data record be the result of changes in the processing environment: a fully characterized calibration history of the instrument, a consistent set of ancillary data, a stable set of algorithms, etc... Then, combining data records from various ocean colour missions for time series analyses may introduce spurious temporal artifacts resulting from inter-mission systematic differences. Eventually, constructing a consistent multi-mission data record requires a thorough knowledge of each mission-specific series, and complete inter-mission comparisons. A direct implication is that this effort is fundamentally connected to, and dependent on, mission temporal overlaps.

The presentation will focus on the two ocean colour variables considered as essential climate variables (ECV) by GCOS [1], the spectrum of water-leaving radiance (or remote sensing reflectance, R_{RS}) and the concentration of chlorophyll-a (Chla). In both cases, the emphasis is on inter-comparison results and the implications in terms of data set consistency and trend detection.

Analysis of the remote sensing reflectance data record

A complete inter-mission comparison is conducted on the SeaWiFS, MODIS-Aqua and MERIS R_{RS} data sets. This is done by accumulating the matching pairs of R_{RS} spectra for each spatial bin and day over the periods of mission overlaps. Before comparison, differences in spectral band specifications between sensors are also accounted for using a bio-optical model.

The inter-comparison statistics document two major characteristics of the R_{RS} data sets. First, a spatially resolved estimate of the random error of the R_{RS} uncertainty budget for SeaWiFS, MODIS and MERIS is computed through an analysis of variance and covariance terms over the comparison ensemble. Then, it

is particularly important to assess, and correct for, inter-mission biases since they can lead to artificial trends in combined data sets that would lessen the usefulness of the series for climate studies. Inter-mission biases vary with wavelength, time and space, but they show well defined spatial patterns that are discussed using a new optical classification. The development of inter-mission bias models is introduced.

Time series analysis of chlorophyll-a concentration

Differences existing between the monthly time series of Chla from SeaWiFS, MERIS, MODIS-Aqua and MODIS-Terra are also analyzed through various statistical indicators like average differences, correlation, or their inherent variances. The trends displayed by each mission are also illustrated, showing significant differences between them (example on figure; updated from [2]).

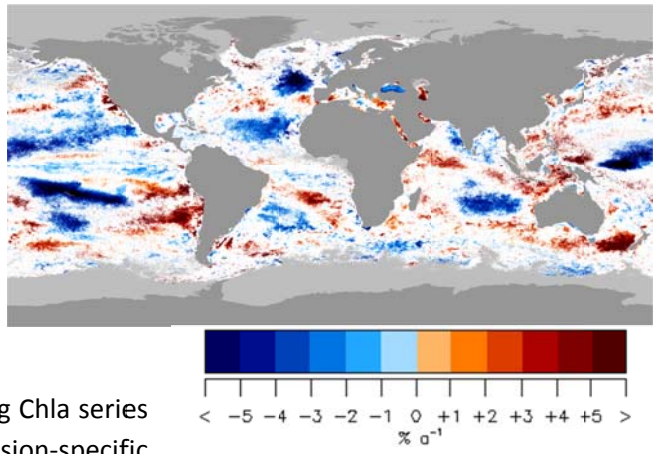

Trends for SeaWiFS Chla, 1998-2007 (non-parametric seasonal Kendall, statistics, p<0.05). Only statistically significant trends are shown. Grey areas show points with not enough data for analysis.

Trends are then computed on data sets combining Chla series from different missions, and compared with mission-specific trends. The part of these trends resulting from biases between missions is analyzed using artificial series made of climatologies. Finally, the level of inter-mission biases that can be tolerated for trend detection is discussed.

Conclusion

Ideally, the field of ocean colour should move from a mission-centric stance to a variable-centric distribution more attractive for users. Besides the continuous presence of ocean colour instruments in space, this requires a continued effort to produce a multi-mission consistent data record and appropriate statistical approaches to account for remaining inter-mission differences.

Acknowledgements

NASA and ESA are duly acknowledged for the distribution of satellite data. This work has been supported by various colleagues, the contributions of which are warmly recognized.

References

[1] GCOS (2011). Systematic observations requirements for satellite-based data products for climate. Supplemental details to the satellite-based component of the Implementation Plan for the Global Observing System for Climate in Support of the UNFCCC.

[2] Vantrepotte, V., and Mélin, F. (2011). Inter-annual variations in the SeaWiFS global chlorophyll *a* concentration (1997-2007). Deep-Sea Res., I, 58, 439-441.

A hybrid halo-optical remote sensing model for characterizing particulates in optically complex waters

Montes-Hugo, M.A.*, Seneville S., St-Onge Drouin S., Mohammadpour G., Bouakba H.

Institut des Sciences de la Mer de Rimouski, Université du Québec à Rimouski, 310 Allée des Ursulines, Office P-216, G5L 3A1, Rimouski, Québec, Canada

*corresponding author (e-mail: martinalejandro_montes@uqar.ca, phone: 418-723-1986, ext. 1961)

Abstract

Light attenuation in the Saint Lawrence Estuary (SLE) can be mainly attributed to changes on light absorption due to chromophoric dissolved organic matter (a_{CDOM}) and detritus (a_d). In coastal systems influenced by freshwater discharge, the magnitude of a_{CDOM} and a_d is inversely correlated with surface salinity. Therefore, salinity can be used as a complementary variable for obtaining more accurate optical closures in waters where optical properties are dominated by non-covarying components. This possibility was investigated using a hybrid inversion technique (hereafter OCSI) based on simulated surface salinity (Laboratoire d'analyse et de simulation des Systèmes océaniques, LASSO) and satellite-based remote sensing reflectance measurements at 440, 490 and 670 nm obtained from SeaWiFS (Sea-viewing Wide Field-of-view Sensor). OCSI-derived estimates for the spectral slope (γ) of the total backscattering coefficient (b_b) were positively correlated with b_b ratios computed between two wavelengths, 450 and 532 nm, and obtained in surface waters (i.e., 0-3 m) of the SLE during Spring 2001. In general, main uncertainties on OCSI products were related to errors on estimating a_{CDOM} and detritus a_d values based on surface salinity (relative bias up to 36.7%) and assuming a constant spectral slope of a_{CDOM} during the survey (up to 43%).

The performance of globally-tuned bio-optical algorithms have been shown to vary in different oceanic basins (Szeto et al, 2011) and different optical environments (Moore et al, 2009). As a consequence, the uncertainties of ocean color products based on these algorithms also vary spatially and are not uniform. Single, bulk statistics without regard to optical environment do not realistically represent how the products are performing spatially. It is important to capture the spatial variation in product uncertainty for assimilation models and for gaining a deeper understanding in how to focus improvements of algorithms to reduce errors in ocean color products. In this work, we present our results of uncertainty analysis on ocean color products for select semi-analytic algorithms. We compare the distribution of uncertainty from matchup data sets for different ocean colors satellites from the viewpoint of optical water types. We also examine these results in the context of how the uncertainties are spread over optical water types using the NOMAD data set. While using matchup data sets has its own sources of error, these comparisons shed light on how algorithms and satellite products are faring for different water types and different sensors. The approach allows for a mapping of product uncertainty by water type for different satellites. These are companion (yet independent) products associated with their corresponding ocean color geophysical products.

Evolution of the MERIS Bright Pixel Atmospheric Correction: accounting for glint.

Gerald, Moore[1], Jean-Paul, Huot[2], Constant, Mazeran[3]
[1]Bio-Optika, Gunnislake,PL18 9NQ,UK
[2]ESA ESTEC, Netherlands
[3]ACRI,France
Email: geraldfmoore@gmail.com

Abstract

The bright pixel atmospheric correction (BPAC)[1] has been part of the operational processor for MERIS on ENVISAT since its launch, and is implemented for the proposed OLCI processor. The BPAC consists of a coupled atmosphere-hydrological model that is parameterised by the Ångström exponent, the properties of pure water and those of particulate matter in the near infra-red (NIR). The BPAC has been used in the operational processor for the MERIS, in order to correct for the multiple scattering [2] atmospheric correction for excess NIR reflectance in case 2 or other waters, where backscatter from particulates results in a significant NIR signal. As part of the evolution for the potential 4th reprocessing of the MERIS archive, and for the OLCI on Sentinel 3 the BPAC has been substantially upgraded. A new version of the BPAC has been developed for the 4th MERIS reprocessing; the revised algorithm uses an analytical solution, and in addition to modelling the spectral signature of particulates and atmosphere, it accounts for the specular scatter from sun glint. The hydrological model is fully described in the MERIS ATDB [3]. The model separates the spectral signature of particulates relying on their similarity spectra [4].

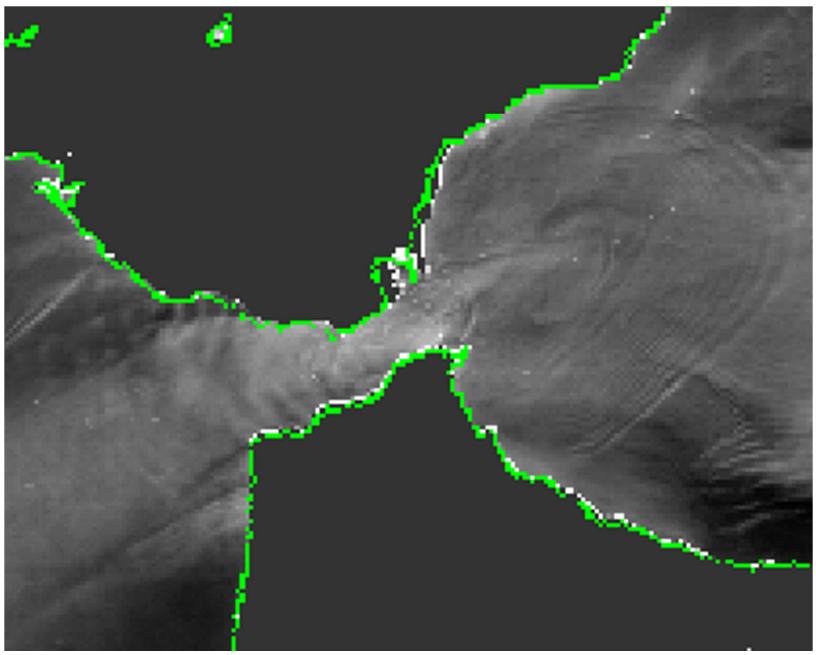

Glint Extracted from MERIS - Mediterranean Sea

Hitherto the glint component in MERIS and other ocean colour sensors has been estimated from the wind-field and a Cox and Munk [5] or similar model of wave slope. This approach has disadvantages, since in terms of operational forecasting remote sensing the true wind field in not known in near real time. The modelled wave slope assumes that the wave field has reached a steady state and that there are no effects due to land. For the coastal zone, where the BPAC can provide NIR backscatter estimates, the wave-slope and wind-field can be influenced by the nearby land topography and the local bathymetry. The example image above are shows the retrieved glint from the Mediterranean Sea, where the surface signature of the internal waves radiating from the Straits of Gibraltar can be clearly seen. Such patterns of increased reflectance can potentially be confused with TSM or chlorophyll when glint is not fully corrected. Further examples

of retrieved glint in coastal inlets, and around islands where noticeable wakes are visible will be presented... The retrieved glint is also compared with that derived from a Cox and Munk model [5]; The BPAC produces estimates of the spectral backscatter in the NIR, although these are not available as routine MERIS products. In contrast to the visible spectral regions currently used for geophysical algorithms, the NIR / Red spectral region shows relatively little CDOM absorption, thus the spectral backscatter provides a robust estimate of TSM. The TSM product is using in-situ data from the North-Western Baltic Sea, a mesotrophic region in the south-west of Portugal and the NOMAD dataset. Using the NOMAD data, the potential to use the BPAC to provide a long term European time series of backscatter using MERIS is demonstrated. The spectral backscatter derived from the BPAC enables estimates of spectral absorption to be made in the red spectral region. The estimates of absorption are used to provide estimates of chlorophyll absorption, and the derived chlorophyll, since the pigment / packaging effect is considerably reduced at red wavelengths. The chlorophyll derived is validated using in-situ data from the North-Western Baltic Sea and the NOMAD dataset.
The glint field providers a partial correction for the land ocean adjacency effect [6].

References

[1] Moore, G. F., Aiken, J., & Lavender, S. J. (1999). The atmospheric correction of water colour and the quantitative retrieval of suspended particulate matter in Case II waters. *Int. J. Remote Sensing*, *20*(9), 1713–1733
[2] Antoine, D., & Morel, A. (1999). A multiple scattering algorithm for atmospheric correction of remotely sensed ocean colour (MERIS instrument): principle and implementation for atmospheres carrying various aerosols including absorbing ones. *International journal of remote sensing*, *20*(9), 1875–1916.
[3] Moore, G. & Lavender, S. MERIS ATDB
[4] Ruddick, K. G., De Cauwer, V., Park, Y. J., & Moore, G. (2006). Seaborne measurements of near infrared water-leaving reflectance: The similarity spectrum for turbid waters. *Limnology and Oceanography*, *51*(2), 1167–1179
[5] Cox, C., & Munk, W. (1956). Slopes of the sea surface deduced from photographs of sun glitter. *Bull. Scripps Instit. Oceanogr. Univ. Calif.*, *6*, 401–488.
[6] Santer, R., & Schmechtig, C. (2000). Adjacency effects on water surfaces: primary scattering approximation and sensitivity study. *Applied optics*, *39*(3), 361–75

HICO-Based NIR-red Algorithms for Estimating Chlorophyll-*a* Concentration in Inland and Coastal Waters – the Taganrog Bay Case Study

W. J. Moses[1], A. A. Gitelson[2], S. Berdnikov[3], J. H. Bowles[1], V. Povazhnyi[3], V. Saprygin[3], and E. J. Wagner[1]

[1]Naval Research Laboratory, Remote Sensing Division, Washington, D.C., USA.
[2]Center for Advanced Land Management Information Technologies (CALMIT), University of Nebraska-Lincoln, USA.
[3]Southern Scientific Center of the Russian Academy of Sciences, Rostov-on-Don, Russia.
E-mail: wesley.moses@nrl.navy.mil

Summary

The results presented here demonstrate the strong potential of the spaceborne hyperspectral sensor HICO as a reliable tool for monitoring coastal water quality, which is critically relevant for coastal ocean color research, especially with the recent demise of MERIS. Two-band and three-band NIR-red algorithms, which have been used very successfully with MERIS data for estimating chlorophyll-*a* (chl-*a*) concentration in coastal waters, yielded accurate estimates of chl-*a* concentration when applied to HICO images. Given the uncertainties in the radiometric calibration of HICO, the results illustrate the robustness of the NIR-red algorithms, validate the radiometric corrections applied to HICO data as they relate to estimating chl-*a* concentration in productive coastal waters, and provide an indication of what could be achieved with future spaceborne hyperspectral sensors.

Introduction

Algorithms that use reflectances in the red and near infrared (NIR) regions of the spectrum are suitable for estimating chl-*a* concentration in optically complex coastal waters (e.g., [1]). NIR-red algorithms based on the spectral channels of MERIS have been shown to yield consistent, highly accurate estimates of chl-*a* concentration for inland and coastal waters from various geographic locations (e.g., [2,3]. The recent demise of MERIS has caused a potentially serious gap in the availability of reliable coastal ocean color data, considering the limitations of MODIS for coastal water quality analysis and the fact that no multispectral or hyperspectral sensor with characteristics that are similar to or better than those of MERIS is scheduled to be launched in the immediate future. In this study, we have used data collected from multiple campaigns on the Taganrog Bay to test the ability of the space borne Hyperspectral Imager for the Coastal Ocean (HICO) to provide accurate estimates of chl-*a* concentration and serve as a reliable tool for coastal water quality analysis.

Discussion

Four *in situ* data collection campaigns were undertaken on the Taganrog Bay between July and Sep 2012, resulting in data from 31 stations, with chl-*a* concentrations ranging between 27.06 and 172.77 mg m^{-3}. The following two-band [4] and three-band [1] NIR-red models were applied to HICO images acquired concurrently with *in situ* data collection:

$$\text{Two-Band HICO NIR-red Model: Chl-}a \propto \left[\bar{R}_{665}^{-1} \times R_{708}\right] \quad (1)$$

$$\text{Three-Band HICO NIR-red Model: Chl-}a \propto \left[\left(\bar{R}_{665}^{-1} - R_{708}^{-1}\right) \times R_{754}\right] \quad (2)$$

where, *Rx* is the reflectance at *x* nm and $\bar{R}_{665}$ is the average of the reflectances at 662 nm and 668 nm. Both NIR-red models had close linear relationships with chl-*a* concentrations (Fig. 1), with determination coefficients of 0.83 and 0.86. The NIR-red algorithms were validated by the leave-one-out cross validation procedure and found to yield accurate estimates of chl-*a* concentration. For the two-band NIR-red algorithm, the Root Mean Square Error (RMSE) and the Mean Absolute Error (MAE) were only 13.52% and 10.89% of the total range of chl-*a* concentration; the corresponding figures for the three-band NIR-red algorithm were 12.02% and 9.12%, respectively. The NIR-red algorithms were used to generate chl-*a* maps that accurately portrayed the spatial and temporal variation of chl-*a* concentration in the bay.

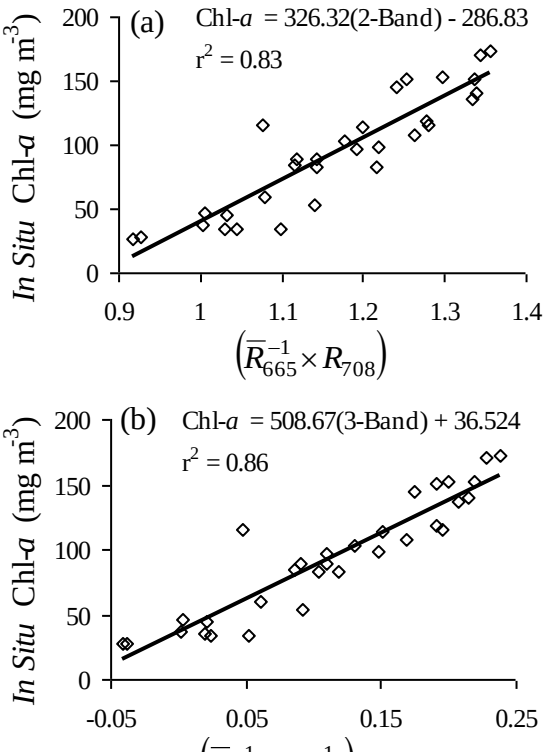

Fig. 1. Plots of chl-*a* concentrations measured in situ versus the (a) two-band and (b) three-band NIR-red model values.

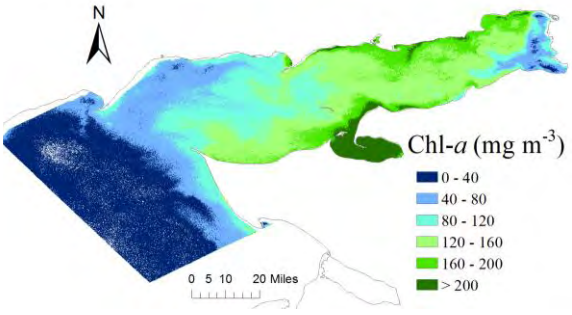

Fig. 2. Chl-*a* map generated from a HICO image using the two-band NIR-red algorithm.

Conclusion

The accuracy of the results obtained illustrates the robustness of NIR-red algorithms and the potential of HICO as a reliable tool for monitoring water quality in coastal waters. It also validates the radiometric and atmospheric corrections applied to HICO [5] as they relate to estimating chl-*a* concentration.

References

[1] Dall'Olmo, G. and Gitelson, A. A. (2005). "Effect of bio-optical parameter variability on the remote estimation of chlorophyll-a concentration in turbid productive waters: experimental results", *Appl. Opt.*, 44(3): 412-422.

[2] Moses, W. J., Gitelson, A. A., Berdnikov, S., Saprygin, V., and Povazhnyi, V. (2012). "Operational MERIS-based NIR-red algorithms for estimating chlorophyll-*a* concentrations in coastal waters – The Azov Sea case study", *Remote Sens. Environ.*, 121: 118-124.

[3] Gitelson, A. A., Dall'Olmo, G., Moses, W., Rundquist, D. C., Barrow, T., Fisher, T. R., Gurlin, D. and Holz, J. (2008). "A simple semi-analytical model for remote estimation of chlorophyll-a in turbid waters: Validation", *Remote Sens. Environ.*, 112(9): 3582-3593.

[4] Gitelson, A. (1992). "The peak near 700 nm on radiance spectra of algae and water - relationships of its magnitude and position with chlorophyll concentration", *Int. J. Remote Sens.*, 13(17): 3367-3373.

[5] Gao, B. -C., Li, R. -R, Lucke, R. L., Davis, C. O., Bevilacqua, R. M., Korwan, D. R., Montes, M. J., Bowles, J. H., and Corson, M. R. (2012). "Vicarious calibrations of HICO data acquired from the International Space Station", *Appl. Opt.*, 51(14): 2559-2567.

Phytoplankton size variability in the global ocean

C. B. Mouw[1]
[1]Michigan Technological University, Houghton, 49931, USA
Email: cbmouw@mtu.edu

Summary

Phytoplankton groups are important to biogeochemical and food web processes. They can be determined based on their ecological role or cell size and are able to be optically differentiated. In this study, the Mouw and Yoder (2010) approach that retrieves percent microplankton (> 20 µm) within a phytoplankton community is utilized. Variability of satellite-derived percent microplankton across the global ocean is explored in the context of the chlorophyll concentration record from the SeaWiFS and MODIS missions. Empirical orthogonal function analysis is used to identify dominant statistical modes in the phytoplankton size and chlorophyll concentration imagery time series. There is evidence of temporal and spatial decoupling between chlorophyll and phytoplankton size. These cases over broad regions of the global ocean are explored in depth. Implications of the observed variability are investigated in the context of biogeochemistry, carbon cycling and flux.

Introduction

The ecology and biogeochemistry of the world's oceans are tightly interconnected. The physical and chemical environment shape microbial community structure which, in turn, mediates biogeochemical pathways including the export of organic matter to the deep ocean and ocean carbon storage. Phytoplankton are a key part of this community and their functional diversity has biogeochemical implications. Motivated by these factors, recent efforts to observe the abundance and activity of the marine phytoplankton from space have placed emphasis on resolving aspects of this diversity; notably broad functional and size classes. Satellite-based observations are revealing the variability of phytoplankton populations on inter-annual to decadal scales. Satellite retrieved estimates of percent microplankton in the phytoplankton assemblage (S_{fm}) [1] and semi-analytical inversion retrieval of chlorophyll concentration ([Chl]) [2] are considered together to understand the relationship between phytoplankton size and [Chl]. This work provides a quantitative comparison of the temporal and spatial relationship between these parameters for near-surface global ocean waters through the use of empirical orthogonal function analysis.

Discussion

Monthly mean percent microplankton [1] and [Chl] [2] imagery time series were investigated with empirical orthogonal function (EOF) and trend analysis. EOF analysis is used to simultaneously examine both temporal and spatial variability. It is useful for compressing the spatial and temporal variability of time series data into a series of orthogonal functions or statistical modes. The temporal variance of the data can be partitioned into modes, revealing spatial functions having time-varying amplitudes, also known as principle components. Prior to EOF analysis, temporal gaps in the data were filled and the data were temporally demeaned. EOF analysis was run on global images of S_{fm} and [Chl] individually and jointly (figure 1). The individual EOF indicates, that with the exception of ENSO, [Chl] mode 1 amplitude time series displays adjustments to the seasonal cycle. However, the S_{fm} amplitude time series suggests a decreasing trend. An advantage of the joint EOF is that both variables will have the same principle components (time-varying amplitudes), thus making it easy to detect and interpret common temporal (seasonal) patterns. The mode 1 amplitude time series of the joint EOF (figure 1) is very similar to the

mode 1 S_{fm} individual amplitude time series, suggesting the dominant variance in time is related to S_{fm}. Spatially, the greatest variability in both parameters in the equatorial Pacific associated with ENSO. The locations of high variability in the S_{fm} individual and S_{fm} and [Chl] joint spatial patterns correspond to regions of the ocean identified [3] as having significant temporal trends. This spatial correlation suggests phytoplankton size structure plays an important role beyond biomass.

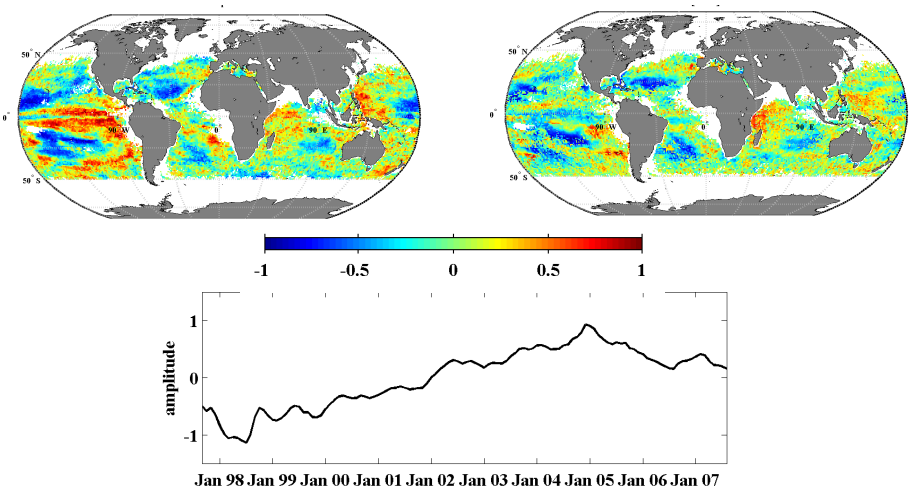

Figure 1. *Mode 1 empirical orthogonal function analysis performed on chlorophyll concentration ([Chl]) and phytoplankton percent microplankton (S_{fm}) jointly. Spatial eigenfunctions for S_{fm} (top left panel) spatial eigenfunctions for [Chl] (top right panel), and time varying amplitudes for both parameters. S_{fm} and [Chl] (bottom panel) both display substantial spatial variability associated with significant temporal variability. It is important to note that S_{fm} and [Chl] spatial variability are not identical, indicating phytoplankton size is not simply responding linearly with [Chl].*

Given ENSO plays such a large role in global spatial and temporal patterns, regional analyses were also carried out to understand emergent patterns at smaller spatial scales. EOF and The decadal climatology and demeaned trends of S_{fm} and [Chl] were determined for the North Atlantic, Equatorial Pacific and Southern Ocean regions.

Conclusions

The EOF analysis indicates S_{fm} and [Chl] spatial variability are not identical, indicating phytoplankton size is not simply responding linearly with [Chl]. In terms of climatology, phytoplankton size generally tracks chlorophyll over an annual cycle but deviations from a linear relationship are evident.

References

[1] Mouw, C., & Yoder, J. (2010). Optical determination of phytoplankton size composition from global SeaWiFS imagery. Journal of Geophysical Research, 115(C12018). doi:10.1029/2010JC006337.

[2] Maritorena, S., Siegel, D., & Peterson, A. (2002). Optimization of a semianalytical ocean color model for global-scale applications. Applied Optics, 41(15), 2705–2714.

[3] Gregg, W., Casey, N., & McClain, C. (2005). Recent trends in global ocean chlorophyll. Geophysical Research Letters, 32(3), L03606. doi:10.1029/2004GL021808.

[4] Alvain, S., Moulin, C., Dandonneau, Y., & Loisel, H. (2008). Seasonal distribution and succession of dominant phytoplankton groups in the global ocean: A satellite view. Global Biogeochem. Cycles, 22(GB3001), doi:10.1029/2007GB003154.

[5] Bricaud, A., Ciotti, A. M., & Gentili, B. (2012). Spatial-temporal variations in phytoplankton size and colored detrital matter absorption at global and regional scales, as derived from twelve years of SeaWiFS data (1998–2009). Global Biogeochemical Cycles, 26(1). doi:10.1029/2010GB003952.

Comparison of atmospheric corrections of HICO images of a subtropical estuarine region in Brazil.

M.A. Noernberg[1,3], S. Lavender[2,3], J.D. Hedley[4], R. Gould[5]
[1] Federal University of Paraná, Center for Marine Studies, Pontal do Paraná, 83255-976, Brazil
[2] Pixalytics Ltd, Tamar Science Park, Plymouth, Devon, PL6 8BX, UK
[3] Plymouth University, School of Marine Science & Engineering, Plymouth, Devon, PL4 8AA, UK
[4] Environmental Computer Science Ltd., Tiverton, Devon, EX16 6LR, UK
[5] Naval Research Laboratory, Stennis Space Center, Mississippi, USA
Email: m.noernberg@ufpr.br

Summary

The quality of ocean color retrieved products depends on accurate atmospheric correction, and this remains a challenging task. Despite the huge scientific contribution of Hyperspectral Imager for the Coastal Ocean (HICO) the spectral quality of this rapidly developed proof of concept instrument also presents challenges. The work presented here investigated different atmospheric correction approaches and the consequences for bio-optical algorithms when retrieving products such as absorption coefficient curves. The results from the approaches are of mixed quality, illustrating that HICO presents challenges for current off-the-shelf atmospheric correction algorithms. However, undertaking this ensemble approach where this is limited *in situ* data provides a greater understanding of the environmental optics and suggests future research that will ultimately lead to a solution that can be applied in an operational monitoring context.

Introduction

The Hyperspectral Imager for the Coastal Ocean (HICO) sensor is the first spaceborne hyperspectral imager designed specifically for the coastal environment. It became operational on the International Space Station in September 2009 and combines high signal-to-noise ratio, contiguous 10 nm wide spectral channels over the range 400 to 900 nm, and a scene size of 42 × 190 km, designed to capture the scale of coastal dynamics. The quality of ocean color retrieved products depends on accurate atmospheric correction, and this remains a challenging task. It has been demonstrated that assuming that sea-water absorbs all the light in the red and near-infrared (NIR) region of the spectrum, referred as the black-pixel assumption (Gordon & Wang, 1994 – GW94), introduces significant errors when applied in turbid waters. Numerous algorithms have been developed with alternative hypotheses taking into account non-negligible NIR ocean contribution to the measured signal. Further, the challenge of atmospheric correction is greater when the need is to retrieve products from areas with few *in situ* measurements. This is the case of the Paranaguá Estuarine Complex, located in south-eastern Brazil, which is a large interconnected subtropical estuarine system, hence frequently turbid and in an area with little resources for in situ radiometric data collection.

Despite the huge scientific contribution of HICO the spectral quality of this rapidly developed proof of concept instrument also presents challenges. The near infra-red (NIR) wavelengths are noisy, which hinders the atmospheric correction. The work presented here investigated different atmospheric

correction approaches and the consequences for bio-optical algorithms when retrieving products such as absorption coefficient curves.

Since Jun 2011, 46 HICO images were acquired over the area or interest; 13 were largely free of clouds. For the same period 24 campaigns for monitoring the absorption coefficients of the three major optically active substances: colored dissolved organic matter, non-algal particles and phytoplankton were realized. At least five sample points were visited near the inlet giving a total of 105 samples. The atmospheric correction required for retrieving the bio-optical absorption coefficients was implemented using four different approaches:

1) Convolution of the hyperspectral bands to "MODIS-like" multispectral bands, and then applying standard GW94 [1] atmospheric correction routines that NASA use for SeaWiFS and MODIS, with near-IR iteration turned on for coastal radiances, to reduce negative water-leaving radiance retrievals. This is processed by the NRL Automated Processing System (APS).
2) An approach originally designed to correct Compact Airborne Spectrographic Imager (CASI) [2], which has the MERIS Bright Pixel approach included [3].
3) The Fast Line-of-sight Atmospheric Analysis of Spectral Hypercubes (FLAASH) available in the ENVI software. Unlike the previous atmospheric corrections that interpolate radiation transfer properties from a pre-calculated database of modeling results, FLAASH incorporates the MODTRAN4 radiation transfer code.
4) An image-driven approach in which the atmosphere reflectance (L_a) is calculated from a pair of adjacent pixels that are in and out of a cloud shadow, with the transmittance and irradiance estimated using the reflected radiance from the top of clouds [3]. The limitation of this method is that it requires distinctive cloud shadow in a near uniform water area, and this shadow cannot be from thin clouds. Also, it does depend on the assumption that L_a is nearly uniform for the study area.

The results from the approaches are of mixed quality, illustrating that HICO presents challenges for current off-the-shelf atmospheric correction algorithms. However, undertaking this ensemble approach where this is limited *in situ* data provides a greater understanding of the environmental optics and suggests future research that will ultimately lead to a solution that can be applied in an operational monitoring context.

References

[1] Gordon, H.R. & Wang, M. (1994). Retrieval of water-leaving radiance and aerosol optical thickness over the oceans with SeaWiFS: A preliminary algorithm. App. Optics, 33:443-452.
[2] Lavender, S.J. & Nagur, C.R.C. (2002). Mapping coastal waters with high resolution imagery: atmospheric correction of multi-height airborne imagery. J. Opt. A: Pure Appl. Opt., 4:S1–S.
[3] Moore, G.F., Aiken, J., Lavender, S.J., (1999). The Atmospheric correction of water colour and the quantitative retrieval of suspended particulate matter in case 2 waters: application to MERIS. Int. J. of Remote Sens., 20:1713–1733.
[4] Lee, Z.P., Casey, B., Arnone, R.A. Weidemann, A.D., Parsons, A.R., Montes, M., Gao, B.C., Goode, W.A., Davis, C., Dye, J. (2007). Water and bottom properties of a coastal environment derived from Hyperion data measured from the EO-1 spacecraft platform. J. Appl. Remote Sens., 1(1):011502.

The multivariate *Partial Least Squares* regression technique for the retrieval of algal size structure from particle and phytoplankton light absorption spectra

E. Organelli, A. Bricaud, D. Antoine, J.Uitz

Laboratoire d'Océanographie de Villefranche, UMR 7093,
CNRS and Université Pierre et Marie Curie, Paris 6, 06238 Villefranche sur Mer, France
Email: emanuele.organelli@obs-vlfr.fr

Summary

The *Partial Least Squares* (PLS) regression technique is here used for the retrieval of the three phytoplankton size classes (micro-, nano- and pico-phytoplankton) from a nine-year time series of *in situ* particle and phytoplankton absorption measurements in the Mediterranean Sea (BOUSSOLE site). PLS models were established for the quantification of concentrations of total chlorophyll *a* (Tchl *a*), of the sum of 7 bio-markers pigments (DPs) and of pigments associated with micro-, nano- and pico-phytoplankton separately. When training PLS models with a dataset including light absorption and HPLC pigment measurements from the Mediterranean Sea only, good accuracy in predicting the algal community structure and its temporal changes at the BOUSSOLE site was observed. A lower accuracy of prediction of phytoplankton size classes over the BOUSSOLE time series was instead revealed by PLS models trained with data from various locations of the world's oceans. Similar performances between PLS models trained with both particle and phytoplankton absorption measurements open the way to an application of this approach also to absorption spectra derived from inversion of field or satellite radiance measurements.

Introduction

The PLS is a multivariate analysis technique that relates a data matrix of predictor variables to a data matrix of response variables by regression. Thus, the PLS method can be used for the prediction of one or several dependent variables from several independent variables [1]. This method is frequently used in chemistry for spectroscopy analysis but only scarcely applied in oceanography, e.g. for the retrieval of information concerning algal populations. An application performed by Stæhr and Cullen [2] showed, however, remarkable skills of PLS in predicting the fraction of chlorophyll biomass of the harmful algae *Karenia mikimotoi*. This led to hypothesize a potential PLS application also for the detection of other phytoplankton types in natural environment.
Two extensive datasets of *in situ* light absorption and HPLC pigment measurements were used for training the PLS technique in order to retrieve concentrations of pigments associated with the three phytoplankton size classes (micro-, nano- and pico-phytoplankton). The fourth-derivatives of particle ($a_p(\lambda)$) or phytoplankton ($a_{phy}(\lambda)$) absorption spectra were selected as the predictor variables while concentrations of Tchl *a*, of the sum of 7 bio-markers pigments (DPs) and of pigments associated with the three phytoplankton size classes [3] were selected as the response variables. A first training dataset consisted of 716 simultaneous HPLC pigment and light absorption measurements collected during several cruises across the world in different years and seasons (hereafter denoted GLOCAL). A second training dataset comprised only data from the Mediterranean Sea (n=239, hereafter denoted MedCAL). The PLS trained models were tested using the nine-year time series (January 2003-May 2011) of absorption measurements at the BOUSSOLE site (n=484; Mediterranean Sea) and the predicted pigment concentrations were compared with those retrieved from HPLC pigment measurements.

Discussion

GLOCAL PLS trained models revealed good accuracy only in predicting Tchl *a* and total DPs content at the BOUSSOLE site. Predicted values of pigments associated with the three size classes separately were actually correlated with HPLC measured values (r^2>0.42) but predictions were systematically overestimated for micro-phytoplankton and underestimated for nano- and pico-phytoplankton. Algal biomass and concentrations of pigments associated with the three size classes were predicted with very good accuracy by the MedCAL trained PLS models. Predicted values were significantly correlated with the measured ones (r^2>0.52) and the points were very close to the 1:1 line. More importantly, $a_p(\lambda)$ and $a_{phy}(\lambda)$ trained models showed similar performances. MedCAL PLS-predicted pigment concentrations reproduced satisfactorily HPLC pigment temporal changes over the entire BOUSSOLE time series (Fig.1).

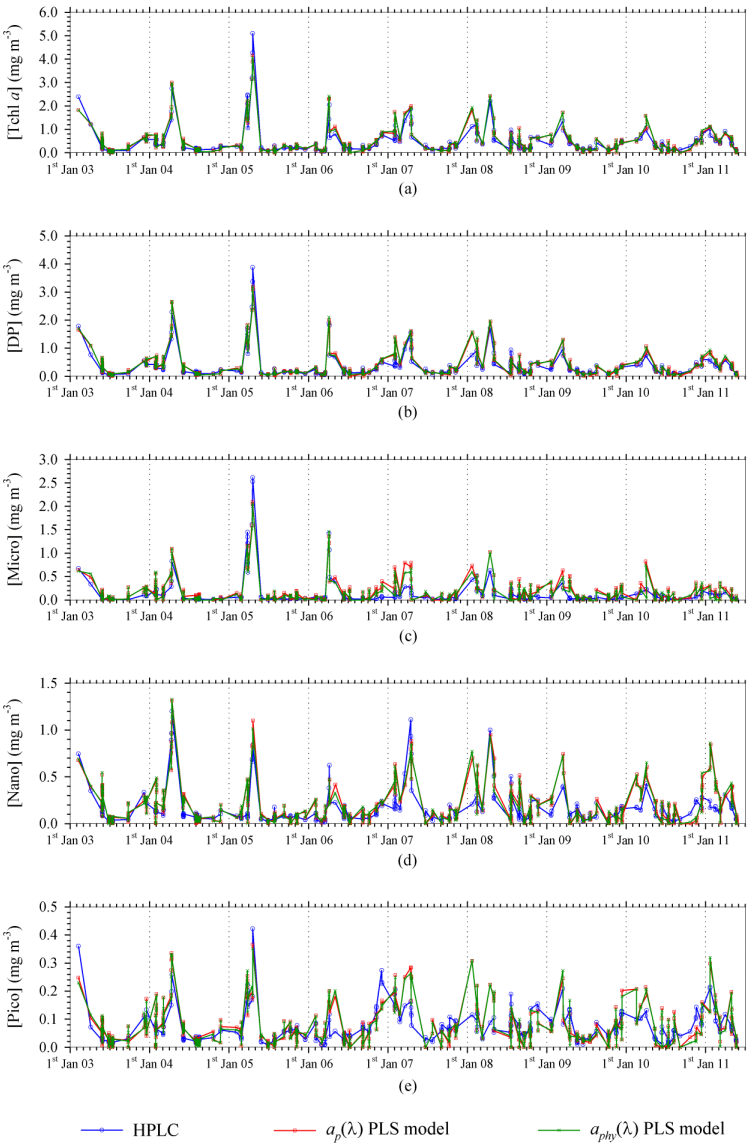

Figure 1 BOUSSOLE time series of pigment concentrations as derived from HPLC pigment measurements and from MedCAL trained PLS models.

Conclusions

The PLS technique represents an encouraging method for retrieving algal biomass and size structure from *in situ* absorption properties especially when models are trained with a regional dataset. Similar performances of $a_p(\lambda)$ and $a_{phy}(\lambda)$ trained models open the way to the application of the PLS method to absorption spectra derived from hyperspectral *in situ* or satellite radiances.

References

[1] Martens, H. and Næs, T. (1989). Multivariate Calibration, Wiley & Sons.

[2] Stæhr, P.A. and Cullen, J.J. (2003). Detection of *Karenia mikimotoi* by spectral absorption signatures. J. Plankton Res., 25: 1237-1249.

[3] Uitz, J., Claustre, H., Morel, A. and Hooker, S.B. (2006). Vertical distribution of phytoplankton communities in open ocean: an assessment based on surface chlorophyll. J. Geophys. Res., 111**:** C08005.

A novel algal discrimination algorithm based on first principles of aquatic optics and applied to hyperspectral remote sensing imagery of the coastal ocean

Sherry L. Palacios[1], Heidi M. Sosik[2], Tawnya D. Peterson[3], Liane S. Guild[1], Raphael M. Kudela[4]

[1]NASA Ames Research Center, Biospheric Science Branch, MS 245-4, Moffet Field, CA 94035 USA
[2]Woods Hole Oceanographic Institute, MS 32, Woods Hole, MA 02543 USA
[3]Oregon Health and Science University, Science & Technology Center for Coastal Margin Observation and Prediction, Beaverton, OR 97006 USA
[4]University of California – Santa Cruz, Ocean Sciences, 1156 High St., Santa Cruz, CA 95064 USA
Email: sherry.l.palacios@nasa.gov

Summary

A new hyperspectral bio-optical algorithm was developed to discriminate phytoplankton taxa in optically complex, case 2 waters. The semi-analytical, phytoplankton detection with optics (PHYDOTax) algorithm is based on first principles of bio-optics with applications to biogeochemical modeling, testing phytoplankton functional type (PFT) models, and detecting and monitoring harmful algal blooms (HABs). PHYDOTax can presently differentiate among diatoms, dinoflagellates, haptophytes, chlorophytes, cryptophytes, and cyanophytes with its existing signature library. PHYDOTax is unique as it discriminates between dinoflagellates and diatoms, a distinction historically considered challenging using chlorophyll-*a*, other pigments, or light absorption spectra alone. With increased availability of hyperspectral imagery from existing satellites, and the launch of new satellites, PHYDOTax holds promise for validating PFT models, modeling biogeochemical cycles, and monitoring harmful algae in optically complex coastal waters. The feasibility of applying the algorithm to other imaging spectrometers (e.g. the AVIRIS simulation of Hyperspectral Infrared Imager- HyspIRI and the Hyperspectral Imager for the Coastal Ocean –HICO) of the Monterey Bay is explored.

Introduction

An initial goal of ocean color remote sensing was to estimate global phytoplankton chlorophyll-a biomass in case 1 waters to address questions related to the ocean's role in carbon uptake and the global carbon budget. Over time, sophisticated algorithms evolved to address more than just chlorophyll-a concentrations in case 1 waters to include: deriving inherent optical properties, cell bio-volume, red-tide indices, water mass detection, and primary productivity in both case 1 and case 2 waters. The bulk chlorophyll-a pool has been further differentiated to quantify the incumbent taxa using pigment-based [1] and ocean color remote sensing algorithms [e.g. 2]. These phytoplankton discrimination algorithms are varied and address specific questions related to carbon flow through aquatic ecosystems, PFTs, and the detection and monitoring of HABs.

The Monterey Bay, CA (USA) is an open bay located along an eastern boundary current. Physical forcing drives nutrient availability to phytoplankton and two of the three oceanographic seasons are characterized by dominant phytoplankton taxa: Upwelling (Mar – Aug)- diatoms and Oceanic (Sep – Oct)- dinoflagellates. This climatological pattern can be disrupted within-season resulting in blooms of mixed assemblages of phytoplankton. This is of particular interest in northern Monterey Bay as extensive dinoflagellate blooms occur in the "red-tide incubator" and may mask co-occuring toxic diatom blooms that pose a threat to ecosystem and human health. The objective of this study was to discriminate phytoplankton taxa contained within algal blooms in case 2 waters using first principles of

bio-optics to identify both the presence of a taxon and to quantify the relative proportions of taxa contained within a bloom to address the need to detect and monitor HABs over a large spatial scale. The algorithm we developed can also be applied to questions related to validating PFT models and carbon uptake within the coastal zone, a region where the understanding of carbon flux is not yet well characterized.

Results and Discussion

PHYDOTax is composed of three parts: 1) a signature library of R_{rs} for phytoplankton taxa found in the coastal ocean derived from measured inherent optical properties (IOPs) of algal cultures and radiative transfer equations, 2) an inverse-matrix approach to deconvolve the signature library from R_{rs} spectra collected from natural waters, and 3) the computation of relative proportions of the total chlorophyll-a pool represented by the constituent taxa. Like its conceptual predecessor, CHEMTAX, the predictions from PHYDOTax are dependent on the taxa represented in the input signature library. The library was developed using IOPs of cultures from thirteen phytoplankton species, representing six taxa commonly found in Monterey Bay: diatoms, dinoflagellates, haptophytes, chlorophytes, cryptophytes, and cyanophytes. Validation with synthetic mixtures confirmed correlation between algorithm predictions and known mixture proportions for all taxa except *Emiliana huxleyi*. Field validation in Monterey Bay, CA in 2006 and 2010 demonstrated a strong correlation between measured and modeled taxon-specific biomass for all taxa except cryptophytes (cyanophytes could not be field validated). PHYDOTax was applied to hyperspectral imagery of Monterey Bay from 2006 and it predicted a bloom with proportions of >60% dinoflagellates and ~20% diatoms; a pattern confirmed with *in situ* cell counts.

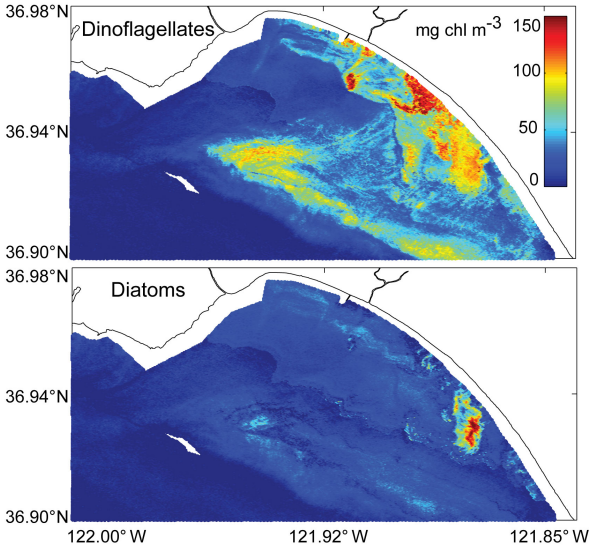

Fig. 1. Predicted taxon-specific biomass: dinoflagellates and diatoms during a major red-tide in northern Monterey Bay, CA (USA). In-water measurements of taxon assemblage validated predictions by PHYDOTax. SAMSOM Hyperspectral airborne sensor (Sep 12, 2006).

Conclusions

PHYDOTax is one of the first bio-optical algorithms to discriminate between dinoflagellates and diatoms in the coastal ocean, a distinction historically considered challenging. It is now possible to track carbon flow through either diatom- or dinoflagellate-dominated ecosystems using hyperspectral remote sensing imagery. PHYDOTax is being evaluated in calibration and validation efforts for the NASA Coastal and Ocean Airborne Science Testbed (COAST) mission in Oct. 2011 and the HyspIRI satellite simulations (AVIRIS airborne imager) in 2013 and 2014, and with other satellite imagers such as HICO.

References

[1] Mackey, M. D., Mackey, D. J., Higgins, H. W. & Wright, S. W.(1996).CHEMTAX - A program for estimating class abundances from chemical markers: Application to HPLC measurements of phytoplankton. Mar Ecol-Prog Ser 144, 265-283.

[2] Alvain, S., Moulin, C., Dandonneau, Y. & Breon, F. M.(2005). Remote sensing of phytoplankton groups in case 1 waters from global SeaWiFS imagery. Deep-Sea Research Part I-Oceanographic Research Papers 52, 1989-2004, doi:10.1016/j.dsr.2005.06.015.

Validation of the WISP algorithm for 9 years of MODIS observations on Dutch monitoring stations

S. Peters [1], K. Poser [1], N. deReus [1], M. Laanen [1], A. Hommersom [1]

Water Insight BV, Wageningen, 6709 PG, The Netherlands

Email: Peters@waterinsight.nl

Summary

Time series of MODIS derived Chl-a and TSM at the locations of Dutch monitoring stations from 2003-2011 were compared to in-situ observations. The MODIS results were obtained by applying the MUMM atmospheric correction and the Water optics Iterative Semi-analytical Processing suite of algorithms (WISP-algorithm). Within this algorithm choices can be made which spectral bands contribute to one of the subalgorithms for Chl-a, TSM and CDOM.

Introduction

Ocean Colour remote sensing in coastal zones with complex waters requires dedicated sensors with high radiometric accuracy, a dedicated spectral band set, specific atmospheric correction methods and algorithms that are able to separate Chlorophyll-a from TSM and CDOM in waters with highly variable concentrations of these components. Between MERIS and SENTINEL, the only usable sensor for this region is MODIS (and VIIRS in the near future). Therefore we have investigated the optimal combination of atmospheric correction and an semi-analytical algorithm to be able to continue providing these services. Using the MUMM atmospheric correction and an adapted version of the WISP algorithm we now are able to prove that Chl-a retrieval with MODIS at elevated TSM concentrations is possible; and that TSM retrieval is at least as good with MODIS as with MERIS.

Discussion

The WISP algorithm (Peters, in preparation) is a semi-analytical approach that uses an iterative scheme to calculate Chl-a, TSM, CDOM. Within the iterative scheme use is made of separate algorithms for each parameter. This allows the use (within the scheme) of band ratio's for Chl-a determination and single band algorithms for TSM and CDOM calculation. The calculation is based on [1] LUTs and the 4^{th} degree polynomial formulation for the reflectance function proposed by these authors. One other attractive aspect of the iterative approach is that per iteration a determination can be made if the water seems to contain high or low concentrations of Chl-a and TSM and to adapt the sub-algorithms (in terms of band choices) automatically to these concentration ranges. From literature we know that low Chl-a concentrations in waters with low TSM are best detected using blue-green band ratio's, while in other cases the red-NIR band ratio provides better results. Similar choices for spectral bands are known for TSM algorithms. The WISP algorithm is therefore one of the first algorithms that adapts itself to various conditions. The algorithm is very successful in case-2 waters using the MERIS band set because of the presence of the 705 nm reference band. Since this band is missing in MODIS alternatives had to be investigated. For Chl-a estimations a value is calculated from the blue green band ratios (443/531,

469/531, 488/531) in the cases that Chl-a is the only important optical active component in the water. In other cases either the band ratio 645/667 or 667/678 is used. Our investigations indicate that the ratio 645/667 contains a clear Chl-a signal for stations close to the coast, while the ratio 667/678 contains the information on high biomass blooms in open waters. For TSM a green band was used in case of low concentrations; in case of higher concentrations we used a red band such as the 678 band. The WISP algorithm is semi-analytical; its parameterization is formulated based on generally accepted SIOP functions according to the SIOP models used in Hydrolight and e.g. in the Coastcolour Round Robin Simulations [2]. Phytoplankton absorption is based on the Bricaud functions; but for the North Sea the absorption at the Chlorophyll-a red absorption band (667 nm) is elevated based on earlier observations. Compared to the CoastColour simulations settings we chose a lower value for the scaling factor for the specific backscattering of mineral particles (0.31).

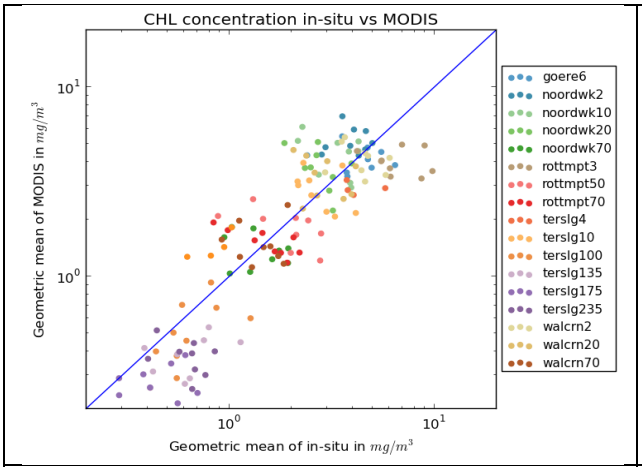

Yearly Chl-a averages at the MWTL stations for MODIS versus in-situ for 2003-2011: R2: 0.78 Slope: 1.02, Intercept: -0.03, RMSE: 0.2, MEA: 0.17

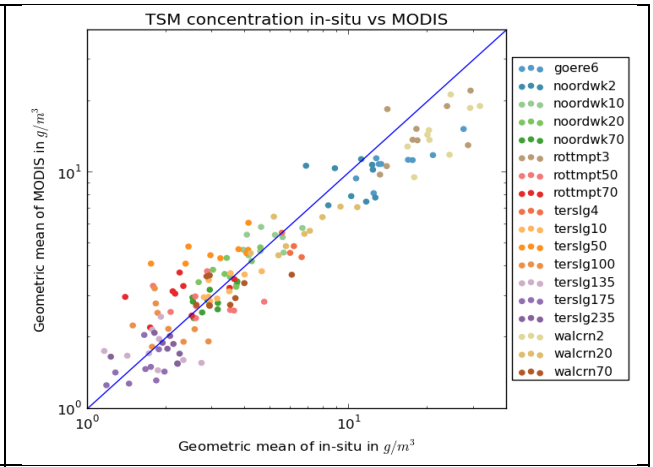

Yearly averages at the MWTL stations for MERIS versus in-situ for 2003-2011: R^2: 0.89, Slope: 0.81, Intercept: 0.11, RMSE: 0.13, MEA: 0.1

Conclusions

The correlation for the yearly geometric mean values is good, both for Chl-a and TSM, although the in-situ station has about 10-20 observations per year while MODIS realizes between 200 and 800 observations per station per year. We can conclude that this version of the WISP algorithm with the optimized selection of MODIS bands provides an effective determination of concentration both at the low end and high end of the values. Even at a distance of 2 km to the coast the values are still reasonable. We find that to improve the results even further, we need stripe removal algorithms and improved cloud flagging, especially at cloud edges.

References

[1] Y. Park and K. Ruddick, "Model of remote-sensing reflectance including bidirectional effects for case 1 and case 2 waters," Appl. Opt. 44, 1236-1249 (2005).

[2] Nechad, B. and Ruddick, K.: DUE CoastColour Round Robin – Harmonized comparison of algorithms Version 2.1 November 2012

A new oil spill detection methodology for MODIS and MERIS satellite imagery: an application to the Mediterranean Sea

A. Pisano[1], S. Colella[1], F. Bignami[1], R. H. Evans[2], R. Santoleri[1]

[1]CNR, ISAC, Rome, 00133, Italy
[2]University of Miami, RSMAS, Miami, 4600, USA
E-mail: andrea.pisano@artov.isac.cnr.it

Summary

We present an innovative automated methodology developed to detect and classify oil spills and look-alikes in MODIS high resolution (250 m) and MERIS full resolution (300 m) top of atmosphere reflectance images. Oil spill detection in optical satellite imagery is very recent and there is a lack of detection algorithms in literature. Our aim is to provide an efficient tool for this detection and thus an additional and complementary cost-effective support to SAR oil spill monitoring of the marine environment. This OS detection procedure was developed within the Italian PRIMI project, as part of the PRIMI operational oil spill monitoring and an oil slick forecasting system.

Introduction

MODIS and MERIS sensors, thanks to their increased spatial resolution, large swath and short revisit time, are now able to resolve small oil spills [1] which represent a prime source of marine hydrocarbon pollution resulting from illegal discharge. Also, these optical sensors, with their near-real time data and availability free of charge, can complement SAR sensors routinely used in oil spill (OS) detection and thus provide a more cost-effective and timely detection approach.

The mechanism behind MODIS (MERIS) oil feature detection mainly depends on the spectral information between oil and surrounding water (e.g. oil-water contrast) and illumination-view geometry of the incident light and satellite (e.g. sun glint condition). Experimental results proved the detectability and observability of oil films on the sea surface with the MODIS sensor [2,3] but there is still a lack of automated detection procedures.

Our oil spill detection procedure first determines where sun glint contamination is present in the image, since the relative oil/water contrast switches depending on the presence of glint. Then, a correction procedure ("image flattening") is applied to the image to remove or at least minimize atmospheric and oceanic natural variability from top of the atmosphere radiances, so as to enhance oil-water contrast. Next, the flattened image is fed to a segmentation algorithm to obtain "oil spill candidate" cluster regions in the image, by discarding non-slick cluster regions. Finally, a set of "feature parameters", defined to discriminate between slicks and look-alikes, are calculated for each OS candidate, leading to further non-slick pruning and to the assignment of a probability score to the remaining, most probable, OS candidates, the score expressing the likeliness of being a true OS.

This OS detection procedure was also used pre-operationally and validated in the framework of the oil spill detection and forecast system developed during the Italian PRIMI project (PRogetto pilota Inquinamento Marino da Idrocarburi/ marine hydrocarbon pollution pilot project).

Discussion

This detection methodology was developed using a set of MODIS and MERIS images of oil spill cases in the Mediterranean Sea for which *in situ* validation observations are available. We built an OS database, consisting of 15 images and 161 slicks. The OS database can be considered representative of the

Mediterranean oil slicks, given the variety of OS geometric (large and small illegal discharge OSs) and illumination/view characteristics.

The definition of feature parameters (e.g. OS area, perimeter, oil-water contrast etc.) and scores is based on the spectral, geometric and statistical analysis carried out on the OS dataset, in which both slicks and look-alikes are known. This analysis has also allowed to estimate the threshold values associated to each feature. These parameters are used to eliminate most non-slick or look-alike cluster regions in an image and to assign a score to the remaining probable oil spills.

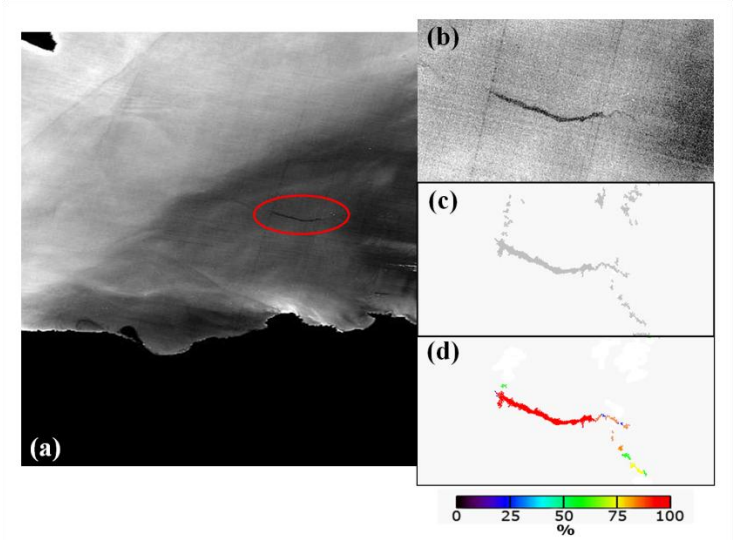

Figure 1. (a) Input flattened image from MERIS (865nm band, August 7 2008 09:50 UTC, off Algeria), oil spill in red ellipse; (b) zoom of the OS area; (c) cluster image; (d) oil spill candidate image after pruning, with color-coded associated scores.

The figure shows the representative steps of the OS detection methodology. The input image, containing the oil spill (in red ellipse of Fig. 1a and enlarged in Fig. 1b) to be detected, is the flattened 865 nm reflectance band relative to the MERIS sensor. By applying the OS detection algorithm to the input band, we obtain the cluster image shown in Fig. 1c, where grey regions represent both candidate oil spill and look-alikes. Finally, Fig. 1d shows the oil spill candidate image, after pruning and score assignment, where slicks are classified with score around 90%.

The method has been tested over the entire OS dataset and demonstrated its capability to detect also small slicks coming from illegal discharges. Validation showed that the method was able to detect 85% of the known slicks of the database. Preliminary validation was also performed on OS cases outside the OS database with encouraging results.

Conclusions

We have developed a methodology for the automatic detection and characterization of oil spills in MODIS and MERIS satellite top of atmosphere reflectance bands, using a set of in situ certified oil spills (OS database) in the Mediterranean Sea. This OS detection procedure was also used pre-operationally and validated in the framework of the oil spill detection and forecast system developed during the Italian PRIMI project (PRogetto pilota Inquinamento Marino da Idrocarburi/ marine hydrocarbon pollution pilot project).

References

[1] Hu, C., Li, X., Pichel, W. G. and Muller-Karger, F. E. (2009). Detection of natural oil slicks in the NW Gulf of Mexico using MODIS. Geophys. Res. Lett., 36, L01604.

[2] Bulgarelli, B. and Djavidnia, S. (2012). On MODIS Retrieval of Oil Spill Spectral Properties in the Marine Environment. IEEE Geoscience and Remote Sensing Letters, 9(3), 398-402.

[3] Adamo et al. (2009). Detection and tracking of oil slicks on sun-glittered visible and near infrared satellite imagery". International Journal of Remote Sensing Vol. 30, No. 24, 6403-6427.

Satellite views of global phytoplankton community distributions using an empirical algorithm and a numerical model

Cecile S. Rousseaux[1,2], Taka Hirata[3], Watson W. Gregg[1]

[1] *Global Modeling and Assimilation Office, NASA Goddard Space Flight Center, Greenbelt, Maryland, USA*
[2] *Universities Space Research Association, Columbia, Maryland, USA*
[3] *Faculty of Environment Earth Science, Hokkaido University, Japan*

Phytoplankton composition plays a major role in biogeochemical cycles in the ocean. The intensity of carbon fixation and export is strongly dependent on the phytoplankton community composition. The approaches to characterize the phytoplankton community composition at a global scale can be roughly classified in two categories: modelling approaches and satellite-derived approaches. In the modeling approach, data assimilation techniques can also be used to constrain the model to track observations time series and to optimize certain variables.

Models and satellite-derived approaches have been used to assess global changes in phytoplankton biomass and community composition at various time scales. Temporal oscillations of phytoplankton biomass are often very variable. The number, timing and magnitude of annual blooms may differ remarkably among locations. In this study we compared the functional response of a numerical model (NASA Ocean Biogeochemical Model, NOBM; Gregg et al., 2003) versus an empirical algorithm (Hirata et al., 2011) in describing the spatial distribution and seasonal variation of four phytoplankton groups phytoplankton (diatoms, cyanobacteria, coccolithophores and chlorophytes) globally and in 12 major oceanographic basins. Global mean differences of all groups were within ~15% of an independent observation data base for both approaches except for satellite-derived chlorophytes. Diatoms and cyanobacteria concentrations were significantly ($p < 0.05$) correlated with the independent observation data base for both methods. Coccolithophore concentrations were only correlated with the in situ data for the model approach and the chlorophyte concentration was only significantly correlated to the in situ data for the satellite-derived approach.

This comprehensive global comparison of a data assimilating biogeochemical model and a satellite-derived approach with extensive in situ archives indicate an overall good agreement of the spatial distribution and seasonal variation in phytoplankton community composition. Using the model, high diatom concentrations were spatially more widespread than using the satellite-derived approach (Figure 1). For example, the North Pacific was the region where the model identified the highest diatom concentration (0.33 mg m^{-3}) whereas the satellite-derived average concentration was 0.15 mg m^{-3}. Although not as productive (in terms of chlorophyll concentration) as the northernmost latitudes, Antarctic was also a region of abundant diatoms and where both approaches differed. Both approaches agreed on the overall distribution of cyanobacteria, except for high latitude and upwelling regions. For example, the satellite-derived approach identified the North Atlantic and Pacific as the regions with highest cyanobacteria concentrations (~0.05 mg m^{-3}, Figure 2 & 3) whereas the model detected low cyanobacteria concentrations (<0.01 mg m^{-3}) in these two regions. This was also the case for the

Antarctic where satellite-derived cyanobacteria concentrations were of ~0.04 mg m^{-3}, while the model did not identify the presence of any cyanobacteria in this region.

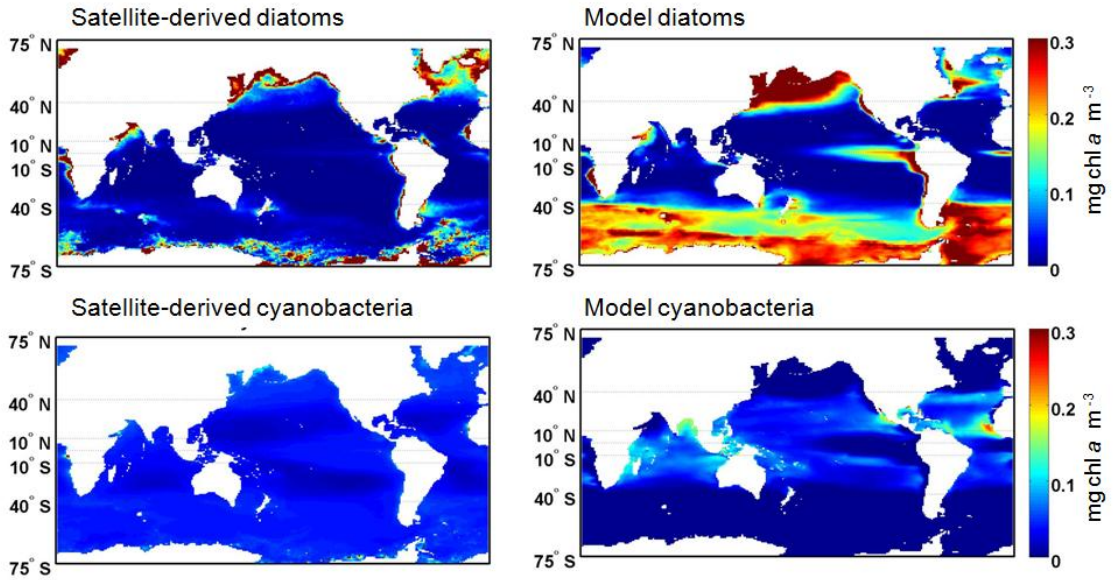

Figure 1: Climatology (1998-2007) of the spatial distribution of diatoms and cyanobacteria using the satellite-derived approach and the NASA Ocean Biogeochemical Model. Note that the satellite-derived prokaryotes are compared to cyanobacteria from the model.

Using monthly means from 2002-2007, the seasonal variation from the satellite-derived approach and model were significantly correlated in 11 regions for diatoms and in 9 for coccolithophores but only in 3 and 2 regions for cyanobacteria and chlorophytes. Most disagreement on the seasonal variation of phytoplankton composition occurred in the North Pacific and Antarctic where, except for diatoms, no significant correlation could be found between the monthly mean concentrations derived from both approaches. Chlorophytes were the group for which both approaches differed most and that was furthest from the in situ data. These results highlight the strengths and weaknesses of both approaches and allow us to make some suggestions to improve our approaches to understanding phytoplankton dynamics and distribution.

Publication:

Rousseaux C.S., T. Hirata and W.W. Gregg, 2013. Satellite views of global phytoplankton community distributions using an empirical algorithm and a numerical model. *Biogeosciences Discuss.*, 10, 1083-1109, doi:10.5194/bgd-10-1083-2013, 2013.

References:

Gregg, W. W., Ginoux, P., Schopf, P. S., and Casey, N. W.: Phytoplankton and iron: Validation of a global three-dimensional ocean biogeochemical model, Deep Sea Research Part II: Topical Studies in Oceanography, 50, 3143-3169, 2003.

Hirata, T., Hardman-Mountford, N. J., Brewin, R. J. W., Aiken, J., Barlow, R., Suzuki, K., Isada, T., Howell, E., Hashioka, T., and Noguchi-Aita, M.: Synoptic relationships between surface chlorophyll-a and diagnostic pigments specific to phytoplankton functional types, Biogeosciences, 8, 311-327, 2011.

The saturation reflectance in turbid waters

K.G. Ruddick[1], A.I. Dogliotti[2], D. Doxaran[3], B. Nechad[1]

[1] Royal Belgian Institute for Natural Sciences (RBINS), 100 Gulledelle, 1200 Brussels, Belgium
[2] Instituto de Astronomía y Física del Espacio (IAFE), CONICET/UBA, P.O: 67 Suc. 68 (C1428ZAA), Buenos Aires, Argentina
[3] Laboratoire d'Océanographie de Villefranche (LOV), CNRS/UPMC, B.P. 8, Quai de la Darse, Villefranche-sur-Mer, 06238, France
Email : K.Ruddick@mumm.ac.be

Summary

It is well-known that for turbid waters there is a maximal value for the marine reflectance, termed here the "saturation reflectance". As suspended particulate matter concentration increases, marine reflectance tends asymptotically towards this "saturation reflectance" limit. This limit has previously been considered as not useful for remote sensing purposes and, for example, suspended particulate matter retrieval algorithms generally avoid exploiting data close to the saturation reflectance. In the present study it is shown that important new information can be extracted from the saturation regime. The saturation reflectance is analysed here using radiative transfer simulations, satellite data and in situ reflectance measurements in highly turbid waters.

Introduction

Ocean colour remote sensing is now well-established as a method for mapping of concentrations of optically active water constituents. Satellite-based ocean colour sensors provide daily maps of parameters such as suspended particulate matter (SPM) concentration by inversion of models relating marine reflectance to inherent optical properties such as absorption, a, and backscattering, b_b , coefficients. It is relatively well-established [1] that the marine reflectance tends towards an asymptotic limit, termed here "saturation reflectance", for infinitely increasing SPM concentration. As this limit is approached the marine reflectance for a given wavelength becomes less and less sensitive to changes in concentration. For example, the in situ measurements of [2] (see Figure) show almost no variability of water reflectance for the wavelength range 400-550nm while SPM varies between 39 and 527 mg/l, whereas significant variation is found for wavelengths 700-1000nm, monotonically increasing with SPM.

Because of the reduction in sensitivity to SPM concentration it is sometimes recommended that the asymptotic limit be avoided for ocean colour remote sensing applications, for example by preferentially using wavelengths with higher pure water absorption where the saturation effect is only reached for correspondingly higher concentrations [3, 4]. While it is true that as reflectance approaches the saturation reflectance there is less and less information on particulate concentration, there is conversely more and more information relating to particulate type or, more specifically, b_{bp}/a_p, the backscatter:absorption ratio of particles. This is in turn related to the refractive index and size distribution of particles. This information is valuable and is currently not adequately exploited in ocean colour remote sensing data.

Discussion

Investigation of the saturation reflectance is beyond the scope of most analytical marine reflectance models. Models, which are based on the quasi-single scattering assumption, typically express reflectance as a linear or quadratic function [5] of $b_b/(a+ b_b)$, and do have an asymptotic limit for high

b_b/a. However, the limit given by such models is simply incorrect, by a factor that can exceed two. Better modelling of the saturation reflectance can be achieved by the use of a two-flow irradiance approximation, as used for example by [4], since this model is more appropriate for highly diffusive media with strong multiple scattering.

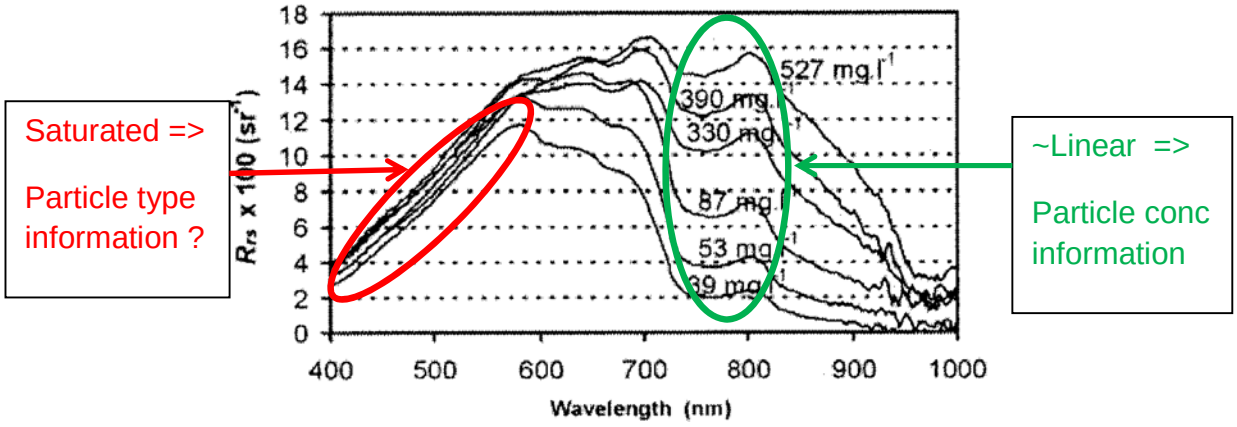

Reflectance spectra measured in the Loire Estuary for different SPM concentrations. Background figure reproduced from [2].

In this study radiative transfer simulations are made to investigate how the saturation depends on optical properties of particulate matter. Approximate analytical models are tested against the radiative transfer simulations. In situ reflectance measurements and satellite data for extremely turbid waters are used to validate the findings of the radiative transfer simulations.

Conclusions

Water reflectance in turbid waters is limited by a maximal value, termed here saturation reflectance. This saturation reflectance cannot be modelled using typical analytical models giving marine reflectance as a linear or quadratic function of $b_b/(a+ b_b)$. The value of saturation reflectance depends on b_{bp}/a_p and the particle volume scattering function. This suggests that remote sensing for saturated wavelengths will provide information on particle type to complement the information on particle concentration that can be retrieved from unsaturated wavelengths.

References

[1] Bowers, D.G., Boudjelas, S. and Harker, G.E.L. (1998), The distribution of fine suspended sediments in the surface waters of the Irish Sea and its relation to tidal stirring. Int J Rem Sen 19(14): p. 2789-2805.
[2] Doxaran, D., Froidefond, J.-M. , and Castaing, P. (2003). Remote-sensing reflectance of turbid sediment-dominated waters. Reduction of sediment type variations and changing illumination conditions effects by use of reflectance ratios. Applied Optics 42(15): p. 2623-2634.
[3] Nechad, B., Ruddick, K.G. , and Park, Y. (2010). Calibration and validation of a generic multisensor algorithm for mapping of Total Suspended Matter in turbid waters. Rem Sens Env 114: p. 854-866.
[4] Shen, F., et al. (2010). Satellite estimates of wide-range suspended sediment concentrations in Changjiang (Yangtze) estuary using MERIS data. Estuaries and Coasts. 33: p. 1420-1429.
[5] Gordon, H.R., et al. (1998). A semianalytical radiance model of ocean color. J Geophys Res 93(D9): p. 10909-10924.

Calibration and validation of ocean color bio-optical models

M. S. Salama[*1,2], R. Van der Velde[1], H. Van der Woerd[3], J. Kromkamp[2], C. Philippart[2]

[1]University of Twente, ITC, The Netherlands
[2]Royal Netherlands Institute for Sea Research (NIOZ), The Netherlands
[3]Amsterdam Free University, IVM, The Netherlands
Email: s.salama@utwente.nl

Summary

We present a method to calibrate and validate bio-optical models that interrelate derived ocean color products to the governing bio-geophysical variables.

The match up set of ocean color observations and measurements is subdivided into calibration (Cal) and validation (Val) data sets. Each Cal/Val pair is used to derive the coefficients (from the Cal set) and the accuracy (from the Val set) of the bio-optical model.

Combining the results from all Cal/Val pairs provides probability distributions of the model coefficients and model errors. The results demonstrate that the method provides robust model coefficients and quantitative measure of the model uncertainty. This approach is easily scalable to different model structures and can be applied to infer the accuracy of ocean color algorithm products.

Introduction

In this paper we present the stochastic approach of Salama et al. [1] for selecting calibration and validation (Cal/Val) sets and demonstrate its use for ocean color bio-optical models. The approach combines the bootstrapping method of Efron and Tibshirani [2] with the Jackknife technique (which leaves out one, or more, observation) and adapts the sample size at each iteration. Bootstrapping and Jackknife methods are usually used to provide the standard error of the derived "plug in" estimates and have been employed for validating ocean color models. However, the combination of bootstrapping without replacement with Jackknife sampling and changing the sample size, at each iteration, is novel and provides not only the accuracy of regressed estimates, but also the underlying probability distribution of regressed estimates and their errors. The developed method samples from a complete matchup set to populate many sets of Cal/Val pairs. Each pair is used to derive the model coefficients and their associated errors, from which the probability distributions of the calibration and validation result is determined.

The method is demonstrated for matchups of chlorophyll-a (Chl-a) concentrations and derived absorption coefficients obtained from the NASA bio-Optical Marine Algorithm Data (NOMAD, version 2a [3]). The general practice is to derive the absorption coefficients from the observed radiance spectra using semi-analytical ocean color models (e.g. Salama and Shen 2010). Lambert-Beer law is then employed to estimate the absorption per unit mass from derived absorption coefficients and measured concentrations as:

$$a_{chla} = a^*_{chla} \times C_{chla} + \epsilon \quad (1)$$

Where a_{chla} is the absorption coefficient of Chl-a in m^{-1}, a^*_{chla} absorption per unit concentration of Chl-a in $m^2.mg^{-1}$, C_{chla} the concentration of Chl-a in $mg.m^{-3}$ and ϵ is an offset term in m^{-1}. The presented method is applied on the *n* (424) match-up data points to derive a^*_{chla} and ϵ from Eq. (1) using the GeoCalVal model [1].

Discussions

The determination coefficients, R^2, of the Cal set are plotted against those of the Val set in Fig. 1-a for all possible combinations. The data point position with respect to the x-axis is an indication for the ability of the model to fit the matchups of the Cal set, whereas its position with respect to the y-axis represents the model's performance in deriving Chl-a absorption coefficient. NOMAD matchup produces a narrow region of Cal/Val pairs, for which the calibration R^2 is similar to validation R2, about 0.75–0.85 (light-grey coloured data points in Fig. 1-a. In other words, within these Cal/Val subdivisions the model validity and the accuracy assessment are balanced. This region defines the optimal setups for subdividing matchups into Cal/Val sets. The underlying mechanisms of the data points in this region are investigated further. We found that the optimal Cal/Val sets are obtained when the arithmetic mean and dispersion of each set are equal to those of the original data set. Figures 1-b,c show the derived probability distributions (PD) of model coefficients, and the associated uncertainties, for the NOMAD matchup set. The resulting PD of model's slope a^*_{chla} have high kurtosis (acute peak around the mean) values and flat tails, i.e. more prone to outliers. The reason for having flat tails is due to the fact that the accuracy of model coefficients depends on the size of the Cal set. In other words, for a large Cal set we expect to have higher accuracy as most data points are used; however, this makes them also sensitive to outliers in the Val set, because most of the data points have been used to create the Cal set. The proposed method reveals the shape of the underlying probability distribution without any a priori assumption on its parameters (e.g. degree of freedom). In the shown example (linear model of Eq.1), the t-probability density function (fitted black lines in Fig. 1-b and c) should be employed to describe the distributions of model coefficient and uncertainties. For non-linear models there is no straightforward theoretical approximation of the expected probability distribution. If we would follow the theory, we would have no means to justify our assumption on the underlying probability distribution and its parameters.

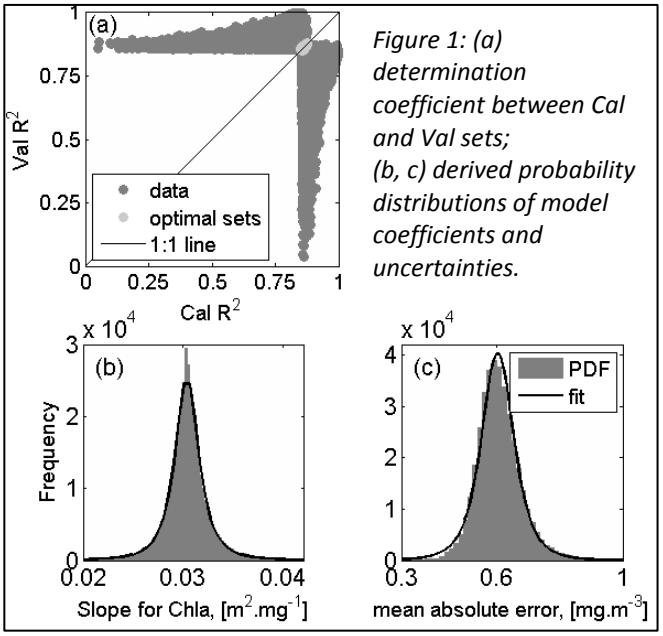

Figure 1: (a) determination coefficient between Cal and Val sets; (b, c) derived probability distributions of model coefficients and uncertainties.

Conclusions

i– The method provides an optimal setup for subdividing matchups into Cal/Val sets; ii– The coefficients and associated uncertainties of linear observation models follow the t-location scale distribution; iii– the optimal Cal/Val sets are obtained when the arithmetic mean and dispersion of the Cal/Val sets are equal to those of the original data set; iv– the presented method is applicable to any data set and can be adjusted to any observation model regardless of the application area.

References

[1] Salama M. S, van der Velde, R., van der Woerd, H.J., Kromkamp, J.C., Philippart, C.J.M., Joseph, A.T., O'Neill, P.E., Lang, R.H., Gish, T., Werdell, P.J. and Su, Z. (2012) Technical notes : Calibration and validation of geophysical observation models. Biogeosciences, 9,6, 2195–2201.

[2] Efron, B. and Tibshirani T. (1993) An introduction to the Bootstrap, 57, Monographs on Statistice and Applied Probability, Chapman & Hall/CRC.

[3] Werdell, J. and Bailey, S.: An improved in-situ bio-optical data set for ocean color algorithm development and satellite data product validation, Remote Sens. Environ., 98, 122–140, 2005.

Linking terrestrial fluxes and biogeochemical variability in the coastal ocean: the role of hydrological models and new satellite ocean color and salinity sensors.

Joseph Salisbury, Ocean Process Laboratory, University of New Hampshire
Douglas Vandemark, Ocean Process Laboratory, University of New Hampshire
Nico Reul, Laboratoire d'Océanographie Spatiale, IFREMER
Severine Fournier, Laboratoire d'Océanographie Spatiale, IFREMER
Bertran Chapron, Laboratoire d'Océanographie Spatiale, IFREMER
Wilfred Wollheim, Complex Systems Research Center, University of New Hampshire

Improvements in hydrological modeling and new satellite sensors for ocean color and salinity are poised to provide data that will enable major advances in our understanding of biogeochemical processes at the land sea interface. These data streams will include information from two new salinity sensors currently in orbit, proposed polar orbiting ocean color sensors with improved spectral and spatial resolution, and geostationary sensors capable of imaging at time scales consistent with the temporal variability of coastal processes. We highlight interdisciplinary research currently underway using hydrological and constituent flux models in conjunction with ocean remote sensing data to estimate the flux and fate of dissolved carbon and to understand processes controlling the variability of coastal absorption features.

Detection of linear trends in multi-sensor time series in presence of auto-correlated noise: application to the chlorophyll-a SeaWiFS and MERIS datasets and extrapolation to the incoming Sentinel 3 - OLCI mission.

Bertrand Saulquin (1, 2), Ronan Fablet (2, 3), Antoine Mangin (1), Grégoire Mercier (2, 3), David Antoine (4), Odile Fanton d'Andon (1).

(1) ACRI-ST, Sophia-Antipolis, France. (2) Institut Mines-Telecom Bretagne, Brest , France. (3) Université Européenne de Bretagne, Rennes, France. (4) Laboratoire d'Océanographie de Villefranche (LOV), France.

Contact: bertrand.saulquin@acri-st.fr

Summary

The detection of long-term trends in geophysical time series is a key issue in climate change studies. This detection is affected by many factors: the amplitude of the trend to be detected, the length of the available datasets, and the noise properties. Although the auto-correlation observed in geophysical time series does not bias the trend estimate, it affects the estimation of its uncertainty and consequently the ability to detect, or not, a significant trend. Ignoring the auto-correlation level typically leads to an over-detection of significant trends.

Satellite time series have been providing remote observations of the sea surface for several decades. Due to satellite lifetime, usually between 5 and 10 years, these time series do not cover the same period and are acquired by different sensors with different characteristics. These differences lead to unknown level shifts (biases) between the datasets, which affect the trend detection. We propose here a generic framework to address the detectability of a linear trend and its significance from multi-sensor datasets.

Introduction

From a methodological point of view, we extend the statistical analysis of linear trends in single-sensor time series in presence of auto-correlated noise [Tiao *et al.*, 1990; Weatherhead *et al.*, 1998] to multi-sensor time series. In particular we address both time overlaps and time gaps between time series. We report and discuss an application to the MERIS and the SeaWiFS chl-a datasets, which clearly demonstrate the gain of this joint analysis.

We investigate how also the time overlap between successive satellite missions could be optimized to improve the detectability of long-term trends and exploit the proposed statistical methodology to evaluate the duration of the S3-OLCI observation series required to improve the joint SeaWiFS-MERIS trend detection based on the hypothesis that the OLCI-MERIS level shift uncertainty will be of the same magnitude than the SeaWiFS-MERIS one.

Discussion

Given a two-sensor dataset, we assume that the two time series share the same long-term trend and seasonal patterns but involve an unknown level shift and correlated noise processes:

$$y_t = \mu + \omega.t + S_t + N_{1t},\ t = 1..n_1 \qquad \text{with} \qquad N_{1t} = \Phi_1 N_{1t-1} + \varepsilon$$

$$y_t = \mu + \omega.t + \delta.U + S_t + N_{2t},\quad t = T_0..n_2 \quad \text{with} \quad N_{2t} = \Phi_2 N_{2t-1} + \varepsilon$$

where the time t is in any case relative to the start of the first time series, which is considered as the reference. T0 is the starting time of the second time series, and n1, n2, are respectively the length of the first and second time series. μ and ω are respectively the intercept term and the linear trend shared by the two time series. δ is the unknown level shift of the second time series compared to the first one, supposed here as constant in time and N_1 and N_2 the first order residuals (AR1). The trend uncertainty $\sigma_{\hat{W}}$ can then be expressed as a function of the weighted white noise variances and the trend coefficient uncertainty, $G = f(n_1, n_2, \Phi_1, \Phi_2, DT, \alpha)$ with DT the overlap or time interval between the two time series and α the correlation coefficient between the two white noise processes.

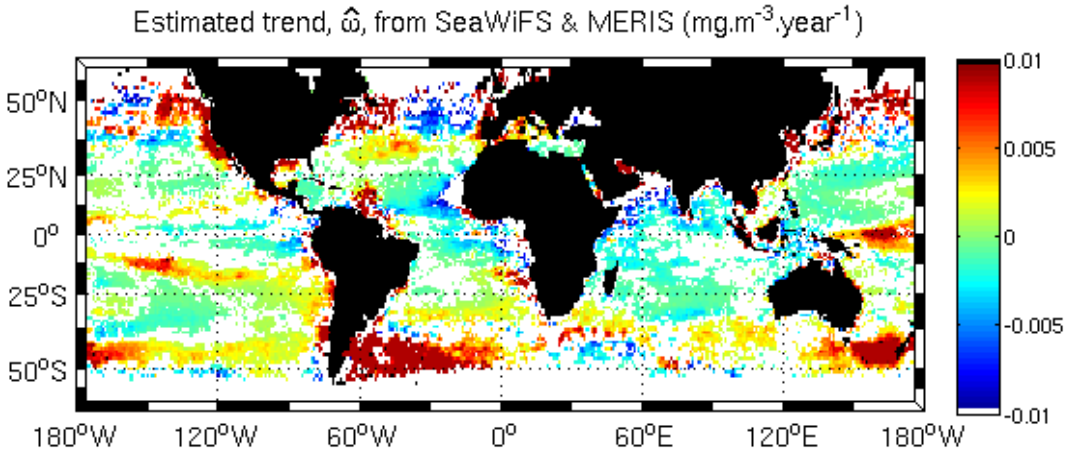

Figure 1: Estimated significant trend estimated from the multi-sensor model using the SeaWiFS and the MERIS dataset (1998-2011).

Conclusion

When two time series are available, the trend detection depends on the uncertainty on the level shift between the datasets. In case of an overlap, the shift uncertainty is diminished. The use of the joint chl-a SeaWiFS-MERIS dataset over the period 1998-2011 led to the detection of 60% of significant trends, compared to 41 % for the SeaWiFS dataset only and 50% for the MERIS dataset only, contributing to a better characterization of region-specific patterns in the detected trends. Using the same model, we estimated the minimal region-dependent duration of the Sentinel 3 - OLCI mission necessary to improve the detection of long-term linear trends issued from the SeaWiFS-MERIS dataset. We estimated a mean value of 53 months for the needed Sentinel 3 – OLCI observations, with some region-dependent fluctuations between 40 to 68 months. This simulation was carried out using an uncertainty level on the shift between OLCI and MERIS of the same magnitude than the one estimated between SeaWiFS and MERIS. These results are coherent with the expected lifetime of the Sentinel 3-OLCI mission, and suggest that the analysis of the global long-term patterns should actually benefit from the joint analysis of SeaWiFS, MERIS and Sentinel 3-OLCI datasets.

Water typed merge of chl-a algorithms and the daily Atlantic (1km) and global (4km) chlorophyll-a analyses of MyOcean II.

Bertrand Saulquin (1), Francis Gohin (2), Garnesson Philippe (1), Odile Fanton-d'Andon (1)

(1) ACRI-ST, Sophia-Antipolis, France. (2) Ifremer Brest , France.

Contact: bertrand.saulquin@acri-st.fr

Summary

The provision of continuous (cloudless) daily fields of chlorophyll-a (chl-a) remains today a challenge. Such products are nevertheless of great interest for users and modellers. We propose here a simple methodology to merge the chl-a fields estimated using several algorithms depending on their validation results on determined water types. The merged fields of chl-a are then optimally interpolated to provide the global MyOcean II chl-a analysis at 4 km resolution and the Atlantic MyOcean II chl-a analysis at 1km resolution. The validation results performed using matchups show a clear added value of both, the merging of algorithms and the spatio-temporal interpolation. The level 4 chl-a analyses are available on a daily base using the MyOcean II facilities.

Introduction

Many algorithms are available for the community to estimate the chl-a concentration from satellite data. The OCx algorithms were calibrated for open ocean (case 1) waters, where the observed spectral shape is constrained by the water and the chl-a absorption spectrum. In coastal waters, the reflectance of the suspended matters and the absorption of the yellow substances influence also the observed spectrum. Today, many 'regional' algorithms have been derived by the scientists to estimate the chl-a locally. We propose here to determine reference water types from the shape of in-situ radiometric profiles. Once the reference water types estimated, we use the membership probability of the satellite derived spectrum to merge the chl-a fields in an optimal way for the end user, i.e. the 'best' algorithm is used on its better domain.

Discussion

We used 7952 in-situ spectra, extracted from the MERMAID database (http://hermes.acri.fr/mermaid) that gathers today more than 30 independent datasets including the NOMAD and AERONET-OC datasets. Each spectrum is defined using 6 wavelengths: 412, 442, 490, 510, 555 and 670 nm. These in-situ measurements have been gathered all over the word and the sampling is considered therefore as representative of the natural variability. The distance used in the segmentation procedure is the mean angle between a reference and the observed spectrum:

$$\boldsymbol{\theta = arcos}\left(\sum_{\boldsymbol{\lambda}} \frac{\boldsymbol{sp(\lambda) * sp\_ref(\lambda)}}{\boldsymbol{|sp| * |sp\_ref|}}\right) \qquad (1)$$

We use and iterative procedure and after convergence, 3 reference spectra were defined: for clear waters, chl-a dominated waters, and coastal waters. The posterior probability of a spectrum i to belong to the water type k is estimated as:

$$P(i,k) = \frac{\left(\frac{1}{\theta(i,k)}\right)}{\sum_{k=1}^{N} 1/\theta(i,k)} \quad (2)$$

The most popular chl-a algorithms were validated on each water type and the 'better' chl-a algorithm is in the merging procedure. To ensure a continuous transition between the algorithms & the water types, the merging between the algorithms is obtained as a weighted sum, depending on, the probability P to belonging to the water types.

$$Chla(i) = \sum_{k=1}^{N} P(i,k) * Chla(i,k) \quad (3)$$

Once the chl-a merged (Figure 1, left), we use the simple kriging estimator with a regional estimation of the covariance structure to interpolate the chl-a fields (Figure 1, right):

$$V_K = -\sum_{i=1}^{n}\sum_{j=1}^{n}\lambda_i\lambda_j\gamma(x_i,t_i;x_j,t_j) + 2\sum_{i=1}^{n}\lambda_i\gamma(x_i,t_i;x_0,t_0). \quad (4)$$

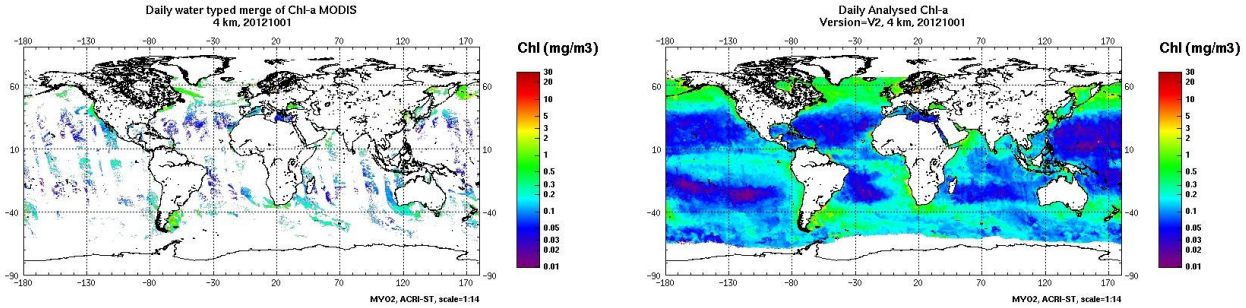

Figure 1: left, the water-typed merge of daily chl-a fields (here 3 different algorithms were used). Right, the corresponding daily optimal interpolation provided in MyOcean II.

Conclusions

The daily spatial coverage has increased from 14 % for the MODIS daily coverage at global scale, to 90 % for the analysed product and from 14% to 90% over the Atlantic. Results of the analyses validation show the same quality in term of bias and standard deviation compared to the merged fields of chl-a, with an increase of in mean X4.5 of the number of matchups. Using GSM only the results of the matchups were nb= 217, S= 1.23, R=0.74, Bias = 0.06, while for the merged chl-a fields the results were nb= 279, S= 1.13, R=0.79, Bias = 0.03 underlying the added value of the merging of chl-a fields derived from different algorithms approach adopted for MyOcean 2.

Acknowledgements

This research was supported by the European Community's Seventh Framework Programme FP7/2007-2013 under grant agreement FP7-SPACE-2009-1/ Collaborative project N° 241759 FP7. These research work is part of a national program on ocean color (GIS–COOC) supported by CNES.

Satellite Derived Primary Productivity Estimates for Lake Michigan

Robert A. Shuchman[1], Michael Sayers[1], Gary L. Fahnenstiel [1], George Leshkevich[2]
[1]*Michigan Tech Research Institute (MTRI), Michigan Technological University* Ann Arbor, MI 48105
[2]*National Oceanic and Atmospheric Administration (NOAA)/Great Lakes Environmental Research Laboratory (GLERL)* Ann Arbor, MI 48108
Email: shuchman@mtu.edu

Summary
A new Case II water color satellite algorithm to estimate primary production (PP) has been generated and evaluated for Lake Michigan. The Great Lakes Primary Productivity Model (GLPPM) is based on a mechanistic model that utilizes remotely sensed observations as input for some variables. The Color Producing Agent Algorithm (CPA-A) [1] is a full spectrum three color component retrieval approach used to derive chlorophyll *a* values and the diffuse attenuation coefficient (K_d) for Photosynthetically Active Radiation (PAR). Satellite derived PP estimates were used to estimate a preliminary Lake Michigan annual primary production of 8.5 Tg C/year. The new algorithm can be used to generate PP time series estimates dating back to late 1997 and will contribute to improved assessment of Great Lakes primary productivity changes as a result of *Dreissenid* mussel invasions, climatic change and anthropogenic forcing.

Introduction
The rate of primary production (PP) is a fundamental property of aquatic systems and measurements of primary production are critical to our understanding of those ecosystems. The amount of primary production can determine the amount of matter and energy available to higher trophic levels and is thus an important measure for management decisions. While simulated in situ experiments provided accurate estimates of primary production in small volumes of water their application to large lakes was limited. Moreover, these in situ and simulated in situ experiments provide an integrated measure of production that is dependent of many variables, (e.g. phytoplankton biomass, light, temperature, etc.), thus limiting their predictive value. In the early 1970s, Fee [2] developed a mechanistic modeling approach that could provide estimates of primary production based on a limited number of input parameters, i.e., chlorophyll, incident irradiation, and photosynthesis-irradiance parameters. The Great Lakes Primary Production Model (GLPPM) is a satellite based implementation of the Fee model following the methods of Lang and Fahnenstiel [3]. The purpose of this program is to develop, evaluate and utilize a new remote sensing approach for estimating primary production in Lake Michigan. This method is an improvement over previous methods in that it requires less input than the wavelength resolving method of Lohrenz et al. (2004, 2008) and utilizes more robust satellite chlorophyll retrievals from ocean color sensors such as MODIS. Because high quality continuous remote sensing imagery exists back to 1997 (SeaWiFS), the application of remote sensing approaches allow one to determine lake-wide primary production in response to various stressors such as invasive species, climate change, oligotrophication, and anthropogenic forcing.

Discussion

The GLPPM was implemented in Lake Michigan using MODIS reflectance imagery along with Lake specific rates of photosynthesis as a function of irradiance. The GLPPM uses chlorophyll a concentrations estimated from the full spectrum three color component Color Producing Agent Algorithm (CPA-A) retrieval approach. The CPA-A uses lake specific Inherent Optical Property (IOP) cross sections as input to solve the inverse radiative transfer equation with respect to water constituent concentration. GLPPM production estimates were compared to in situ production observations for a single year to assess GLPPM accuracy. The GLPPM performs best in the spring and fall when the euphotic zone is well mixed, while it underestimates during periods of water column stratification in the summer. The GLPPM was applied to three dates in early April 2007, 2008, and 2009 to investigate the annual variation in Lake Michigan production. This analysis clearly showed that late winter/early spring primary productivity varies significantly in space and time at both nearshore and offshore regions. The new GLPPM enables, for the first time, estimates of lake-wide primary production. Using four dates in 2008 (Figure 1) and extrapolating to the shoreline for hatched areas, lake-wide production was calculated, excluding Green Bay, to be 9922 mt/d for March 20, 18846 mt/d for May 12, 33569 mt/d for July 5, and 32845 mt/day for September 1. Furthermore, if one assumes these individual dates to be representative of longer time periods, preliminary annual lake-wide primary production can be calculated. A preliminary estimate of annual lake-wide primary production is approximately 8.5 Teragrams (Tg) of carbon fixed per year. This annual production represents approximately 0.02% of the global oceanic annual carbon fixation.

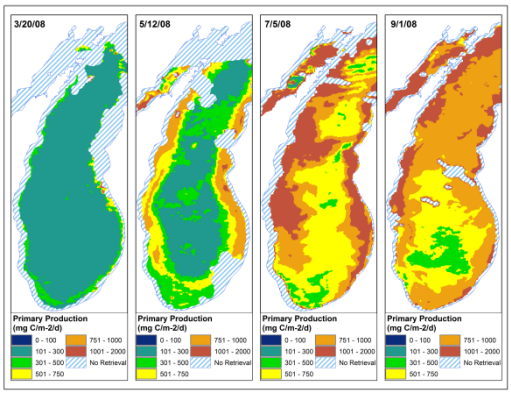

Figure 1. 2008 seasonal primary production estimated from the GLPPM

Conclusions

The satellite based GLPPM was developed for Lake Michigan using Great Lakes specific chlorophyll a concentrations and photosynthetic rates. The model compared well with in situ observations particularly in the spring and fall when the lake is not yet stratified. The GLPPM is able to provide, for the first time, accurate lake wide production estimates that can be used to examine spatial and temporal trends as well as derive yearly total carbon fixation estimates. These observations over time provide insight into the effects climate change, invasive species, and anthropogenic forcing have on Great Lake ecosystems.

References

[1] Pozdnyakov, D., Shuchman, R., Korosov, A., Hatt, C., 2005. Operational algorithm for the retrieval of water quality in the Great Lakes. Remote Sensing of Environment. 97, 353-370.

[2] Fee, E.J., 1973. A numerical model for determining integral primary production and its application to Lake Michigan. J. Fish. Res. Bd. Can. 30, 1447-1468.

[3] Lang, G.A., Fahnenstiel, G.L., 1996. Great Lakes primary production model - methodology and use. NOAA Tech. Memo. ERL GLERL-90, NOAA Great Lakes Environ. Lab, Ann Arbor, MI.

CDOM a useful surrogate for salinity: Mapping the extent of riverine freshwater discharge into the Great Barrier Reef lagoon from MODIS observations

Schroeder T.[1], Brando V.E.[2], Devlin M.J.[3], Dekker A.G.[2], Brodie J.E.[3], Clemenston L.A.[4], McKinna L.[5]

[1] CSIRO Land and Water, Brisbane, QLD 4102, Australia
[2] CSIRO Land and Water, Canberra, ACT 2601, Australia
[3] James Cook University, Townsville, QLD 4811, Australia
[4] CSIRO Marine and Atmospheric Research, Hobart, TAS 7001, Australia
[5] Curtin University, Perth, WA 8645, Australia
Email: Thomas.Schroeder@csiro.au

Summary

Daily ocean colour observations from MODIS-Aqua have been used to map the inter-annual extent of riverine freshwater flood plumes into the Great Barrier Reef (GBR) lagoon between 2002 and 2010. To enable a reliable mapping of low salinity waters we applied a regionally adapted physics-based coastal ocean colour algorithm [1],[2], that simultaneously retrieves chlorophyll-a, non-algal particulate matter and coloured dissolved organic matter (CDOM), from which we used CDOM as a surrogate for salinity (S) for mapping the freshwater plume extent.

Introduction

Riverine freshwater plumes are the major transport mechanism for nutrients, sediments and pollutants into the Great Barrier Reef (GBR) lagoon and connect the land with the receiving coastal and marine waters. Knowledge of the variability of the freshwater extent into the GBR lagoon is relevant for marine park management to develop strategies for improving ecosystem health and risk assessments. The inverse correlation between CDOM and S makes CDOM a useful tracer for lower salinity flood waters. In the open ocean, CDOM absorption originates predominantly from bacterial decomposition of phytoplankton cells, whereas in coastal waters, CDOM is dominated by humic and fulvic acids of terrestrial origin transported to the seas through freshwater runoff from the land as well as autochthonous CDOM from salt marshes, mangroves, inter- and sub tidal benthic microalgae, sea grasses, macro-algae and corals. Water types in the GBR, especially during the wet season, are a complex mixture ranging from clear blue oceanic waters to extremely turbid waters affected by river run-off and with high concentrations of suspended matter (up to 300 mg m^{-3}) and dissolved organic material (CDOM absorption at 443 nm up to 2 m^{-1}). River runoff in the GBR is highly seasonal and correlated with precipitation, with two-thirds of annual rainfall occurring during the wet season from December to April. In addition, there is a large inter-annual variability in precipitation and runoff observed depending on the intensity of the monsoon and the frequency of tropical cyclones.

The optical complexity of the GBR coastal waters especially during run-off conditions requires a model or physic-based inversion approach to distinguish the overlapping absorption features of phytoplankton, non-algal particulate matter and CDOM. In this study, CDOM absorption across the entire GBR World Heritage Area (coast line ~2,300 km) was estimated from a semi-analytical model with variable specific inherent optical properties [2]. Spatially coherent sampling of such a large area is not feasible with in-

situ methods. The application of remote sensing in the GBR however provides a fast and efficient tool for large scale monitoring.

Discussion and conclusions

For each wet season between 2002 and 2010 the freshwater extent was estimated from daily MODIS measurements (Fig. 1) by applying a threshold of 0.24 m^{-1} to maps of seasonally aggregated maximum CDOM absorption at 443 nm. The CDOM absorption threshold was derived from linear regression of 250 concurrent in-situ CDOM and salinity measurements covering the inner most GBR lagoon and corresponds to a salinity of S=30. This rather conservative threshold was established to enable robust automated image classification and to avoid mapping of any autochthonous CDOM production within the reef matrix. Further, the selected threshold is of ecological relevance as some coral species in the GBR have been reported to bleach at a salinity level of S=30 depending on exposure period and water temperature.

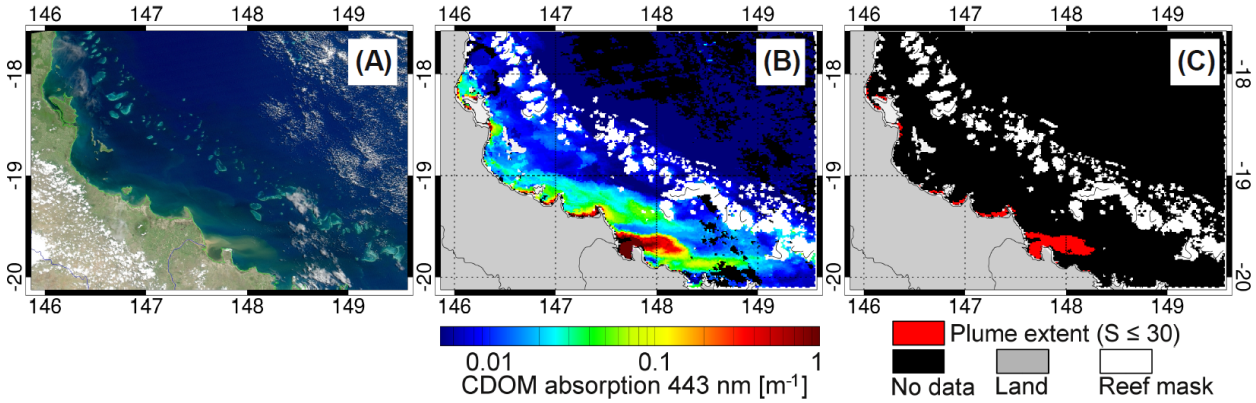

Fig. 1. Pseudo true-colour image of a sub-region in the central GBR (Burdekin) (A) captured by MODIS-Aqua on 02 Feb 2005 and associated CDOM absorption at 443 nm (B) and calculated freshwater plume extent with salinity values S≤30 (C).

The inter-annual extent analysis showed that lower salinity waters (S≤30) were found to reach a number of inner and mid-shelf reefs, but none of the outer shelf reefs located at the edge of the continental shelf. Across the entire GBR World Heritage Area the inter-annual variation in estimated freshwater plume areal extent was found to be highly correlated with flow data from stream gauges (R^2=0.73) and to a lesser degree with Southern Oscillation Index (SOI) data (R^2=0.66). The maximum freshwater extent over the entire GBR was observed in 2008 with an estimated area of approximately 22,000 km^2. Future applications of this method should provide additional information on coral reef exposure duration to various salinity levels, which in combination with sea surface temperature data, may assist Marine Park management in their risk assessment of coral health in the GBR.

References

[1] Schroeder, T., Behnert, I., Schaale, M., Fischer, J., and Doerffer, R. (2007). Atmospheric correction algorithm for MERIS above case-2 waters, International Journal of Remote Sensing 28 (7), 1469-1486.

[2] Brando, V.E., Dekker, A.G., Park, Y.J., and Schroeder, T. (2012). Adaptive semianalytical inversion of ocean color radiometry in optically complex waters, Applied Optics 51 (15), 2808-2833.

SEASONAL DYNAMICS OF SURFACE CHLOROPHYLL CONCENTRATION AS AN INDICATOR OF HYDROLOGICAL STRUCTURE OF THE OCEAN (BY SATELLITE DATA)

A. Shevyrnogov[1,3], G. Vysotskaya[1,2]

[1] Institute of Biophysics of SB RAS, Krasnoyarsk, 660036, Russia
[2] Institute of Computational Modelling of SB RAS, Krasnoyarsk, 660036, Russia
[3] Siberian Federal University, Krasnoyarsk, 660074, Kirensky St., 26, Russia
E-mail: ap_42@mail.ru

Summary

Continuous monitoring of phytopigment concentrations and sea surface temperature in the ocean by space-borne methods makes possible estimating ecological conditions of ecosystems in critical areas. Unlike land vegetation, hydrological processes largely determine phytoplankton dynamics, which may be either recurrent or random. The types of chlorophyll concentration dynamics and sea surface temperature can be manifested as zones quasistationary by seasonal chlorophyll dynamics, quasistationary areas (QSA).

Introduction

The authors of the papers [4,5] showed the existence of zones that are quasi-stationary with similar seasonal dynamics of chlorophyll concentration at surface layer of the ocean. Results were obtained on the basis of processing of time series of SeaWiFS satellite images. It was shown that fronts and frontal zones coincide with dividing lines between quasi-stationary areas, especially in areas of large oceanic streams. To study the dynamics of the ocean for the period from 1985 through 2012 we used data on the temperature of the surface layer of the ocean and chlorophyll concentration (AVHRR, SeaWiFS and MODIS) [1,2,3]

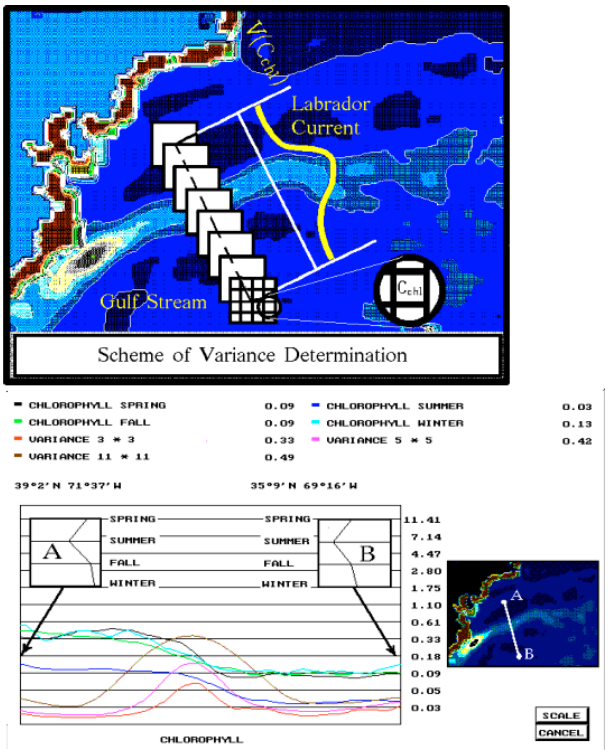

Fig.1 Determination of moving variance of chlorophyll concentration

Discussion

Biota of the surface oceanic layer is more stable in comparison with the quickly changing surface temperature. It enables circumventing the influence of a high-frequency component (for example, a diurnal cycle) in studying the dynamics of the spatial distribution of surface streams. In addition, an analysis of nonstable ocean productivity phenomena, stood out time series of satellite images, showed the existence of areas with different types of instability in the all Global Ocean. They are observed as adjacent nonstationary zones of

different size, which are associated by different ways with known oceanic phenomena. It is evident that dynamics of a spatial distribution of biological productivity can give an additional knowledge of complicated picture of surface oceanic layer hydrology.

Figure 1 shows the diagram of deriving moving variance using the intersection of the frontal zone between the Labrador Current and the Gulf Stream as an example. Even though the seasonal progress of dynamics in chlorophyll concentration is different and so are the absolute chlorophyll concentrations, the variance on both sides of the frontal zone is small. The variance drastically increases at the intersection of the interface between the waters with different seasonal dynamics of chlorophyll concentration. The value of the moving variance is shown in the chart with different optical density.

Figure 2 demonstrates different origins of the appearance of quasistationary zones in the ocean. We can see that the border between quasistationary zones is an indicator of the front between the Labrador Current and the Gulfstream, another example of revealed phenomenon is a quasistationary area around of the British Isles that correlates with the relief of the oceanic *bottom*.

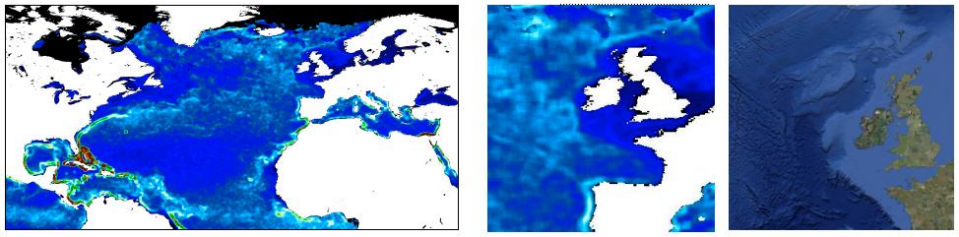

Conclusions

Considering that the QSA maps are calculated almost for all surface of the Global Ocean, not all QSA can be explained, especially those of small size. However, some small QSA are interesting. There are also local QSA near estuaries of large rivers and large industrial centers, which can be result of human impact.
In sum, satellite data is a powerful instrument for investigation of dynamic oceanic processes, their stability and instability. The result of such study can be used for monitoring of long-term changes and their correlation with climate dynamics.

References

[1] Behrenfeld M.J., O'Malley, R.T., Siegel, D.A., McClain C.R., Sarmiento J.L., Feldman, G.C., Milligan, A.J., et al. 2006. Climate-driven trends in contemporary ocean productivity. Nature, 444, 752-755
[2] Chavez, F. P., Strutton, P. G., Friedrich, G. E., Feely, R. A., Feldman, G. C., Foley, D. G., and McPhaden, M. J. 1999. Biological and chemical response of the equatorial Pacific Ocean to the 1997–98 El Niño. *Science*, 286: 2126–2131.
[3] McClain, C.R., Cleave, M.L., Feldman, G.C., Gregg, W.W., Hooker, S.B., Kurig, N., 1998. Science quality SeaWiFS data for global biosphere research. Sea Technology. 39, 10–16
[4] A. Shevyrnogov, G. Vysotskaya, E. Shevyrnogov, A study of the stationary and the anomalous in the ocean surface chlorophyll distribution by satellite data. International Journal of Remote Sensing, Vol. 25, №7-8, pp. 1383-1387, April 2004
[5] A. P. Shevyrnogov, G. S. Vysotskaya, J. I. Gitelson, Quasistationary areas of chlorophyll concentration in the world ocean as observed satellite data *Advances in Space Research*, *Volume 18, Issue 7*, *Pages 129-132*, *1996*

Sea ice properties in the Bohai Sea measured by MODIS-Aqua: Satellite Algorithm and Study of Sea Ice Seasonal and Interannual Variability

Wei Shi[1,2*] and Menghua Wang[1]

[1]NOAA/NESDIS Center for Satellite Applications and Research (STAR),
E/RA3, 5830 University Research Ct., College Park, MD 20740, USA

[2]CIRA, Colorado State University, Fort Collins, CO, USA
[*]Presenter, Email: wei.1.shi@noaa.gov

1. Satellite algorithm development (Shi and Wang, 2012a)

Based on the fact that sea ice reflectance drops significantly in the shortwave infrared (SWIR) wavelengths, black pixel assumption is assessed for three SWIR bands for the Moderate Resolution Imaging Spectroradiometer (MODIS)-at 1240, 1640, and 2130 nm-over the sea ice in the Bohai Sea in order to carry out atmospheric correction for deriving sea ice reflectance spectra. For the SWIR 1240 nm band, there is usually a small (but non-negligible) reflectance contribution over sea ice. Although there is a slight sea ice reflectance contribution at the MODIS 1640 nm band over sporadic land-fast or hummock ice, the black pixel assumption is generally valid with the MODIS bands 1640 and 2130 nm in the Bohai Sea. Thus, the SWIR-based atmospheric correction algorithm using MODIS bands at 1640 and 2130 nm can be conducted to derive sea ice optical properties in the region. Based on spectral features of the sea ice reflectance, a regionally optimized ice-detection algorithm is proposed. This regional algorithm shows considerable improvements in detecting sea ice over the Bohai Sea region, compared with a previous MODIS global sea ice detection algorithm. The sea ice coverage as identified in the new algorithm matches very well with the sea ice coverage from both the MODIS true color image and the imagery from the Interactive Multisensor Snow and Ice Mapping System (IMS).

2 Study of sea ice seasonal and interannual variability (Shi and Wang, 2012b)

During the 2009-2010 winter, the Bohai Sea experienced its most severe sea ice event in four decades, which caused significant economic losses, affected marine transportation and fishery, and impacted the entire marine ecosystem in the region. Measurements from the Moderate Resolution Imaging Spectroradiometer (MODIS) on the Aqua satellite from 2002 to 2010 and surface atmosphere temperature (SAT) data from the National Centers for Environmental Prediction (NCEP) are used to study and quantify the extreme sea ice event in the 2009-2010 winter and the interannual variability of the regional sea ice properties, as well as the relationship between sea ice and the climate variability in the Bohai Sea. The mean sea ice reflectance from MODIS-Aqua visible and near-infrared wavelengths are 933%, 13.26%, and 12.60% in the months of December 2009, January 2010, and February 2010, respectively, compared with the monthly average sea ice reflectance values (from 2002 to 2010) of 9.35%, 11.21%, and 11.41% in the same three winter months. The sea ice monthly average coverages are similar to 5427, similar to 27,414, and similar to 21,156 km(2) in these three winter months. These values are significantly higher than the averages of monthly sea ice coverage of similar to 2735, similar to 11,119, and similar to 10,287 km(2) in the Bohai Sea in December, January, and February between 2002 and 2010. Most of the sea ice coverage was located in the northern Bohai Sea. Both the intra-seasonal and interannual sea ice variability in the Bohai Sea is found to

be related closely to SAT. The mechanism of anomalous SAT and intense sea ice severity are also discussed and attributed to large-scale climate changes due to the variability of the Arctic Oscillation (AO) and Siberian High (SH).

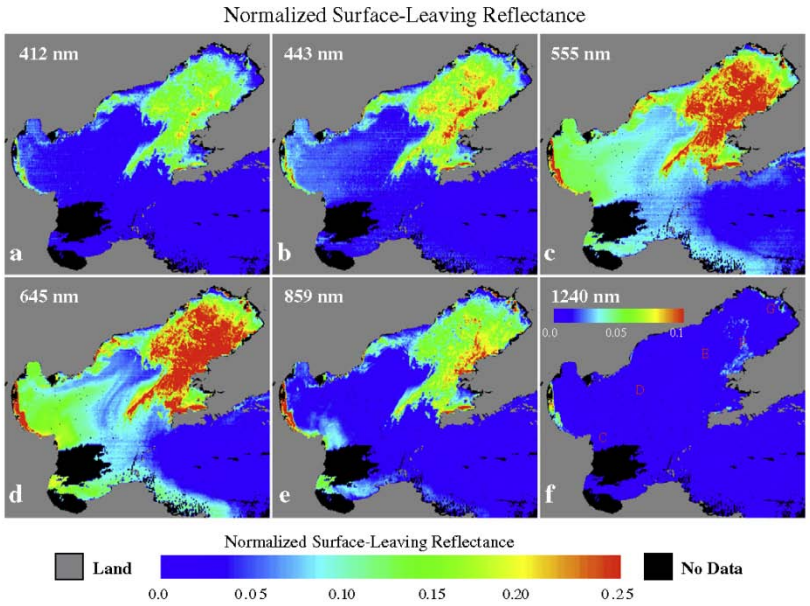

Figure caption:
Normalized surface-leaving reflectance at wavelengths of (a) 412 nm (deep blue), (b) 443 nm (blue), (c) 555 nm (green), (d) 645 nm (red), (e) 859 nm (NIR), and (f) 1240 nm (SWIR) derived from MODIS-Aqua measurements on February 12, 2010.

References

[1] SHI, W., and M. H. WANG. 2012a. Sea ice properties in the Bohai Sea measured by MODIS-Aqua: 2. Study of sea ice seasonal and interannual variability. Journal of Marine Systems **95:** 41-49, DOI 10.1016/j.jmarsys.2012.01.010.

[2] SHI, W., and M. H. WANG. 2012b. Sea ice property in the Bohai Sea measured by MODIS-Aqua: 1. Satellite algorithm development. J. Marine Systems **95:** 32-40.

Vicarious Calibration Efforts for VIIRS Operational Ocean Color EDR

Menghua Wang[1], Wei Shi[1,2,*], Lide Jiang[1,2], Liqin Tan[1,2], Xiaoming Liu[1,2], and SeungHyun Son[1,2]

[1]NOAA/NESDIS Center for Satellite Applications and Research (STAR), E/RA3, 5830 University Research Ct., College Park, MD 20740, USA

[2]CIRA, Colorado State University, Fort Collins, CO, USA
[*]Presenter, Email: wei.1.shi@noaa.gov

Ocean color products have been routinely produced from the Visible Infrared Imaging Radiometer Suite (VIIRS) on the Suomi National Polar-orbiting Partnership (S-NPP) using the Interface Data Processing Segment (IDPS) since its launch in October of 2011. Recently, VIIRS ocean color Environmental Data Records (EDR), e.g., normalized water-leaving radiance spectra $nL_w(\lambda)$, chlorophyll-a concentration (Chl-a), have been declared as the Beta status. Thus, VIIRS ocean color EDR is now available to public through NOAA Comprehensive Large Array-data Stewardship System (CLASS). Although IDPS-produced ocean color EDR is quite reasonable compared with in situ data, on-orbit vicarious calibration has not been carried out for the IDPS ocean color products. There are some bias errors in the current IDPS-produced ocean color products. It is well known that, in order to derive accurate satellite ocean color products, post-launch on-orbit vicarious calibration is necessary [1]. In this presentation, we describe a vicarious calibration approach for deriving vicarious gains for VIIRS M1 to M7 bands for the IDPS operational ocean color data processing. The vicarious gains for VIIRS sensor are derived using the in situ $nL_w(\lambda)$ data that have been acquired with the Marine Optical Buoy (MOBY) system over oligotrophic waters off Hawaii [2]. With the vicarious calibration gains applied to the VIIRS M1 to M7 bands, ocean color products ($nL_w(\lambda)$ and Chl-a) from VIIRS IDPS operational data processing can be significantly improved.

Specifically, in the vicarious calibration approach, the gain coefficients for the VIIRS two near-infrared (NIR) bands (M6 and M7) at wavelengths of 745 and 862 nm are first derived and tested over the MOBY site and the South Pacific Gyre region. MOBY in situ $nL_w(\lambda)$ data for VIIRS spectral bands since January 2012 have been used to iteratively compute the vicarious gains for the VIIRS M1 to M5 bands. Based on results from iterative $nL_w(\lambda)$ matchup procedure, VIIRS vicarious gains are adjusted and derived for VIIRS bands M1 to M5 with the best matchups of satellite versus MOBY in situ measurements.

From results of extensive evaluations and assessments, we show that with the vicarious calibration VIIRS IDPS-produced ocean color products are significantly improved. In addition, some detailed analyses and discussions for the impact of vicarious calibration on ocean color products are provided. We show that, although there are still some important issues, VIIRS can potentially provide high-quality global ocean color products in support of the science researches and various operational applications.

References

[1] Gordon, H. R. (1998). In-orbit calibration strategy for ocean color sensors. *Remote Sens. Environ.*, 63, 265-278.

[2] Clark, D. K., H. R. Gordon, K. J. Voss, Y. Ge, W. Broenkow, and C. Trees (1997). Validation of atmospheric correction over the oceans. *J. Geophys. Res*, 102(D14), 17081-17106.

Title: A Mechanistic Assessment of Global Ocean Carbon Export From Satellite Observation

Authors: D.A. Siegel[1], K.O. Buesseler[2], S.C. Doney[2], S. Sailley[2], M.J. Behrenfeld[3], P.W. Boyd[4]

1 – University of California, Santa Barbara, Santa Barbara, CA USA
2 – Woods Hole Oceanographic Institution, Woods Hole, MA, USA
3 – Oregon State University, Corvallis, OR, USA
4 – University of Otago, Dunedin, New Zealand

Abstract:

The biological carbon pump is thought to export anywhere from 5 to 12 Pg C each year from the surface ocean depth in the form of settling organic particles and its functioning is crucial for the global carbon cycle. Assessments of the global export flux have either been through the extrapolation of point measurements to global scales or the results of ocean system model experimentation. Satellites resolve relevant space and time scales providing guidance to the empirical extrapolation problem, but they do not quantify directly carbon export. Here, we introduce a mechanistic approach for assessing global carbon export by accounting for 1) the size distribution of phytoplankton leading to the direct sinking of algal carbon biomass and 2) upper ocean mass budgeting of phytoplankton carbon and the production of fecal export mediated by zooplankton grazing. The resulting export flux model does an excellent job reproducing regional export flux observations and it reproduces the basic patterns of export spatially and seasonally, predicting a global export of 5.9 (±1.3) Pg C per year. A sensitivity analysis shows a relatively weak dependence of the global flux summaries to large changes in the four model parameters. Our approach provides many insights for future research on carbon export and ecosystem trophic dynamics.

Seasonal to Interannual Variability in Phytoplankton Biomass and Diversity on the New England Shelf: In Situ Time Series to Evaluate Remote Sensing Algorithms

Heidi M. Sosik
Biology Department, MS 32
Woods Hole Oceanographic Institution
Woods Hole, MA 02540-1049
hsosik@whoi.edu

Hui Feng
Ocean Process Analysis Laboratory (OPAL)
University of New Hampshire
Durham, NH 03824
Hui.Feng@unh.edu

We are exploring and evaluating algorithms that can be applied to remotely sensed ocean color data, extending beyond phytoplankton biomass to the possibility of functional group or size-class-dependent biomass retrievals. We have approached this challenge with unique phytoplankton time series observations made possible by new sensor technology deployed at an ocean observatory on the New England Shelf near Woods Hole, Massachusetts. Observations of phytoplankton and optical properties are being made at the Martha's Vineyard Coastal Observatory (MVCO), with focus on the combination of automated submersible flow cytometry and automated above water ocean color radiometry (AERONET-OC) (Figure 1).

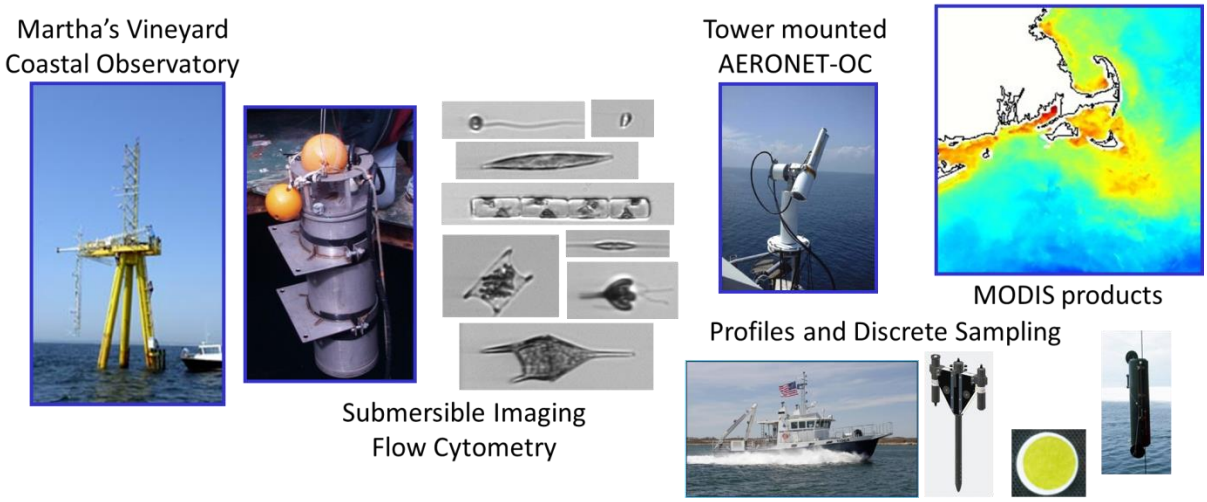

Figure 1. Autonomous sampling strategies at the Martha's Vineyard Coastal Observatory offshore tower site include an AERONET-OC SeaPRISM unit deployed on the rail of the tower, and Imaging FlowCytobot, shown here in its pressure housing ready for underwater deployment on the tower. Additional measurements and sample collection are conducted as part of water column profiles on trips to the site on a coastal vessel.

Our results show the MVCO study site is an excellent test case for a range of optical approaches to characterizing phytoplankton properties. The time series acquired to date emphasize that there are dramatic seasonal and some interannual fluctuations in the phytoplankton community, both

with respect to size structure (Figure 2) and taxonomic composition, thus providing a means to determine which types of algorithms can capture these changes.

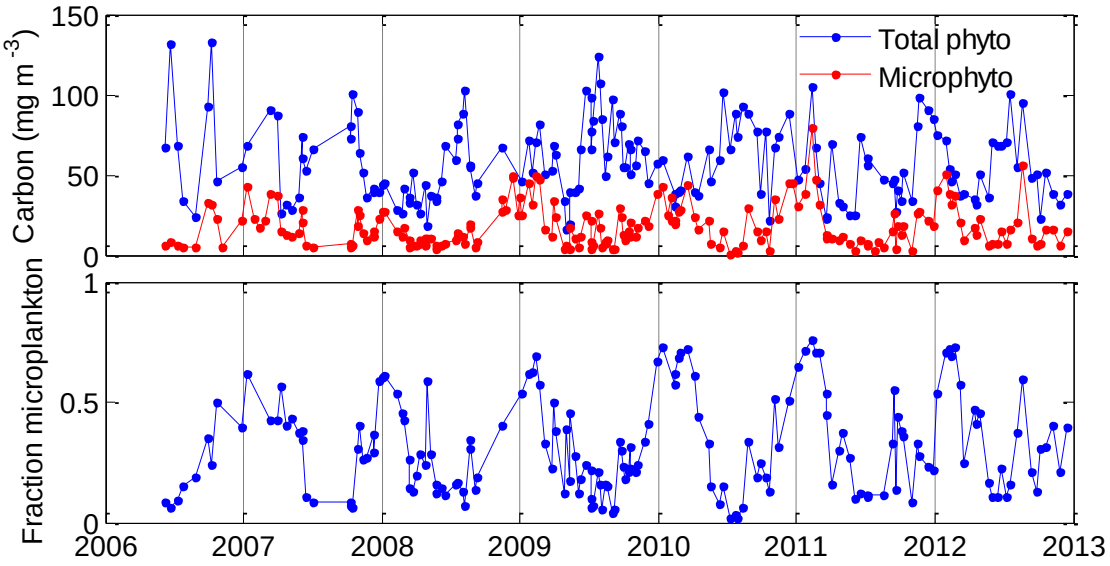

Figure 2. Time series of phytoplankton carbon biomass for the whole community and the microplankton (>20 μm) size fraction (upper panel) and the corresponding fraction of carbon in the microplankton (lower panel) at MVCO. Individual cell biovolumes are estimated from light scattering for small cells (Olson et al. 2003) and from 2D images for large cells and chains (Moberg and Sosik 2012); then carbon is estimated from cell volume according to published relationships (Menden-Deuer and Lessard 2000). Results shown here are for time points that include complete manual verification of image classification results ensuring highest quality estimates not affected by errors such as possible misidentification of detrital particles as plankton by automated classification approaches (Sosik and Olson 2007).

Efforts to date have focused primarily on evaluation of absorption- and pigment-based estimation of community cell size properties and pigment-based characterization of broad taxonomic groups. We find that published absorption- and pigment-algorithms both reproduce general patterns of seasonality, but tend to overestimate the contribution of microplankton in this system. In situ carbon-based taxonomic contributions are correlated with taxon biomass as Chl-a derived from published HPLC pigment algorithms, though relationships are non-linear and unexplained variance can be high, likely due in part to variation in carbon-to-Chl ratio with taxa and growth conditions. Preliminary assessment of published remote sensing algorithms for taxonomic indicator pigments shows they tend to underestimate at high concentrations such that retrieved seasonality is damped compared to in situ assessment.

Retrieval of aerosol and marine parameters in coastal environments: The need for improved bio-optical models

Stamnes[1], Knut, Li[1], Wei, Fan[1], Yongzhen, Stamnes[1], Snorre, Chen[1], Nan, and Stamnes[2], Jakob

[1]Stevens Institute of Technology, Hoboken, New Jersey 07030, USA
[2]University of Bergen, Bergen N-5000, Norway.

Simultaneous (one-step) retrieval of aerosol and marine parameters by means of inverse techniques based on coupled atmosphere-water radiative transfer modeling and optimal estimation can yield a considerable improvement in retrieval accuracy based on radiances measured by MERIS, MODIS, and similar instruments (Li et al., Int. J. Rem. Sens., 29, 5689-5698, 2008) compared with traditional (two-step) methods based on atmospheric correction which frequently lead to negative water-leaving radiances in turbid coastal waters. This one-step approach relies on adequate models describing the inherent optical properties (IOPs) of the atmosphere (aerosols) and the turbid water. However, recent experience (ftp://ccrropen@ftp.coestcolour.org/RoundRobin/CCRRreport.pdf with an annex: ftp://ccrropen@ftp.coastcolour.org/RoundRobin/CCRR_report_OCSMART.pdf) shows that IOPs produced by currently available bio-optical models do not match *in situ* measured IOPs very well, and give pigment absorption values that are smaller than the measured ones for high concentrations of pigmented particles found in turbid coastal waters. To remedy this problem we describe a different approach similar to that advocated by Stramski et al. (Applied Optics, 40, 2929-2945, 2001), and more recently by Zhang et al. (Applied Optics, 51, 5085-5099, 2012), in which we adopt two different groups of particles, one to mimic pigmented particles (characterized by its size distribution and refractive index with respect to water), and another group representing non-pigmented particles (characterized by its own size distribution and refractive index). Then we use the measured IOPs to determine that combination of size distributions, refractive indices, and mixing proportions of pigmented and non-pigmented particles which gives the optimum match between modeled and measured IOPs. This approach to IOP modeling of scattering and absorbing particles in the water is analogous to that currently used by NASA to describe aerosol IOPs (Ahmad et al., Applied Optics, 49, 5545-5560, 2010). It will be demonstrated that this consistent description of atmospheric and water IOPs leads to improved ability to retrieve aerosol and marine parameters in coastal environments through a one-step forward-inverse modeling approach based on coupled atmosphere-water radiative transfer modeling and optimal estimation.

Polymer: a new approach for atmospheric and glitter correction

F. Steinmetz, D. Ramon, P. Y. Deschamps
HYGEOS, Lille, 59000, France
Email: fs@hygeos.com

Summary

The POLYMER algorithm has been initially developed to process MERIS imagery, in particular in presence of intense sun glint. It has proven to be reliable, accurate and insensitive to many artifacts like light cloud contamination, improving greatly the usefulness of the MERIS data. Work is under progress to adapt the Polymer concept to other present ocean color sensors like MODIS and VIIRS. We are presenting preliminary results of application to VIIRS.

Introduction

The POLYMER algorithm [1] has been developed initially to improve atmospheric and glitter correction because of the two following rationales:

- The MERIS data exhibits large areas of sun-glint contamination that could not be treated correctly by the current atmospheric correction schemes extrapolating from the NIR
- The model of atmospheric scattering is simplified by using a polynomial of the wavelength, that allows to account for the multiple interactions between molecular and aerosol scatterings (and glitter) without reference to a specific aerosol model

It has been selected as the MERIS processor in the frame of the Ocean Colour Climate Change Initiative after an extensive comparison with other atmospheric correction algorithms [2].

MERIS processing

An example of the L2 product is given in Fig.1. The standard product processed by the standard MERIS Ocean Colour product (processed by MEGS) is also shown for comparison. Polymer allows retrieving effectively a consistent Chlorophyll pattern along the West Coast of Madagascar that is affected by an intense glitter pattern (up to 20% reflectance) and blacked out by the Megs processing. The POLYMER product is also less affected by the presence of clouds and less noisy than the Megs product. These merits are of paramount importance when compositing L3 products over a period.

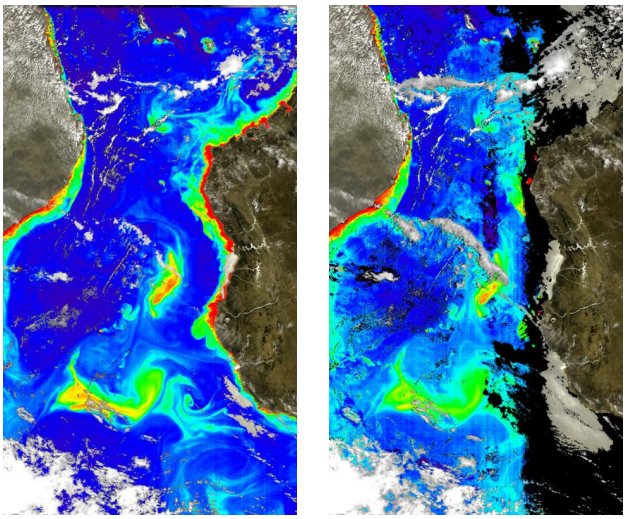

Fig.1: Example of level 2 chlorophyll-a concentration products from Dec. 21, 2003 over the Mozambique Canal, derived from MERIS data with Polymer (left) and MEGS (right) processors

VIIRS Processing

The POLYMER algorithm has been adapted to the processing of VIIRS data using its channels in the Visible and NIR. Preliminary results are shown in Fig.2 as well as the standard processing by NASA (processed by SeaDAS). We can see that the spatial coverage is higher for Polymer, and unlike the standard processing, do not show artifacts in the vicinity of the sun glint pattern.

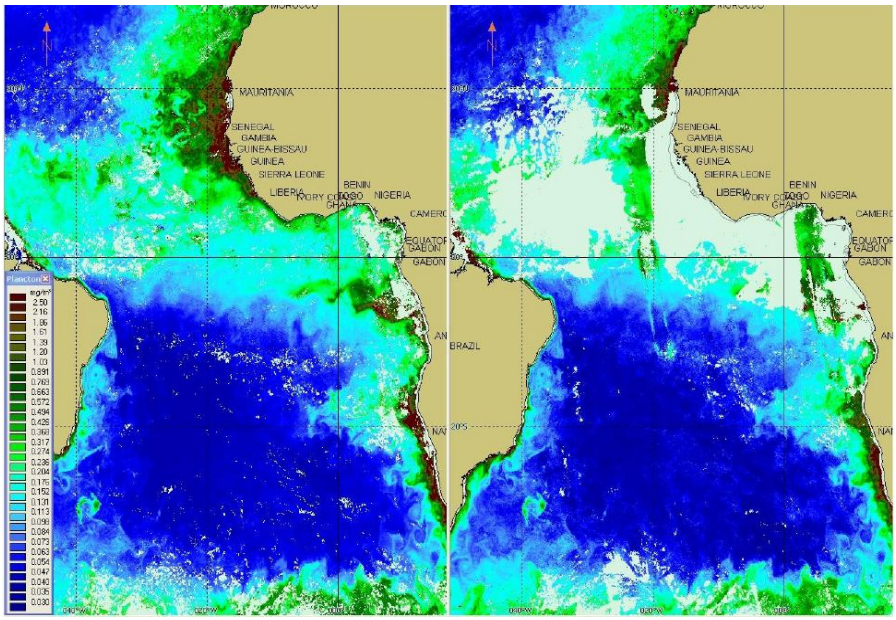

Fig. 2: example of level 3 composite of VIIRS chlorophyll-a concentration in the Atlantic Ocean from March 1-4, 2012, processed by Polymer (left) and SeaDAS (right).

Discussion

Due to a sensor-independent approach and an already successful application to multiple sensors, Polymer is an obvious candidate to the processing of OLCI data at Level 2. It performs best when applied to MERIS who has an excellent inter-band radiometric calibration thanks to its in-flight solar panel calibration and is less sensitive to the absolute radiometric calibration. It is a recommendation to the future to have a strong requirement on the specification of the inter-band radiometric.

References

[1] Steinmetz, F., Deschamps, P. Y. and Ramon, D. (2011). Atmospheric correction in the presence of sun glint: Application to MERIS. Optics Express, 19, 10, 9783-9800.
[2] Müller, D.; Krasemann, H.; Brewin, R.; Brockmann, C.; Deschamps, P-Y.; Doerffer, R.; Fomferra, N.; Franz, B.A.; Grant, M.G.; Groom, S.; Mélin, F.;Platt, T.; Regner, P.; Sathyendranath, S.; Steinmetz, F.; Swinton, J. (2012). The OC-CCI Assessment of Atmospheric Correction Processors. Sentinel-3 OLCI/SLSTR and MERIS/(A)ATSR workshop, ESRIN, Frascati, Italy.

Validation SIMEC adjacency correction for Coastal and Inland Waters?

S. Sterckx[1],E. Knaeps[1]
K.G. Ruddick[2], S. Kratzer[3,4], A. Ruescas[4]

[1] Flemish Institute for Technological Research (VITO), Boeretang 200, B-2400 Mol, Belgium
[2] Royal Belgian Institute for Natural Sciences (RBINS), 100 Gulledelle, 1200 Brussels, Belgium
[3]Stockholm University, Stockholm, Stockholm, SE-106 91, Sweden
[4]Brockmann Consult GmbH, Max-Planck-Str. 2, 21502 Geesthacht, Germany

Email: Sindy.Sterckx@gmail.com

Summary

In many coastal and inland waters environment effects hamper the correct retrieval of water quality parameters from remotely sensed imagery. SIMEC (SIMilarity Environment Correction), a new approach for the correction of adjacency effects is presented in this paper. SIMEC is applied to a MERIS match-up dataset over coastal and inland waters.

Introduction

Several new satellites such as Sentinel-2, Sentinel-3 and the hyperspectral satellites EnMAP and PRISMA will be launched in the near future. These EO sensors will provide a wealth of new data at increased spatial, spectral and temporal resolutions. Although not all conceived as being ocean colour missions, the inland and coastal water community could benefit considerably from these new data sources. A higher spatial resolution extends the existing monitoring efforts to cover even the first nautical mile from coast where the Water Framework Directive (WFD) is still in force or to lakes which are small and have irregular shapes and can not be monitored with the existing missions.

However for these nearshore coastal and inland waters adjacency effects complicate the atmospheric correction process. Light reflected from the nearby land can be forward scattered by the atmosphere into the sensor field of view. This causes a "blurring" of the signal and the effect, generally known as adjacency, background or environment effect, modifies the spectral signature of the observed pixel.

Here, we present a sensor-generic adjacency pre-processing method, the SIMilarity Environment Correction (SIMEC). This correction method was first proposed by Sterckx et al. (2010) [1] for the correction of airborne hyperspectral imagery. The correction algorithm estimates the contribution of the background radiance based on the correspondence with the NIR similarity spectrum [2]. A key aspect of the method is that no assumptions have to be made on the NIR albedo.

The objective of this paper is to validate SIMEC on MERIS images acquired from coastal and inland waters. SIMEC is applied to correct the TOA radiance signal for adjacency effects for a series of MERIS FR data covering the Belgian North Sea coastal waters, the turbid Scheldt estuary and a lake Vänern in Sweden, the third largest lake in Europe. Next, the standard MERIS processor (MEGS) is applied using the ODESA (Optical Data processor of ESA) software, in order to retrieve the water reflectance and to compare with in-situ measured water reflectance.

Discussion

The normalized water reflectance retrieved from ODESA-MEGS processing on MERIS FR images with and without first applying SIMEC are compared to the in-situ measured normalized water reflectance. For several sampling stations the MERIS retrieved normalized water reflectance is strongly underestimated

without SIMEC pre-processing with often negative water reflectance values for the first two MERIS bands (Figure 1). The correspondence between MERIS retrieved normalized water reflectance and in-situ measured normalized water are quantified on the basis of the Root Mean Square Error (RMSE) and the correlation coefficient (R^2). A significant decrease in RMSE and increase in R^2 is observed for several stations after SIMEC pre-processing.

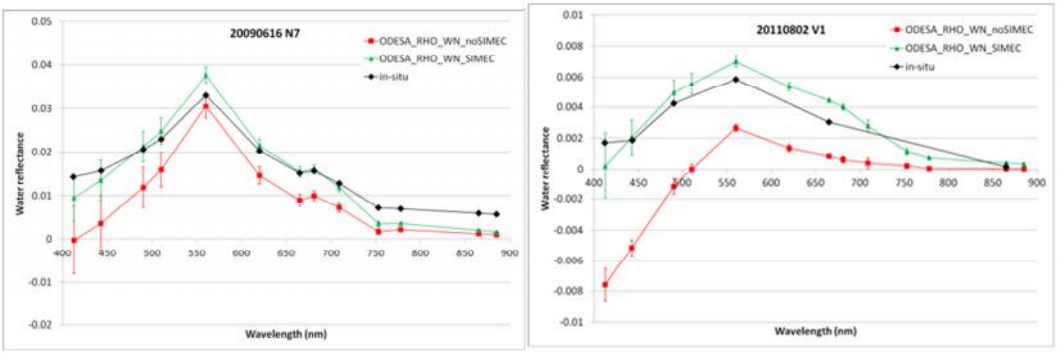

Fig. 1: Comparison between in-situ measured normalized water reflectance (black diamonds) and the normalized water reflectance extracted from MERIS FR within a 3x3 pixel box around the in-situ point derived from the ODESA-MEGS processor with (green triangles) and without (red squares) SIMEC pre-processing for North Sea (N) and Lake Vänern (V) sampling points. Error bars refer to the standard deviation calculated from the retrieved MERIS water reflectance for a 3 by 3 pixel window.

Conclusions

SIMEC is a sensor-generic approach and can therefore directly be applied to future. The performance of SIMEC was tested on MERIS FR images acquired over coastal areas, estuaries and lakes. SIMEC had a positive or neutral effect on the retrieved water reflectance calculated with the MERIS MEGS processor. A decrease in the RMSE up to 400 % was observed after SIMEC pre-processing.

References

[1] Sterckx, S., Knaeps, E., Ruddick, K., 2010, Detection and Correction of Adjacency Effects in Hyperspectral Airborne Data of Coastal and Inland Waters: the Use of the Near Infrared Similarity Spectrum. International Journal of Remote Sensing, 32(21), 6479-6505.

[2] Ruddick, K., De Cauwer, V., Park, Y., 2006, Seaborne measurements of near infrared water-leaving reflectance: The similarity spectrum for turbid waters, Limnol. Oceanogr., 51(2), 1167-1179.

Development of the Black Sea bio-optical algorithms: applications and some results based on ocean color scanner data sets

V. Suslin[1], T. Churilova[2]
[1]Marine Hydrophysical institute of National Academy of Sciences, Kapitanskaya str., 2, Sevastopol, 99011, Ukraine
[2]Institute of Biology of the Southern Seas of National Academy of Sciences, , 2 Nakhimov Ave. Sevastopol, 99011, Ukraine
Email: slava.suslin@gmail.com

Presently the Black Sea is the basin through which not only the transport streams of supply, metal and energy sources are passed, but also output of natural resources including hydrocarbon production takes place on shelf. The main wealth of the Black sea region is its recreational potential: comfortable weather conditions from May to October, unique natural landscape, properties of sea water (salinity ~ 17 ‰ and Secchi disk ~ 15 m on the southern coast of the Crimea) and a lot of historical places. So in near future its using will increase. Suitable tool is needed to track current ecological state of the Black Sea, to forecast and to calculate possible scenarios of various processes and events. Currently the cooperative operational hydrodynamical and ecological model of the Black Sea is this tool [1]. The models of such class induce development of regional algorithms which provides continuous stream of quantitative and qualitative information about biooptical characteristics of the upper layer of the Black Sea.

Main sources of these data are the measurements of the spectral radiances of the ocean-atmosphere system which are made by color scanners on the Earth orbit. Key element of regional biooptical algorithm for the Black Sea is the procedure of separation of the light absorption by phytoplankton and by colored detrital matter (sum of detritus and colored dissolved organic matter) [2, 3]. The example of this separation is shown on the figure. Biooptical characteristics of sea water such as particle backscattering coefficient in visible spectrum, spectral slope of particle backscattering coefficient [4], which is an integral part of inherent optical properties of seawater (*IOPs*), can be recovered, knowing the spectral characteristics of the coefficient of the light absorption by phytoplankton and by colored detrital matter and with remote sensing reflectance. Together with *in situ* measurements of taxonomic composition of phytoplankton they allows to analyze of links between *IOPs* and phytoplankton functional groups.

Based on the established features of the vertical distribution (statistics of field measurements of profiles) of concentrations of chlorophyll *a* and parameterization of the light absorption by all optically active components for the individual seasons and areas, it can restore the downward shortwave radiation field in the upper layer of the Black Sea [5]. This is necessary in the spectral approach to assess the primary production [6] and the contribution of short-wave radiation to the thermodynamic properties of seawater [7].

Acknowledgments

Source Data Credit: NASA/GSFC/OBPG, projects ODEMM, MyOcean-2, PERSEUS, DEVOTES, Russian-Ukrainian project “The Black Sea as a simulation model of the Ocean”, “Fundamental problem of operative oceanography” and “Riski” of

National Academy of Sciences of Ukraine.

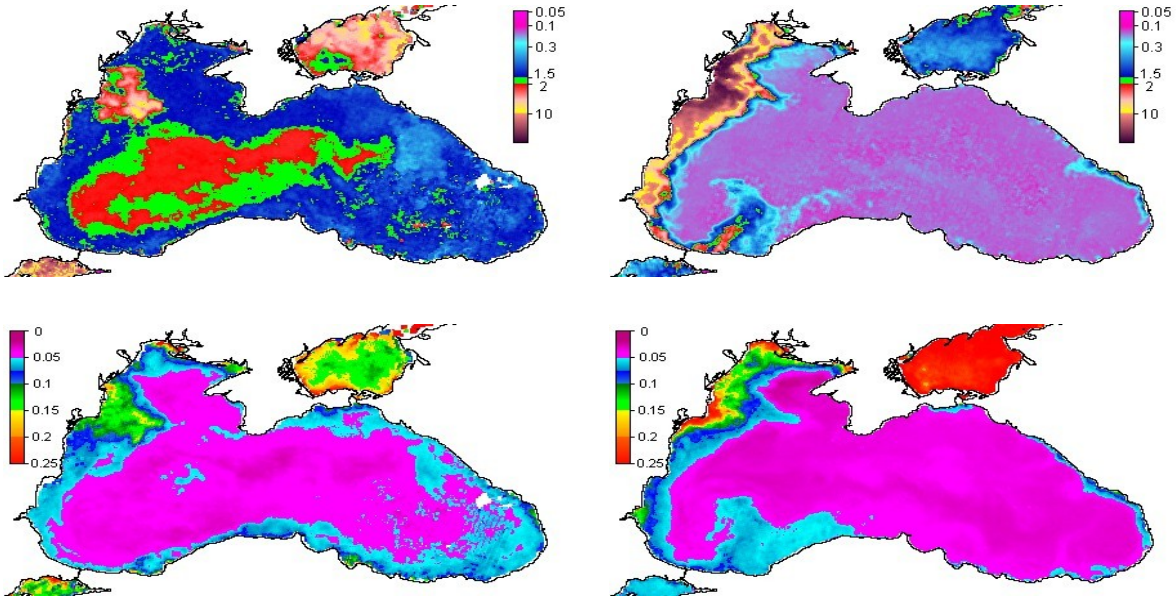

Figure. Example of merge products of chlorophyll a concentration (up, in mg m^{-3}) and absorption coefficient of colored detrital matter at 490 nm (bottom, in m^{-1}) in the 2nd half of March, 2004 (left) and in the 1st half of June, 2006 (right)

References

[1] Korotaev, G. K., Oguz, T., Dorofeyev, V.L., Demyshev, S. G., Kubryakov, A. I. and Ratner, Yu. B.: Development of Black Sea nowcasting and forecasting system, Ocean Sci., 7, 1–21, 2011.
[2] Suslin V., Churilova T., Sosik H. The SeaWiFS algorithm of chlorophyll a in the Black Sea // Marine Ecological J., 2008, Vol. VII, No. 2, p. 24-42, (in Russian)
[3] Suslin V., Sosik H., Churilova T., Korolev S. Remote Sensing of Chlorophyll *a* Concentration and Color Detrital Matter Absorption in the Black Sea: A Semi-Empirical Approach for the Sea-Viewing Wide Field-of-View Sensor (SeaWiFS) // Proceeding of XIX Ocean Optics conference, 6-10 October 2008, Tuscany, Italy, CD.
[4] Suslin V.V., Churilova T.Ya. The Black Sea *IOPs* based on *SeaWiFS* data // Ocean Optics XXI, Glasgow, Scotland, October 8-12, 2012, 9 p. OO121107_Suslin__Vyacheslav_Vladimirovich_OO121107.pdf
[5] Churilova T., Suslin V., Sosik H. Bio-optical spectral modelling of underwater irradiance and primary production in the Black Sea // Proceeding of XIX Ocean Optics conference, 6-10 October 2008, Tuscany, Italy, CD.
[6] Churilova T.Ya., Suslin V.V. Seasonal and inter-annual variability in waters transparency, chlorophyll a content and primary production in the Black Sea simulated by spectral bio-optical models based on satellite data (*SeaWiFS*) // Ocean Optics XXI, Glasgow, Scotland, October 8-12, 2012, 13 p. OO121251_Churilova__Tetyana_OO121251.docx
[7] Kubryakov A., Suslin V., Churilova T., Korotaev G. Effects of Penetrative Radiation on the Upper Layer Black Sea Thermodynamics // MyOcean Science Days, Toulouse, 1-3 December 2010, http://mercator-myoceanv2.netaktiv.com/MSD_2010/Abstract/ Abstract_KUBRYAKOVa_MSD_2010.doc

Accuracy assessment of satellite Ocean colour products in coastal waters.

Gavin Tilstone, Aneesh Lotliker[1], Steve Groom.

Plymouth Marine Laboratory, Prospect Place, West Hoe, Plymouth, PL1 3DH, UK
[1]Indian National Centre for Ocean Information Services (INCOIS), "Ocean Valley", P.B No.21, IDA Jeedimetla P.O, Hyderabad, 500 055, India

The use of Ocean Colour Remote Sensing to monitor phytoplankton blooms in coastal waters is hampered by the absorption and scattering from substances in the water that vary independently of phytoplankton. In this paper we compare different ocean colour algorithms available for SeaWiFS, MODIS and MERIS with in situ observations of Remote Sensing Reflectance, Chlorophyll-a (Chla), Total Suspended Material and Coloured Dissolved Organic Material in coastal waters of the Arabian Sea, Bay of Bengal, North Sea and Western English Channel, which have contrasting inherent optical properties. We demonstrate a clustering method on specific-Inherent Optical Properties (sIOP) that gives accurate water quality products from MERIS data (HYDROPT) and also test the recently developed ESA CoastColour MERIS products. We found that for coastal waters of the Bay of Bengal, OC5 gave the most accurate Chla, for the Arabian Sea GSM and OC3M Chla were more accurate and for the North Sea and Western English Channel, MERIS HYDROPT were more accurate than standard algorithms. The reasons for these differences will be discussed. A Chla time series from 2002-2011 will be presented to illustrate differences in algorithms between coastal regions and inter- and intra-annual variability in phytoplankton blooms

Coastal and Inland Water Data Product from the Hyperspectral Infrared Imager (HyspIRI)

Kevin R. Turpie[1]
on behalf of the HyspIRI Aquatic Data Products Working Group (HADPWG)

[1]University of Maryland, Baltimore County/JCET, Catonsville, USA, 20902
Email: kevin.r.turpie@nasa.gov

Summary

A team of about three dozen scientists in the coastal and inland water remote sensing community began a dialogue on how the upcoming HyspIRI mission could support the generation of coastal and inland data products and applications using its Visible to Short-wave Infrared hyperspectral (VSWIR) imager, eight thermal bands with high spatial resolution. This group, known as the HyspIRI Aquatic Data Products Working Group (HADPWG), demonstrated from the literature and their research with similar data sets that benefit of the HyspIRI mission of providing global remote sensing in these regions could be transformational. This report provides an overview of their conclusions and their vision for the future.

Introduction

HyspIRI is currently planned to include an imaging spectrometer with 213 spectral channels between 0.38 to 2.5 μm on 0.01 μm centers and a multispectral thermal infrared (TIR) instrument with eight spectral channels (one at 4 μm and seven between 7.5–12 μm) [1]. Both instruments will have a spatial resolution of 60 m at nadir. The spacecraft is also planned to be in an ascending polar orbit, crossing the equator at 10:30 AM local time. The equatorial revisit times will be 19 and 5 days for the VSWIR and TIR instruments, respectively [1]. The instrument will have 14bit radiometric resolution, 2% polarization sensitivity, and a 4° degree westward tilt to reduce solar specular reflectance. The projected SNR of HyspIRI is better than that of Hyperion, comparable to that of the Hyperspectral Imager for the Coastal Ocean (HICO) sensor on board the International Space Station (ISS), and is considered reasonably adequate for accurately retrieving hyperspectral reflectance from water surface for typical coastal conditions.

Discussion

Coastal ecosystems are amongst the most productive in the world, playing a major role in water, carbon, nitrogen, and phosphorous cycles between land and sea. Furthermore, coastal regions are home to about two thirds of the world's population [3]. Coastal counties in the USA alone produced nearly 40% of that country's GDP[4]. The wellbeing these human communities and their economies depends on the status of coastal ecosystems. Significant degradation and loss of wetlands [5], corals, submerged aquatic vegetation (SAV), have occurred [6]. Studies of coastal and inland water ecosystems structure and function, and how they interrelate, are critical to understand and protect these valuable resources.

These marginal regions between land and sea support valuable ecotones that are highly vulnerable to shifts in the environment, whether from climate change and its consequences (e.g., sea-level rise), human activities (e.g., eutrophication or changes to existing watershed hydrology), or natural

disturbances (e.g., storms or tsunamis). The so-called "Decadal Survey" (NRC 2008) [7], which defines the need for the HyspIRI mission, also identifies climate change as being more critical to coastal regions than any other. Establishing baseline maps and inventories for these ecosystems would be an important contribution to that end. Because these drivers of changes can occur on large scales or even globally, spaceborne remote sensing is a key tool for studying these environments. In particular, hyperspectral imagery is a valuable tool to assess coastal ecosystem status, distribution, and composition [8]. The HyspIRI mission in particular is well situated to produce global maps of coastal ecosystems and improve our understanding how these communities are distributed, structured, and function. This supports coastal ecosystem research and environmental conservation and management.

Conclusions

The HADPWG has pooled its resources and research, performed further analyses regarding specific technical issues, and synthesized the compiled information into a list of prioritized data products and applications. These are broken into five major areas:

1. Wetland Cover Classification and Mapping – e.g., tidal marshes, mangrove forests, fresh water wetlands, and boreal wetlands).
2. Water Surface Features and Floating Vegetation (Pleuston) – e.g., oil emulsions, kelp, sargassum mats, sea lettuce, floating debris)
3. Water Column Constituents – e.g., inherent and apparent optical properties, phytoplankton pigments, CDOM, and tripton.
4. Benthic Cover Classification and Mapping – e.g., coral and mollusk reefs, submerged aquatic vegetation, and algal mats.
5. Shallow Water Bathymetry

References

[1] Roberts, D.A., Quattrochi, D.A., Hulley, Hully, G.C., Hook, S.J., Green, R.O., (2012). Synergies between VSWIR and TIR dta for the urban environment: An evaluation of the potential for the Hyperspectral Infrared Imager (HyspIRI) Decadal Survey mission, *Remote Sensing of Environment*, 117, 83-101.

[3] Cracknell, A.P. (1999). Remote sensing techniques in estuaries and coastal zones – an update. International Journal of Remote Sensing, 19(3), 485-496. ISSN 0143-1161.

[4] Kildow, J.T., Colgan, C.S., Scorse, J. (2009). State of the U.S. Ocean and Coastal Economies – 2009. National Ocean Economics Program (NOEP). 60pp.

[5] Barbier EB; Hacker SD; Kennedy C; Koch EW; Stier AC, and Silliman BR., (2011). The value of estuarine and coastal ecosystem services. Ecological Monographs 81(2):169-193.

[6] Klemas, V .V ., (2001). Remote sensing of landscape-level coastal environmental indicators. Environmental Management 27(1): 47-57.

[7] National Research Council (2007). Earth science and applications from space: national imperatives for the next decade and beyond. Committee on Earth Science and Applications from Space: A Community Assessment and Strategy for the Future. 456 pp. (ISBN: 0-309-66714-3).

[8] Zomer, R. J., Trabucco, A. & Ustin, S. L., (2009). Building spectral libraries for wetlands land cover classification and hyperspectral remote sensing. *Journal of Environmental Management*, 90, 2170- 2177.

Improving remote sensing water quality algorithms

Twardowski, M., H. Groundwater, J. Sullivan, N. Stockley, Z. Lee

Work on improving algorithms for determining suspended particulate matter (SPM) and chlorophyll concentration from inherent optical property (IOP) measurements will be presented, as this is a critical link to developing improved semi-analytical algorithms for determining these parameters from remotely sensed reflectance. Data collected in northern Lake Michigan in the summer of 2012 will be included in the analysis. One of the limitations of using IOPs such as attenuation or backscattering as proxies for a parameter such as SPM is those relationships are dependent on the composition of the particle population, most importantly variability in size distributions and bulk refractive index. Other techniques have been developed, however, to estimate these particle characteristics from certain IOPs, so that there is potential for combining algorithms to determine water quality parameters with a semi-analytical or fully analytical algorithm from a suite of IOPs with greater accuracy than current empirical relationships.

Atmospheric trace-gas dynamics and impact on ocean color retrievals in urban estuarine and coastal ecosystems

Maria Tzortziou [1, 2], Jay R. Herman [3, 2], Ziauddin Ahmad [4,2], Chris Loughner [1, 2]

[1]University of Maryland, Earth System Science Interdisciplinary Center, College Park, MD, 20742, USA
[2] NASA Goddard Space Flight Center, Greenbelt, MD, 20771, USA
[3]University of Maryland, Joint Center for Earth Systems Technology, Baltimore, MD, 21228, USA
[4] Science and Data Systems, Inc., Silver Spring, MD, 20906, USA

Summary

Spatial and temporal dynamics in trace gas pollutants were examined over urban estuarine and coastal ecosystems in the US, Europe and Korea, using a new network of ground-based Pandora spectrometers. Our measurements showcase the strong temporal and spatial gradients in atmospheric nitrogen dioxide (NO_2) typically observed in moderately to highly polluted coastal areas in both developed and developing countries. Ground based measurements were combined with satellite observations from Aura-OMI, air-quality model simulations, and radiative transfer calculations to assess impacts on ocean color atmospheric corrections and retrievals of coastal ocean biogeochemical variables.

Introduction

Among the largest sources of uncertainty for satellite ocean color retrievals in near-shore waters close to heavily polluted urban centers is the strong temporal variability and spatial gradients in atmospheric absorbing trace gases (e.g., NO2) associated with industrial emissions, traffic, construction, heating and other anthropogenic activities [1]. Atmospheric pollution over near-shore waters can be transported back inland through sea breeze circulations, and converge with freshly emitted pollutants, aggravating air pollution levels and deposition of atmospheric pollutants along the shoreline. Moreover, strong, prolonged sea breeze events can transport a large amount of urban air pollution into the free troposphere, where pollutants have longer lifetime and are susceptible to long range transport offshore and over adjacent shelf and open ocean environments [2]. If not adequately corrected, this variability in coastal atmospheric composition can impose a false impression of temporal and spatial variability on the coastal ocean optical and biogeochemical properties retrieved from space [3]. Consideration of these errors is important for measurements from polar orbiting ocean color (OC) satellite sensors, but becomes particularly critical for geostationary satellite missions that aim at providing higher frequency and higher spatial resolution observations of ocean dynamics from a geostationary orbit.

Discussion

High frequency (every 2 min) measurements from our network of ground-based Pandora spectrometers provided the capability to capture the strong temporal and spatial variability typically characterizing atmospheric composition in coastal urban areas [1] [4] [5]. Our measurements in US, European and South Korean coastal areas show that NO_2 changes frequently exceed 0.5 DU over a period of an hour and 1 DU over a period of less than 3 hours (Figure 1). Local maxima in $TCNO_2$ typically occur early in the morning with secondary peaks often observed later in the afternoon associated with rush-hour NO_x emissions. With a footprint of approximately 12 km x 24 km at nadir, and less sensitive to NO_2 concentrations near the surface where NO_x is emitted, Aura-OMI does not typically capture the strong

spatial and temporal variability in NO_2 observed by the Pandora network and predicted by air quality models such as CMAQ (Community Multi-scale Air Quality model). On a sun-synchronous polar orbit and with an overpass at around 13:30 local time, Aura-OMI misses the morning and late afternoon rush-hour peaks in $TCNO_2$ observed by the Pandoras and predicted by the air-quality model over urban areas, providing a satellite image of $TCNO_2$ under relatively low near-surface emission conditions. Pandora observations were combined with high-resolution CMAQ simulations, and detailed radiative transfer calculations to evaluate how the observed variability in NO_2 affects ocean color retrievals from polar orbiting or geostationary satellite sensors if not corrected, or if atmospheric correction is based on climatology, measurements from other satellite instruments in sun-synchronous orbits (e.g. Aura-OMI), or coarser (and non-coincident) geostationary observations.

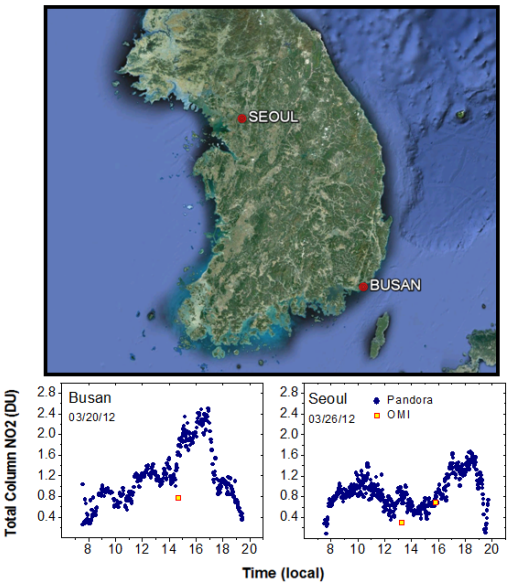

Figure 1 TCNO2 variability in Seoul and Busan

Conclusion

Our results show that high spatial and temporal resolution measurements of atmospheric NO_2 are critical in urban coastal areas to 1) better understand atmospheric dynamics at higher spatial resolution than is currently available from satellite observations, 2) capture the high temporal variability associated with local pollution patterns and photochemical processes, and 3) apply results to improve ocean color atmospheric corrections and retrievals of coastal ocean biogeochemical variables from space.

References

[1] Tzortziou M., J. R Herman, C. P Loughner, A.Cede, N. Abuhassan, S. Naik (2013). Spatial and temporal variability of ozone and nitrogen dioxide over a major urban estuarine ecosystem. Journal of Atmospheric Chemistry, Special Issue PINESAP, DISCOVER-AQ.

[2] Loughner C.P., M. Tzortziou, M. Follette-Cook, K. E. Pickering, D. Goldberg, C. Satam, A. Weinheimer, J. H. Crawford, D. J. Knapp, D. D. Montzka, G. B. Diskin, and R. R. Dickerson (2013; In Review). Impact of bay breeze circulations on surface air quality and boundary layer export. Atmospheric Environment.

[3] Fishman J.; Laura T Iraci; J Al-Saadi; P Bontempi; K Chance; F Chavez; M Chin; P Coble; C Davis; P DiGiacomo; D Edwards; Eldering, A.; J Goes; J Herman; C Hu; D Jacob; C Jordan; S R Kawa; R Key; X Liu; S Lohrenz; A Mannino; V Natraj; D Neil; J Neu; M Newchurch; K Pickering; J Salisbury; H Sosik; Subramaniam, A.; M Tzortziou; J Wang; M Wang (2012). The United States' Next Generation of Atmospheric Composition and Coastal Ecosystem Measurements: NASA's Geostationary Coastal and Air Pollution Events (GEO APE) Mission. Bulletin of the American Meteorological Society. doi:10.1175/BAMS-D-11-00201.1.

[4] Herman J.R., A. Cede, E. Spinei, G. Mount, M. Tzortziou, N. Abuhassan (2009). NO_2 Column Amounts from Ground-based Pandora and MFDOAS Spectrometers using the Direct-Sun DOAS Technique: Intercomparisons and Application to OMI Validation. J. Geophys. Res., 2009JD011848.

[5] Tzortziou M., Herman J.R., Cede A., Abuhassan N. (2012). High precision, absolute total column ozone measurements from the Pandora spectrometer system: Comparisons with data from a Brewer double monochromator and Aura OMI. J. Geophys. Res., 117, D16303, doi:10.1029/2012JD017814

A benchmark dataset for the validation of MERIS and MODIS ocean colour turbidity and PAR attenuation algorithms using autonomous buoy data.

Q. Vanhellemont[1], N. Greenwood[2], K. Ruddick[1]

[1] Royal Belgian Institute of Natural Sciences (RBINS), Management Unit of Mathematical Models (MUMM), Brussels, 1200, Belgium

[2] Centre for Environment, Fisheries & Aquaculture Science (CEFAS), Lowestoft, Suffolk, NR33 0HT, United Kingdom

Email: quinten.vanhellemont@mumm.ac.be

Summary

We present a dataset that combines marine reflectance spectra and several standard L2 products from MERIS and MODIS, with turbidity (T), Photosynthetically Available Radiation (PAR) at different depths, and fluorescence (F) from three autonomous buoys (CEFAS' Smartbuoys) located in turbid coastal waters of the North Sea and the Irish Sea. Our dataset contains several hundreds of matchups between in situ and satellite, and is a powerful benchmarking tool for validating satellite products and retrieval algorithms for turbidity and PAR attenuation.

Introduction

Ocean colour remote sensing is becoming well-established for the monitoring of coastal waters and marine science applications. Validation of satellite-derived products remains problematic, as simultaneous matchups of in situ data and cloud-free satellite data are sparse, and costly to obtain with ship-based measurements. Optical instruments on autonomous platforms can provide many more matchups, typically one per cloud free pixel. For moderate resolution ocean colour sensors (MODIS/MERIS) this is typically one matchup per cloud-free day at temperate latitudes, giving tens of matchups per year and hundreds over the lifetime of a satellite.

Smartbuoys are autonomous buoys operated by CEFAS that record several parameters multiple times per hour. Measurements from three turbid water buoys with deployments between 2002 and 2010 were used: WARP, (Warp Anchorage, 51.5°N, 1°E, Turbidity [5-95%]: 3-53 FTU), WGAB (West Gabbard, 52°N, 2°E, Turbidity [5-95%]: 1-18 FTU), and LIVB (Liverpool Bay, 53.5°N, 3.3°E, Turbidity [5-95%]: 1-21 FTU). Level 2 data from MODIS Aqua (R2012.0) and MERIS (2^{nd} and 3^{rd} reprocessing) was used, distributed respectively by NASA (OBPG - http://oceancolor.gsfc.nasa.gov/) and ESA (MERCI - http://merci-srv.eo.esa.int/merci/welcome.do). A kernel of 25 pixels (5x5) over each station is extracted from the remote sensing data, and is combined with the closest available in situ data within 60 minutes of the overpass (usually < 15 minutes). Fully cloudy or invalid kernels are skipped.

Datasets included from the MODIS data are: Remote sensing reflectance (Rrs, water-leaving radiance with air-sea interface reflection removed divided by downwelling irradiance) at wavelengths 412, 443, 469, 488, 531, 547, 555, 645, 667, and 678 nm. Some OBPG standard products are also included: aot_869, angstrom, chlor_a, cdom_index and Kd_490. Data was screened using the l2_flags, removing data where any of the following flags were raised: CLOUD, HISUNGLINT, LOWLW, MAXAERITER, HILT, HISUNGLINT and STLIGHT. Pixels with negative values in the dataset or negative values in Rrs 412, 443 or 488 and aot_869 were dropped. For chlor_a the respective product flag (CHLFAIL) was also checked.

Datasets included from the MERIS data are: water leaving radiance reflectance (ρ_w=Rrs·π) at wavelengths 413, 443, 490, 510, 560, 620, 665, 681, 708, 753, 778, 865 nm, aero_epsilon_865, aer_opt_thick_865, algal_1, algal_2, yellow_subs, and total_susp. The appropriate product confidence flags (PCD flags) and the CLOUD and HIGH_GLINT flags were used to mask bad data.

Discussion

The merged dataset contains the reflectance spectra from MODIS and MERIS with the corresponding in situ optical instrument data for hundreds of matchups between 2002 and 2010. The dataset allows for a validation of different reflectance based algorithms for turbidity (T) and PAR attenuation (Kpar). The Figure to the right shows an example validation of 596 high quality (with 25 unmasked pixels in the image kernel) MODIS turbidity [1] matchups. A robust relationship is found, with low relative errors. Some scatter is found in the lower T range, where the satellite gives lower values than the buoy. These discrepancies could be due to differences in the sampling of the scattering (backscatter/sidescatter), differences in sampling volume (a few cm^3 for the T sensor), erroneous atmospheric correction, or fouling of the in situ sensor.

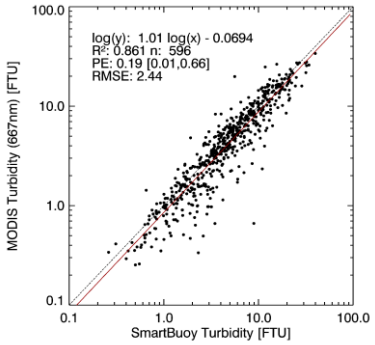

Example MODIS Aqua Turbidity matchups

In situ Kpar can be calculated for the buoys from the PAR sensors at different depths, and can be compared with Kpar products derived from remote sensing, such as [2,3]. The in situ fluorescence data is also included, but is known to have a bad correspondence to HPLC chlorophyll *a* concentrations. However, its relative signal can be relevant, and the data can also be useful in explaining differences between the in situ and remote sensing T or Kpar.

Conclusions

A reference dataset for coastal water ocean colour algorithm testing is presented that combines reflectance data from satellites and turbidity, fluorescence and PAR data from continuously measuring autonomous buoys. The instruments on the buoys were not intended for ocean colour remote sensing validation and could moreover be subject to fouling problems during extended deployments. However, the long time series of data, the large number of matchups, the wide concentration range, the relevant parameters and the high level of quality control of the datasets makes them very useful for coastal water algorithm testing. Following their successful use in studies from one team (http://www2.mumm.ac.be/remsem/publications.php), it was considered useful to make this dataset more widely and easily available for the ocean colour community.

References

[1] Nechad, B., K. G. Ruddick and G. Neukermans (2009). Calibration and validation of a generic multisensor algorithm for mapping of turbidity in coastal waters. SPIE European International Symposium on Remote Sensing, Berlin.

[2] Devlin, M. J., Barry, J., Mills, D. K., Gowen, R. J., Foden, J., Sivyer, D., & Tett, P. (2008). Relationships between suspended particulate material, light attenuation and Secchi depth in UK marine waters. Estuarine, Coastal and Shelf Science, 79(3), 429-439.

[3] Lee, Z. P., Du, K. P., & Arnone, R. (2005). A model for the diffuse attenuation coefficient of downwelling irradiance. Journal of Geophysical Research, 110(C2), C02016.

The Mediterranean Ocean Colour Observing System: product validation

G. Volpe, S. Colella, V. Forneris, C. Tronconi, R. Santoleri

Istituto di Scienze dell'Atmosfera e del Clima, CNR, Via Fosso del Cavaliere 100 - 00133 - Roma, Italy

Email: gianluca.volpe@cnr.it

Summary

This paper presents the product validation activity performed in the context of the Mediterranean Ocean Colour Observing System. Two validation schemes are presented: the offline and the online validation. The former refers to the computation of basic statistical quantities between satellite-derived product and the in situ counterpart. There is an overall good agreement between satellite and in situ chlorophyll. Among the analysed sensors SeaWiFS is the best performing. A method for assessing the near real-time product quality (online validation) is developed and its limitation discussed. Main results are concerned with the degradation, starting from mid-2010, of the MODIS Aqua channel at 443 nm with its successive recover thanks to the new calibration scheme implemented in the recently released SeaDAS version 6.4.

Introduction

To ensure a sustainable use of the marine resources, an accurate description and a reliable prediction of the ocean state and variability is crucial. An essential element of the Mediterranean Ocean Colour Observing System is tied to data reliability in terms of both the scientific accuracy and the temporal consistency. To address these issues two validation approaches are here described: an offline validation, every time a significant change in the processing chain takes place, and a daily online validation aimed at assessing the degree of data reliability based upon data time consistency.

Discussion

Offline validation

Offline validation refers to the comparison between single sensor (SeaWiFS, MODIS-Aqua and MERIS) satellite observations and the corresponding *in situ* measurements in terms of basic statistical quantities. The present analysis relies on the most up-to-date in situ CHL dataset for the Mediterranean Sea, whose quality has been improved through a careful analysis of the single CHL profiles. There is an overall good agreement between satellite-derived CHL and in situ OWP (Optically Weighted Pigment concentration). This work presents the first validation exercise performed over MODIS and MERIS Mediterranean-adapted algorithms in the basin. Scatterplots highlights a general underestimation by MODIS and MERIS (2^{nd} reprocessing), while SeaWiFS appears to be the best performing. Despite the lower number of observations, MERIS statistics perform slightly better than those of MODIS; both sensors, however, underestimate in situ OWP. Panels in **Errore. L'origine riferimento non è stata trovata.** show that this underestimation is particularly evident, for MODIS, in correspondence of OWP values lower than 1 mg m^{-3}, while larger values do agree quite well; on the other hand, MERIS underestimation is concerned with the entire CHL range of variability.

Online Validation

The aim of the online validation is to assess the temporal consistency of daily satellite observations through the use of both previous day data and of the daily climatological satellite data. These climatology maps have been created using the data falling into a moving temporal window of ± 5 days, and include the daily climatological standard deviation (STD) on a pixel-by-pixel basis. The current day data temporal consistency is evaluated into two successive steps.

First, checking, on a pixel-by-pixel basis, whether the difference between the current day observation and that of the previous day fall within or outside four climatological STD. These pixels fall in the statistics named "IN/OUT PrevDay". In case previous day data do not cover all of the current day pixels, the difference between these current day pixels and the corresponding current day SeaWiFS climatology is computed and compared against four climatological STD. These pixels fall in the statistics named "IN/OUT Clima". All pixels for which neither the first nor the second approach can be applied are marked as "Missing". The main outcome of this analysis, performed over the 2010-2011 sensors' time series, is that MODIS-derived chlorophyll exhibits, starting from mid-2010, a severe drift towards the low end of its range of variability. This drift depends in turn on the degradation of the channel at 443 nm.

Conclusions

Two distinct validation processes are performed within the Mediterranean Ocean Colour Observing System: the offline and the online validations. The offline validation refers to the product quality assessment performed via the in situ data comparison, and is performed every time a significant change in the processing chain takes place, e.g., in case of an algorithm update. Main results highlight the SeaWiFS product to be the most reliable in terms of basic statistical quantities, while MODIS- and MERIS-derived products do show a slight but systematic underestimation of the in situ field. The analysis also shows that there has been a slight SeaWiFS performing worsening as compared to previous results. The two most plausible causes have been identified: the processing software and the sensor degradation with time. As for the former, despite the evidence for the improvement of the CHL retrieval at global scale with SeaDAS 6.1, our analysis do demonstrate that the CHL retrieval remains below the quality target expectations in the Mediterranean Sea. Moreover, there is also evidence of a drift in the SeaWiFS signal, which has not fully corrected by the vicarious calibration meant to prevent the signal degradation with time. The second type of CHL quality evaluation presented in the work is the online validation. This system can thus be used to inform both the end-users and the upstream data providers about the quality of the product and of the data sources, respectively. A new SeaDAS release was recently issued with a new calibration scheme. This new SeaDAS version has demonstrated to successfully address the MODIS calibration issues in the Mediterranean and Black Sea. Based on these results the Mediterranean Ocean Colour Observing System has implemented, since June 2012, SeaDAS 6.4 in its operational processing chains to provide users with state-of-the-art products with outstanding scientific quality as fully demonstrated in this work.

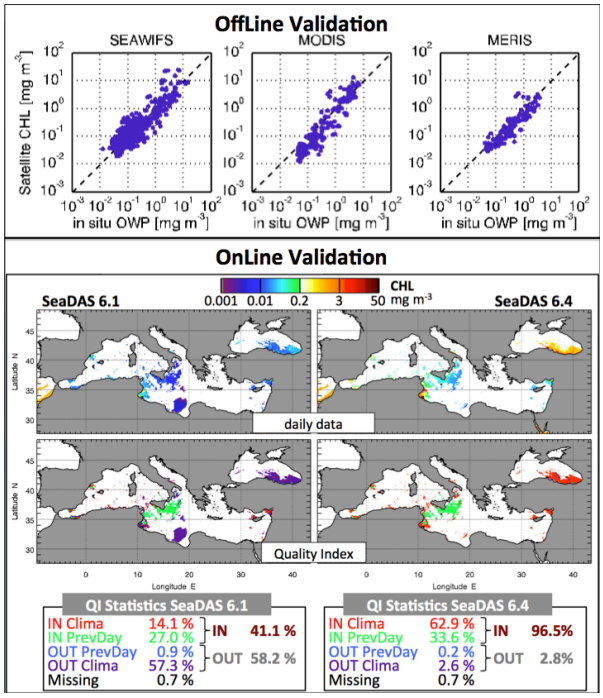

Figure 1: Upper panels show the offline validation the operational CHL observations. Left, middle and right panels represent SeaWiFS, MODIS and MERIS respectively. Lower panel shows an example of the online validation analysis over MODIS CHL image of the December the 13th, 2011. Left (right) panels refer to the analysis performed using SeaDAS 6.1 (6.4), and are the daily MODIS CHL image and the Quality Index, respectively.

The Influence of Raman Scattering on Ocean Color Inversion Models

Toby K. Westberry,[1] Emmanuel Boss,[2] Zhongping Lee[3]

[1]Oregon State University, Corvallis, OR 97331-2902, USA,
[2]University of Maine, Orono, ME 04469-5706, USA
[3]University of Massachusetts Boston, Boston, MA 02125, USA
Email: toby.westberry@science.oregonstate.edu

Summary

Raman scattering can be a significant contributor to the emergent color spectrum of the surface ocean. Despite its importance, previous efforts to account for this phenomenon have not been readily incorporated into routine bio-optical inversions of ocean color data. Here, we use radiative transfer simulations to quantify biases in optical properties retrieved from semi-analytical inversion models that are due to Raman scattering. Of particular interest are significant errors (>50%) in estimates of the particulate backscattering coefficient (b_{bp}). We present an analytical approach to directly estimate the Raman contribution to remote sensing reflectance in all ocean color satellite wavebands. For application to satellite remote sensing, spectral irradiance products in the ultraviolet from the OMI instrument are merged with MODIS data in the visible. The resulting global fields of Raman-corrected b_{bp} show significant differences from standard b_{bp} estimates, particularly in the clearest ocean waters where average biases are ~50%. Given the interest in transforming b_{bp} into biogeochemical quantities (e.g., particulate organic carbon or phytoplankton carbon), Raman scattering must be accounted for in semi-analytical inversion schemes.

Introduction

Ocean color inversion models provide a means of relating the emergent radiance spectrum to various absorbing and scattering components in the surface ocean. However, the accuracy of retrieved quantities depends upon our ability to account for all significant processes affecting light transmission and propagation in the ocean and atmosphere. One such physical process that affects the ambient light field is Raman scattering, a form of inelastic scatter in which photons that interact with the medium (e.g., seawater) are re-emitted at wavelengths differing from the excitation source (Raman and Krishnan 1928).

Past efforts have demonstrated that Raman scattering can contribute significantly to the marine upwelling radiance field across all visible wavelengths to a variable degree (see Gordon, 1999 and references therein). As a result, failure to account for Raman scattering when will result in errors in any relationships linking in-water properties to upwelling radiance or equivalently, remote sensing reflectance, $R_{rs}(\lambda)$. Select works have accounted for the phenomenon (Sathyendranath and Platt, 1998; Loisel and Stramski, 2000), but these efforts have not been carried forward in subsequent studies or in the comprehensive report by the IOCCG (IOCCG volume 5).

Here, we express $R_{rs}(\lambda)$ as the sum of an elastic scattering component and an inelastic scattering component due to Raman:

$$R_{rs}(\lambda, 0^-) = R_{rs,E}(\lambda, 0^-) + R_{rs,Raman}(\lambda, 0^-) \quad (1)$$

We are subsequently able to develop an analytical expression for the Raman component of Rrs:

$$R_{rs,Raman}(0^+,\lambda_{em}) = \frac{t}{n^2}\frac{\tilde{\beta}^r(\theta_s\rightarrow\pi)b_r(\lambda_{em})E_d(0^+,\lambda_{ex})}{(K_d(\lambda_{ex})+\kappa_L(\lambda_{em}))E_d(0^+,\lambda_{em})}\left[1+\frac{b_b(\lambda_{ex})}{\mu_u(K_d(\lambda_{ex})+\kappa(\lambda_{ex}))}+\frac{b_b(\lambda_{em})}{2\mu_u\kappa(\lambda_{em})}\right] \quad (2)$$

where the subscripts λ_{ex} and λ_{em} refer to excitation and emission (satellite) wavelengths. In practice, initial estimates of inherent optical properties (IOPs) are required, as well as incident spectral irradicances at excitation and emission wavelengths, $E_d(0^+, \lambda_{ex})$ and $E_d(0^+, \lambda_{em})$, respectively. Thus, the procedure is applied iteratively. In this work, we employ two inversion models currently used by NASA to generate evaluation products, the GSM model (Maritorena et al., 2002) and the QAA (Lee et al., 2002).

Results and Discussion

Results obtained with simulated data (HydroLight) show that 1) the relative error in each IOP due to Raman scattering differs greatly between each IOP, 2) errors differ between inversion models (GSM versus QAA), 3) errors are greatest at low *Chl* and decrease with increasing *Chl*, and 4) errors are greatest in the retrieval of $b_{bp}(443)$. *Chl* and $a_{ph}(443)$ are overestimated by ~15-25% under the most oligotrophic conditions (Chl<0.02 mg m^{-3}), and decrease to ~5% when *Chl*>0.3 mg m^{-3}. Errors in $a_{CDM}(443)$ are negligible across all trophic conditions. Errors in $b_{bp}(443)$, however, can be >100% under oligotrophic conditions and are still ~20% when *Chl*>0.3 mg m^{-3}.

Application to a single monthly field of satellite remote sensing data (June 2004) yields patterns consistent with those diagnosed from simulated data. For the GSM model, median Chl decreases only slightly (~8%) from 0.12 mg m^{-3} to 0.11 mg m^{-3} after correction for Raman. Median phytoplankton absorption ($a_{ph}(443)$) estimated from the QAA decreases similarly (8%) following correction. Retrievals of CDOM and detrital absorption, $a_{CDM}(443)$, are particularly insensitive to the presence of Raman scattering and only change by <3% for either inversion model. The largest differences resulting from the Raman correction are observed in $b_{bp}(443)$. Global distributions of Raman-corrected $b_{bp}(443)$ for both models show values that are much lower across most of the mid-latitudes, and to a lesser extent at high latitudes. As a global average, Raman-corrected $b_{bp}(443)$ from GSM and QAA are shifted downward by ~30% and 20%, respectively, but up to 30% of the ocean has errors due to Raman in excess of 50%. This suggests that $b_{bp}(443)$ is significantly overestimated over much of the ocean when using either model without correction for Raman scatter. This is of particular interest is we are to accurately transform these optical proxies into biogeochemical quantities.

References

Gordon HR (1999) Contribution of Raman Scattering to Water-Leaving Radiance: a Reexamination. Appl Optics 38 (15):3166-3174.

Lee ZP, Carder KL, Arnone RA (2002) Deriving inherent optical properties from water color: A multiband quasi-analytical algorithm for optically deep waters. Appl Optics 41 (27):5755-5772.

Loisel H, Stramski D (2000) Estimation of the inherent optical properties of natural waters from the irradiance attenuation coefficient and reflectance in the presence of Raman scattering. Appl Optics 39 (18):3001-3011. doi:10.1364/ao.39.003001.

Maritorena S, Siegel DA, Peterson AR (2002) Optimization of a semianalytical ocean color model for global-scale applications. Appl Optics 41 (15):2705-2714.

Raman CV, Krishnan KS (1928) A new type of secondary radiation. Nature 121:501-502.

Sathyendranath S, Platt T (1998) Ocean-color model incorporating transspectral processes. Appl Optics 37 (12):2216-2227. doi:10.1364/ao.37.002216.

Assessment of bio-optical algorithms for satellite radiometers in coastal waters of the Baltic Sea using in situ measurements

M. Woźniak, B. Wojtasiewicz, K. Bradtke

University of Gdansk, Institute of Oceanography, Department of Physical Oceanography, Gdansk, 80-952, Poland

Email: m.wozniak@ug.edu.pl

Summary

The assessment of ocean color satellite algorithms was performed for coastal waters of the Baltic Sea. The formulas for chlorophyll *a*, K_d(490), CDOM absorption at 400 nm, TSM and Secchi depth were tested. The in situ reflectance data gathered in the Gulf of Gdansk using RAMSES hyperspectral radiometers were applied in the validation. The obtained results suggest that after calibration of the coefficients the formulas can be used for OLCI coastal data.

Introduction

The Baltic Sea which is affected by eutrophication suffers from frequent algae blooms. A part of bloom-forming organisms, like cyanobacteria, can form extensive summer blooms which can possibly have toxic influence on other organisms, including human beings.Thus they can affect the recreational use of coastal areas. Therefore, there is a need to predict and monitor the development of mass occurrence of phytoplankton whose dynamics has to be studied with relevant spatial and temporal resolution. Remote sensing techniques can provide extensive spatial coverage (synoptic view) and time-series that are necessary to study this problem. However, standard remote sensing algorithms often fail badly in the Baltic Sea waters due to high concentrations of colored dissolved organic matter (CDOM) and suspended particulates (SPM).A big effort to the calibrate the algorithms and to validatethe products has been made for the ocean color radiometers (i.a. [1]; [2]; [3]; [4]; [5]). New measuring opportunities will be anticipated in the Sentinel-3 mission which is planned to begin in the nearest future. The aim of this project was to select the most accurate formulas which could be used to derive optical parameters based on the Sentinel-3 data in the coastal waters of the Baltic Sea. The following parameters were considered: the chlorophyll *a* concentration, the spectral diffuse attenuation coefficient of downwelling irradiance at 490nm K_d(490), the absorption coefficient of CDOM (also called yellow substance) at 400nm, total suspended matter (TSM) and the Secchi depth. We validated the algorithms developed for previous ocean color radiometers. The spectral bands used in these algorithms were within the Sentinel OLCI ones.

Discussion

The input data were the reflectance values measured *in situ* with the use of the hyperspectral radiometer TriOS RAMSES. All the reflectances used were recalculated into the Sentinel-3 bands. The data were collected from May to September, 2012 in the Gulf of Gdansk (Southern Baltic Sea) at five stations (Fig. 1). We chose nine algorithms for chlorophyll *a* (chl-*a*) concentration. Four of them were proposed by HELCOM [6] three were provided by Darecki & Stramski [2],whereas the remaining two were developed in theDESAMBEM project [5]. The best accuracy (Mean Normalised Bias (MNB) -29% and Root Mean Square (RMB) of 26%) was obtained using one of the DESAMBEM algorithms, whereas the worst was observed in the case of OC4 standard algorithm. It is not surprising, because this algorithm was developed for typical case 1 waters. The values of MNB and RMB for the other algorithms were below 100%,except for one of the algorithms proposed by Jorgensen and Berastegui (HELCOM) for

which the MNB and RMB were higher than 120%.In the case of K_d(490)we chose algorithms proposed by Kratzer [3], Alikas [1], Darecki & Stramski, [2] and Mueller [4].The lowest bias was noted when the algorithm proposed by Mueller was applied, beside the fact that it was developed for case 1 waters. However the statistics obtained for the remaining formulas were very similar. The algorithms for a_{ys}(400) and TSM were taken from Darecki's PhD thesis [7]. He proposed more than four algorithms for these two components, but we chosen these with the lowest errors. Kratzer in her paper [3] beside the algorithm for K_d(490) proposed also the algorithm for the SD which was the only one tested in our study, but the results weresatisfactory (MNB of 1% and RMB 19%).

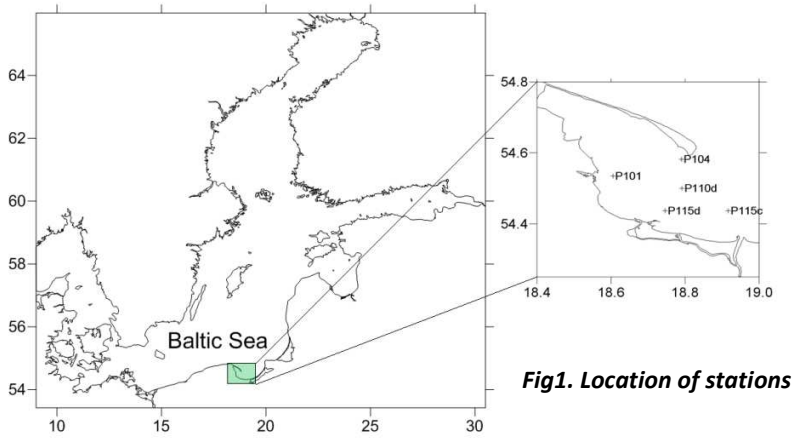

Fig1. Location of stations

Conclusions

The results of the validation prove the accuracy of the algorithms which were applied for previous ocean color space-borne sensors. It can be expected that they can be also used for OLCI sensor. However, in the case of coastal areas it is necessary to calibrate the coefficients used in these formulas.

References

[1] Alikas K., Kratzer S., ReinartA. (2012). Robust Kd(490) and Secchi algorithms for remote sensing of optically complex waters. Proceedings of XXI OO conference

[2] Darecki M., Stramski D. (2004). An evaluation of MODIS and SeaWiFS bio-optical algorithms in the Baltic Sea. Remote Sensing of Environment 89, pp 326–350

[3] Kratzer S., Brockmann C. , Moore G. (2008). Using MERIS full resolution data to monitor coastal waters — A case study from Himmerfjärden, a fjord-like bay in the northwestern Baltic Sea. Remote Sensing of Environment 112, pp 2284–2300

[4] Mueller J.L. (2000). SeaWiFS Algorithm for the Diffuse Attenuation Coefficient Kd(490) Using Water-Leaving Radiances at 490 and 555nm. Chapter 3 of O'Reilly, J.E., and 24 Coauthors, 2000: *SeaWiFS Postlaunch Calibration and Validation Analyses*, Part 3. NASA Tech. Memo. 2000–206892, Vol. 11, S.B. Hooker and E.R. Fire-stone, Eds., NASA Goddard Space Flight Center, pp. 24-28

[5] Woźniak B., Krężel A., Darecki M., Woźniak S.B., Majchrowski R., Ostrowska M., Kozłowski Ł., Ficek D., Olszewski J., Dera J. (2008). Algorithms for the remote sensing of the Baltic ecosystem (DESAMBEM). Part 1: Mathematical apparatus. Oceanologia, 50 (4), pp. 451–508.

[6] HELCOM, (2004). Thematic Report on Validation of Algorithms for Chlorophyll a Retrieval from Satellite Data of the Baltic Sea Area.

[7] Darecki M. (1998). Analiza wpływu składników wód Baltyku na spektralne charakterystyki oddolnego pola światła. PhD thesis (in Polish).

Inherent Optical Properties of Coccolithophores: Emiliania Huxleyi

P. Zhai[1], Y. Hu[2], C. R. Trepte[2], D. M. Winker[2], D. B. Josset[1] and P. L. Lucker[1]

[1]SSAI, MS 475 NASA Langley Research Center, Hampton, VA, 23681, USA
[2]MS 475 NASA Langley Research Center, Hampton, VA, 23681, USA
Email: Pengwang.zhai-1@nasa.gov

Summary

In this paper we simulate and report the Inherent Optical Properties (IOP) of Emiliania Huxleyi (EHUX), the most abundant species of the coccolithophores. The IOPs include the Mueller scattering matrix, extinction and scattering cross sections. A realistic non-spherical model is built for EHUX based on electron micrograph of coccolithophore cells. The coccolithophore model includes a near-spherical core with refractive index of 1.04, and a carbonate shell formed by smaller coccoliths with refractive index of 1.2. The Amsterdam Discrete Dipole Approximation (ADDA) code [1] is used to simulate light scattering by non-spherical particles. The impacts of different cell configuration and size on the Mueller scattering matrix elements are studied. We compare our results with a previous theoretical model based on detached coccoliths [2] and ocean water Mueller matrix measurements [3]. Potential usage of this modeled Mueller matrix on ocean color remote sensing will be explored.

Introduction

Coccolithophores, or coccolithophorids, are unicellular and photosynthetic and are found in large numbers in global ocean waters. They provide important food sources for aquatic environment. An interesting feature of coccolithophores is that they generate calcium carbonate plates called coccoliths. The production of coccoliths play important roles in carbon cycle by their $CaCO_3$ production in response to the CO_2 partial pressure change. Emiliania Huxleyi (EHUX) is the most abundant species of coccolithophores. They can produce massive blooms that have large impacts on the environment and fisheries. In the global scale, it is indispensible to use ocean color sensors such as MODIS and VIIRS to study the effects of coccolithophore primary production on the carbon cycle and to monitor EHUX bloom events. The CALIOP satellite lidar system provides valuable information on ocean waters [4]. The combination of passive and active systems will generate a plethora of multidimensional information on coccolithophores and other oceanic particles.

In assisting the interpretation of both passive ocean color satellite images and active lidar signals, it is necessary to have the knowledge of Inherent Optical Properties (IOP) of these particles. A short list of these properties include absorption and scattering coefficients, beam attenuation coefficient, scattering matrix, and a few other parameters used in different applications. Both theoretical simulations and experimental measurements are used to obtain the IOP for oceanic particles. The microscopic images of coccolithophores and other particles show that overall these particles are not spherical. Nevertheless spherical models are used to simulate IOP for oceanic particles due to the significant difficulties of simulating light scattering by large non-spherical particles. On the other hand, the experimental measurements of ocean waters are mostly focused on absorption and extinction coefficients, sometimes volume scattering function (the 11 element of the scattering matrix). The complete Mueller matrix measurements for ocean water have been done by Voss and Fry in 1984 [3] and are still widely cited after almost 30 years. Theoretical efforts have been made to simulate light scattering by small

detached coccoliths [2]. In this paper we present an effort of simulating the IOP for the whole EHUX cells. The results are compared to the detached coccoliths and differences are observed.

Model and results

Our model is based on the scanning electron micrograph of a single coccolithophore cell (see Fig. 1(a)). The coccolith model is built similar to the wagon wheel model presented in Gordon (2007) [2]. The coccoliths are rotated and rearranged around a nearly spherical core to form a representation of the EHUX cell (see Fig. 1(b) for an example). The index of refraction is set to 1.2 for the coccoliths and 1.04 for the spherical core. A random number generator is used to produce realistic irregularities for the EHUX cell. The model is then transformed into dipole representations which can be used as inputs to the Amsterdam Discrete Dipole Approximation code (ADDA) [1] to calculate the complete set of IOP for this cell. Figure 1(c) shows the scattering matrix element S_{22}/S_{11} of the EHUX cell shown in Fig. 1(b) for different sizes. The average scattering matrix measurement of ocean water by Voss and Fry [3] is also shown for comparison. It is observed that the theoretical simulations for this element is smaller than that of the average ocean water for scattering angle smaller than 120 degrees and it is larger if scattering angle is larger than 120 degrees. It is also interesting to see the sharp peak around the backscattering which suggests a difficulty in the extrapolation of the measurements towards 180 degrees. We will present some systematic results for other elements.

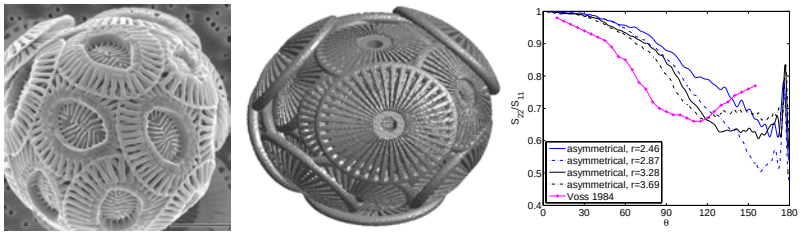

Figure 1 From left to right: (a) A scanning electron micrograph of a single coccolithophore cell. Image credit: Alison R. Taylor (University of North Carolina Wilmington Microscopy Facility) (b) a realistic model representing the coccolithophore cell (c) the scattering matrix element S_{22}/S_{11} for the model presented in Fig. 1(b) for different sizes (unit micron). The measurement for ocean water by Voss and Fry 1984 is also plotted for comparison.

Summary

A realistic nonspherical model for EHUX is built and the optical properties are calculated using the ADDA code. The results show large deviations from the average ocean water measurements. The spike at the backscatter suggests the necessity of measuring scattering matrix for the whole set of scattering angles.

References

1. Yurkin, M.A. and Hoekstra, A. G. (2011) The discrete-dipole-approximation code ADDA: capabilities and known limitations. J. Quant. Spectrosc. Radiat., 112: 2234–2247 .
2. Gordon, H.R. (2007) Backscattering of light from disk-like particles with aperiodic angular fine structure. Opt. Express 15: 16424-16430.
3. Voss, K.J. and Fry, E.S. (1984) Measurement of the Mueller matrix for ocean water. Appl. Opt. 23: 4427-4439.
4. Hu, Y. and coauthors, 2010: Presentation at the A-Train Symposium, “Ocean Carbon Cycle Studies Using CALIOP and High Spectral Resolution Lidar (HSRL)”, http://a-trainneworleans2010.larc.nasa.gov/pdf/CCES-PM/04_Hu.pdf

Accurate estimation on floating algae area in Lake Taihu, China

Y.C. Zhang, R.H. Ma, H.T. Duan

Nanjing Institute of Geography and Limnology, Nanjing, 21008, P. R. China
Email: yczhang@niglas.ac.cn

Summary

Various floating algae area detecting methods have been reported using remote sensing data in open oceans, coastal waters and inland lakes. Yet partial coverage of floating algae in sub-pixels is always neglected besides atmospheric correction and diverse algae index, so that different estimations are always achieved in spite of using the same remote sensing image. Here, a novel algorithm to detect floating algae absolute area based on floating algae index (FAI)[1], namely algae pixel-growing algorithm (APA), is developed and applied to quantify timely floating algae area in Lake Taihu of China using MODIS data.

Introduction

According to the FAI definition [1] and the fundamental property of water color remote sensing, FAI value of a MODIS pixel has the linear relation with FAI values of MODIS sub-pixels. Considering that it is difficult to achieve the FAI of sub-pixel, we suppose that two kinds of sub-pixels make up the target pixel, which have the same FAI to the maximum and minimum value of a 3×3 pixels window (the target pixel is the central pixel of the window), which could be expressed as,

$$\mathrm{FAI}_{MODIS}{}^{pixel} = \gamma \cdot FAI_{MODIS}(Max^{pixel}) + (1-\gamma) \cdot FAI_{MODIS}(Min^{pixel}) \quad (1)$$

where r is the decomposition parameter. For a mixed pixel of MODIS, we definite the algae coverage is the proportion of area covering by floating algae in a mixed pixel. Considering that the thickness of floating algae is variant in different area, we think that all of the mixed pixels are covered by the thinnest floating algae. Suppose that the relationship of FAI and coverage of a mixed pixel could be expressed as follows,

$$FAI = \alpha \cdot FAI_{algae} + (1-\alpha) \cdot FAI_{non-algae} = \left(FAI_{algae} - FAI_{non-algae}\right) \cdot \alpha + FAI_{non-algae} \quad (2)$$

where α is coverage of a mixed pixel, FAI_{algae} and $FAI_{non\text{-}algae}$ are the FAI threshold of floating algae and non-algae respectively. Then the FAI of max pixel and min pixel in a 3×3 pixels window could be expressed as,

$$FAI_{MODIS}(Max^{pixel}) = \mathrm{m} \cdot \alpha_{Max} + \mathrm{k} \qquad FAI_{MODIS}(Min^{pixel}) = \mathrm{m} \cdot \alpha_{Min} + \mathrm{k} \quad (3)$$

where m and k are the slope and intercept respectively; α_{max} and α_{min} are the coverage of max and min pixels in a 3×3 pixels window respectively. Integrating Equations (1) & (3), coverage of mixed pixel could be described as,

$$\alpha_{MODIS}{}^{pixel} = \gamma \cdot \alpha_{Max} + (1-\gamma) \cdot \alpha_{Min} \quad (4)$$

Discussion

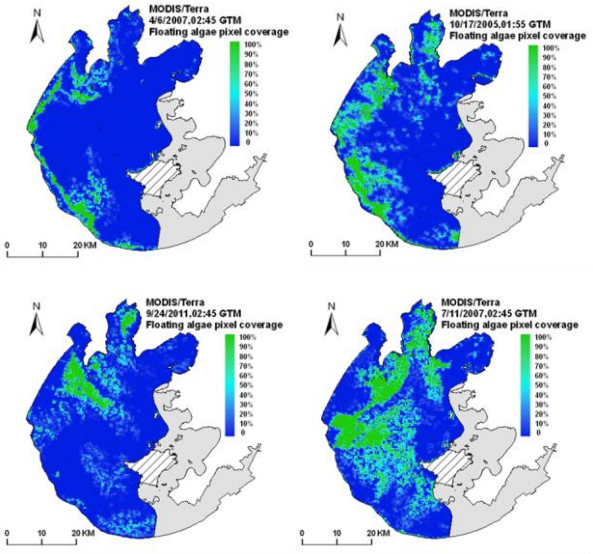

Examples of algal bloom spatial distribution from algal pixel-growing algorithm using MODIS data.

Figure 1 shows some examples of algal bloom spatial distribution from algal pixel-growing algorithm using MODIS data. Algal bloom area identified from 24 Landsat TM/ETM+ images ranges from 14.8 to 505.7 km^2. Compared with TM/ETM+ images, RSE (Relative Standard Error) of APA and LA (Linear algorithm) [2] in synchronous MODIS images is 15.2 and 24.8 respectively, and corresponding RE (Relative Error) is 9.9% and 17.3%. Whatever algal bloom area is, APA shows better and more stable results than LA. Further confirmed by comparing MODIS algal bloom coverage histograms resulted from APA and LA with paired TM/ETM+ coverage histogram resized from 30 to 250 m. In our study, instead of choosing minimum value of different algal bloom thresholds, all pixels completely covered by pure algae in 24 MODIS images were pooled together to compute the FAI histogram as well as the mean and standard deviation. Considering the decentralized distribution of FAI value of pure algae pixels, a universal algal bloom threshold was determined as the mean (0.115) minus the standard deviation (0.065), which was approximately 0.050, which could include 85.4% pure algae pixels of 24 MODIS images. The universal algal bloom threshold (FAI=0.05) was chosen as a time-independent FAI threshold to distinguish pure algae blooms from waters partially covered by floating algae. We also gathered all pixels from 24 MODIS images, the floating algae coverage of which is below 5% but not zero. It reveals that FAI values of low-coverage algal bloom are not fixed or centralized, which ranged from -0.03 to 0.02, and 85.4% of which were less than -0.002.

Conclusions

Algae pixel-growing algorithm (APA), a novel algorithm, is introduced here to detect floating algae absolute area in Lake Taihu, based on the Floating Algae Index (FAI) which is less sensitive to changes in environmental and observing conditions such as aerosols and solar/viewing geometry. Data comparison with synchronous Landsat TM/ETM+ data, APA could obtain more accurate and more stable results than traditional linear mixing algorithm (LA).

References

[1] Hu, C. M. (2009). A novel ocean color index to detect floating algae in the global oceans. Remote Sensing of Environment, 113(10), 2118-2129.

[2] Hu, C. M., Lee, Z. P., Ma, R. H., Yu, K., Li, D. Q., & Shang, S. L. (2010). Moderate Resolution Imaging Spectroradiometer (MODIS) observations of cyanobacteria blooms in Taihu Lake, China. Journal of Geophysical Research-Oceans, 115, C04002. doi: 10.1029/2009JC005511.

Evaluation of the Quasi-Analytical Algorithm for estimating the inherent optical properties of seawater from ocean color: Comparison of Arctic and lower-latitude waters

Guangming Zheng, Dariusz Stramski, and Rick A. Reynolds

Marine Physical Laboratory, Scripps Institution of Oceanography, University of California San Diego, La Jolla, CA 92093-0238, U.S.A.
Email: Guangming Zheng, E-mail: gzheng@ucsd.edu

There is strong interest to use remote sensing of ocean color and in situ optical observations as tools for monitoring the ecosystem response and feedback to the environmental changes in Arctic waters. Current inverse reflectance algorithms were typically developed for lower-latitude waters and their application to the Arctic waters needs to be evaluated because the optical properties of the Arctic waters can differ significantly from those of lower latitudes. However, such an evaluation has not been done owing largely to a lack of comprehensive field data collected in the Arctic waters.

Recently, a large set of field data with concurrent measurements of both inherent optical properties (IOPs) of seawater and radiometric quantities that enable determinations of apparent optical properties (AOPs) including the reflectance of the ocean were collected in the Chukchi and Beaufort Seas. Using this new dataset and a lower-latitude dataset collected in the eastern South Pacific and eastern Atlantic, we evaluated the performance of the Quasi-Analytical Algorithm (QAA) [1], version 5 [2], for deriving the spectral total absorption, $a(\lambda)$, and backscattering, $b_b(\lambda)$, coefficients of seawater from input spectrum of remote-sensing reflectance, $R_{rs}(\lambda)$.

We found that the performance of QAA for estimating $a(\lambda)$ varies from very good to fair (bias on the order of ~10%) depending on light wavelength and the oceanic region (Figure 1). For $b_b(\lambda)$, the QAA typically shows overestimation from small to as large as about 35%, with higher overestimation for clear waters (Figure 1). We also conducted a sensitivity analysis to identify and quantify major sources of errors for output variables $a(\lambda)$ and $b_b(\lambda)$. The results show that, for both the Arctic and lower-latitude data, the parameter u [$\equiv b_b/(a+b_b)$] at the reference wavelength of 555 nm generally contributes the most significant bias to $b_b(\lambda)$ at all wavelengths within the spectrum of visible light, whereas the interplay between $u(555)$ and $u(\lambda)$ generally dominates the errors of QAA-derived $a(\lambda)$ except for the reference wavelength. The $u(\lambda)$ parameter tends to be overestimated for relatively clear waters, leading to overestimation of $b_b(\lambda)$. One of main reasons for overestimating $u(\lambda)$ is that the QAA parameterization does not account for Raman scattering effect, which is particularly important for relatively clear

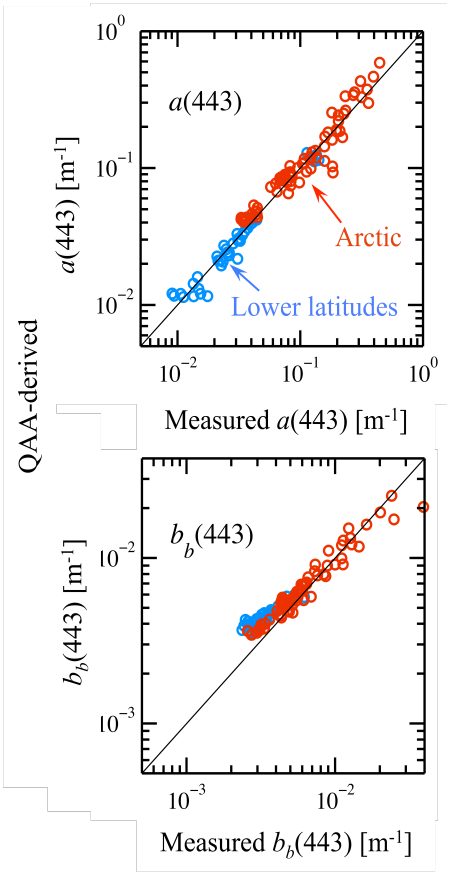

Figure 1. Comparison between QAA-derived and measured total absorption and backscattering coefficients at example wavelength of 443 nm for data collected in the Arctic and lower-latitude waters.

waters [e.g., 3, 4]. For QAA-derived $a(\lambda)$, the biases resulting from $u(555)$ and $u(\lambda)$ tend to compensate each other. At short wavelengths, QAA-derived power spectral slope, η, of the particulate backscattering coefficient, $b_{bp}(\lambda)$, as well as the choice of formula [5, 6, 7] for calculating the pure water backscattering coefficient, $b_{bw}(\lambda)$, are also important sources of bias for both $b_b(\lambda)$ and $a(\lambda)$. The latter source is particularly important in clear waters. Our findings provide guidance for future efforts towards refinement of the QAA and potentially also for the development of other inverse models.

References

[1] Lee, Z. P., Carder, K. L., and Arnone, R. A. (2002). Deriving inherent optical properties from water color: A multiband quasi-analytical algorithm for optically deep waters. Appl. Opt., 41: 5755–5772.
[2] Lee, Z. P., et al. (2011). An assessment of optical properties and primary production derived from remote sensing in the Southern Ocean (SO GasEx). J. Geophys. Res., 116: C00F03, doi:10.1029/2010JC006747.
[3] Gordon, H. R. (1999). Contribution of Raman scattering to water-leaving radiance: A reexamination. Appl. Opt., 38: 3166–3174.
[4] Morel, A., and Gentili, B. (2004). Radiation transport within oceanic (case 1) water. J. Geophys. Res., 109: C06008, doi:10.1029/2003JC002259.
[5] Morel, A. (1974). Optical properties of pure water and pure seawater, In: *Optical Aspects of Oceanography*, Jerlov, N. G. and Nielson, E. S. (Ed), Academic, San Diego, California.
[6] Buiteveld, H., Hakvoort, J. H. M., and Donze, M. (1994). The optical properties of pure water. Proc. SPIE, Ocean Optics XII, 2258: 174–183.
[7] Twardowski, M. S., Claustre, H., Freeman, S. A., Stramski, D., and Huot, Y. (2007). Optical backscattering properties of the “clearest” natural waters, Biogeosciences, 4: 1041–1058.